Research and Technology

Fiscal Year 1985 Annual Report Marshall Space Flight Center

JAN198 6
RECEIVED
NASA STI FACILITY
ACCESS DEPT.

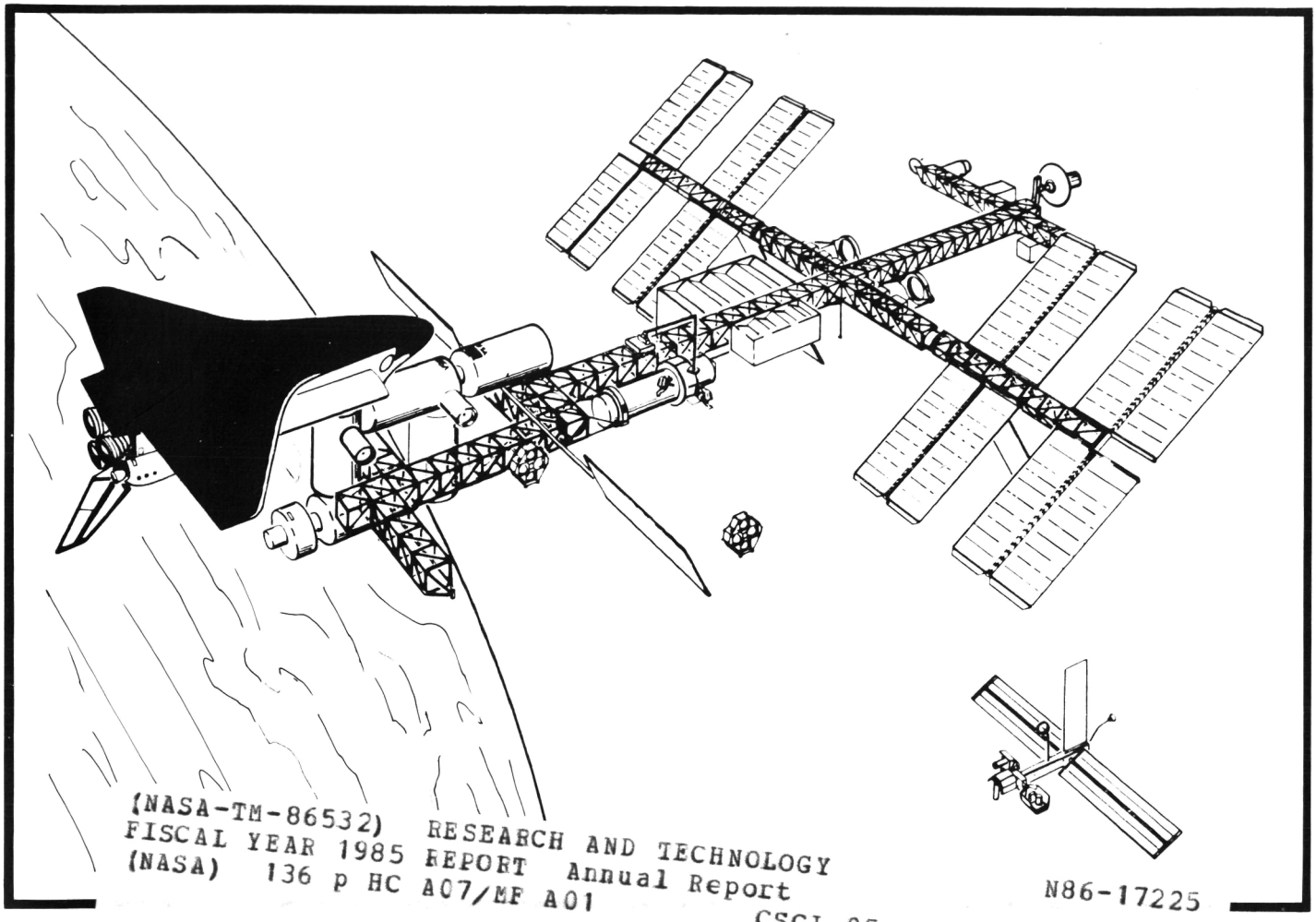

(NASA-TM-86532) RESEARCH AND TECHNOLOGY
FISCAL YEAR 1985 REPORT Annual Report
(NASA) 136 p HC A07/MF A01
CSCL 05A
N86-17225
Unclas
G3/85 05186

November, 1985

NASA

25 Marshall Space Flight Center 1960-1985

INTRODUCTION

A quarter of a century is but a moment on the cosmic calendar. Now that Marshall Space Flight Center has reached its 25th Anniversary, it seems just moments ago that President Dwight D. Eisenhower stood on these grounds and formally dedicated the George C. Marshall Space Flight Center in Huntsville, Alabama. This Fiscal Year 1985 Research and Technology Report reflects the wide spectrum of activities closely linked with the Center's mainstream spaceflight developments. Past accomplishments testify to the success of getting deeply involved in the science and technology of our projects – 32 Saturn launches, Pegasus, the Skylab missions, three High Energy Astronomy Observatory missions, the Apollo – Soyuz mission, and an accelerating schedule of successful Shuttle, Spacelab, and Shuttle payload missions. The Center continues to be involved in engineering development, scientific research, and technology. At the beginning of our second quarter century, the experience and dedication of our engineers and scientists, and the success of our collaboration with industry and academia will now be aimed at the next great endeavor, the Space Station.

W. R. Lucas,
Director

PREFACE

The point of contact at Marshall Space Flight Center for this report is F. A. Speer, DS01, (453 – 3033), who provided overall supervision. He was assisted by an editorial committee consisting of W. C. Snoddy, A. J. Dessler, J. W. Littles, I. Akbay, and J. W. Campbell. Detailed editorial support was supplied by A. Howard, L. Menteer, and S. Goodman, with production assistance from W. Smith and J. Robinson. To assist the reader, an MSFC contact, office code, telephone number, and sponsoring agency is included at the end of each article. The work at MSFC is a cooperative effort. Because of space restrictions, it is impossible to list all those involved in the projects described in this report.

TABLE OF CONTENTS

ADVANCED STUDIES

Introduction	W. C. Snoddy	1
Space Station		
Space Station	L. E. Powell	1
Space Station Technology	C. C. Gregg	2
Transportation Systems		
Orbital Maneuvering Vehicle	W. G. Huber	3
Aeroassist Flight Experiment	R. E. Austin	4
Orbital Transfer Vehicle	C. L. Varnado	5
Advanced Launch Vehicles	M. A. Page	6
Space Transportation System Propellant Scavenging	M. A. Page	7
Advanced Recovery System for Space Transportation System Applications	M. A. Page	7
Aft Cargo Carrier	J. E. Hughes	8
Space Systems		
Advanced X-Ray Astrophysics Facility	D. C. Cramblit	9
Gravity Probe-B	A. K. Neighbors	10
Pinhole Occulter Facility	J. R. Dabbs	11
Advanced Solar Observatory	W. T. Roberts	12
Solar Terrestrial Observatory	W. T. Roberts	13
Extending Very Long Baseline Interferometry to Space	S. Morgan	13
Deployable Antenna Flight Experiment	W. E. Thompson	15
Space Based Ultraviolet/Optical Phased Arrays	M. E. Nein	15
Tether Applications in Space	G. F. von Tiesenhausen	17
Long Term Orbital Cryogenic Storage Facility	U. Hueter	18
The Human Role in Space	S. B. Hall	19
Experimental Geostationary Facility	R. H. Durrett	20
Manned Mars Mission	J. M. Butler	21
Commercial Materials Processing in Space	K. R. Taylor	23

RESEARCH PROGRAMS

Introduction	A. J. Dessler	25
Microgravity Sciences		
Introduction	R. J. Naumann	25
Crystal Growth and Characterization	S. L. Lehoczky	25
Metal Model Material for Modeling Low Gravity Solidification of Alloys	W. D. Hamilton	26

Model Immiscible Systems	D. O. Frazier	27
Solution Crystal Growth	R. L. Kroes	27
Advanced Furnace Technology for Materials Processing in Space	D. B. Griner	28
Low – G Solidification of Alloys	P. A. Curreri	29
Undercooling of Peritectics	M. B. Robinson	31
Study of the Reactive Element Effect on Oxidation	E. C. Ethridge	32
Surface Film Effects on Drop Tube Undercooling Studies	E. C. Ethridge	33
Organic Crystal Growth	R. J. Naumann	33
Protein Crystal Growth	R. S. Snyder	34
Phase Partitioning	R. S. Snyder	35
Electrophoresis	R. S. Snyder	36
Effects of Microgravity on Model Polymer Systems	B. E. Goldberg	36
Monodisperse Latex Reactor	D. M. Kornfeld	37
Solar Physics		
Introduction	R. L. Moore	38
Solar Magnetic Fields	M. J. Hagyard	39
Transition Region	R. L. Moore	41
Ultraviolet Spectrometer and Polarimeter	E. A. Tandberg – Hanssen	42
Coronal and Interplanetary Dynamics	S. T. Suess	44
Statistical Solar Studies	R. M. Wilson	45
Magnetospheric Physics		
Introduction	C. R. Chappell	47
Observations of Global Ion Outflows	J. H. Waite, Jr.	47
Spacecraft Charging at High Altitudes Data Analysis	P. D. Craven	49
Superthermal Ion Composition Studies	T. E. Moore	50
Body – Plasma Electrodynamic Interaction Studies	N. H. Stone	52
Retarding Potential Analyzer Differential Ion Flux Probe	N. H. Stone	53
Spacecraft Plasma Interactions	A. P. Biddle	54
Low – Energy Charged Particle Flight Instrumentation	A. P. Biddle	55
Space Physics Analysis Network	J. L. Green	56
Space Experiments with Particle Accelerators	D. L. Reasoner	57
Astronomy		
Introduction	R. Decher	58
X – Ray Astronomy	M. C. Weisskopf	59
Advanced X – Ray Telescope Designs	R. B. Hoover	60
Gamma – Ray Astronomy	G. J. Fishman	62
Cosmic Ray and Particle Physics	T. A. Parnell	63

Mid – Infrared Array Camera	C. M. Telesco	64
Infrared Astronomy	E. W. Urban	64
Atmospheric Sciences		
Introduction	W. W. Vaughan	65
Geophysical Fluid Flow Cell	F. W. Leslie	65
Theoretical and Experimental Studies of Baroclinic Processes	T. L. Miller	66
Contributions to Monte Carlo Turbulence Simulation	C. W. Campbell	67
Global Wind Measurement by Satellite Doppler Lidar	D. E. Fitzjarrald	68
Analysis of Airborne and Ground – Based Doppler Lidar Data	J. Rothermel	69
Doppler Lidar Research and Development	J. W. Bilbro	70
Low Altitude Flow Conditions	M. B. Alexander	70
Satellite Infrared Remote Sensing of the Formation and Development of Convective Storms	R. E. Smith	71
TECHNOLOGY PROGRAMS		
Introduction	J. W. Littles	73
Liquid Propulsion Systems		
Application of Powder Metallurgy Techniques to Produce Improved Bearing Materials for Rocket Engine Turbopumps	B. N. Bhat	73
Rolling Contact Fatigue Behavior of Ion Plated Bearing Materials	R. L. Thom	74
Methane Heat Transfer Investigation	D. H. Blount	75
Rocket Engine Turbopump Bearing and Seal Material Tester	W. N. Myers	76
The Development of Single Crystal Turbine Blades for the Space Shuttle Main Engine	R. A. Parr	76
Improvements in Turbine Airfoil Low Cycle Fatigue Life	L. A. Gross	77
Vacuum Plasma Spray Coating Development	R. R. Holmes	78
Space Shuttle Main Engine Hot Gas Manifold Analysis	H. G. Struck	78
Turbomachinery Whirl Elimination with Damping Seals	G. L. von Pragenau	79
Forces on Turbomachinery Rotors	T. H. Fox	81
Development of Hydrogen Resistant Alloys	W. B. McPherson	82
Advanced High Pressure Oxygen – Hydrogen Propulsion Instrumentation	T. N. Marshall	82
Measurement of Very Small Thrust Forces in a Space Environment	A. R. Felix	84

Optically Beamed Energy Transfer Mechanisms	T. D. McCay	85
Solid Rocket Propulsion Systems		
Ignition Overpressure from Solid Rocket Motor Firings	S. H. Guest	87
Effects of Sodium Hydroxide on Carbon – Phenolic Material	B. E. Goldberg	88
Solid Rocket Booster High Temperature Sealants Development	C. H. Jackson	88
Filament Winding Automation and Kinematic Simulation	W. R. Colberg	89
Processes		
Variable Polarity Plasma Arc Welding on the Space Shuttle External Tank	E. O. Bayless, Jr.	90
Large Weld Tooling Technology Development	J. H. Ehl	91
Space Shuttle Main Engine Robotic Weld System	C. S. Jones, Jr.	91
Weld Modeling	A. C. Nunes, Jr.	93
External Tank Spray – on Foam Insulation Flowrate Instrumentation System	E. Martinez	94
Space Shuttle External Tank Foam Application Development	C. H. Jackson	95
Process Control Automation	E. Martinez	96
Sprayable Ablator Process for Solid Rocket Booster Structures	W. E. Hill	97
Materials		
An Electrochemical Study of the Corrosion Behavior of Primer Coated 2219 – T87 Aluminum	M. D. Danford	99
Formulation/Cure Technology for Ultra – High Molecular Weight Silphenylene – Siloxane Polymers	N. H. Hundley	99
Cure Monitoring Methodology for Advanced Composite Materials	B. E. Goldberg	101
Orbital Atomic Oxygen Effects on Thermal Control and Optical Materials	A. F. Whitaker	102
Liquid Oxygen/Gaseous Oxygen Compatible Elastomers	W. J. Patterson	103
Space Power		
Low – Temperature Semiconductors	R. F. DeHaye	104
Autonomously Managed Power System	D. J. Weeks	105
Battery Protection and Reconditioning Circuit as Used on the Hubble Space Telescope	L. F. Lollar	106

Miniature Cassegrainian Concentrator Solar Array — M. R. Carruth, Jr. — 107

Robotics and Teleoperations
Robotics and Teleoperations — D. R. Scott — 108

Information Systems
A Laser Optical Disk in a Data Base Management System — D. T. Thomas — 109

Structures and Dynamics
Space Deployable Structures — E. E. Engler — 110
Solar Array Flight Experiment/ Dynamic Augmentation Experiment — R. W. Schock — 112
Composite Structures Development — G. H. Gordon — 113
Development and Test of Advanced Composite Components — E. E. Engler — 114

Heat Transfer/Fluid Mechanics
Fluid Interface and Bubble Experiment — F. W. Leslie — 115
Thermal Energy Storage and Transport Utilizing Microencapsulated Phase Change Materials — J. W. Owen — 116
Heat Transport Across Structural Boundaries — J. W. Owen — 117
Cryogenic Fluid Management Breadboard — R. A. Brodowski — 119
Warm Fog Dispersal Research — V. W. Keller — 120

TECHNOLOGY UTILIZATION

Introduction — I. Akbay — 123

Advanced Lightweight Firefighting Module — R. A. Burns — 123
Firefighters' Communication Equipment — D. Stone — 124
Emergency Management Computer Aided Trainer — K. A. Smith — 125
Prosthetic Urinary Sphincter System — J. R. Richardson — 126
Photorefractor Ocular Screening System — J. R. Richardson — 127

Advanced Studies

Advanced studies are the beginning. They match future development goals with technology. Each challenges the other.

Many past goals have become reality during Marshall Center's first 25 years. They include President Kennedy's vision of placing "a man on the moon and returning him safely to the Earth"; orbiting our first space station, Skylab; establishing a highly versatile Space Transportation System that evolved from the Redstone rockets through the giant Saturn series of launch vehicles and culminated with the current Space Shuttle propulsion systems; developing a facility which converts the Orbiter into a temporary space station, Spacelab; and fashioning far-seeing "eyes" like the Apollo Telescope Mount and the High Energy Astronomy Observatories – instruments that have advanced the frontiers of space sciences.

Goals that will soon be reality include the Hubble Space Telescope, an observatory capable of seeing to the edge of the universe; a capability for lowering instrument-laden packages from the Shuttle on a 60-mile long tether to study the atmosphere and magnetosphere; and the exploitation of the low-gravity environment. In microgravity, we are witnessing the beginnings of creating new medicines, electro-optical materials, alloys and other products which could provide tremendous benefits to mankind.

Today we establish new goals and pursue new technology. These fresh visions of the future include the permanently manned Space Station, manned interplanetary missions, geostationary facilities, and the commercial use of space. Advancements in technology include orbital servicing and assembly, even larger optical systems in space, advanced launch and inter-orbital vehicles, and a host of scientific spacecraft designed to observe the celestial sphere as well as our solar terrestrial environment.

Space Station

In January 1984 President Reagan directed NASA to develop a permanently manned Space Station within a decade, to invite other countries to participate in its development, and to promote private sector investment in space. Although this represented a firm commitment by the Administration to support the development of a Space Station, the project itself was not new to NASA.

In May 1982 the NASA Administrator established a Space Station Task Force consisting of the scientific community, other government agencies, potential international partners and United States aerospace firms. The Task Force provided the focus and direction for the Agency's space station activities and identified mission requirements. In the spring of 1983 a Concept Development Group (CDG) was formed as part of the Task Force. This group led the agency-wide engineering and integra-

ORIGINAL PAGE IS
OF POOR QUALITY

tion effort to develop space station concepts as well as architectural and system requirements. The MSFC Science and Engineering and Program Development Directorates participated by performing numerous trade studies and analyses to support this agency-wide activity. MSFC's previous experience provided significant insight into the design challenges of the Space Station (Figure 1).

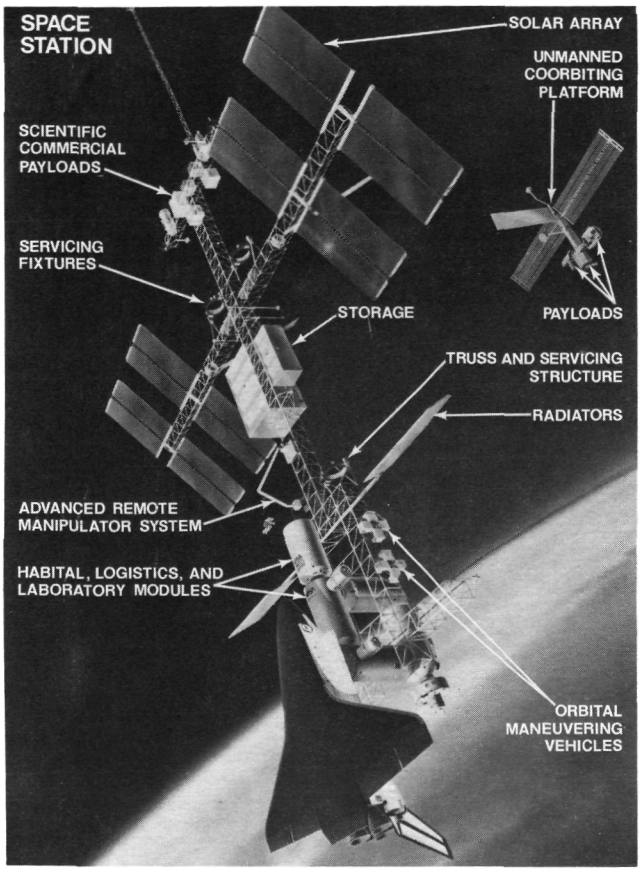

Figure 1. Space Station.

By May 1984 the data resulting from the Task Force and most of the participants were relocated to the Johnson Space Center (JSC) to support the Space Station "Skunk Works" activity. The Skunk Works' mission was to develop a Space Station Reference Configuration, to prepare a requirements document, and to prepare the Request for Proposal for the preliminary design procurement. Work assignments were established by the NASA Administrator for the four centers, and by October, the Space Station Projects Office was established at MSFC with responsibility for overall project management of the Space Station elements and Space Station Systems Engineering and Integration tasks assigned to the Center. This office is aligned to the management of the Common Module, Laboratory Module, Logistics Module, Propulsion and Vehicle Accommodations, Project Integration and Program Control.

Since that time MSFC has continued to focus on user involvement, both commercial and international, and to develop a flexible program that will provide users with a Shuttle-dependent, space facility that is continuously habitable, readily maintainable, and resuppliable, as well as technologically evolutionary. The Station will be an on-orbit laboratory for scientific application and technological development and will provide a permanent observatory, a space transportation node, and a servicing and repair facility for free-flyers and space platforms, both manned and unmanned. Commercial applications include manufacturing and assembly facilities for future products manufactured in space.

L. E. Powell/KA01
(205) 453-0541
Sponsor: Space Station

Space Station Technology

MSFC has a major role in the development of technological advancements which support the Space Station Program. NASA's aim is to develop and demonstrate technology for the Space Station which builds upon the Agency's strong research and technology program. Detailed and thorough assessments concluded that enhanced current technology in selected disciplines is necessary to build the Space Station. Technological areas selected for further study include propulsion systems to maximize efficiency of fuel utilization, technology needed for berthing as opposed to docking of the STS with elements of the Space Station, the closed loop aspects of an Environmental Control Life Support System (ECLSS) to eliminate or reduce the life cycle cost, and the technology required for more efficient power generation.

MSFC was assigned lead center responsibilities for advanced development in the areas of attitude control and stabilization, onboard propulsion and fluids, and structures and mechanisms. MSFC also has a major supporting role in the advanced development areas of electrical power, environmental control and life support, human productivity, data management, communications, and thermal control.

During the past year, 40 procurements for advanced development test bed activities were initiated and work is underway primarily in the areas of Attitude Control, ECLSS, Propulsion, and Structures/Mechanisms/Materials. Total accumulated test time of 2,896 seconds has been achieved on the gaseous oxygen/hydrogen thruster at varying mixture ratios and time deviations. Also, the MSFC ECLSS team has produced a facility layout and begun purchasing and assembling hardware for a prototype test facility. More detailed discussions of specific Space Station technology results will be covered in other sections of this report.

Cecil Gregg/KA01
(205) 453 – 0541
Sponsor: OSS

Transportation Systems

Orbital Maneuvering Vehicle

With the advent of the Space Shuttle, it is now possible to efficiently deliver a spacecraft to and from low Earth orbit. This payload performance can be further enhanced by using an Orbital Maneuvering Vehicle (OMV) which has been studied at MSFC for several years. This activity originated with the Teleoperator Retrieval System (TRS), which was designed to reboost/deboost the Skylab, and has continued in an effort to optimize the OMV to accommodate a wide range of mission applications. The OMV will operate in orbits higher than the Shuttle or Space Station orbit and may also be used in geosynchronous orbit when delivered by high – energy upper stages such as the Transfer Orbit Stage (TOS), Centaur, and Orbital Transfer Vehicles (OTVs).

In – house and contracted conceptual (Phase A) studies were concluded in October 1983. Definition (Phase B) contracts were awarded to LTV, Martin Marietta, and TRW in August 1984, and will be completed by the end of August 1985. These conceptual and definition studies have defined a highly efficient vehicle which can be used for a wide range of services. A representative configuration, shown in Figure 2, depicts the use of the vehicle to support the delivery, retrieval, reboost, viewing, and servicing of free – flying satellites.

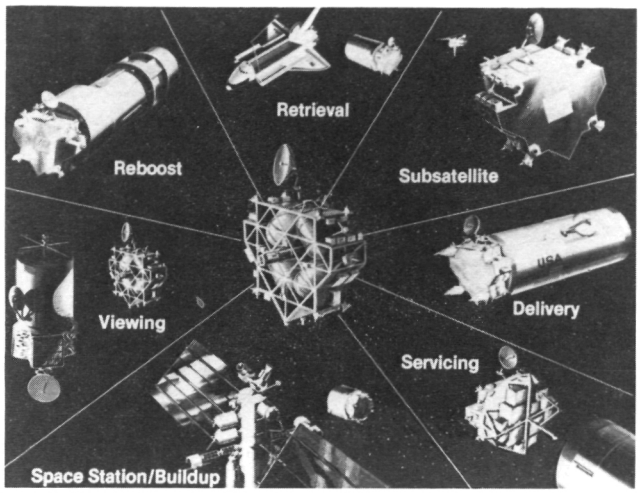

Figure 2. OMV Operational.

Many advanced OMV missions are visualized, including on – orbit refueling functions by the addition of tanker kits and remote servicing with the addition of manipulator systems. In addition, specialized docking systems and/or end effectors will make it possible to collect debris and retrieve tumbling spacecraft. The OMV will also be available for assembly and build – up of the initial Space Station, and later, will provide augmentation and enhancement to the facility.

Several configuration approaches are being defined, but the vehicle can generally be described as a relatively thin wafer, approximately three to five feet thick and approximately fifteen feet in diameter. This design allows it to be directly mounted to the Shuttle longerons

and keel without the use of a cradle and thereby minimizes the need for airborne support equipment and maximizes the Shuttle payload manifesting flexibility.

The Shuttle – transported OMV will be based at the Space Station. Shuttle – supported operations will be utilized for high inclination orbits not accessible from the Space Station. The OMV Operations Control Center will be located on the ground; however, the OMV will be controlled from the Space Station when operating in the vicinity of the Space Station.

The Phase B effort is being supported by concentrated MSFC supporting development activities in the rendezvous and docking simulation areas, including the design, testing, and evaluation of various docking interfaces and docking/rendezvous aids. Primary areas of design deal with the remote rendezvous and docking sensors and aids needed by the pilot to assure final approach and docking of the OMV to both stable and slowly rotating targets. In this category, the need for range and range rate radar is being investigated in addition to television and lighting type and quality. Communication time delays and the operator tolerance/capability is being studied and evaluated by having pilots fly high fidelity demonstrations on both the OMV Robotic Flat Floor Facility (which has six degrees of freedom capability) and the Target Motion Simulator. Simulations are also being accomplished utilizing alternative docking interfaces. Primary efforts have been focused on the possibility of adapting the Remote Manipulator System (RMS) end effector to be the OMV docking interface.

Another area of concentration involves the requirements for a three – point docking system to interface with payloads equipped with three hard points, such as the Flight Support System currently being utilized by the Multi – Mission Spacecraft (MMS), the Hubble Telescope, and other large observatory spacecraft. MSFC activities are being closely integrated with the contractor simulations. These simulation activities, other supporting development work, and contracted definition studies are providing a sound base of knowledge on which to start the OMV development program.

William G. Huber/PF14
(205) 453 – 5311
Sponsor: OSF

Aeroassist Flight Experiment

The Aeroassist Flight Experiment (AFE) will simulate the atmospheric flight phase of an Aeroassisted Orbital Transfer Vehicle (AOTV) returning from geosynchronous orbit. The definition phase of the program, begun in 1983, involved MSFC and the Johnson, Langley and Ames Centers. A Project Initiation Agreement (PIA) developed in 1985 between these centers and the OSF and OAST Headquarters Program Offices is in the final phase of negotiations. The first phase of the experiment is planned for 1990, and like the AOTV, the AFE will skim through the upper levels of the atmosphere and target a preset orbit that would be suitable for Orbiter retrieval.

The AFE will be composed of a carrier vehicle and the aerobraking subsystem (Figure 3). The carrier will serve as the basic structure of the simulation and will house the avionics and propulsion system and provide integration support for the aerobraking subsystem. The aerobraking subsystem consists of the aerobrake structure which has instruments designed to measure the environmental parameters necessary for technological development. The flight experiment cannot be accomplished through ground tests or analyses because determinations must be made concerning nonequilibrium radiation predictions, real gas aerodynamic predictions, and performance of flexible aeroassist devices.

Environmental and vehicle design technology will also benefit from the experiment. The environmental technology includes nonequilibrium convective heating, wall catalysis, and aerodynamics, while the vehicle design technology involves enhanced flight performance, Thermal Protection System materials, avionics, guidance algorithms and deployable devices.

ORIGINAL PAGE IS
OF POOR QUALITY

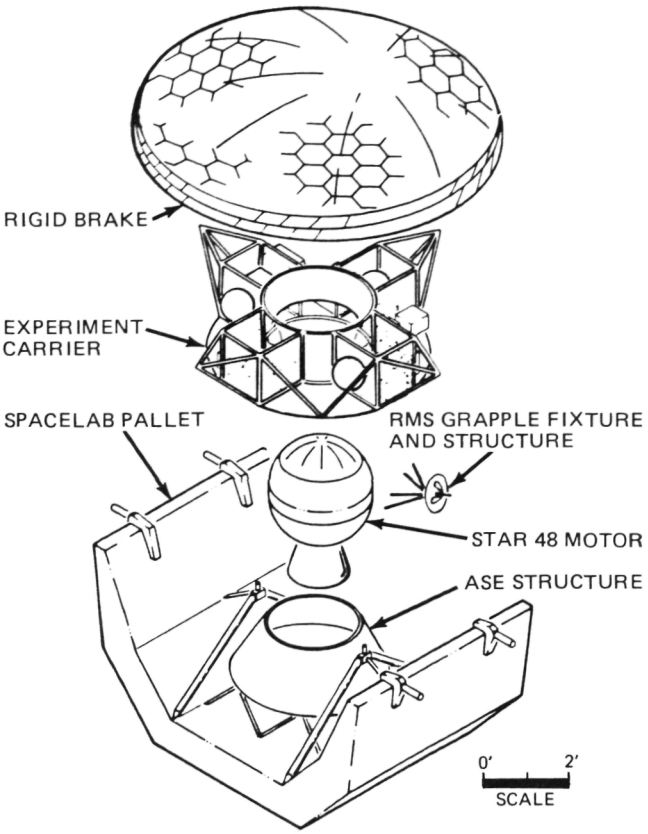

Figure 3. Aeroassist Flight Experiment – Baseline Rigid Brake Concept – Exploded View.

These technological designs are strongly influenced by atmospheric variations in the upper atmosphere.

Two concepts are being considered: the rigid brake system and the flexible system in the form of a ballute. The concept using the brake is currently planned for the first flight, while the flexible brake is a possibility for the second. The second flight is currently under investigation as an option to the program pending the results of current Orbital Transfer Vehicle Studies. In 1985 substantial definition activities have been accomplished by the in-house NASA AFE Steering Committee, and through contracted studies which led to baseline definitions of these two concepts.

Gene Austin/PS03
(205) 453-0162
Sponsor: OSF and OAST

Orbital Transfer Vehicle

For many years NASA has been involved in defining the requirements and designing the systems which will satisfy the nation's future space transportation needs. The advent of the Space Shuttle opened a new era in space transportation by providing low cost access to low Earth orbit. Studies of future payload requirements indicate that efficient and cost effective transportation from low Earth orbit to higher Earth orbits and beyond will be needed in the 1990's. These transportation requirements have been identified from the analysis of NASA's long range planning in science, application, and technology, as well as from forecasts of future commercial activities in space. Analyses of these various sources resulted in the definition of transportation systems known as Orbital Transfer Vehicles (OTV).

A broad spectrum of orbital transfer system concepts (Figure 4) is being studied to determine the best method of meeting future mission requirements. These studies, conducted by three contractors, Boeing Aerospace, Martin Marietta, and General Dynamics/Convair, are scheduled to be completed late in 1985. System requirements derived from a NASA-developed OTV Mission Model, and candidate vehicle concepts were defined to assess alternative evaluationary approaches to meeting mission requirements. Space Station accomodations and interface requirements were also identified for the support of a space-based OTV fleet

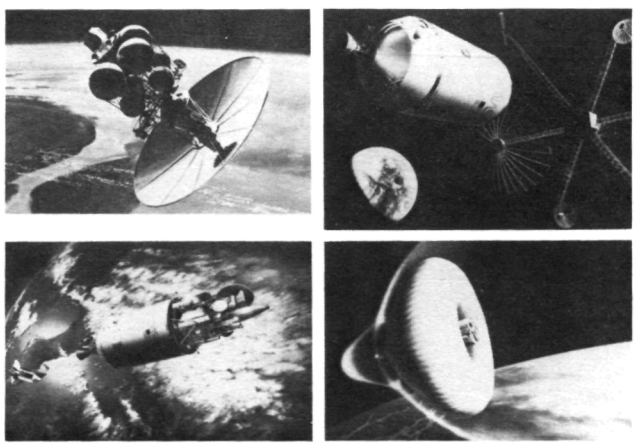

Figure 4. Orbital Transfer Vehicle Concept.

and presented to the Space Station Program for assessment of initial Space Station impacts. The results of these Studies will be combined with earlier studies and in – house NASA investigations to identify the most promising concepts or approaches and to determine areas requiring technological advancement.

Lee Varnado/PS03
(205) 453 – 0162
Sponsor: OSF

Advanced Launch Vehicles

A number of payloads currently under study for launch after 1995 are too large and heavy to be accommodated by the Space Transportation System (STS), and many do not require a manned flight for their deployment. These payloads are critical to the needs of NASA and other government agencies; therefore, the development of cost effective intermediate and heavy lift launch vehicles is necessary if these payloads are to be flown.

Advanced launch vehicle studies at MSFC have continued in an effort to satisfy these potential needs with two basic approaches being identified. The first is to use Shuttle components to design unmanned vehicles that have increased payload weight and size capabilities, with emphasis on designs that can evolve into a Heavy Lift Launch Vehicle (HLLV). This will result in a group of Shuttle Derived Vehicles (SDVs) with initial payloads in the intermediate range (80k–160k lb), evolving to the HLLV range of 200k–500k lb. The basic designs are the side mount vehicle in which the Orbiter is replaced with a cargo carrier and a Propulsion/Avionics (P/A) module, and the in – line vehicle where the Orbiter is removed, a P/A module is placed under the External Tank (ET), and the payload is atop the ET. Both configurations use standard STS Solid Rocket Boosters (SRBs). Each concept has been studied with both expendable and reusable main engine propulsion systems. Both vehicle concepts can evolve into vehicles with increased performance by replacing the SRBs with Liquid Rocket Boosters using liquid oxygen/hydrocarbon (LOX/HC) engines (Figure 5).

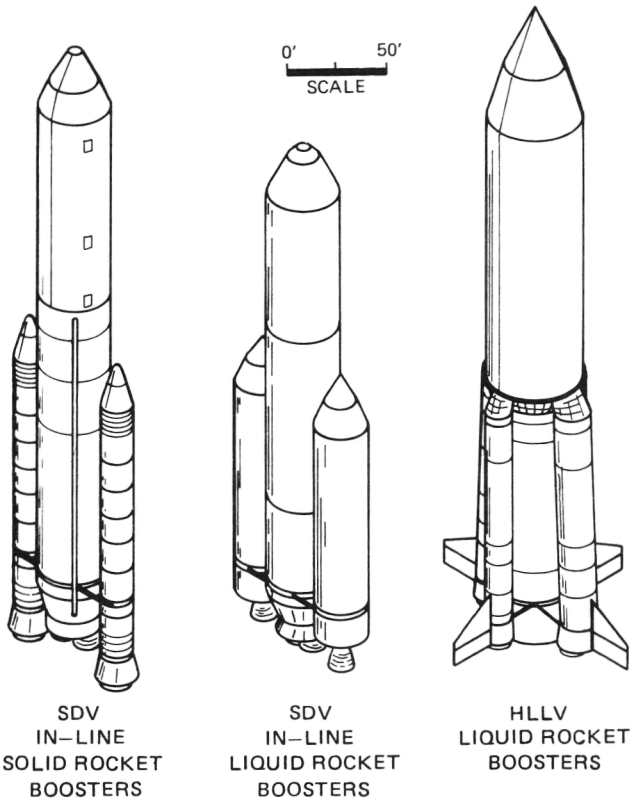

Figure 5. Shuttle Derived Vehicles (SDV)/Heavy Lift Vehicles (HLLV).

The second approach that has been investigated is to start with a HLLV having new propellant tanks, LOX/HC engines, new boosters, and new avionics. The launch system could evolve into smaller vehicles through independent use of selected boosters and other components, thus satisfying the space transportation needs with a vehicle family of non – SDV components. An in – house preliminary definition and cost analysis of HLLV concepts was completed in 1985.

In both approaches, recovery of the boosters and P/A module has been investigated as a means of reducing costs. The technology required for the development of the SDV and HLLV concepts, including potential cost savings were developed in 1985, including the LOX/HC and LOX LH_2 engines, recovery sys-

tems, avionics, improved operations, advanced materials, and improved manufacturing methods.

M. A. Page/PS03
(205) 453 – 0162
Sponsor: OSF

Space Transportation System Propellant Scavenging

The periodic resupply of consumables will be an inherent part of extended space operations. The Space Station and the reusable Orbital Transfer Vehicle (OTV), based at the Space Station, will require large quantities of cryogenic propellant and the Orbital Maneuvering Vehicle (OMV) will require storable propellants. The Propellant Scavenging Study investigates scavenging of residual and performance reserves from the External Tank and propellant lines after the Shuttle flight requirements have been met.

Two scavenging concepts are being investigated for feasibility and estimation of the amount of cryogenic propellants that can be scavenged over a 10 year period (1991–2000). One scavenging concept considered was to collect and store the residual propellant in tanks located in the Aft Cargo Carrier. The tanks could then be separated from the Shuttle and transferred to a position in Low Earth Orbit (LEO) to be picked up and delivered to the Space Station orbit by an OMV. The 1985 Study identified a potential to scavenge 2.15 million pounds of cryogenic propellant in the 1991 – 2000 time frame. The second concept is to locate the collecting tanks in the Orbiter's Cargo BAY concept and transfer them from LEO to the Space Station orbit by OMV. The In – Cargo Bay concept will also apply to scavenging storable propellants from the Orbiter Maneuvering System (OMS). This concept was shown in this year's study to have a potential of scavenging 1.25 million pounds of cryogenic propellant, and 1.40 million pounds of OMS storable propellants in the 1991 – 2000 time frame.

MSFC is sponsoring the Aft Cargo Carrier Concept while the Johnson Space Center is sponsoring the In – Cargo Bay Concept. Both concepts are designed for system return to Earth via the Shuttle Cargo Bay. Conceptual designs of both scavenging systems were developed in this year's studies. Each concept established the feasibility of obtaining substantial amounts of scavenged propellants on – orbit at a relatively low cost.

Technology required to transfer cryogenic propellants under zero gravity from the External Tank into the transfer tanks and from the transfer tanks into the orbital holding/storage tanks in the Space Station vicinity will need to be developed. Measuring the amount of cryogenic propellant in a tank in a weightless environment is also a technology that requires development. Demonstrations to test the concepts/systems will be needed.

M. A. Page/PS03
(205) 453 – 0162
Sponsor: OSF

Advanced Recovery Systems for Space Transportation System Applications

During fiscal year 1985 a study of Advanced Recovery Systems for Space Transportation System (STS) Applications was accomplished. Experience with the STS solid rocket booster (SRB) has demonstrated the economic benefits of using parachutes for recovery and reuse of launch vehicle hardware; however, since the selection of the SRB recovery system, the materials and fabrication technology has progressed to the point where further investigation of advanced recovery systems is desirable.

The study considered the recovery of a 70,000 lb object such as the reusable Propulsion/Avionics Module (P/A), using either the parawing/parafoil concept, or the modified Rogallo wing (Figure 6). The parawing/parafoil is a lifting device used in the subsonic through

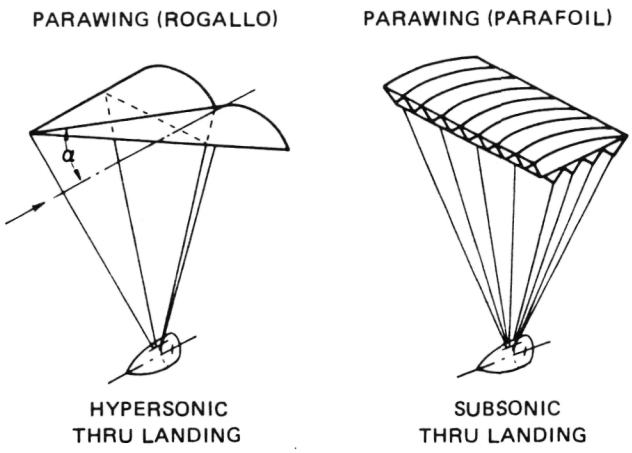

Figure 6. Advanced Recovery Systems—Basic Concepts.

landing range, while the Rogallo wing is used in the hypersonic through landing range and can be used to return items directly from orbit. Each concept has remotely controlled guidance which allows precision landing control with near zero vertical velocity resulting in minimal payload damage.

Both the parawing/parafoil and Rogallo concepts appear to be feasible. The parawing/parafoil concept can be applied to booster and subsonic P/A modules, while the Rogallo system may be applicable to other payloads. Proposed studies will further develop the advanced recovery methods and will lead to demonstration plans and programs.

M. A. Page/PS03
(205) 453-0162
Sponsor: OSF

Aft Cargo Carrier

The Aft Cargo Carrier (ACC) has been studied as a method to increase the payload volume capability of the Space Transportation System (STS) to Low Earth Orbit (LEO) and Geosynchronous Orbit (GEO). The use of the ACC will permit accommodation of payloads with diameters of 25 ft as compared to 14 ft for the Orbiter Cargo Bay. It would be used to transport large Orbital Vehicles, Large Diameter Reflector subassemblies, propellant scavenging tanks and additional payloads deployed by the Payload Assist Module. This increase in payload diameter capability would also be available to other governmental agencies and commercial organizations (Figure 7).

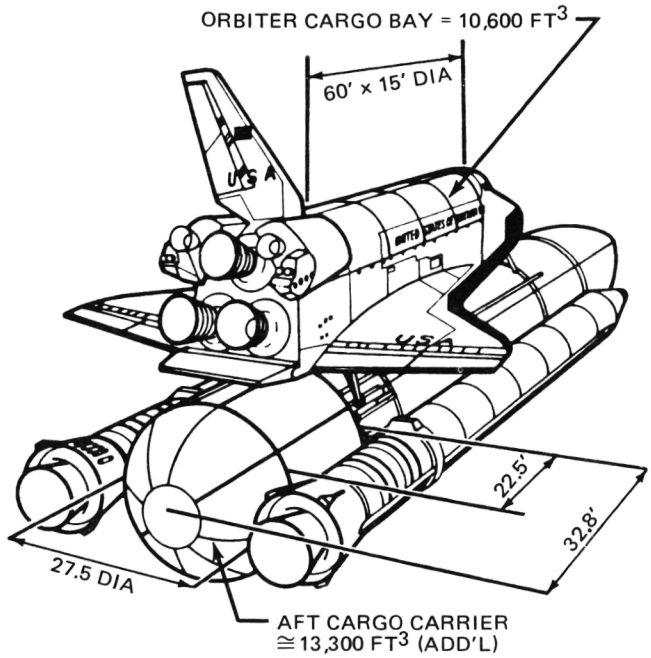

A. C. C. INCREASED PAYLOAD

- ADDITIONAL PAYLOAD VOLUME:
  - FOR VOLUME LIMITED FLIGHTS
  - FOR PAYLOADS DIFFICULT TO INSTALL IN ORBITER
- POTENTIAL A. C. C. PAYLOADS:
  - SPACE STATION MODULE
  - LARGE STRUCTURES
  - PROPULSIVE STAGE PLUS PAYLOAD
  - CRYOGENIC ORBIT TRANSFER VEHICLE

Figure 7. Shuttle Derived Vehicle/Aft—Cargo Carrier (ACC).

Tests to determine the external acoustic and overpressure environment in the vicinity of the ACC during the Shuttle lift-off phase have been conducted. Data from these tests indicate that the feasibility of matching the acoustic environment to that of the Orbiter Cargo Bay is well within design capability. Tests also were conducted to determine if the acoustic levels reaching the payload inside the ACC could be reduced by purging the interior of the ACC with helium at low pressures dur-

ORIGINAL PAGE IS
OF POOR QUALITY

ing the boost phase of the Shuttle flight. Results of these tests verified that the acoustic environment in the ACC can be made equal to that in the Orbiter Payload Bay. Technology and advanced development required to further enhance the performance and economics of the ACC include: refined fabrication methods, thermal protection materials, separation devices and methods, and demonstrations to test the system.

James E. Hughes/PS03
(205) 453-0162
Sponsor: OSF

Space Systems

Advanced X-Ray Astrophysics Facility

The Advanced X-Ray Astrophysics Facility (AXAF) program has moved from the conceptual phase to the definition phase. Two prime contractor teams led by TRW and Lockheed Missiles and Space Company were selected to analyze alternative concepts for this free-flying x-ray observatory. Based on the conceptual studies performed by MSFC and its project team member, the Smithsonian Astrophysical Observatory, AXAF will weigh about 20,000 lb and have a length of approximately 43 ft (Figure 8). Launch is planned for the early 1990's, and AXAF will operate through on-orbit servicing over a 15-year lifetime. The heart of the observatory will be a large, high-precision, x-ray telescope with scientific instruments located at the focal plane. These instruments are capable of performing several detection techniques for long-term, detailed studies of x-ray radiation. They will be periodically replaced on orbit throughout the observatory's operating lifetime.

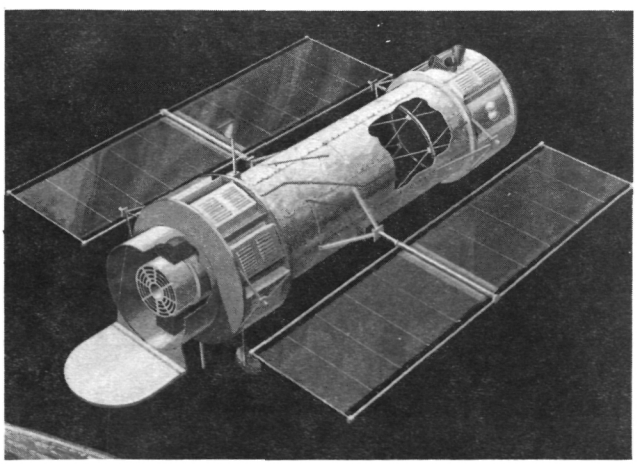

Figure 8. Advanced X-Ray Astrophysics Facility.

Systems studies by the prime contractors continue to support the feasibility of the mirror concept and the conclusions of previous conceptual studies. The only critical technology area in the AXAF concept is the high precision optical system. The goal for the flight x-ray optical system is to achieve a resolution capability approximately eight times that of High Energy Astronomy Observatory-2 (HEAO-2). This improved resolution, along with a fourfold increase in the collecting area and high sensitivity detectors at the focal plane, is expected to improve the overall x-ray telescope performance 50-100 times over that of its predecessor.

A Technology Mirror Assembly (TMA) was initiated in 1982 to demonstrate the feasibility of AXAF optical system goals and to improve the technology base within the industry. Perkin-Elmer and ITEK were contracted to design, fabricate, assemble, and test two x-ray mirror assemblies which were implemented using fabrication processes and metrological techniques related to the AXAF flight mirror assembly. The principal technology goal of the program was to determine the specifications for the AXAF mirror element surface finish and figure. To achieve this goal, it was recognized that the high-precision/accuracy aspects of fabrication, metrology assembly, alignment, and x-ray performance testing required technological development.

The TMA shown in Figure 9 is a two-element paraboloid/hyperboloid grazing incidence telescope. It is a scaled down version of an AXAF mirror pair with the same surface finish and figure requirements. The mirror elements have a 0.5 degree grazing angle and are coated

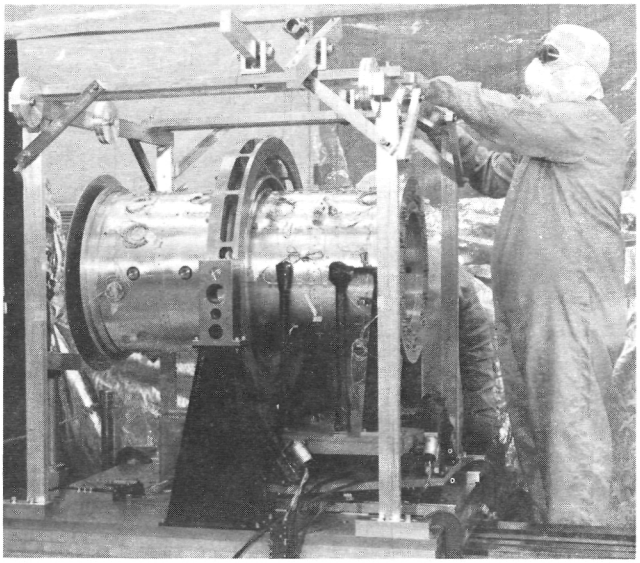

Figure 9. TMA Two Element Paraboloid/Hyperboloid Grazing Incidence Telescope.

with 500Å of gold to provide reflectivity over the energy range of 0.1 to 10 keV. The mirror elements, fabricated by Perkin-Elmer from Zerodur, are supported in a mirror (cell) support system designed and fabricated by the Smithsonian Astrophysical Observatory. The focal length of the TMA is limited to 6 m (10 m for AXAF) to permit x-ray performance testing in the existing MSFC X-Ray Test Facility.

An x-ray detector assembly equipped with three detectors is used in the x-ray performance test. The detectors include a high resolution imager, a larger area proportional counter with pinholes and/or slits, and a position-sensitive proportional counter. Precision motion provides the capability to map the x-ray image and provide subarcsecond resolution. A quad cell based motion detection system was designed and fabricated by MSFC to correct for image smear caused by relative motion between the TMA and x-ray detectors. The results of the x-ray test program will be provided to the prime contractors for use in the Phase B studies and for establishing specifications for the AXAF flight mirrors.

David C. Cramblit/PF19
(205) 453-0788
Sponsor: OSSA

Gravity Probe-B

Gravity Probe-B is a new test of Einstein's General Theory of Relativity using an Earth-orbiting satellite to measure with extreme precision the precessions of gyroscopes with respect to a telescope pointed at a suitable guide star. The purpose of this mission is to measure two predicted principal relativity effects. The geodetic precession due to the orbital motion of the gyroscope through the curved spacetime surrounding the Earth and the frame-dragging or "gravitomagnetic" precession due to the rotation of the Earth itself will be measured. In a 650 km orbit the values of the two effects predicted by the Einstein theory are 6.6 arc/sec/yr and 0.042 arc/sec/yr, respectively.

In early 1984 NASA, in response to statements of support from several eminent scientists, through the Office of Space Science and Applications directed MSFC and Stanford University to develop and present a plan for the engineering development of Gravity Probe-B. The approach outlined in this plan is to build a Shuttle Test Unit for flight on the Shuttle and a similar test unit for additional tests on the ground. The Shuttle Test Unit will consist of a full-scale flight dewar and an instrument with support electronics. The instrument will have four gyroscopes mounted in a quartz block and enclosed in a probe assembly which slides into the dewar (Figure 10). Extensive operational and performance checks will be made on the gyroscopes as they fly on an approximate seven-day Shuttle Mission.

Certain portions of the Gravity Probe-B instrument, in particular the reference telescope and fine pointing system, cannot be fully evaluated with the Shuttle Test Unit. For this and other reasons a separate Ground Test Unit with a probe assembly essentially identical to that of the Shuttle Test Unit will be developed and tested on Earth in an inexpensive laboratory dewar. In addition, the Ground Test Unit will incorporate the telescope and fine pointing system.

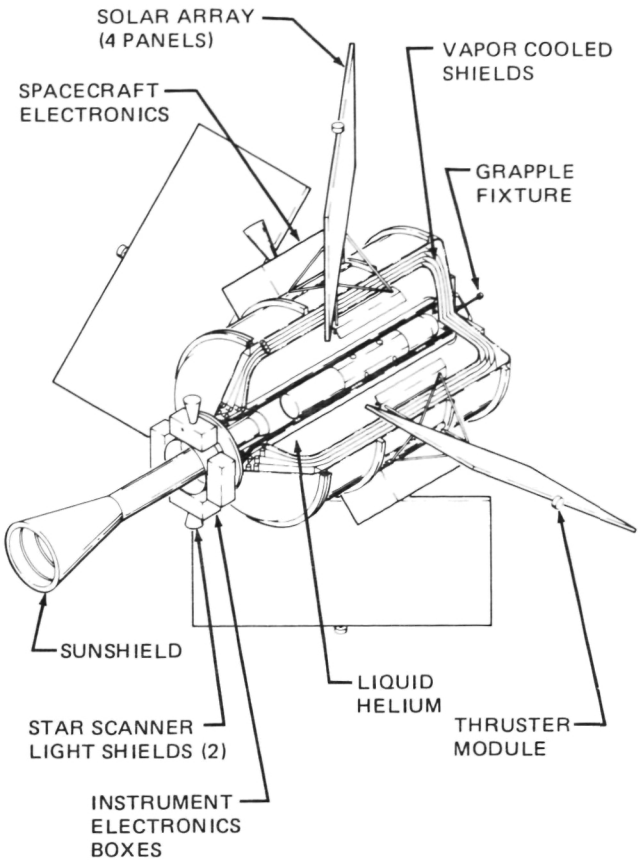

Figure 10. Gravity Probe-B.

The design, building, and testing of these two units, coupled with analytical activities, should provide the experience, knowledge, and insight necessary to assure a successful science mission that can be accomplished with reduced risks. A contract with Stanford for this development activity was signed on March 29, 1985. The planning and scheduling for the engineering development effort will support a science mission starting in 1989.

The dewar was delivered and acceptance testing was completed. Two important tests were made. First, the alignment of the dewar center line relative to the spin axis was measured. The requirement is that these two axes be within one degree or better. The measurements demonstrated that the angle between these two axes is seven minutes of arc.

Second, helium boil-off measurements were made to confirm the test values reported by the dewar manufacturer. After achieving equilibrium, the helium boil-off rate reached five liters/day. This is two liters/day below the guaranteed seven liters/day.

A rough design of the Quartz Block Assembly and inner actuator was produced and analyzed using a finite element model for stress and strain during launch and on-orbit. An important initial result is that the maximum tensional stress level in the quartz is about 250 psi. This should result in an adequate design margin based on the expected tensile strength of quartz (not less than 1500 psi).

Current research involves the creation of $\sim 10^{-7}$ G magnetic field at the first gyro in a 9 in diameter lead bag, and the design of the quartz housing and quartz block to minimize their sizes while satisfying the magnetic shielding and spin-up requirements on the gyro rotors. Other areas of research include the analysis and design of the necks of the dewar and the probe to facilitate integration and to satisfy the requirement to allow the experiment to be immersed in liquid helium while achieving low heat leak and assuring adequate dewar life as well as to test a single gyro in a tilting, rotating dewar to demonstrate the ability to accurately predict and analyze the drift of the gyroscope.

A. K. Neighbors/PF16
(205) 453-5584
Sponsor: OSSA

Pinhole Occulter Facility

The Pinhole Occulter Facility (POF), which will eventually become part of the Space Station or an associated facility, is an observatory imaging the Sun and celestial objects in hard x-rays and observing the solar corona in visible and ultraviolet wavelengths. A 32 m deployable boom will position an occulting mask between the solar instruments and the solar disk. The solar corona around the edge of the disk will be observed utilizing the coronal imaging instrumentation while multiple aperture imaging systems make possible the obser-

vation of the hard x-ray activity of the Sun. The Instrument Pointing System (IPS) positions and stabilizes the imaging systems, occulting mask, and deployable boom. The system can be used to form high resolution images of celestial objects in much higher energies than has previously been possible (Figure 11).

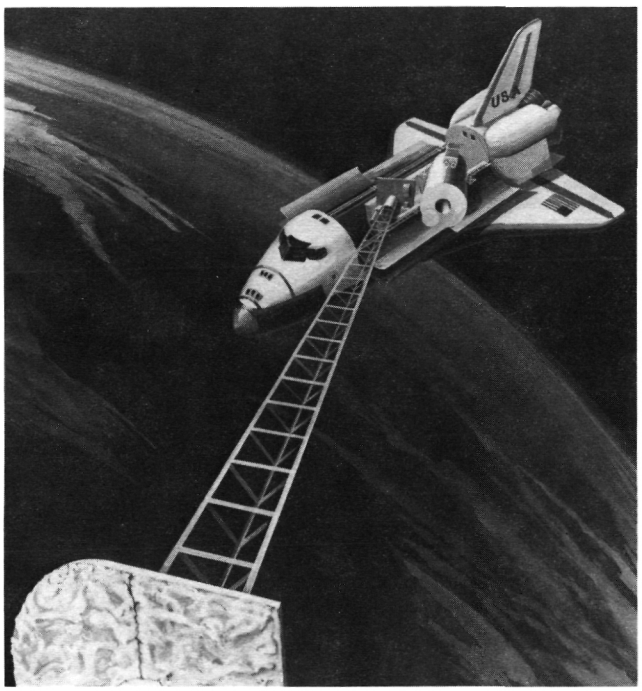

Figure 11. Pinhole Occulter Facility.

A feasibility study was concluded and documented in 1984. Since then, a science workshop was held in the spring of 1985 and drew wide participation from the solar science community. Documentation of this effort will be completed by fall of 1985. Engineering efforts have verified the controllability of the boom, and current studies are directed toward developing implementation of the control laws previously developed. In addition, studies are underway to define experimental requirements necessary for integration with the Spacelab.

Joseph R. Dabbs/PS02
(205) 453-3430
Sponsor: OSSA

Advanced Solar Observatory

The Advanced Solar Observatory (ASO) is an integrated array of instruments capable of observing the complete electromagnetic emission spectrum of the Sun. It consists of a Solar High Resolution Telescope Cluster, a Solar Low Frequency Radio Facility, a Solar High Energy Facility, and a Pinhole/Occulter Facility (Figure 12). There are several reasons for studying the Sun in such depth. First, it is the only star which can be examined in sufficient detail to allow stellar phenomena to be studied at the level of basic atomic physics, nuclear

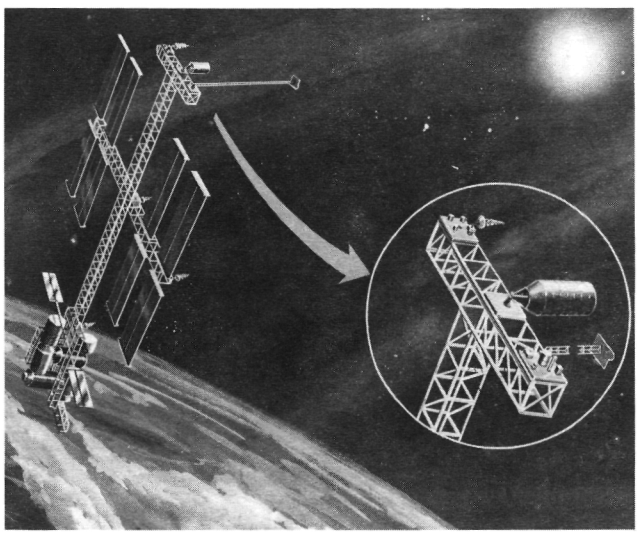

Figure 12. Advanced Solar Observatory on the Space Station.

physics, plasma physics, and magnetohydrodynamic processes underlying these phenomena. Second, the Sun is the predominant factor in shaping the interplanetary space within the solar system. The interaction of the heliosphere with planetary magnetospheres, ionospheres, and atmospheres form the discipline of space physics. Finally, the Sun has a profound influence on the Earth's ecosphere, and therefore on humanity. The Advanced Solar Observatory will fly in component form on the Space Shuttle evolving eventually into a long-duration Space Station.

Studies have revealed several technology areas associated with the implementation of

ORIGINAL PAGE IS
OF POOR QUALITY

the ASO which need to be addressed. These include the development of a pointing system capable of both arc/second pointing and the thermal dissipation of several kilowatts of power. Large quantities of data (~50 mbps) will also be generated for display on the manned Space Station and on the ground. These technology areas are being addressed as a part of the planning and definition process leading to the implementation of the ASO.

Walker, A. B.: A Golden Age for Solar Physics. Physics Today, November 1982.

William T. Roberts/PS02
(205) 453 – 3430
Sponsor: OSSA and Space Station

Solar Terrestrial Observatory

The Solar Terrestrial Observatory (STO) is a combination of scientific instruments which provide information about the physical processes of solar terrestrial space. At this time the role of these processes in the variability of the solar terrestrial system is poorly understood. Although we have superficial knowledge of many relationships between the Sun, interplanetary space, the Earth's magnetosphere, and atmosphere, we have an incomplete understanding of the actual physical and chemical processes that underlie these relationships. This lack of understanding precludes a reliable predictive capability. The STO will be able to make unique measurements that will contribute an adequate understanding of many of these processes.

The Solar Terrestrial Observatory (Figure 13) will be a major payload for the Space Station (or Space Platform) and initially will use instruments originally built for, and flown on, Shuttle/Spacelab missions. These missions will be used to establish basic instrument and experiment techniques and capabilities.

A mini – workshop on STO was held this year in conjunction with the SESAC Task Force on Scientific Uses of Space Station. The workshop reiterated the need for flying an STO

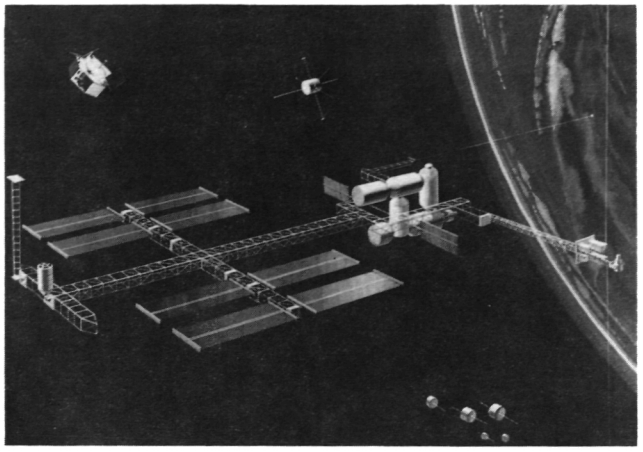

Figure 13. Solar Terrestrial Observatory on the Space Station.

on the initial Space Station, and defined the requirements for an evolutionary STO program, using the existing inventory of Spacelab experiments. The output of this study was also used to define the requirements for a study which has been initiated on the definition of requirements for typical solar terrestrial instruments on the early Space station.

Technological issues to be addressed include the evolution of energy storage systems (or direct electrical power from the Space Station) to provide high power (~60 kW) for the periodic operation of active instruments, the effects of contamination on instruments, the dynamic effects of the deployed tether, and the orientation requirements of microgravity experiments. Since the initial STO will consist mainly of instruments originally developed for Shuttle/Spacelab missions, the primary requirement is to develop a technological bridge across which this transition to the Space Station can move.

William T. Roberts/PS02
(205) 453 – 3430
Sponsor: OSSA

Extending Very Long Baseline Interferometry to Space

Very Long Baseline Interferometry (VLBI) will provide astronomers with their highest – resolution look at the universe. By combining

the output of two radio astronomy antennas thousands of kilometers apart, angular resolution of one-thousandth of an arc/second or better is obtained. Current VLBI observations are limited in resolution by the largest antenna-to-antenna separation available (one Earth diameter) and in their information content by small numbers of antennas in use at one time. Extension of VLBI techniques to include one or more antennas in space will relieve both of these constraints and result in marked improvement in our ability to map distant radio sources at the highest resolution. The rapid movement of the space antenna around the Earth yields a space antenna-ground antenna separation with wide range and rapid change capacity, resulting in a much more complete map of each source.

In March 1981 an opportunity to participate in a proposed large antenna Shuttle demonstration prompted the Office of Space Science and Applications to appoint a Technical Working Group to aid MSFC in the design of a VLBI experiment within the Deployable Antenna Program. The VLBI experiment was part of an engineering flight test and measurement program to evaluate and demonstrate a large aperture antenna in space. In March 1985 the VLBI science working group sent NASA Headquarters a favorable recommendation for a Shuttle-attached experiment using a 15 m model.

Future VLBI missions will be international in scope. The working group has met with scientists from the European Space Agency (ESA) to develop a joint European and U.S. VLBI mission. One concept being pursued is Quasat. It is based on a joint U.S./ESA proposal to fly a 14 m to 25 m antenna in a 15,000 km apogee orbit.

A 15 m antenna was built and tested under The Office of Aeronautics and Space Technology Development Program. Deployment tests were completed in March 1985. Although the antenna was a ground-test version, it was constructed of flight-type materials. To bring the antenna up to full flight quality will require retrofit of the deployment drive motors, addition of flight-quality lubricants, addition of thermal control blankets, qualification tests, and the rework of the reflector surface to meet the VLBI reflector geometry. Radio frequency tests in the Martin Marietta Near Field Facilities were also successful this year.

The proposed orbital VLBI experiment test to be flown on the Shuttle will provide a significant test of space antenna technology, aid in the development of the Quasat antenna and instrumentation, provide a demonstration of space-based VLBI operation, and contribute to the understanding of active galactic nuclei, quasars and interstellar masers. The deployment of a 15 m diameter antenna will be a significant test of antenna technology, especially if it is operated at or near K-band. Areas of interest include the accuracy of deployment, the stability over time of the antenna, and the integrity of the support structure and mesh. Of particular importance is a test of the thermal distortions of the support structure and surface in a space environment. Study efforts at MSFC are continuing to concentrate on a cooperative venture with Langley Research Center to modify the 15 m Hoop-Column antenna developed as a ground-test version by the Harris Corporation.

Burke, B. F.: Radio Telescopes Bigger Than Earth. Astronautics and Aeronautics, 70, 10, p. 44, October, 1982.

Morgan, Samuel H. and Roberts, David H.: Shuttle VLBI Experiment: Technical Working Group Summary Report. NASA TM-82491, July, 1982.

Roberts, D. H., Morgan, S. H., Burke, B. F., Jordan, J. F., Preston, R. A. and Hamilton, E. C.: SPIE Conference Proceedings: The National Symposium and Workshop on Optical Platforms. Huntsville, AL, 1984.

S. Morgan/PS02
(205) 453-3430
Sponsor: OSSA

ORIGINAL PAGE IS
OF POOR QUALITY

Deployable Antenna Flight Experiment

The Deployable Antenna Demonstration (Figure 14) is an engineering flight test on the Space Shuttle to evaluate and demonstrate space antenna performance capabilities which are essential to building future large communications satellites and Earth monitoring systems. Large antennas may eventually be used in geosynchronous orbit, with each antenna system efficiently replacing several small satellites. Flight definition, planning, and antenna test article evaluation continue at MSFC in conjunction with technology efforts at other NASA centers and other Government agencies. The Deployable Antenna Test Program addresses configuration and performance capabilities for space application of microwave radiometry, multibeam communications, spaceborne radar, and radio astronomy.

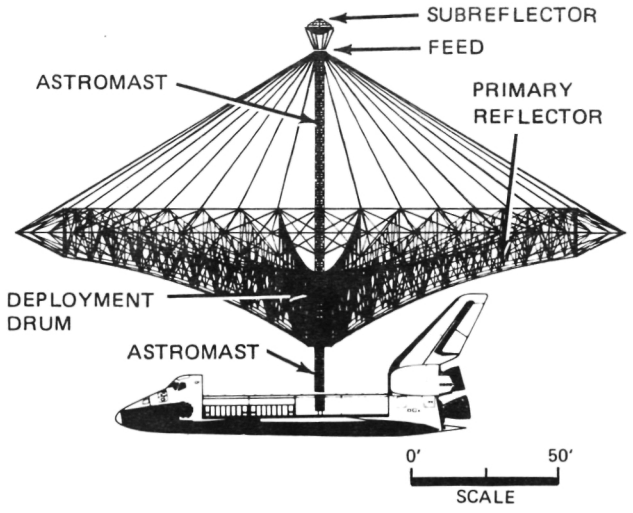

Figure 14. Deployable Antenna Flight Experiment.

Candidate test articles have sizes ranging from 10 m to 50 m, and all designs utilize lightweight precision structure to support development of high precision, high gain antennas. Baseline configurations proposed for development are a generic structure with provisions to accommodate either mesh reflector apertures or phased array membranes for varied mission requirements.

Currently, antenna test articles are being designed for structural ground tests and a subsequent flight test. On-going test article designs are based on recently developed radiating membrane configurations with enhanced performance capabilities. Initial flight testing is currently targeted in 1988 with objectives to measure structural dynamics and antenna performance in the orbital environment.

Wilbur E. Thompson/PS04
(205) 453-2792
Sponsor: NASA and OSF

Space Based Ultraviolet/Optical Phased Arrays

Advanced ultraviolet/optical telescopes of the future must provide increased resolution and larger light collecting area. Increasing telescope performance by simply scaling conventional telescope configurations has reached its limit with the Space Telescope's 2.4 m diameter monolithic mirror on one hand and the largest conventional ground-based telescope in the free world, the 4.5 m diameter Hale Telescope, on the other. Of all new design concepts, the segmented mirror (Figure 15) and phased array telescopes have attracted the most attention.

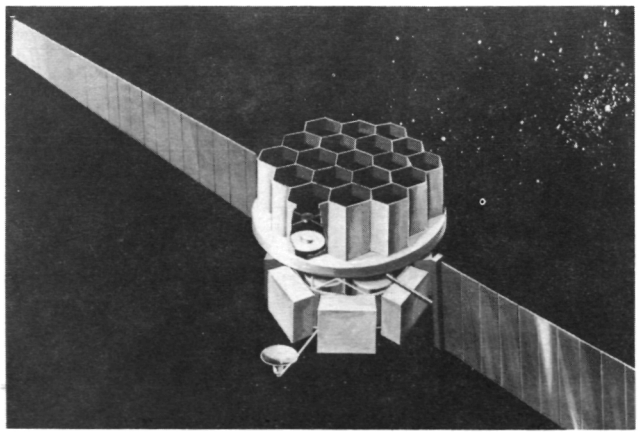

Figure 15. Modular Multi-Mirror Telescope.

The key to high angular resolution is that light remains coherent over large distances. Diffraction-limited performance of an array of

telescopes requires coherence of all participating wavefronts. Such a method has been used successfully to study radio sources at very high resolution (0.001 arc/sec) by using data from simultaneously observing radio telescopes on baselines stretching over the diameter of the Earth. Theoretically, the same resolution can be achieved at optical wavelengths by devices one hunbdred thousand times smaller in scale; however, the beams from the individual optical telescopes must be phased and combined coherently before detection. In radio telescopes the beams can be combined after detection since the longer radio wavelengths allow precise time tagging of the incoming wavefronts at each telescope. As a consequence, optical phased arrays depend on maintaining the optical path lengths to extreme precisions on the order of one-tenth to one-hundredth of a wavelength (typically 3 to 10 parts per billion). To achieve such high performance most economically, unconventional aperture shapes such as elongated, partially filled apertures, and minimum redundant mirror spacings mimicking circular apertures are being investigated as potential space telescopes of the future.

Despite the high degree of complexity, the phased array telescopes have definite advantages which warrant further investigation. For instance, the linear arrangement which is possible is particularly suitable for storage in the Shuttle Payload Bay. Other designs provide short distances between primary and secondary mirrors and reduce the mass moments of inertia, resulting in lower control torque requirements which improve pointing and slewing capability.

The previously studied Coherent Optical System of Modular Imaging Collectors (COSMIC) concept is a large linear array. The initial array contains four afocal interferometric telescopes with a beam combining telescope at one end. A major disadvantage of this concept is the fact that the array must rotate slowly in space to build up a uniformly good image. Figure 16 shows a concept consisting of nine afocal telescopes spaced in a particular

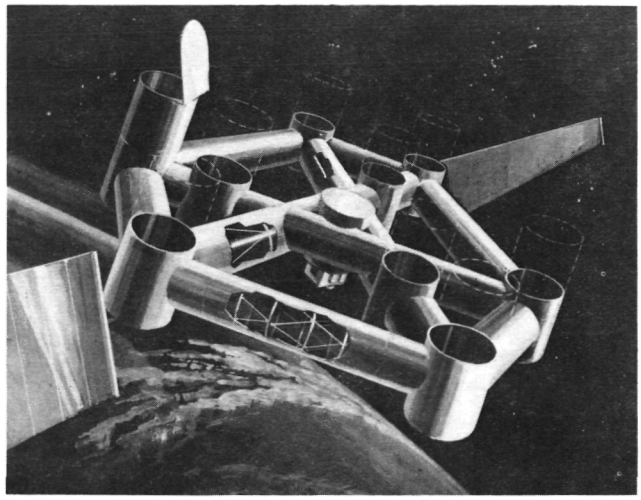

Figure 16. "Golay 9" Coherent Array.

arrangement to optimize sampling of the spatial frequencies while approaching a circular overall aperture that does not require rotation of the array.

In 1980 an in-house study of different concepts for phased arrays was initiated to investigate various telescope configurations and launch options. In June of 1984 a study was initiated to assess the technology requirements for creating realistic telescope designs with major focus on the optical concepts and technology which facilitate orbital assembly and maintenance. Results thus far indicate that the nonredundant, two-dimensional Golay patterns provide the widest spread of aperture that avoids zeros in the optical transfer functions, correspondingly giving the lowest noise gain among candidate multiple aperture arrangements. However, the problem associated with two-dimensional unfilled arrays having afocal telescopes is the very small field of view, a small number of reflections and therefore good UV throughput. The disadvantage is a very large outer structure on which to place the secondary mirror, making the overall telescope very long and thus difficult to assemble on-orbit. The large outer structure also makes it difficult to control the dimensional micrometer tolerances.

Davis, B. G., Korsch, D. and Nein, M. E.: Coherent Optical System of Modular Imaging Collectors (COSMIC): *An Approach for a Large Aperture*

High Angular Resolution Telescope in Space. SPIE Proceedings: Synthetic Aperture Systems, 440, 1984.

Max E. Nein/PS02
(205) 453 – 3430
Sponsor: OSSA

Tether Applications in Space

Tethers to be used in space are long, relatively thin, flexible cables which connect two or more masses moving together in parallel trajectories. The distance between the masses can be fixed or variable and the tether connections may be permanent or temporary, permitting the masses to be disconnected. Tethers may be conductive to carry electrical current or nonconductive for the transmission of loads.

Two new developments supporting tether applications are in progress at present funded by the Small Business Innovative Research Office. One involves a simple expendable tether payload deployment system. During 1985, hardware design and production were started and assembly and testing were begun. A prototype system will be available in 1987. This deployer is planned to be used for flight demonstrations of critical areas in the tether applications program. The other effort resulted in the development this year of a new type of conducting tether where the conducting metal is deposited on Kevlar filaments thus providing a unified, composite material with combined strength and conductivity characteristics. During 1986/87, we expect the development of a coating facility using the proprietary process for tether lengths up to 100 km.

Since the early 1970's, NASA has ventured into a number of space tether applications which make use of dynamic, static, and electrodynamic properties. Gravity – gradient and rotating tethers were tested and used during the Gemini Program. In the last decade more attention has been devoted to the tether concept and future applications may include using tethers for trolling satellites through the Earth's upper atmosphere, for power generation and orbit maintenance, and for communications and power links.

One of the presently studied applications is the insertion of spacecraft into orbit from the Shuttle Orbiter which transfers momentum from the Shuttle to the payload. This would send the payload into a higher altitude without additional expenditure of propellant. The Shuttle perigee will be reduced making it easier for the Shuttle to reenter the Earth's atmosphere.

Other applications where studies are in progress involve the tethered deployment of various space vehicles from the Space Station. The tethered deployment of an Orbiter from a Space Station would transfer angular momentum from the Orbiter to the Space Station accelerating the Station and decelerating the Orbiter. This would result in less orbit maintenance for the Station and considerable propellant savings for the Orbiter reentry (Figure 17 a and b).

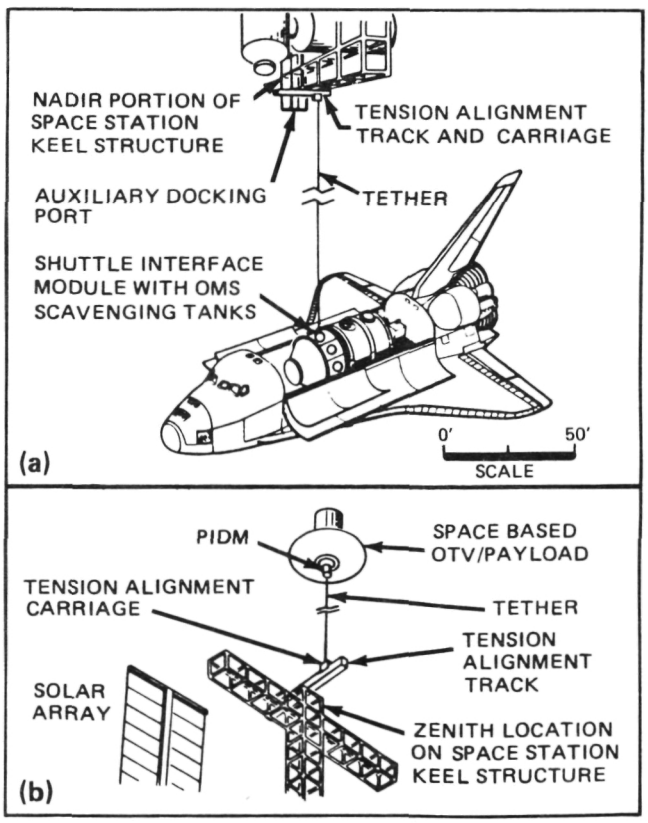

Figure 17. (a) Tether Deorbit of Shuttle from Space Station.
(b) OTV Tether Launch Assist.

In addition, under study at this time is the upward tethered launch of an Orbital Transfer Vehicle (OTV) from the Space Station which results in an increased OTV velocity and altitude and an associated increase in payload capacity or propellant savings. The resulting altitude loss of the Station would be made up during the next Orbiter deployment.

Present studies are also defining how the Space Station could be accompanied by tethered platforms. These platforms would require no guidance mechanisms, propulsion systems, and little maintenance. The tethers could provide direct data relay and could also serve as power and communication links.

During the next year a study will address the tethered deployment of small reentry capsules from the Space Station which would be a simple way to return materials processing or biological samples to Earth. This would make it unnecessary to wait for the next Orbiter flight.

An early Shuttle – based flight demonstration will be defined using an available reentry capsule.

The above concepts, and others mentioned, will be candidates for a detailed cost/benefit analysis during the next year. Required research and technology advancements have been derived from the studies and are listed in Table 1.

Georg von Tiesenhausen/PS01
(205) 453 – 2789
Sponsor: OSF and SBIR

Long Term Orbital Cryogenic Storage Facility

Long term, cryogenic, fluid storage facilities for periods of five years or longer will be required to support future programs in space such as the Space Station Orbital Transfer Vehicles

Table 1. Tether Research and Technology.

REQUIRED RESEARCH AND TECHNOLOGY ADVANCEMENTS HAVE BEEN DERIVED FROM THESE STUDIES AND INVOLVE:

A. TETHER MATERIALS AND CONFIGURATIONS
- MEASUREMENT AND CATALOGUING OF TETHER MATERIAL PROPERTIES
- TETHER PROTECTIVE COATINGS
- ELECTRODYNAMIC TETHER INSULATION
- ELECTRODYNAMIC TETHER CONDUCTORS
- ON-ORBIT TETHER REPAIR CONCEPTS
- HIGH STRENGTH TETHER CONFIGURATIONS

B. TETHER APPLICATIONS ENGINEERING INSTRUMENTATION
- TETHER DAMAGE DETECTION
- DEFINITION OF EXISTING INSTRUMENTATION CAPABILITIES
- DEFINITION OF ADDITIONAL NECESSARY FLIGHT DATA FOR:
  - MISSION CONTROL
  - POST FLIGHT PERFORMANCE ANALYSIS
  - MISSION DESIGN VERIFICATION
- DEVELOPMENT AND DEMONSTRATION OF INSTRUMENTATION SYSTEMS
- DEVELOPMENT AND TESTING OF HOLLOW CATHODES

C. TETHER SYSTEM DYNAMICS/ORBITAL MECHANICS SIMULATION:
- DEFINITION OF EXISTING CAPABILITIES OF SIMULATION PROGRAMS
- DEFINITION OF ADDITIONAL CAPABILITIES REQUIRED
- PROVISIONS FOR:
  - PROGRAM PORTABILITY
  - EASE OF USE
  - FLEXIBILITY
  - ECONOMY
- DEVELOPMENT OF REQUIRED PROGRAMS WITH AS UNIVERSAL AN APPLICATION AS ECONOMICALLY PRACTICAL

D. ATMOSPHERIC/AEROTHERMODYNAMIC TECHNOLOGY
- ANALYTICAL METHODS AND COMPUTATIONAL CODES DEVELOPMENT
- UPPER ATMOSPHERIC AEROTHERMODYNAMICS MODELING
  - STANDARDIZED DYNAMIC MODELING AND SIMULATION CAPABILITIES DEVELOPMENT

ORIGINAL PAGE IS
OF POOR QUALITY

(OTVs), Telescopes, and Laser Systems. Minimization of cryogenic boiloff/venting is mandatory to reduce system size and resupply requirements. Reduction of boiloff losses can be achieved by insulation, refrigeration and/or the reliquefaction of gases.

The recent approval of the NASA Space Station and the eventual space basing of a cryogenic OTV will require orbital storage of large quantities, >50,000 kg (>110,000 lb) of cryogenics. The capability to store large quantities of cryogenics in space for long periods of time will require thermally efficient systems to preclude excessive Earth-to-orbit resupply transportation costs. The loss of propellants stored in orbit must be minimized by using advanced insulation design concepts, low conductance structure, zero-g fluid acquisition/transfer hardware and refrigeration/reliquefaction systems. Prior to utilizing a cryogenic fluid storage/resupply facility at the Space Station or on another orbital facility, both advanced technology and verification testing will be required.

The verification program will consist of both ground and flight testing. The flight test program is envisioned as a potential precursor flight in the Space Transportation System (STS) Orbiter. The test article would be a subscale version of the orbital storage facility (Figure 18). The purpose of the test will be to establish the thermal performance of the design prior to utilizing the hardware in a technology demonstration mission on the Space Station with long term effects being determined by usage at the Space Station.

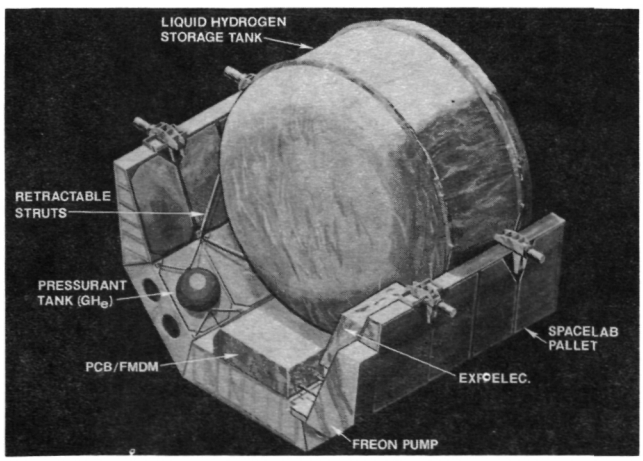

Figure 18. Orbital Cryogenic Storage Facility.

A preliminary study has analyzed a Liquid Oxygen/Liquid Hydrogen (LOX/LH_2) orbital storage system. The study concluded that a coupled tank design utilizing vapor cooled shields, in conjunction with a refrigeration system, with approximately 1.6 cm (4 in) of multilayer insulation appears to be a viable concept. The use of reliquefaction to control boiloff losses resulted in excessive power penalties. Fluid transfer losses of less than five percent per transfer were calculated.

A contracted system study is being conducted to examine orbital cryogenic storage systems for requirements, performance, and reasons for technological studies. The objectives are to conduct performance trade analysis, develop a technology plan, establish a test plan for ground/flight testing, and develop a conceptual design of the test article. It will investigate four basic systems: insulation plus vapor cooled shields (passive system), refrigeration, partial reliquefaction and total reliquefaction (nonventing). Based on the study results, a technology development test program will be established leading to a refrigeration/reliquefaction system supporting a space-based, cryogenic, liquid oxygen, and hydrogen storage facility. The detail design and development of a test article will be performed based on the results of the study. An orbital demonstration flight experiment will obtain data for development of design criteria for future long term cryogenic fluid storage facilities in space.

Uwe Hueter/PD22
(205) 453-4263
Sponsor: OSF

The Human Role in Space

Human abilities must be skillfully integrated with various types of automation in complex space systems to tap the full potential of each. This process of man/machine integration would

be challenging even if it took place in a static environment, but it does not. Space tasks are becoming routine, automation is burgeoning, and crew sizes are increasing. Missions are becoming longer, vehicles larger, mission complexity greater, and in coming years, both man and machine will be sent to distances in space that were previously inaccessible. Systems are usually complicated mixtures of humans and automated equipment, and since the space program is so dynamic, a means was needed to objectively evaluate man/machine systems.

In this context, The Human Role in Space (THURIS) Study has examined how to quantify and define appropriate roles for humans in space by analyzing representative future missions. Initially, the THURIS study organized and consolidated data on human capabilities and limitations, on task performance times, relative costs, and technology readiness to support man/machine analyses. The data were arranged so that complex scenarios could be described using 37 generic activities. For each of these activities, associated time, cost, and technological data were developed at seven automation levels so that various human roles could be compared, expressed in relative terms, and reduced to graphical formats to simplify analyses. Results of that effort are documented in comprehensive reports.

This year's work validates, refines, and extends THURIS techniques and data by applying them to mission elements that differ from the ones examined last year. Elements now under study include refueling an Orbital Maneuvering Vehicle, aerobrake replacement, vehicle assembly/disassembly, engine exchange, payload mating/demating for the Orbital Transfer Vehicle, and sample manipulation and product analysis in a space laboratory environment.

This year's validation effort involves several tasks. It includes assuring that the 37 generic activities, seven levels of automation, and eight categories of technological readiness are necessary, sufficient, and properly defined to analyze new missions. It involves checking the accuracy, consistency, accessibility, breadth of supporting data, and reviewing the overall man/machine allocation approach to assure that it is logical and that its results are relevant.

Last year, THURIS cost relationships and basic data were limited to Low-Earth Orbit Space Station applications. This established a firm conceptual framework using available data. This year's study extends the range of applications to include selected manned missions in geostationary orbit and expands the spectrum of automation to include robots.

In the process of analyzing new missions, this year's effort is also identifying equipment and procedures to enhance human roles in space. These are being reduced to a set of candidate ground-based and in-flight demonstrations. The results of the current study should be especially useful in the preliminary design phase of projects when man/machine tradeoffs are particularly difficult and the impact is far reaching.

Stephen B. Hall/PD24
(205) 453-4197
Sponsor: OSF

Experimental Geostationary Facility

Extensive conceptual study of Geostationary Facility concepts have been performed by NASA since the early 1970's. Recent conceptual studies concluded that a single Shuttle-launched Experimental Geostationary Facility is needed in the early 1990's to pave the way for future operational geostationary facilities. A representative experimental facility was defined which would demonstrate an integrated system of communications, Earth observations/data collection, science, and facility technology. Figure 19 portrays this experimental facility.

This year's studies have been jointly funded by OSSA and OSF. The Lewis Research Center, under OSSA sponsorship, has defined the communications experiments and mission scenarios, while MSFC, sponsored by OSF, is defining the Geostationary Bus and Facility.

ORIGINAL PAGE IS
OF POOR QUALITY

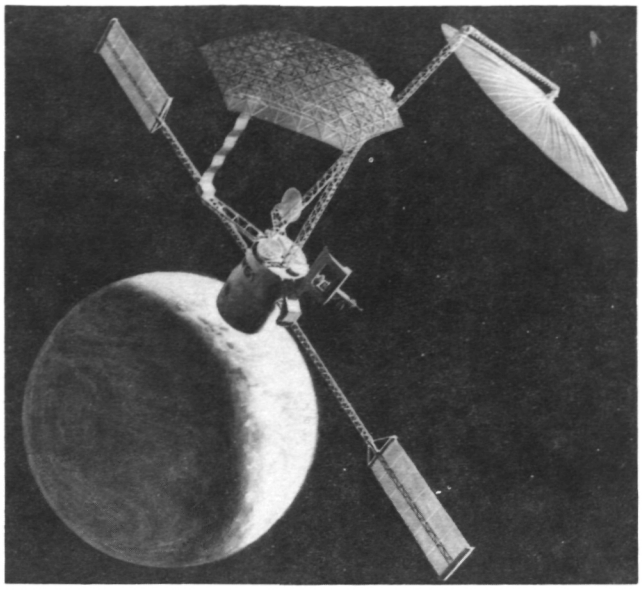

Figure 19. Geostationary Facility.

These studies are exploring the potential economic, technological, and insurability advantages to future operational facilities of utilizing the new Low Earth Orbit (LEO) Space Station for assembly/test/checkout, utilizing the new Orbital Transfer Vehicles (OTVs), and utilizing Geosynchronous Earth Orbit (GEO) versions of Orbital Maneuvering Vehicles for on-orbit servicing and reconfiguration. Also, the earlier conclusions regarding economy-of-scale benefits, practical limitations on frequency reuse through multibeams, feasibility of large-scale aggregation of services, and overall cost effectiveness of GEO facilities are being further examined and refined. Results to date have identified facility bus and payload configuration drivers (dry platform mass, number and diameter of antennas, payload thermal dissipation), servicing requirements, subsystem enabling technologies such as attitude control (ring laser gyro), electrical power (thin silicon solar cell), and how the Space Station can be used to deploy and service Geostationary Facilities.

Regardless of the final form the Experimental Geostationary Facility takes, the technology that will be demonstrated by such a platform includes deployable structures and structural mechanisms; active stabilization of large space structures; a high efficiency AC power system; LEO-to-GEO transfer of deployed structures; automated unmanned servicing at GEO; facility intermodule docking; an integrated attitude control system for docked facility modules; multibeam antennas; scanning beam antennas; accurate beam pointing; interfacility links; onboard communication switching and processing; a facility communications controller/processor; link performance enhancement techniques; effective isotropic radiated high power and small Earth station antennas; dual polarization Ka-band; and use of high-power, long-life, traveling-wave tube amplifiers.

Ramler, J. and Durrett R.: NASA's Geostationary Communications Platform Program., No. AIAA-84-0702, pp. 613-623 New York, 1984.

Robert H. Durrett/PS04
(205) 453-2792
Sponsor: OSF and OSSA

Manned Mars Mission

NASA's Marshall Space Flight Center has been involved in manned Mars mission planning since the 1960's, including several major studies with significant portions being done in-house. Current studies include "flyby" missions, Mars orbit, Mars landing, and missions to the moons of Mars. Investigation is underway into a Mars flight before 2000, and on more sophisticated later flights.

Practical opportunities for certain classes of missions occur only about every two years, with the delta velocity requirements varying significantly between some opportunities. Mission durations are a little greater than one year for "flyby", about two years (including approximately 60 days at Mars) for utilizing planetary opposition alignment, and about three years (including approximately one year stay at the planet) for utilizing planetary conjunction alignment.

Because of the long missions, physiological and psychological factors must be investigated thoroughly. The basic mechanisms of physiological degradation due to reduced or zero

gravity must be better understood, and the potential for reducing degradation by using diet supplements and/or exercise must be investigated. Alternative approaches, such as providing a gravity field as part of the space vehicle, could impose significant design constraints.

Current study activities have centered around an approach which assembles the space vehicle in a Low Earth Orbit (LEO) near the Space Station. Utilization of Space Station technology, designs, concepts, operations, and/or use of the actual flight hardware and operations appears to be possible.

For example, study results indicate that the Space Station – based OTV can contribute significantly by providing orbit transfer of the returned space vehicle to the Space Station orbit. OTV elements and technology can be used directly and/or provide support to the propulsion, propellant transfer/storage and aerobraking needs of the space vehicle. The Space Station OMV can be used to support the LEO assembly of space vehicle elements.

For earlier missions chemical propulsion with aerobraking appears to offer the most readily available capability. This year's studies have shown that the use of cryogenic propellants without aerobraking requires space vehicle weight between 1.5 to 3.5M lb or more, depending on mission type and year of launch. Use of aerobraking (Figure 20), however, can reduce the weight at the high end of the range to around 1.6M lb.

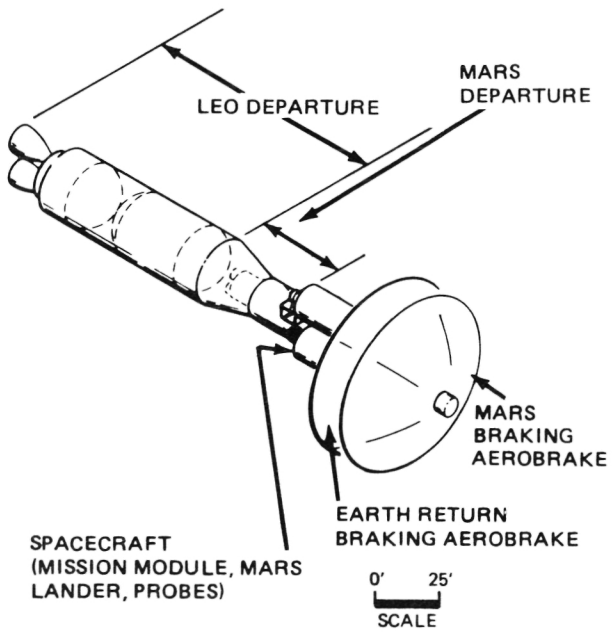

Figure 20. Manned Mars Vehicle Configuration.

Other suggested propulsion concepts are nuclear, electric, solar sail, and hybrids. These concepts for any vehicle propulsion option, a large chemical Earth – to – orbit propulsion capability must be available to launch the space vehicle elements to the assembly orbit. Such capability will be required for many other potential future space activities for both NASA and other government agencies, as well as Mars missions.

Table 2. Potential Areas of Technology/Advanced Development for Manned Mars Mission.

- LONG–DURATION SPACE FLIGHT EFFECTS ON HUMANS, & PREVENTIVE MEASURES
- LONG–DURATION CRYO STORAGE
- LONG LIFE SPACE SYSTEMS
- LIGHT–WEIGHT SPACE SYSTEMS
- OPTIMIZED TRAJECTORIES
- RADIATION EFFECTS & PROTECTIVE MEASURES
- REUSABLE PROPULSIVE VEHICLES
- ON–ORBIT ASSEMBLY
- AUTOMATION/AUTONOMY
- WAYS TO OFFSET/REIMBURSE COST OF SUSTAINED LUNAR/PLANETARY INVOLVEMENT
- ADVANCED PROPULSION SYSTEMS (SEPARATE FOR CARGO & HUMANS) INCLUDING NUCLEAR & LOW THRUST
- ADVANCED POWER SYSTEMS, INCLUDING NUCLEAR
- CLOSED–BIO–LOOP ENVIRONMENTAL CONTROL AND LIFE SUPPORT SYSTEM
- AEROBRAKING
- UTILIZATION OF SPACE STATION AND OTHER THEN–EXISTING CAPABILITIES, EQUIPMENT, OR CONCEPTS
- LONG–DISTANCE, HIGH–RATE COMMUNICATION SYSTEM
- ADVANCED SURFACE TRANSPORTATION VEHICLES
- ADVANCED SCIENCE CONCEPTS & EQUIPMENT
- ADVANCED EXTRAVEHICULAR ACTIVITY EQUIP–MENT

Development of Mars surface infrastructure elements offers challenges in a number of areas. For surface exploration a manned mobile laboratory will be needed. In situ resource production units are needed to produce such resources as propellants, fuel cell reactants, breathable gases, water, etc.. Long-term habitability, food production, construction, and manufacturing elements will be necessary for a more mature base on Mars.

The Mars surface phase is the most critical for electrical power provisioning. Here, reduced solar intensity, surface environment, and long night periods reduce the performance of photovoltaic and solar-thermal power systems, hence research is needed. Nuclear power concepts have more potential development and safety problems than solar systems; however, the possible benefits offered by nuclear systems warrant continued study.

Thermal control challenges on the Martian surface include heat rejection and long-term storage of cryogens in an unfavorable environment. Table 2 provides a partial list of applicable technology/development areas which have been identified as part of this year's study.

John Butler/PD24
(2305) 453-4195
Sponsor: OSF

Commercial Materials Processing in Space

Since the 1960's MSFC has conducted low-gravity processing experiments utilizing ground-based facilities and space flight opportunities. The advent of routine space flights via the Space Transportation System has opened up a new field, Commercial Materials Processing in Space (CMPS). In orbit, gravity levels far below ambient, can consistently be obtained so microgravity becomes a parameter that can be used to optimize materials processes similar to the way pressure and temperature parameters are routinely used to improve material properties here on Earth.

The CMPS program encompasses ground-based analyses, drop tower experiments, low-g ballistic aircraft flights, and space experiments. In addition, NASA has established policies and procedures for making business and legal arrangements with commercial firms and for providing technical assistance to their research and development work aimed at commercial applications of materials processing in space (Table 3).

For example, ground-based work on electronic materials indicates that weightlessness alters the fundamental interaction of heat flow, mass transport and fluid mechanics during crystallization. Early flight experiments in space tend to confirm these expectations and have led to commercial research and development aimed at producing, for example, improved gallium

Table 3. Current Applications of CMPS.

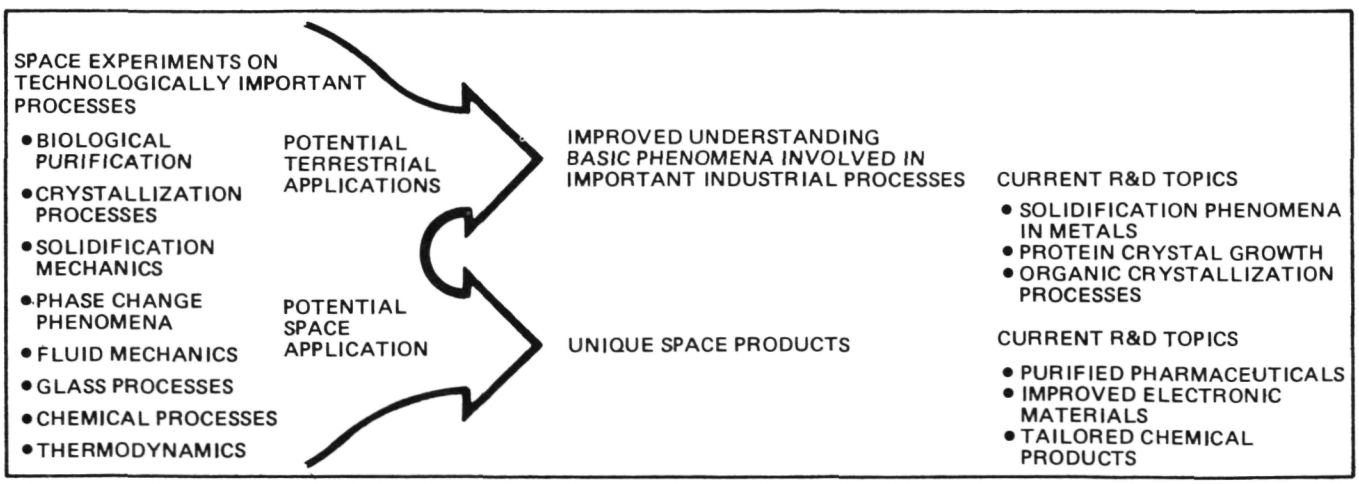

arsenide crystals, wafers, electro-optical crystals, and infrared sensors.

Another area of commercial interest is in the control of the solidification of metals and alloys which is basic to the entire field of metallurgy. Gravitational effects such as bouyancy-driven convection or sedimentation of various phases can greatly influence the macrostructure as well as the microstructure of metals and alloys. Currently, a group of basic metal industry users is forming a Metallic Alloys Research Consortium to do space research on basic solidification phenomena with the goal of improving their ground-based processes.

Fluids and transport phenomena are the common denominator of the wide spectrum of materials processing on Earth. The supply of material to the solidification process is controlled by heat and mass transport phenomena which are dominated by gravity-driven convection or sedimentation. Experiments in space simplify problems by eliminating the gravity-driven set of flows so the other phenomena can be isolated and analyzed. An aerospace company has developed an apparatus to accommodate fluid mechanics investigations in space. This device will be used in cooperation with other industrial research and development firms to study fluids phenomena involved in crystallization and other processes.

A number of biotechnology processes are adversely influenced by gravity effects. These include electrophoresis, isoelectric focusing, phase partitioning, suspension cell culturing, and crystallization of protein. In the case of electrophoresis, joint NASA-commercial work in space has shown large increases in both purity and through-put. Also, preliminary space experiments have already produced much larger protein crystals. Currently, ten non-NASA users have entered into joint agreement to grow protein crystals for medical applications.

Glasses and ceramics research typically takes advantage of the absence of gravity-driven convection and the ability to process samples without contact with a container. In space, materials can be heated, cooled, and manipulated while floating free of contact with container walls. Thus, deep undercooling is possible, corrosive materials are not contaminated by contact with containers, and surface tension tends to determine the shape of samples. Potential applications include novel glasses, fiber optics, laser optics, and fusion targets.

Research in space opens new opportunities for chemical processes. For example, seeded polymerization of latex has been used to grow monodisperse spheres that have become a commercial product. These spheres are sold as standards for calibration and are being considered for a range of biomedical applications.

MSFC's experience in low-g processing, is used in the development of Joint Endeavor Agreements (JEA's), Technical Exchange Agreements (TEA's), and Industrial Guest Investigator's Agreements (IGI's). This capability was instrumental in the development of JEA's with MDAC, 3M, MRA, OSC, and TEA's with Deere and Company, Inco, and Honeywell. This past year MSFC aided in the development and submission of JEA's proposals from Deere, General Motors, Rockwell, Grumman, Boeing, and ISC. Twelve companies and institutions have been added as IGI's to the Protein Crystal Growth Experimental Program (Upjohn, Smith, Kline & French, Schering, Burroughs-Wellcome, Merck, MDAC, Scripps Institute, Dept. of Navy, University of Pennsylvania, and University of Iowa). In the next two years between 10 to 15 companies are expected to sign JEA's, TEA's, or IGI's requiring MSFC participation.

MSFC continues to welcome the interest of CMPS investigators. The Agency has developed literature and a film which give prospective users technical data on materials processing in space and outlines how they can become involved. In addition, NASA has established groups at both NASA Headquarters and at NASA centers dedicated to working technical and business arrangements with commercial users.

Kenneth R. Taylor/PS05
(205) 453-3424
Sponsor: OCP

Research Programs

In conjunction with the many engineering responsibilities carried out by the Marshall Space Flight Center, and in order to support the many space missions managed at this Center, a strong research program has developed over the years. Scientists and engineers have striven to create the best possible environment for research in all areas of interest to MSFC. In so doing, the Center has developed expertise in the areas of Microgravity Science, Space Science, and Atmospheric Science.

In the 1970's, MSFC managed the Apollo Telescope Mount, which opened a new era in space observations. For example, the Center's instruments on Skylab provided new and exciting data on the x-ray Sun, which has given us a new picture of the high-energy, hot plasma of the solar atmosphere. In the early Spacelab flights of the 1980's, the Space Shuttle provided a novel form of space observatory and microgravity laboratory, and has supported a wide range of scientific investigations. For the future, MSFC scientists and engineers are designing and building experiments, both in situ and remote sensing instruments, to take full advantage of the exciting opportunities provided by continuing Shuttle and Spacelab flights and by the pending establishment of a Space Station.

Microgravity Sciences

Experiments on materials in low-gravity began with the Apollo lunar program. Several small "suitcase" experiments were added to the flight manifest of Apollo 14, 16, and 17 and were performed by the crew during the trans-Earth coast. Skylab offered the first opportunity to perform materials processing in a facility dedicated to that purpose. The Apollo-Soyuz Test Project (ASTP) offered the opportunity to fly several new experiments as well as refly several of the Skylab experiments. In general, the solidification and crystal growth experiments performed on Skylab and ASTP did not produce spectacular results, but did confirm that buoyancy-driven convective flows were sufficiently suppressed so that diffusion-controlled conditions could be approached.

The Shuttle Program provided the opportunity to resume extended experiments in a microgravity environment. The first materials processing experiments were performed in the mid-deck of STS-3 in March 1982. Several experiments have followed on Shuttle and Spacelab flights with exciting results. These flights have led to the first commercial product being produced in space using the Monodisperse Latex Reactor. The Shuttle/Spacelab program has provided the opportunity to fly the materials' experiment assembly, furnace experiments, levitation experiments, and bioprocessing experiments in space.

Crystal Growth and Characterization

Over the past several years, research has been conducted in the area of solid-solution semiconductors such as HgCdTe alloys. The purpose of these studies is to provide a data base in 1-g for comparison with low-gravity results to be obtained during space flight experimentation. Considerable progress has

been made in several areas of crystal growth and characterization including experimental and calculational efforts. Studies of ampule preparation and crystal quality show that graphitized ampules reduce nucleation of unwanted crystallographic grains at the ampule wall. Equipment to reproducibly graphitize ampules has been constructed and is being used to determine optimum graphitization parameters.

A thermal model of the Bridgman growth furnace has been enhanced to include radiation heat transfer and to predict shapes of interfaces produced by various furnace temperature profiles. The Advanced Automatic Directional Solidification Furnace (AADSF) has been used successfully to grow Ge and HgCdTe samples. Time constraints severely restricted the use of the contactless resistivity measurement apparatus during the past year. It has now been upgraded to provide improved signal-to-noise ratios, and measurements on HgCdTe alloys have been resumed.

Recently, a new effort was begun to cast HgCdTe alloys under a variety of conditions, including varying the angle with respect to gravity. A compositional map will be made for each ingot and the correlation between casting conditions and compositional distribution in 1-g will be determined. At the same time, a numerical model will be developed to predict the compositional distribution in an ingot. The empirical results and the model will be used together to choose additional Earth-based casting experiments and to provide a basis for making castings in space.

A Fourier Transform Spectrometer (FTS) was installed and operated regularly during 1985. During fiscal year 1985, its principal application was the compositional mapping of HgCdTe wafers and detection of impurity energy bands in the bandgap of HgCdTe. This capability is being used in the analysis of Bridgman crystals and cast ingots. Impurity detection depends on the subsequent installation of a closed-cycle helium refrigerator.

Sandor L. Lehoczky/ES72
(205) 453-3090
Sponsor: OSSA

ORIGINAL PAGE IS
OF POOR QUALITY

Metal Model Material for Modeling Low-Gravity Solidification of Alloys

A metal model material (ammonium chloride) is being investigated for simulation of the solidification of alloys in a low-gravity (approximately 0.01 g) environment. Previous investigations of the effect of gravity on microstructure for both binaries (Sn-Pb, Sn-Bi, Al-Cu) and more complex alloys such as MAR-M246 (Hf) have shown a correlation between the gravity level and the spacing of primary and secondary dendrite arms. The metal model material used in this investigation has also demonstrated similar variations in both ground-based experiments and low-gravity experiments.

The application of long periods of low gravity on the solidification processing of materials requires extensive experimental setup for containment of high temperature (molten) alloys. Preliminary prediction of anticipated growth parameter variation can be used in experimental design applications and may also serve as a screening process for selection of materials for study on the Space Shuttle and Space Station. A series of experiments is being conducted on NASA's KC-135 aircraft. This aircraft flies a

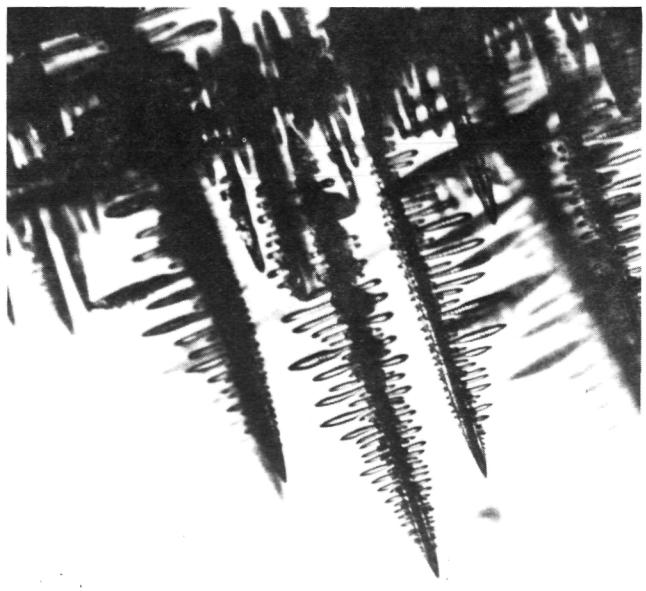

Figure 21. 35 mm Photograph of Dendrites Grown in Zero Gravity (80X).

series of parabolic maneuvers during which the experiment is subjected to both low and high gravity periods.

Four flights of this experimental package have been completed in fiscal year 1985 and five are projected for 1986. Preliminary analysis of the video tapes and still photographs indicates an increase in both primary and secondary dendrite arm spacings with a decrease in gravity (Figure 21). These spacings are being correlated with results from previous studies of metal alloys. An accurate top growth rate and profile will be determined from modifications to be used in experiments planned for fiscal year 1986.

David Hamilton/EH22
(205) 453 – 5513
Sponsor: OSSA

Model Immiscible Systems

Metal alloys are formed from elements that are generally not miscible, nor soluble, in the liquid state. The study of transparent immiscible systems is important to evaluate the properties of metal alloys which are opaque. Several experiments on the succinonitrile – water system provide compelling evidence that preferential wetting and thermal migration are important effects governing distribution in a miscibility gap type system. After liquid nitrogen quenching of "neutrally buoyant" succinonitrile – rich solutions, second phase droplet migration due to interfacial tension gradients drives the minority phase along the thermal gradient toward the hottest region which in these experiments is away from the crucible wall.

Droplet migration rate is largely dependent on droplet size. A complete understanding of factors which determine particle size and number distribution requires an understanding of the Ostwald ripening mechanism. During the precipitation or formation of the secondary phase from a parent phase, under isothermal conditions and in the absence of external forces, the size distribution of droplets of the precipitating phase grows to reduce the surface contact between the two phases with a definite time dependence. The growth rate depends on the degree of precipitating solution saturation. Growth occurs by gradual solvation of small droplets into the matrix and diffusion out of the matrix onto the larger droplets. The size distribution increases with time, initially fairly quickly, and trails off as solution saturation drops. The end result is a lower interfacial area between the phases.

A mathematical development of diffusion – controlled droplet growth by Lifshitz, Seyozov, and Wagner (LSW), is capable of handling only very small secondary phase volume fractions. One important technical objective is to modify the rate equation for droplet growth to account for larger volume fractions by considering interactions of neighboring precipitants. During this reporting period, the rate equation has been extended to include a minority phase volume fraction square root influence on droplet growth rate. Determination of higher order terms is in progress by James K. Baird, at the University of Alabama in Huntsville.

Witherow, W. K. and Facemire, B. R.: Optical Studies of a Binary Miscibility Gap System. Journal of Colloid and Interface Science, 104(1), pp. 185 – 192, 1985.

Donald Frazier/ES73
(205) 453 – 3090
Sponsor: OSSA and CDDF

Solution Crystal Growth

A research effort is being carried out on the study of solution crystal growth with emphasis on the low – gravity environment of an orbiting spacecraft. This study centers around the growth of single crystals of triglycine sulfate (TGS) and includes the development of the Fluids Experiment System (FES). Both a ground – based laboratory effort and the development of a flight experiment are included.

Triglycine sulfate $(NH_2CH_2COOH)_3$ (H_2SO_4) is ferroelectric with a Curie temperature of 49°C.

It is of interest for both its basic scientific properties and for its application as an infrared detector. Its optical, thermal, transport, electrical, and crystallographic properties are under study. The values derived from these studies are used to mathematically model the crystal growth in a low-gravity environment.

A flight experiment was designed, developed, and carried out on Spacelab 3. The objectives for this experiment were to develop a technique for solution crystal growth in a low-g environment, to characterize the growth environment provided by low-g, to determine environmental effects on growth behavior, and to determine how a low-g environment influences the properties of a resulting TGS crystal. Two TGS crystals were successfully grown and hundreds of holograms taken during the execution of this experiment in the FES (Figure 22) on Spacelab 3. The crystals will undergo a series of characterization measurements to determine the effects of low-g environment on their growth. The holograms will be used to study growth process dynamics by constructing schlieren, shadowgraph, and interferometric images of the interaction of the solution with the growing crystal.

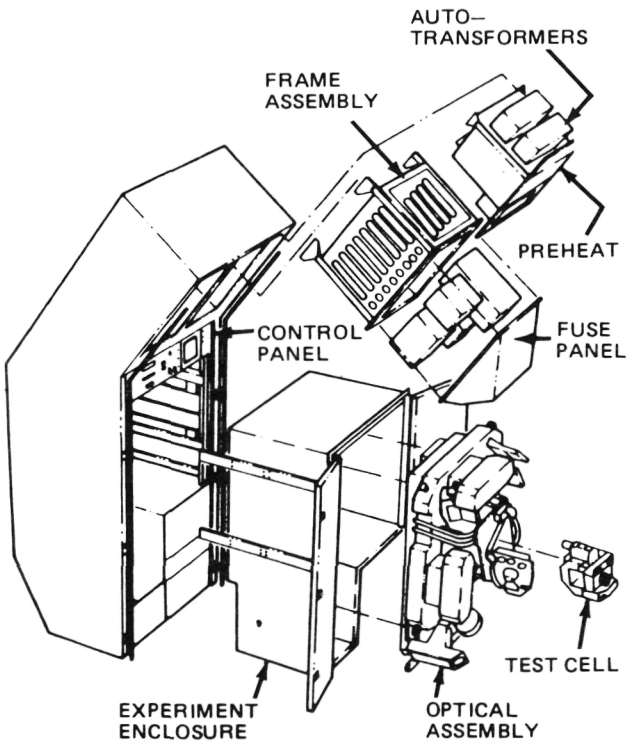

Figure 22. FES Rack – Assembly.

The studies are part of a continuing effort in which other crystalline materials will be studied as well as new, improved techniques developed and applied to future flight experiments.

Kroes, R. L. and Reiss, D. A.: Properties of TGS Aqueous Solution for Crystal Growth. Journal of Crystal Growth, 69, pp. 414-420, 1984.

Kroes, R. L., Reiss, D. A., Silberman, E. and Morgan, S. H.: Diffusion of TGS in Aqueous Solution. Journal of Physical Chemistry, 89, pp. 1657-1658, 1985.

Roger L. Kroes/ES72
(205) 453-0183
Sponsor: OSSA

Advanced Furnace Technology for Materials Processing in Space

In investigating the problems of lasers to melt and zone refine semiconductors or metal crystals, emphasis was placed on techniques to control and maximize the absorption of laser power into the sample. Advanced furnaces for material processing in space will require unusual temperatures, temperature gradients, and zone profiles. The main feature of using laser beams to generate and control the gradients around the melt zones is the high degree of control. The beam can be focused on a small area; it can be rapidly scanned to a new location; and the gradients can be controlled by beam shaping or scan dwell time.

An experimental work station was designed for investigating the effects of scanning a laser beam on a variety of samples. A variable power carbon dioxide laser was selected because of the high efficiency and low cost. The selected laser can range between 10 and 85 W. A rapid scan system moves the focused laser beam to generate a narrow melt zone and a precision stepper motor moves the melt zone along the crystal. The hardware is under

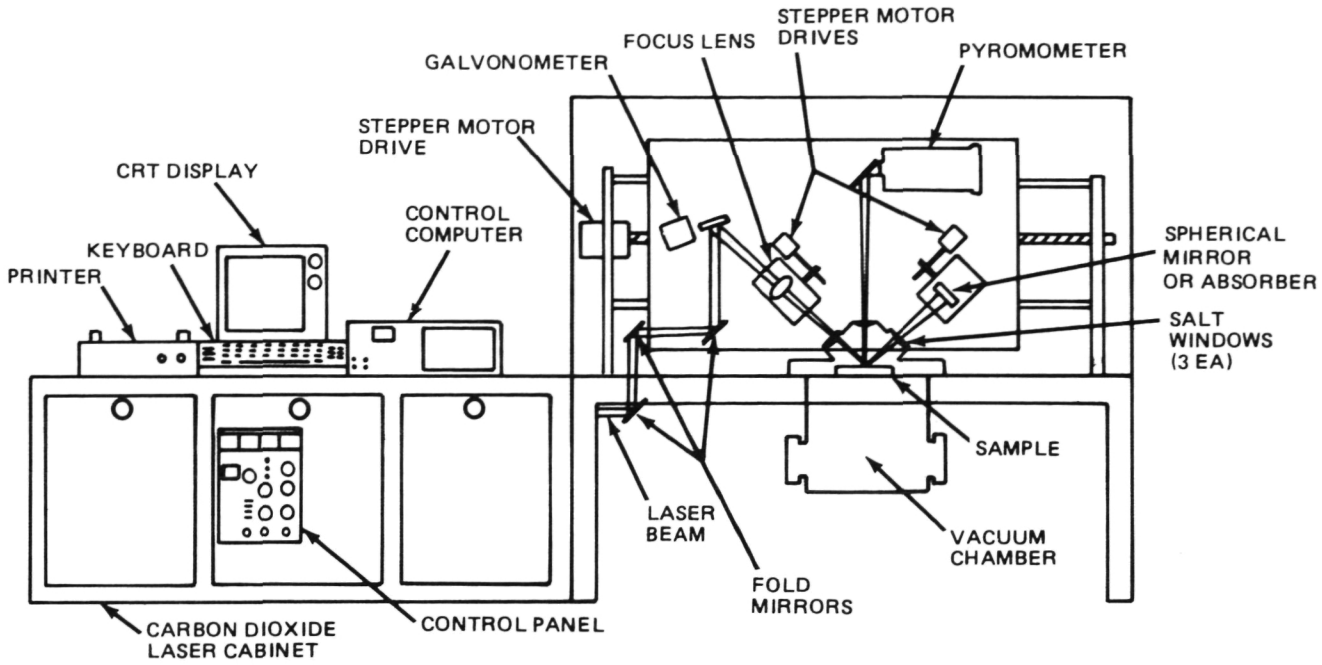

Figure 23. Schematic of Laser Furnace.

computer control to allow flexibility in experimentation. The use of lasers is growing, and melting semiconductors crystals is new and shows exciting promise. Characteristics required to produce well-controlled temperature gradients and melt zones (Figure 23) define the power, scan dwell time, and beam angle of incidence.

Experiments have been performed on silicon and a nickel-based superalloy labeled MAR-M-246. Melt zones were generated in silicon at a laser power setting of just under 50 W. The laser did not have enough power to melt the nickel crystal. The largest use now is in the growth of silicon ribbons and annealing of wafer surfaces.

D. B. Griner/EB23
(205) 453-4700
Sponsor: CDDF

Low-G Solidification of Alloys

Commercial alloys are often complex, empirically derived, multi-component systems. The influence of buoyancy phenomena during solidification on final microstructure and properties of these alloys is not known in most cases. Other alloy classes such as hypermonotectic alloys have not reached their potential for commercial exploitation because of sensitivity to gravity-induced inhomogeneities. Industry is often forced to restrict composition of additives to minimize buoyancy-driven segregation. Convectively stable solidification geometry is often dictated, but the complex geometry of commercial castings such as superalloy turbine blades can make convection stabilization infeasible. The intricate role of gravity during the solidification of complex alloys makes a vigorous Earth-based research program imperative before a space research effort is undertaken.

Cast iron and metal-carbon alloys, in general, are influenced greatly by gravity during their solidification. Since graphite is much less dense than liquid iron, the carbon content of cast iron has been limited to near eutectic composition because of graphite flotation. The effects of gravity on eutectic cell size, dendrite arm spacing, graphite nodule size, and lamellar spacing (in white iron) were unknown before this study. John Deere and Co., through a Technical Exchange Agreement, has been collaborating with NASA in aircraft flight solidification experiments with cast iron for several

years. These experiments involved quenching ingots of cast iron during a single KC – 135 or F – 104 aircraft flight parabola, producing 20 – 40 sec of low gravity. Because of difficulties in control and interpretation of these experiments, a directional solidification furnace was built to fly in the KC – 135 aircraft. The solidification interface can be moved through a cylindrical sample at a controlled rate. The sample can be directionally solidified by a sequence of low – gravity maneuvers. A longitudinal section of the sample can be correlated with accelerometer data, and alternating regions of low and high gravity can be identified on the sample. The effect on microstructure and composition of the gravity level during solidification can then be studied with relative ease. In collaboration with the University of Alabama, a vigorous study of iron – carbon alloys has been undertaken utilizing this furnace system. The experiments have shown that low – gravity solidification graphite flotation can be arrested, and that eutectic cell size, spacing of lamellae, dendrite arm spacing, and solidification interface stability are dependent on gravity level during solidification. These results have formed the basis for a Joint Endeavor Agreement (JEA) proposal to NASA by John Deere and Co. for cast iron solidification experiments in space.

Superalloys are another important class of commercial alloys that can be strongly influenced by buoyancy forces during solidification. Castings must be convectively stabilized to minimize defects and buoyancy considerations can be crucial in selection of additives. KC – 135 experiments with MAR – M 246 nickel – based superalloy have provided the first data on a low – gravity solidified superalloy (Figure 24). Secondary dendrite arm spacing increases with solidification time in low – gravity while the volume fraction of carbides decreases. The morphology and composition of carbides are also a function of gravity level during solidification. A study has begun of primary arm spacing using the single crystal Pratt and Whitney alloy PWA 1480.

Hypermonotectic alloys have not achieved their potential for commercial exploitation because

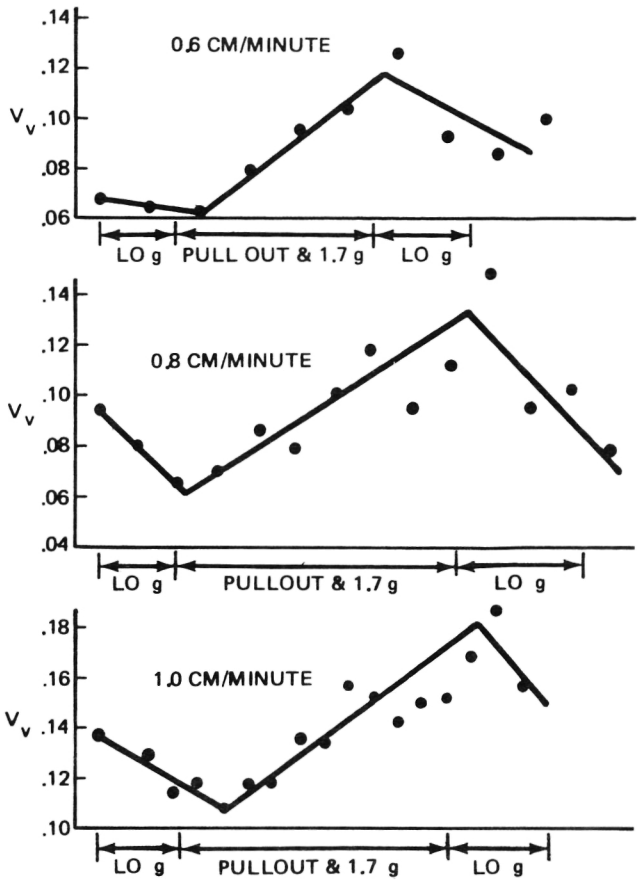

Figure 24. Volume Fraction Carbides.

of gravity – driven segregation of the two immiscible liquid phases during solidification. Experiments attempting to control hypermonotectic microstructure by solidification in low gravity have been unsuccessful due to lack of understanding of surface tension forces which become dominant in low gravity. The relatively routine access to low gravity offered by the KC – 135 system has allowed the study of a number of monotectic alloy compositions in the ternary Al – In – Sn system. It is believed that the addition of the third element, tin, to the aluminum – indium alloy changes the interfacial energy between the solidifying phases. The results of the KC – 135 experiments indicate that gravity level during solidification influences not only incorporation of immiscible phases into the solidification interface but also the alignment and morphology of the resulting microstructure.

Hendrix, J. C., Curreri, P. A. and Stefanescu, D. M.: Directional Solidification of Flake and

Spheroidal Graphite Cast Iron in Low and Normal Gravity Environment. Transactions of the American Foundryman's Society, 92, pp. 435 – 458, 1985.

Johnston, M. J., Curreri, P. A., et al.: Gravity Level Induced Microstructural Variations in a Directionally Solidified Superalloy. Met. Trans., September 1985.

P. A. Curreri/ES72
(205) 453 – 3090
Sponsor: OSSA and CDDF

Undercooling of Peritectics

Two facilities, a drop tube and a drop tower (Figure 25), are presently used at MSFC for low – gravity processing. The vertical stainless steel tube can either be evacuated at 10^{-6} torr or backfilled with an inert gas to enhance sample cooling. Samples are processed in a low – gravity, containerless environment by free falling the length (105 m) of the drop tube (0.25 m diameter) for 4.6 sec. Samples are melted prior to release by either an electron bombardment furnace or an electromagnetic levitator. The thermal history of the sample during melting as well as the brightness trace for each sample during free fall are recorded and stored by a digital data acquisition system and desk top computer. If the sample undercools during processing, it will be recorded by the brightness trace.

The drop tube effort is presently supporting approximately ten research projects. By far the most comprehensive study to date involves the undercooling of Nb and Nb – based alloys. Large degrees of undercooling were recorded and unique microstructures were found. The Nb – based effort is being updated to a space flight experiment.

Drop tower processing involves dropping a large drag shield along vertical rails with an air jet assist to overcome air drag and rail friction. Experimental packages are allowed to "float" within the draft shield for the 4.5 sec of low – gravity time. Data from the experiment are recorded by telemetry and onboard high – speed motion pictures. Currently the facility supports two research efforts with the University of

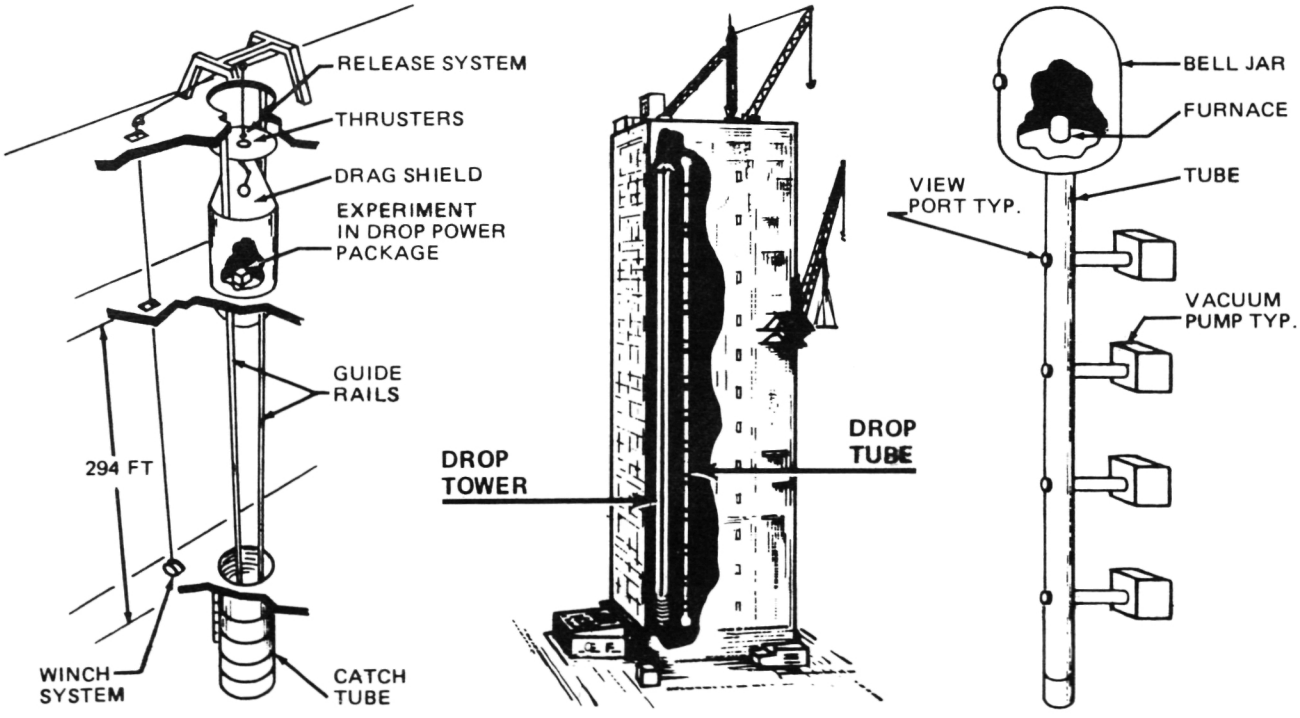

Figure 25. Low Gravity Free-Fall Facility.

Alabama in Huntsville (UAH). One effort involves critical point wetting in carbon tetrachloride, the perfluoro – methyl – cyclohexane; the other effort involves interface superconductors and immiscible metal alloy systems.

During the period covered by this report, samples were processed in a complete vacuum by the electromagnetic levitator. These samples undercooled during the complete length of the facility and solidified only after contact with the catcher. Completion of sample characterization of previously processed Nb – Ge alloys was also accomplished. Several publications and presentations have resulted.

Robinson, M. B. and Lacy, L. L.: High Temperature Containerless Calorimeter. Review of Scientific Instruments, 56(3), pp. 430 – 436, 1985.

Kaukler, W. F., Tcherneshoff, L. M. and Straits, S. R.: Critical Point Wetting Drop Tower Experiment. NASA CP – 2313, p. 306, February 1984.

Michael B. Robinson/ES72
(205) 453 – 2046
Sponsor: OSSA and CDDF

Study of the Reactive Element Effect on Oxidation

The addition of "reactive elements" such as Y, Ce, Th, Hf, or their oxides to alloys containing chrome greatly improves their high temperature oxidation behavior. In particular, a reduction in oxidation rate and an enhancement in adhesion of the passivating oxide are observed compared to the same alloys without "reactive element" additions. This so – called "reactive element" effect has been known for over 40 years, but despite intensive research efforts, the mechanisms of the effect remain largely unknown. It is the goal of this research to determine the mechanisms using low – g prepared samples and the technique of trans verse–section analytical electron microscopy.

It is very difficult to prepare alloys with oxide dispersions using the various techniques that have been attempted in the past. Melting and solidification of such alloys is unsuccessful because of the density difference between the oxide particles and the liquid metal. Agglomeration of the oxide particles is driven by differential Stokes settling. As a result, these types of studies have been abandoned.

In light of encouraging results obtained by the production of dispersions of ThO_2 in Mg and BeO in Be produced by microgravity melting and solidification, an experiment is underway to produce a uniform dispersion of reactive element oxide containing alloys in microgravity. The objective of this work is to prepare samples with a uniform dispersion of Y_2O_3 particles in Fe – 24Cr. The samples are to be utilized to perform oxidation experiments and mechanical tests to determine which of the current theories of the "reactive element" effect are applicable.

The approach is to process a number of samples with the best containerless processing techniques on Earth as controls to those produced in microgravity. Electromagnetic levitation melting and free fall solidification in the Marshall Space Flight Center Drop Tube Facility will establish the limit of Earth processing techniques. Preliminary results indicate that it is not possible to produce uniform dispersions by these techniques. This is due to the melt stirring in an agglomeration that occurs during the electromagnetic levitation melting prior to drop tube containerless low – gravity solidification. In order to produce uniform dispersions, it is necessary to melt as well as solidify the alloy in low gravity.

Future plans are to solidify two samples in an electromagnetic levitation furnace in the Space Shuttle. This appears to be the only possible way for alloys to be prepared for the critical experiments to establish the mechanisms for the "reactive element" effect.

King, W. E., Peterson, N. L. and Reddy, J. F.: Application of Transverse – Section Analytical Electron Microscopy to the Study of Oxidation of Metal Alloys. Proceedings of the 9th International Conference on Metallic Corrosion, 1984.

Edwin C. Ethridge/ES72
(205) 453 – 3917
Sponsor: OSSA and CDDF

Surface Film Effects on Drop Tube Undercooling Studies

A major emphasis of the Materials Processing in Space Program is the containerless processing and solidification of materials. It has been demonstrated that the absence of surface effects from containers during cooling allows bulk melts of some metals to be lowered far below the thermodynamic melting temperature prior to solidification. In other MSFC drop tube studies, molten Pd – Si – Cu has been successfully undercooled in bulk droplets to the glassy state. Alloys of Nb – Ge and Nb have been undercooled by 500°C and 525°C, respectively. Other drop materials such as Cu – Zr and Ni – Al do not seem to exhibit this tendency to undercool significantly. It is believed that surface oxidation plays a significant role in the heterogeneous nucleation. Drop tube experimentation offers the advantage of containerless solidification in the absence of certain nucleation effects so that the effect of surface films on nucleation can be examined.

The objectives of this study are to further develop and understand the role of surface effects during solidification of pure metals and alloys in the MSFC drop tube. This will aid the understanding of heterogeneous nucleation effects and allow optimum use of drop tubes to conduct undercooling studies of metals.

A computer program has been written and a number of oxide stability curves have been calculated using thermodynamic data. These calculations, using free energy of formation data for oxides, have been used to generate working curves to determine under various conditions of low oxygen partial pressures which oxides, if any, are stable. Other calculations include reducing gas agents (i.e., four percent hydrogen) which are effective for stripping surface oxides from some metals. A series of working curves have been drawn to aid potential drop tube users in predicting when surface reaction films are expected to form.

During fiscal year 1985 approximately 60 drop tube experiments were completed. Several elemental metals selected, based on the stability of their surface coatings, were melted and solidified. These include Cu, Pd, Ni, and Rh. The technique utilizes containerless electromagnetic levitation induction melting. After melting, the sample is dropped in free fall through a quench gas and solidifies containerlessly. Metallographic results indicate that samples which achieve large undercoolings result in single or bi – crystals. This is due to the presence of one nucleation event which completely crystallizes the sample prior to another nucleation event. The gaseous conditions for this to occur correspond to the theoretical expectations based upon the absence of surface oxide films. The sample is characteristically shiny with a smooth surface, i.e., no observable features under the scanning electron microscope at 5,000X magnification. Opposed to these results are the samples processed under conditions in which surface oxides are stable. These samples are typified by dull oxidized surfaces and a microstructure consisting of numerous crystal grains and/or dendrites.

Edwin C. Ethridge/ES72
(205) 453 – 3917
Sponsor: OSSA and CDDF

Organic Crystal Growth

The emerging technology utilizing nonlinear optics has intensified the search for new materials with large nonlinear coefficients. A promising family of such materials is organic macromolecular and polymer crystals. Such crystals have proven difficult to grow for a number of reasons, one of which involves Earth's gravity.

The 3M Corporation recently signed a Joint Endeavor Agreement (JEA) with NASA to explore the growth of such crystals in microgravity. MSFC has been working to accommodate the 3M Corporation experiments on the Space Shuttle mid – deck and to model the crystal growth process. The aim of the JEA is to create a nonproprietary material mutually acceptable to both NASA and 3M to be used to test

the growth models in order to advance the technology of growing such crystals in microgravity.

The first experiment of this series was flown on Shuttle Mission 51 – A (November 1984). Six reaction chambers were packaged in the experiment cannister developed for the Monodisperse Latex Reactor and were operated by a small computer control system. The crystals were grown by automatically opening valves in the reaction chambers and allowing solvents containing reactive components to inter – diffuse and precipitate out the compound to be crystallized. The small crystallites remain suspended in the microgravity environment and grow by a process known as Ostwald ripening in which larger crystallites grow at the expense of smaller crystallites in order to reduce the overall surface energy of the system.

The nonproprietary material chosen to model the growth process was urea. Urea was dissolved in methanol and precipitated by the diffusion of toluene which lowers its solubility. The space experiment produced a large number of needle – like crystals, which was surprising since a more compact growth was expected. The optical quality of the crystals is still being evaluated. The mission did have a number of low level accelerations that disturbed the anticipated quiescent growth conditions.

Several of the growth chambers did not open due to electromechanical problems. 3M Corporation scientists reported that the proprietary material grew crystals large enough and with sufficient perfection to allow the first good optical measurements to be made on this particular substance.

Robert J. Naumann/ES71
(205) 453 – 0940
Sponsor: OSSA

ORIGINAL PAGE IS
OF POOR QUALITY

Protein Crystal Growth

One of the techniques responsible for the rapid advancement of molecular biology is the use of x – ray diffraction to determine the three – dimensional structures of complex protein macromolecules associated with living organisms. Since the biological properties of these macromolecules are dependent on certain active sites formed by the folded three – dimensional structure, knowledge of this structure is crucial to understanding how such molecules perform their function. Apart from obtaining knowledge of the inner workings of living systems at the molecular level, this information offers many exciting possibilities in biotechnology. For example, it may be possible to design and produce new enzymes having important applications in industrial chemistry. A number of major industries are becoming actively involved in enzyme engineering. Another important application is drug design. It is known that some chemotherapeutic agents work by binding to specific sites of certain enzymes necessary for the proliferation of cancer cells and inhibit their activity. To date the development of such agents has been largely an empirical trial – and – error process. If the structures of the target enzymes were known, a more efficient approach could be used to design chemotherapeutic agents. This is one of the objectives of the Comprehensive Cancer Center at the University of Alabama in Birmingham (UAB).

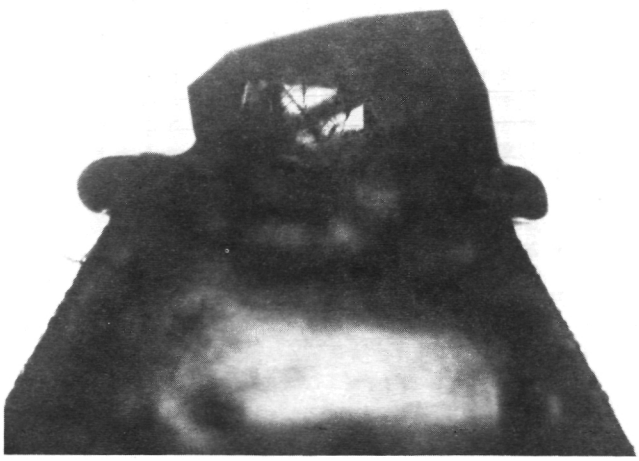

Figure 26. Crystal Growth at End of Syringe.

On Shuttle Mission 51 – D, April 1985, a small (50 cc) Protein Crystal Growth (PCG) apparatus

was operated. The small, hand-held (50 in^3) apparatus was designed to test designs of investigators at UAB and MSFC and to explore the use of the microgravity environment for crystal growth of a variety of proteins with medical and scientific interests. Because of the preliminary nature of the design and relatively high gravity levels encountered during the flight, only one of the returned 36 samples had a large crystal (Figure 26). Preliminary data on this lysozyme (major dimensions – 1.6 mm) show it to diffract out to at least 1.3 Å. This represents a significant advance in capability if borne out by later crystal growth tests.

Robert S. Snyder/ES73
(205) 453-3537
Sponsor: OSSA and CDDF

Phase Partitioning

One of the most important aspects of biotechnical, biomedical manufacturing processes involves separation. In particular, drugs produced by cells in culture must be separated from the culture. Cell types which produce a desired compound must be separated from other, often very similar, cell types not of interest. Many separation methods are available, including centrifugation (separating on the basis of mass and also shape), electrophoresis (separating on the basis of charge), gel chromatography (separating on the basis of size), and affinity techniques (separating on the basis of affinity for a specific ligand or antibody). Often these techniques can be combined to yield very pure compounds or cell populations; however, they all suffer because component cost and energy requirements are cost prohibitive.

One method widely used in industry for the separation of organic compounds is two-phase separation. When polymers such as dextran and polyethylene glycol are mixed in water at low concentrations, two-phase systems form, each being enriched in one of the polymers. On Earth, phase separation proceeds rapidly in these systems due to density differences between the phases. A series of short-duration (20 sec) experiments aboard KC-135 aircraft have demonstrated that, in low gravity, phase separation still proceeds rapidly in spite of appreciable viscosities and low liquid interfacial tensions.

A Phase Partitioning Experiment (PPE) was successfully conducted on the Space Shuttle in April 1985. The object of the PPE was to determine whether the immiscible phase, in a two-phase polymer aqueous phase system, separated in the absence of density differences between the liquids. It was to study the time course of the process and to make initial observations on the effects of particles (biological cells) on the separation. In addition, the effects of varying interfacial tension, phase volume ratio, phase viscosity, polymer type, and phase wall-wetting behavior were studied. An oil/water mixing experiment performed on Skylab did not show separation in space. Comparison of laboratory and Shuttle flight data indicates that: the two polymer phases do separate in microgravity; orientation of the separated phases is determined by which one best wets the cavity wall (the other phase forming an "egg yolk" near the center of the chamber); the presence of cells does not dramatically alter the phase separation in microgravity (Figure 27); and the rate of phase separation was several orders of magnitude greater than predicted by current theories of phase separa-

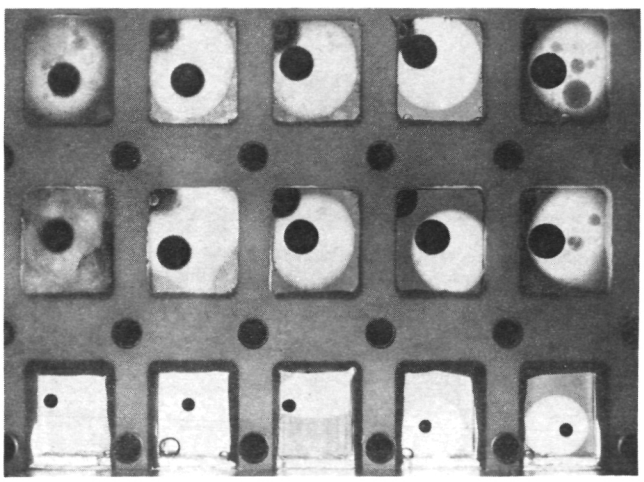

Figure 27. Phase Partitioning.

tion and tension, volume ratio, viscosity, and polymer type. Quantitative data evaluation is currently underway.

Robert Snyder/ES73
(205) 453 – 3537
Sponsor: OSSA

Electrophoresis

Sample stream broadening in Continuous Flow Electrophoresis (CFE) continues to be a major source of resolution degradation both on Earth and in space. Experiments on two Space Shuttle flights have shown significant band spreading with resultant loss in resolution occurring even when the sample and buffer are well matched in conductivity. This is significant if high concentrations are expected for separation in reduced gravity. These high concentrations could cause electrical field distortions which would in turn cause the sample to migrate toward the walls. As the sample deviates from the chamber center plane, viscous and electro – osmotic flows spread the sample along the width of the chamber, degrading resolution. The amount of migration of the sample in a direction perpendicular to the chamber center plane (transverse direction) is vitally important to the performance of CFE on Earth and in space.

The chamber is mounted horizontally (Figure 28) in order to reduce the effect of buoyancy – induced thermal convection on the chamber flow. The chamber may be viewed from three axes so that the samples stream distortion can be completely defined. A sample experiment shows a stream entering from the right with the chamber side walls containing the flow on top and bottom. The voltage gradient is 50 V/cm. The sample is spreading toward the walls just after leaving the nozzle. This transverse spreading would be translated into lateral spreading causing a degradation of resolution in a typical CFE chamber.

In this ground – based chamber the sample settles toward the bottom, thus preventing the study of high concentrations. A future flight

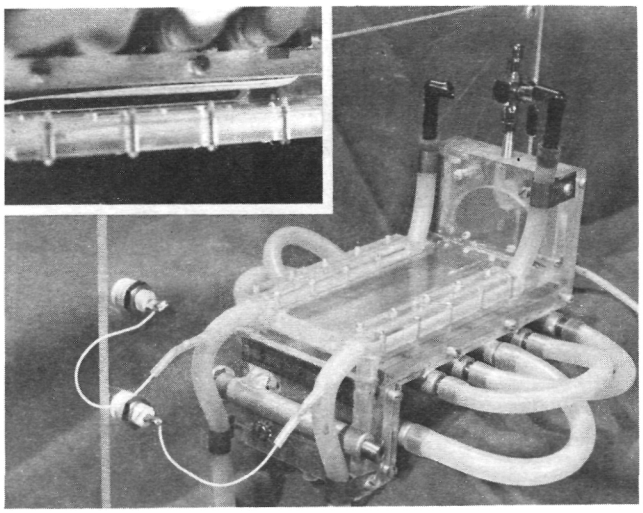

Figure 28. Laboratory Chamber for Multi-Axis Viewing of Sample Stream. Electrophoresis Pipe (inset photo).

experiment is being designed to study the effects of high concentration on sample band spreading using a similar apparatus to assure that space – based CFE can achieve its maximum potential.

In summary, the following progress was realized during the past year. A three – dimensional model was developed that can reproduce the data from both Space Shuttle experiments. Fluid dynamic measurements on the flow profile in continuous flow electrophoresis chambers have been completed showing the sensitivity of flow to the electrical properties of the fluid. Experiments in porous gels have also been done, confirming the above results.

Robert Snyder/ES73
(205) 453 – 3537
Sponsor: OSSA

Effects of Microgravity on Model Polymer Systems

While major resources and research efforts have been expended on metallic and ceramic material behavior in microgravity, little investigation has been done involving polymers. Fabrication of latex spheres has demonstrated

marketability of space/polymer processing technology. Major research efforts that yielded a scientific baseline enabling processing advances for metallic and ceramic materials are nonexistent for polymers. This study, conducted in fiscal year 1985, investigates a small facet of this scientific baseline: the effects of microgravity on polymer chain reptation and crystallization.

All experiments use well characterized model polymer constituents. Gel permeation chromatography and differential scanning calorimetry testing have been performed on all systems to determine baseline parameters. A few selected samples have dielectric monitoring monoprobe sensors imbedded in the matrix, and phase/gain responses are being baselined.

Microgravity conditions are attained on-board the NASA KC-135 aircraft. During the short duration (30 sec) microgravity period provided, thin section polymer samples (9 μm) are melted on a programmable microscope hot stage and quenched in air. Two in situ methods for monitoring the melt have been used: real time video recording and photocell monitoring through the microscope ocular. To date, only one polymer system has been successfully investigated: linear polyethylene (molecular weight 52,000).

Though only two flight series have been completed, initial results are promising. The instrumentation system assembled for this investigation provides the capability for simultaneous recording of up to four monitorial properties. Currently, gravity force, hot-stage temperature, and microscope ocular light intensity traces are generated. The correlation of these data with post-flight analysis (spherulite size, birefringence characteristics, in situ melt temperature, and flight recrystallized melt temperature) is similarly positive.

In situ melt temperature varies as a function of gravity conditions. Samples heated 1.7 to 1.8 times normal gravity melted approximately 3°C below the observed melt temperature of those samples heated in microgravity conditions. It must be noted that this difference may be caused by differing thermal conditions during heating. High-gravity heated samples are pressed in intimate contact with the glass hot-stage slide; microgravity heated samples may float above the slide in the thin (20-25 μm) gap between slide and coverglass.

Birefringence characteristics of the air-quenched crystals also appear to vary with gravity-quench conditions. As birefringence is related to crystal structure, this provides another indication of gravity-affected properties within discrete polymeric moieties.

B. E. Goldberg/EH34
(205) 453-1227
Sponsor: CDDF

Monodisperse Latex Reactor

The purpose of the Monodisperse Latex Reactor (MLR) is to produce monodisperse polystyrene latex in microgravity with particle sizes larger and more uniform than can be manufactured on Earth. Latex is a stable suspension of very tiny (micrometer-size) plastic spheres in water. The objective of this experiment is to form billions of monodisperse microspheres in larger sizes than can be produced on Earth. Monodisperse means all exactly the same size, defined as a standard deviation in diameter of less than two percent for all microspheres in the batch. Batches have been returned to Earth from Shuttle flights with standard deviations better than 1.4 percent (Figure 29). STS 41-B produced 1.7 billion microspheres of 30 μm diameter and 45 billion microspheres of 10 μm diameter. The difference is due to each latex recipe being held constant at about 25 percent total solid content by weight. Latex can only be grown on Earth in quantities up to about 5 μm diameter while remaining monodisperse due to buoyancy and sedimentation. They cannot be stirred since stirring causes coagulation, which destroys the latex. In microgravity, the absence of buoyancy effects has allowed sphere growth thus far to 30 μm diameter at 1.2 percent standard deviation. The MLR hardware has flown five times on the

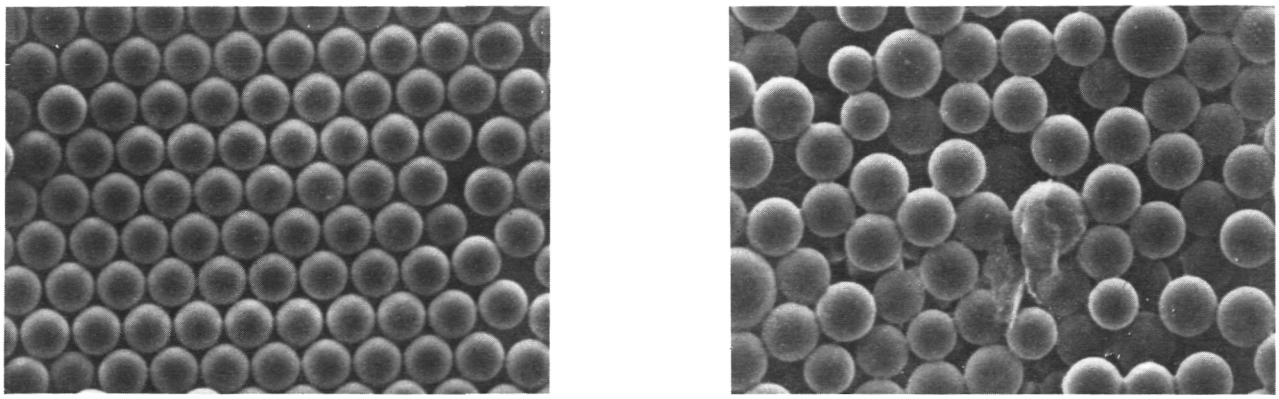

(a) Latex Spheres Made in Zero-G (Space).

(b) Latex Spheres Made on Earth.

Figure 29.

Space Shuttle and three more flights are presently scheduled. It is expected that 100 μm monodisperse particles will be produced by the completion of this flight series.

This experiment resulted in the production of the first space-manufactured commercial material ever to be marketed. The 10 μm particle-size latex was officially accepted by the U.S. National Bureau of Standards (NBS) on July 17, 1984. The bureau completed certification in April 1985, and will begin marketing in July 1985 to researchers worldwide. It is known as United States 10 μm Standard Reference Material (SRM# 1960). NASA transferred 15 g to NBS where it was diluted and packaged into 600 vials, each containing 4 ml of latex at 0.4 percent solids. The vials have a total market value of $230,000, or about $15,300 per gram, or $434,000 per ounce of solid polymer. The proceeds from the sale of this material will be shared by NASA and NBS. In theory, two to three million dollars worth of latex can be produced on each Space Shuttle flight. NBS has requested NASA to produce 30 g of 30 μm latex and 80 g of 100 μm latex which they will also market. Once it is demonstrated that these latexes can be produced in quantity and quality, they can be marketed for many types of scientific applications.

D. M. Kornfeld: Monodisperse Latex Reactor (MLR), A Materials Processing Space Shuttle Mid-Deck Payload. NASA TM-86487, January 1985.

Vanderhoff, J. W., El-Aasser, M. S., Micale, F. J., Sudol, E. D., Tseng, C. M., Silwanowicz, A., Kornfeld, D. M. and Vicente, F. A.: Preparation of Large-Particle-Size Monodisperse Latexes in Space: Polymerization Kinetics and Process Development. Journal of Dispersion Science an Technology, 5, (3&4), 231-245, 1984.

Dale M. Kornfeld/ES73
(205) 453-0185
Sponsor: OSSA

Solar Physics

The Sun is a magnetic variable star (Figure 30). Its magnetic field is the direct cause of the intriguing complexity of the solar atmosphere, structure and activity. Sunspots, plage, spicules, filaments, flares, coronal mass ejections, coronal loops, coronal holes, and coronal streamers are created by the magnetic field and are probably necessary for the existence of the hot corona and solar wind. The research activities of the MSFC Solar Science Branch span the range of major problems associated with the magnetic field: the origin of the field in the solar cycle, the structure and evolution of the field in the observable solar atmosphere, and the major effects of the field including heating of the solar atmosphere, flares, coronal mass ejections, and generation of the solar wind. Main observational tools are presently the Vector Magnetograph at MSFC and the Ultraviolet Spectrometer and

ORIGINAL PAGE IS
OF POOR QUALITY

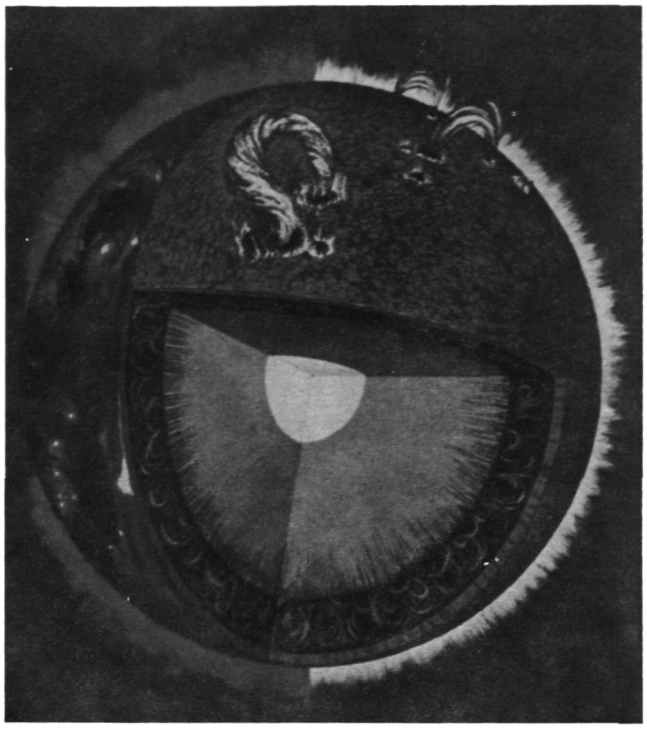

Figure 30. The Sun.

Polarimeter on the Solar Maximum Mission (SMM). Data from these instruments are analyzed in combination with complementary data from other instruments on SMM, other solar space missions, and other ground-based observatories. The results of these empirical studies are combined with theory and computer modeling to construct and test physical models of the observed magnetic phenomena. The results of instrument development, observations, and analyses complement both ongoing SMM and future solar space missions. These include Spacelab 2, Sunlab, International Solar Polar Mission, and Solar Optical Telescope.

Solar Magnetic Fields

The MSFC Solar Vector Magnetograph is a unique instrument for measuring the Sun's magnetic field because it measures the total magnetic vector, not just the line-of-sight component that is measured with magnetographs at other solar observatories. The additional information gained from making observations of the total magnetic vector has contributed significantly to our understanding of the magnetic Sun. Research in vector magnetic fields at MSFC has produced several benchmark results, including the measurement of the vertical gradients of sunspot magnetic fields, observations of magnetic shear, derivation of electric currents, and detection of submergence in the vector magnetic field.

Recent research has centered on observations and analyses of data taken in collaboration with Solar Maximum Mission (SMM) observations as part of the MSFC SMM Guest Investigator Program. One objective of the program is to observe the magnetic field of a sunspot in the solar atmosphere at several different heights above the spot. With the appearance of a suitable sunspot on the solar disk in March 1985, MSFC personnel organized joint observations with the MSFC vector magnetograph, the Haleakala Stokes polarimeter, the SMM Ultraviolet Spectrometer and Polarimeter (UVSP), and the Owens Valley Radio Observatory. The MSFC observations obtained the vector field of the sunspot at the photospheric level, Haleakala obtained data on the chromospheric vector field using a line in the red part of the visible spectrum, the UVSP mapped the field in the transition region, and the radio data provided the field strength in the overlying corona. Data have been obtained on the field of that sunspot from the photosphere through the transition region to the corona, which forms the outer part of the Sun's atmosphere.

In the Bright Point/Electric Current Associations Program, the objective is to determine if there are correlations between the heating events inferred from observed enhancements of already bright points seen in ultraviolet spectroheliograms and sites of photospheric electric current densities inferred from observations of non-potential or sheared magnetic fields. Recent analyses of preliminary data from joint observations with the MSFC magnetograph and the UVSP indicate that there is a relaxation of magnetic shear along the magnetic neutral line in a solar active region at the same time that a series of heating events are

seen in ultraviolet lines with the SMM instrument.

A Bright Points/Coronal Hole Program was initiated by K. Harvey (National Solar Observatory) to study bright points in coronal holes. In 1984 and in April 1985, spectral images in He 10830 were obtained at Kitt Peak along with MSFC vector magnetograms, UVSP spectroheliograms and Big Bear Solar Observatory data (H – alpha and line – of – sight magnetograms). In the April observations, a southern coronal hole was the target area, and the MSFC vector data showed the possible detection of transverse fields in this "quiet" solar area.

In addition to these joint observations, a vigorous research program has been pursued over the past year, analyzing and interpreting data obtained with the MSFC magnetograph. The study of magnetic field configurations involves the investigation of techniques to extrapolate the observed photospheric vector magnetic fields to understand the configuration and energy content of the chromospheric and coronal fields. The formulation linear force – free fields in terms of the transverse magnetic field was developed and published. A computer program has been written for the linear force – free method developed by Alissandrakis (1981) as an extension of the Nakagawa method (1972). Magnetic fields calculated by both the Nakagawa and Alissandrakis methods are compared with the observed field (Figure 31); the methods of Alissandrakis can produce more highly sheared fields and thus can provide more realistic upper limits for the electric currents in active regions. To investigate nonlinear force – free fields, the method of Pridmore – Brown has been adapted to a computer algorithm which has been verified for several test cases and is now being converted to run on a Cray computer. This technique will allow the study of more realistic nonlinear force – free magnetic fields that are believed to exist, and are evidenced, in fields that twist with height.

On April 24, 1984, the Hinotori X – Ray Experiment observed the X13/3B solar flare that began at 23:56 UT in Active Region 4474. This was the largest flare observed since December 1982. Vector magnetic field data for that region were obtained with the MSFC magnetograph both before and after the event. A collaborative analysis of these data was initiated to investigate the characteristics of the x – ray flare with respect to the configuration of the magnetic field.

A collaboration with B. Haisch of Lockheed began during the SMM series of workshops to analyze coordinated observations of an active region. The data include SMM/UVSP and x –

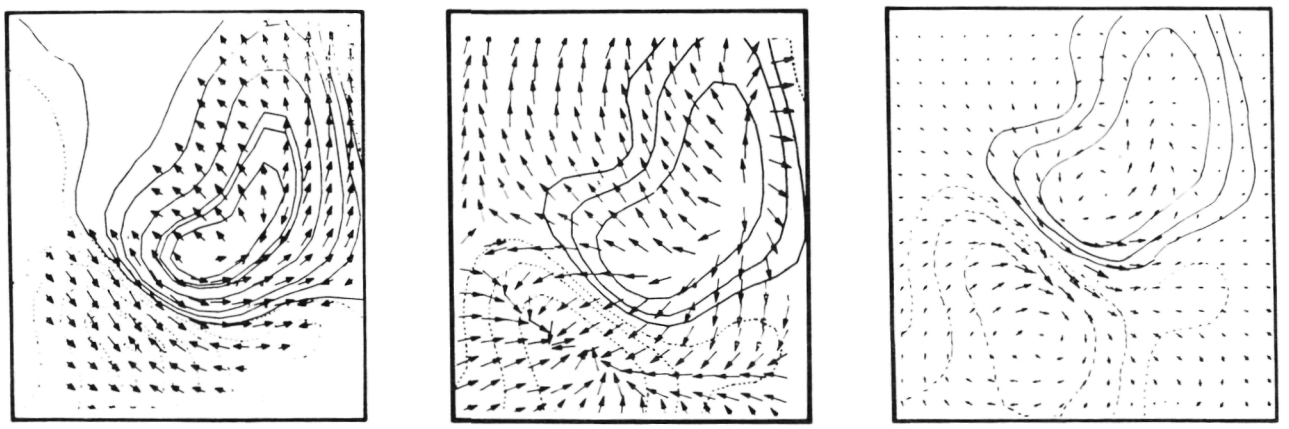

THE OBSERVED TRANSVERSE MAGNETIC VECTOR FIELD SHOWN WITH THE LONGITUDINAL MAGNETIC FIELD CONTOURS.

THE TRANSVERSE FIELD CALCULATED BY THE NAKAGAWA METHOD FOR MAXIMUM ALPHA.

THE TRANSVERSE FIELD CALCULATED BY THE ALISSANDRAKIS CONSTANT ALPHA PROCEDURE ($\alpha = 1$).

Figure 31. Magnetic Fields Calculated by Both the Nakagawa and Alissandrakis Methods.

ray images, MSFC vector magnetograms, and high-resolution Lyman-alpha images from the Transition Region Camera of the Lockheed Rocket Experiment that was flown on September 23, 1980. One part of this analysis consisted of comparing maps of the electric current density (derived from the vector magnetic field data) with bright features seen in the x-ray and ultraviolet images. In another area of this collaboration, an attempt is being made to derive a magnetic field model for this active region by matching the observed magnetic field with the chromospheric and coronal fibril structures seen in H-alpha and Lyman-alpha images. In the course of this analysis, it was found that in one area of the active region the magnetic field rotated with height. This is seen in the comparison of the photospheric field with H-alpha and Lyman-alpha fibrils shown in Figure 32. Such twisting of the

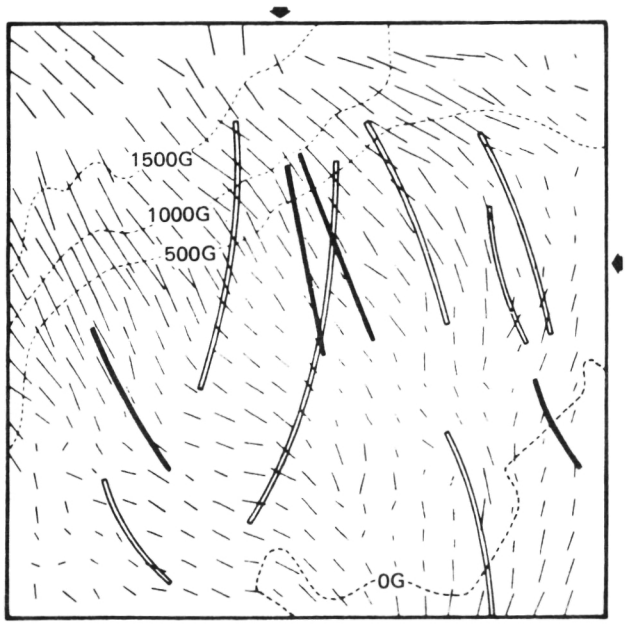

Figure 32. The Magnetic Field Configuration in the Active Region 2684 on September 23, 1980, from the MSFC Vector Magnetograph.

fields with height cannot be modeled with potential or linear force-free fields.

M. J. Hagyard/ES52
(205) 453-0118
Sponsor: OSSA

Transition Region

The chromosphere-corona transition region is the complex interface between the chromosphere and the corona. Through the transition region the temperature increases from that of the chromosphere (~10^4 K) to that of the corona (~10^6 K). The heating of the transition regions is one of the long-standing fundamental puzzles of solar physics. The Sun's magnetic field strongly controls the structure of the transition region. Because the magnetic pressure greatly exceeds the plasma pressure, mass flow and thermal energy transport within the transition region are channeled along the field. Understanding the physics of the transition region hinges on knowledge of the magnetic field threading the transition region.

Most of the recent transition region models have been based on a two-dimensional picture of the magnetic structure, as in Figure 33.

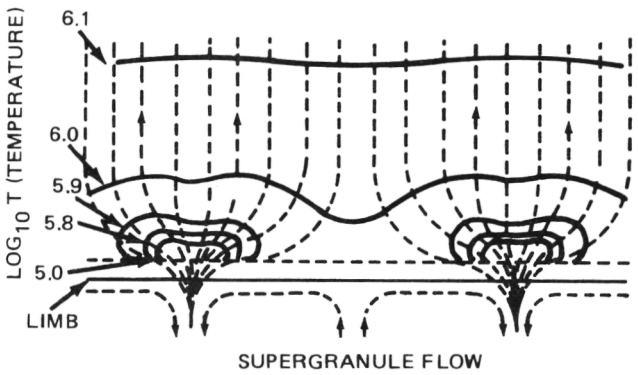

Figure 33. The standard two-dimensional picture of the magnetic structure of the transition region. The magnetic field is concentrated at the supergranulation boundaries in the photosphere, from where it diverges with height to become much more nearly uniform and vertical in the corona.

In this picture the magnetic field is rooted at the boundaries of supergranular cells and diverges rapidly with height to become nearly uniform and vertical in the corona. In these models the entire transition region is magnetically connected to the corona, and the entire radiative energy loss from the transition region

might be supplied from the corona by heat transfer along the field lines. In general agreement with observation, these models produce enhanced transition region emission in the network of magnetic flux concentration along the supergranular boundaries. Because the models are two-dimensional, they cannot explicitly account for the observed strong variation of emission along the network.

On the basis of images of the transition region from Skylab, the Solar Maximum Mission (SMM), and magnetograms from ground-based solar observatories, a revised picture of the transition region has been proposed. The observed fine-scale structure of the transition region and the fine-scale structure of the magnetic field in the photosphere suggest that the transition region has a three-dimensional structure that is inhomogeneous along the network. The added feature is that the part of the transition region at temperatures below ~10^5 K, which is called the "cooler transition region," is mostly in small magnetic loops that contain no hotter plasma. The cooler transition region is thereby magnetically insulated from the corona. This requires the cooler transition region to be heated internally rather than by heat transfer from the corona.

The remainder of the transition region, the part at temperatures above ~10^4 K, is called the "hotter transition region." This region is similar to the standard picture in that it is threaded by field lines that reach into the corona, and its energy losses are supplied by heat transfer from the corona. The main difference is that the constriction of the magnetic field is greater and is three-dimensional rather than two-dimensional (Figure 34).

The constriction of the field may well be great enough that the corona loses much less heat by back conduction than previously thought. This would mean that the amount of heating required to sustain the corona is much less than previously thought.

The extent to which the new picture is valid will be determined by further observations of the transition region, chromosphere, and photosphere with spatial resolution of at least a few arc seconds. Some of the needed observations can be obtained and are being pursued with the Ultraviolet Spectrograph and Polarimeter on SMM and with ground-based magnetographs, including the MSFC Vector Magnetograph. Other key observations will be supplied by the high-resolution solar telescopes to be flown on Spacelab 2 and Sunlab.

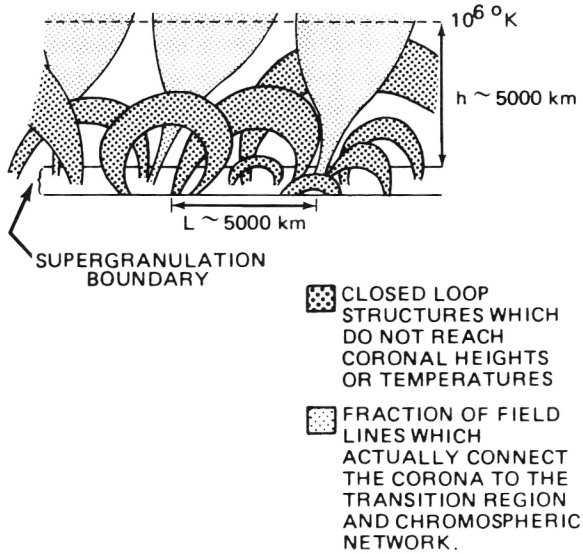

Figure 34. Three-dimensional picture of the magnetic structure of the transition region as proposed by Dowdy, Rabin, and Moore.

R. L. Moore/ES52
(205) 453-0118
Sponsor: OSSA

Ultraviolet Spectrometer and Polarimeter

The rich data obtained during 1980 are still being analyzed, and new observations have been obtained since the repair of the Solar Maximum Mission (SMM) satellite in April 1984. Research relating to both the active Sun (e.g., flares, sunspots) and the quiet Sun (e.g., a spectral atlas of selected wavelength regions) is being pursued.

Studies of data from the Ultraviolet Spectrometer and Polarimeter (UVSP) have helped de-

lineate the dynamic nature of many solar phenomena. This is due to a unique feature of the UVSP. It observes velocities in the Sun's transition region by means of the Doppler shift of carefully selected spectral lines. For example, large roster maps of an active region show patterns of upward and downward motions in areas very close together, indicating an intricate, fine structure with scale less than 2000 km for this layer of the solar atmosphere. Based on such observations, the morphology and function of the transition region are being reconsidered.

One of the main objectives of the SMM is to explore the physics of flares using the UVSP extensively for this purpose. It is generally believed that the energy released in a solar flare is stored in the strong magnetic fields in active regions. These fields form magnetic loops in the solar atmosphere, and flares probably occur when a plasma instability causes a sudden conversion of magnetic energy in the loop. While it has not as yet been possible to detect changes in the strength of the magnetic field during a flare with the UVSP, the instrument has made it possible to pinpoint the location of the flare emission in the loop and to follow the rapid development of the flare plasma. As electrons are accelerated in the flare loop, they stream down and collide with the lower solar atmosphere, heating the plasma which emits the strong UV lines observed by the UVSP. Then using high-energy lines accessible with the UVSP, the manner in which the flare loop is being filled with very hot plasma,~10 million degrees can be seen streaming up from the loop footpoints. As more and more detailed knowledge of the solar atmosphere has become available, better physical models of the atmospheric plasma have been constructed. One region of the solar spectrum that still needs more study to yield necessary data for further improving solar atmospheric models is the region of the UV which the UVSP can observe. This instrument has now observed, with very good spectral resolution, the band from 1200 to 3000 Å, so that appropriate models can be improved. In particular, in the region of 2000 to 3000 Å, the UVSP observations have better resolution and a higher signal-to-noise ratio than previous observations. The models make it possible to better understand the sources of opacity and the abundance of the elements contributing to the opacity in the form of spectral lines and continua. During the 1980 observations, it was discovered that the whole transition region above sunspots oscillates up and down with periods in the range 110 to 200 sec. The nature of these oscillations is now the object of further study. Comparisons with ground-based observations of chromospheric and photospheric lines are being performed to determine the reflection properties of the oscillating waves as they propagate upward through the spot.

During 1985 selected regions of the solar spectrum have been observed in active regions, and the analysis of these data are presently underway to determine the different physical conditions that exist in such regions as compared with the more quiet solar atmosphere. This should lead to a better understanding of how an active region can develop the pre-flare conditions necessary for the cataclysmic flare phenomenon to occur.

Athay, R. G., Gurman, J. B. Henze, W. and Shine, R. A.: Fluid Motions in the Solar Chromosphere-Corona Transition Region I. Line Widths and Doppler Shifts for C IV. Astrophysical Journal, 265, p. 519, 1983.

Gurman, J. B., Leibacher, J. W., Shine, R. A., Woodgate, B. E. and Henze, W.: Transition Region Oscillations in Sun Spots. Astrophysical Journal, 253, p. 939, 1982.

Tandberg-Hanssen, E., Kaufmann, P., Reichmann, E. J., Teuber, D. L., Moore, R. L., Orwig, L. E. and Zirin, H.: Observation of the Impulsive Phase of a Simple Flare. Solar Physics, 90, p. 41, 1984.

Woodgate, B. E., Shine, R. A., Poland, A. I. and Orwig, L. E.: Simultaneous Ultraviolet and Hard X-Ray Bursts in the Impulsive Phase of Solar Flares. Astrophysic Journal, 265, p. 530, 1983.

E. Tandberg-Hanssen/ES01
(205) 453-0027
Sponsor: OSSA

Coronal and Interplanetary Dynamics

The temperature of the Sun's corona is more than one million degrees, causing the outer portion to expand supersonically and form the solar wind. Because of the Sun's magnetic field, the corona is also highly inhomogeneous. Magnetically confined portions are called coronal streamers while magnetically open regions are called coronal holes because of their relatively low density and brightness.

Physical processes in the solar corona and interplanetary medium are being studied through theoretical models and analysis of data. The motivation for this research is the opportunity to develop an understanding of the energetics and dynamics of processes involved in coronal expansion into the interplanetary medium. These include stationary and time-dependent phenomena, the characterization of processes that heat and accelerate the solar wind, and the topological structure of the expansion in three dimensions. The work has proven extremely productive in motivating ideas on a variety of space projects.

The Magnetohydrodynamic (MHD) model of coronal structure gives a reliable simulation of streamers which is the magnetically confined regions. The results from this model have been analyzed by applying a local stability criterium for the condensation mode instability to the interior of the model streamer. The result is that stronger magnetic fields, which give higher densities, lead to instability and the formation of coronal cavities, but weak-field streamers are stable. This not only has identified the mechanism for formation of cavities and the reason why they only occur in some streamers, but also demonstrates that the future coronal theories must include both thermal conduction and radiative losses.

A second analysis using the same streamer model shown in Figure 35 has also been used to estimate wave speeds in streamers and coronal holes. This is difficult since the magnetic field and flow speeds cannot be directly

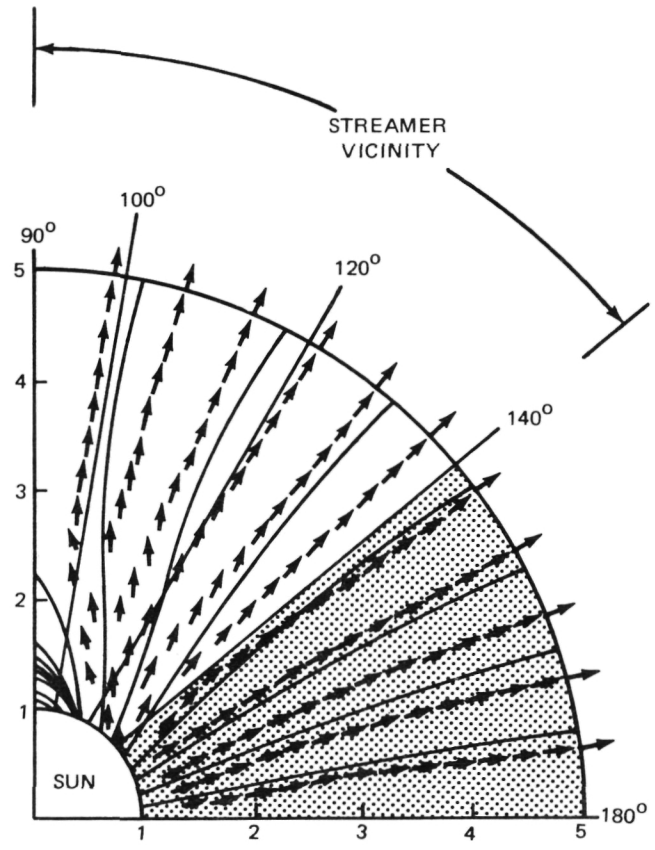

Figure 35. Meridional cut through model solar corona – the south pole is to the right, at 180 degrees. Solid lines are magnetic field lines and the vectors show the magnitude and direction of the flow field.

measured. The results provide a velocity profile in radius that is a lower bound for freely expanding coronal mass ejections (CMEs). CMEs that fall below this line are thus being restrained by the photospheric magnetic field.

In a separate study of MHD processes in the outer solar system, analysis of data from Pioneers 10 and 11 and several different near-Earth spacecraft has shown that magnetic flux is disappearing from the neighborhood of the heliographic equatorial plane. This process is well explained by the theory of MHD meridional transport of mass and magnetic flux poleward from the equator. There is extraordinary agreement between the observations, theory, and analytic expressions (Figure 36). These have been derived for the transport in a general class of stellar winds with large meridional gradients.

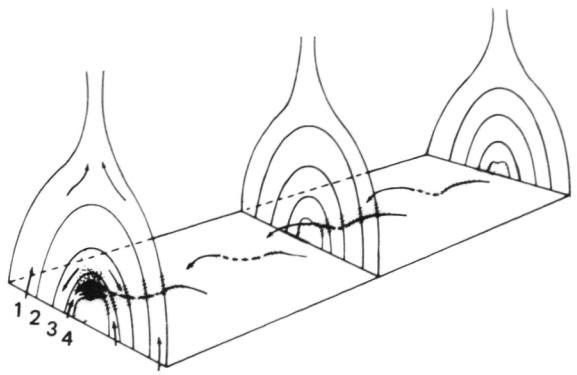

Figure 36. Schematic of the four important regions in a streamer. 1: Steady outflow. 2: Magnetostatic equilibrium. 3: Volume unstable to the condensation mode for sufficiently strong magnetic fields, where a cavity will form. 4: Volume unstable to the condensation mode, where a prominence may form in the presence of a sheared magnetic field that provides support.

In an analysis applied to a yet more distant region of the solar system, a remote detection of the shock wave terminating the solar wind at the outer edge of the heliosphere has been used by scientists at the University of Iowa. This study, together with a theoretical model of that shock wave, places constraints on properties of the local interstellar medium. The remote shock wave detection shows it to lie between 30 and 45 au. This information was combined with the model calculation to give an estimate of the galactic cosmic ray spectrum below 10 MeV outside the solar system. The galactic cosmic ray spectrum below 10 MeV was unknown because those cosmic rays are removed from the solar system by their interaction with the solar wind beyond the terminating shock wave.

Research accomplishments in coronal and interplanetary medium research during 1985 include explanations for the formulation of coronal cavities, the propagation speeds of coronal transients, and the meridional transport of magnetic flux in the outer solar system. Also, a remote detection of the shock wave terminating supersonic solar wind expansion has been used to place limits on the properties of the local interstellar medium.

Suess, S. T. and Moore, R. L.: Wave Speeds in the Corona and the Dynamics of Mass Ejections. Huntsville, Al., May 1985.

S. T. Suess/ES52
(205) 453 – 2824
Sponsor: OSSA

Statistical Solar Studies

During 1985 statistical studies were done in areas of interplanetary "magnetic clouds" and the solar cycle. Interplanetary "magnetic clouds" have been described by Klein and Burlaga as regions in the solar wind having radial lengths of about 0.25 au at Earth where the strength of the magnetic field is high and the direction of the magnetic field changes appreciably by means of rotation nearly parallel to a plane. They are important since they may be a manifestation of the Sun's Earth–directed coronal mass ejections at 1 au. The Sun often displays a violent nature, sometimes ejecting large amounts of material away from its surface into interplanetary space. When these ejections are directed toward Earth, they may be sensed in the solar wind, and possibly have geomagnetic effects.

In an attempt to confirm the hypothesis that magnetic clouds are the effects of Earth–directed coronal mass ejections, an investigation of the relationship between magnetic clouds and solar activity was undertaken in 1984 and 1985. It was found that six of nine magnetic clouds following shocks (called group A clouds) were preceded by flare – related type II meter – wave radio bursts near the Sun's central meridian (within 49 degrees). Control samples had no type II bursts closer than 47 degrees of the central meridian. Thus, at least one group of clouds can be associated with solar activity near the central meridian, activity indicative of coronal mass ejection. No clear associations could be found for the other two cloud groups.

Later, in a 1985 study, the relationship between magnetic clouds and disappearing filaments near the central meridian was investigated. (Disappearing filaments are analogous to "eruptive" or "ascending" prominences when viewed on the Sun's disk.) It was found that a convincing case can be made for associating the disparition brusque of January 18, 1974, with the magnetic cloud preceding an interaction region of January 24, 1974. Chi-square statistical testing revealed that magnetic clouds of groups B and C may be associated with disappearing filaments near the central meridian at a high (98 percent) confidence level. When group A clouds were included, the confidence level was reduced to 95 percent.

Combining the results of the two studies suggests that magnetic clouds are indeed associated with Earth-directed coronal mass ejection, and are primarily associated with two forms of solar activity: group A clouds with flare-related type II meter-wave radio bursts near the central meridian and groups B and C magnetic clouds with disappearing filaments near the central meridian.

Two additional studies are presently underway. The first is an investigation of the association between magnetic clouds and long decay events at x-ray and radio wavelengths. The second is an investigation of possible geomagnetic effects of magnetic clouds.

A second major area of statistical study concerns the solar cycle. Efforts in this area were first reported in 1982. More recently, in 1984, evidence was found that the sunspot cycle may be divided into two groups by cycle duration: short-period cycles (less than 128 months) and long-period cycles (more than 133 months). Surprisingly, no cycles have been observed with durations in the range of 128 to 133 months, which contain the mean cycle duration. Further, short-period cycles were often cycles of high maximum sunspot number, while long-period cycles were often cycles of low maximum sunspot number. Additional investigation revealed that the sunspot cycle is shorter when the "envelope of the sunspot number curve" is rising and longer when it is falling. Furthermore, these trend relationships are disjoint; i.e., the solar cycle has two distinct physical modes: "short-while-growing" and "long-while-declining" with the transition between modes occurring at irregular intervals.

Several follow-on studies are underway and have already yielded interesting results. Cycles 18 and 19, both short-period cycles, peaked simultaneously in terms of smoothed values of the number of sunspots and the 10.7 cm radio flux, while cycles 20 and 21, both either long-period cycles or predicted to be long-period cycles, had maximum smoothed number values which were separated in time by about 1.5 yr with sunspot number peaking first. For cycle 21, the lack of simultaneity in peak values is most pronounced and statistically significant. Because of solar cycle "bimodality," it is tempting to associate long-period cycles and phase lag.

Upon investigation it appears that the mean sidereal rotation rate for all short-period cycles has slowed for cycles 16 to 19. Beginning with cycle 20, the mean sidereal rotation rate has increased. It is inferred that mean sidereal rotation rate per cycle varies with the mode of the solar cycle. Since cycle 21 is predicted to be long-period, it is suggested that its mean sidereal rotation rate will be higher than was observed for cycle 19.

Wilson, R. M. and Hilder, E.: Are Interplanetary Magnetic Clouds 1-AU Manifestations of Coronal Transients? Solar Physics, 91, p. 169, 1984.

Robert M. Wilson/ES52
(205) 453-2824
Sponsor: OSSA

ORIGINAL PAGE IS
OF POOR QUALITY

Magnetospheric Physics

Since the beginning of the space program, the Earthspace environment has been a fundamentally important area of study. The first U.S. Satellite, Explorer 1, identified and measured the Van Allen radiation belts, a region of high-energy charged particles that are trapped in the inner portion of the Earth's magnetic field. This measurement of high-energy particles has been followed by a series of spacecraft missions that have extended the measurement techniques to cover a full range of particle energies and masses as well as the electric and magnetic fields that are present in the Earth's environment.

The Earth's magnetic field has a dipole shape which resembles a pumpkin. The ionized gas or plasma that flows from the Sun, called the solar wind, moves past the Earth at high velocities and distorts the dipole, compressing it on the dayside and stretching it into a long tail in the anti-sunward direction (Figure 37). This magnetic field is called the magnetosphere and forms the structural skeleton that guides the motions of charged particles such as protons and electrons in the Van Allen radiation belts.

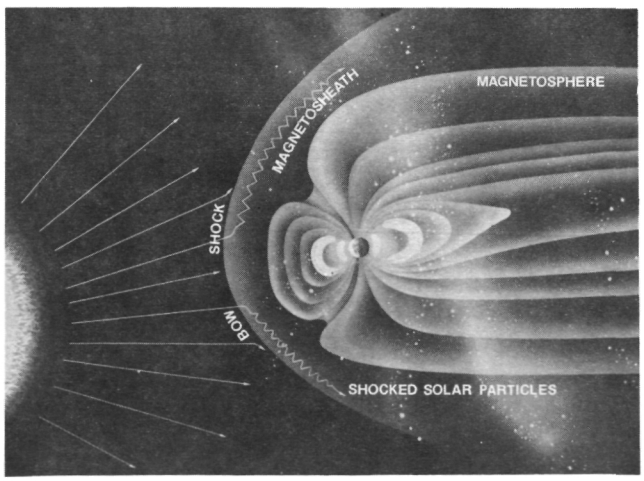

Figure 37. The Solar-Terrestrial Environment.

Measurements have uncovered a variety of lower energy plasmas in the Earth's magnetosphere with a composition similar to the Earth's ionosphere, suggesting that the Earth itself supplies a dominant amount of the plasma to its own environment instead of the Sun as was originally thought.

The importance of this ionospheric source and the processes by which ionospheric plasma is energized and transported into the magnetosphere have been a basic motivation for the MSFC research in magnetospheric physics. This thrust has influenced the design of instrumentation, the analysis of data from multiple spacecraft, the laboratory study of flowing plasmas, the development of ionospheric and magnetospheric models of plasma energization and interchange, and the development of advanced data networking systems. Successful measurements of low-energy plasma characteristics have been carried out from numerous sounding rocket flights, the Spacecraft Charging at High Altitudes (SCATHA), the International Sun-Earth Explorer (ISEE), Dynamics Explorer (DE) satellites, and the Space Shuttle.

Observations of Global Ion Outflows

In August 1981 the Dynamics Explorer 1 and 2 satellites were launched carrying instruments which have revealed a complex pattern of global ion outflow from the Earth. This ion outflow is energized by solar wind magnetosphere interaction processes and modulated by magnetospheric plasma flow dynamics. One of the instruments aboard the Dynamics Explorer satellites, the Retarding Ion Mass Spectrometer, has provided detailed measurements of ion density, composition, and energy. These measurements, along with those of the other Dynamics Explorer instruments, have provided a new and exciting look at the characteristics of Earth's global ion outflow.

Within the magnetosphere, the Earth's magnetic field is strong enough to divert the stream of plasma emanating from the Sun and control the motion of the Earth's internal plasma sources. At the base of this magnetosphere lies the ionosphere. It is in the ionosphere that Earth-borne ions are produced, primarily by neutral particles such as N_2, O_2, and O

through absorption of solar radiation. After they are created, some of these ions flow upward, along with their electrons, to the magnetosphere. A major area of research in magnetospheric physics centers around determining the importance of this ionospheric source in supplying the magnetosphere with its ionized gas.

The rate of ion outflow depends on the latitude of the foot print of the magnetic field line along which outflow is occurring. At the polar cap, the Dynamics Explorer satellites measured predicted ion outflow, known as "polar wind," moving at supersonic speeds. Retarding Ion Mass Spectrometer data showed H^+ ions to have typical velocities of 20 km/sec and a flux of 2×10^8 ions per cm^2/sec. Observations also showed that superimposed on the polar wind flow was an unexpectedly large outflow of O^+ ions with energies greater than those predicted for the polar wind.

In addition to the upward motion of the plasma, motions in high-latitude regions and at the polar cap are affected by an electric field, perpendicular to the magnetic field. This is caused by the interaction of the solar wind and the magnetosphere. This electric field produces ion motions perpendicular to the magnetic field, which results in a substantial horizontal flow superimposed on the vertical field-aligned ion outflow. This phenomenon is dramatically exhibited at the low-latitude edge of the dayside polar cap. The ions in this region flow horizontally upward, spreading the ions throughout the polar cap. Since all ion species seem to be comparably heated in the ionosphere, they move upward at speeds inversely proportional to the square root of their mass. This results in the different ion species being spatially separated across the polar cap. This phenomenon has been aptly named the Geomagnetic Mass Spectrometer, and it is an extremely important source of magnetospheric plasma. During periods of less intense ion heating, heavier ions such as O^+, NO^+, and O_2^+ fall back into the polar ionosphere. This phenomenon is called the "Ion Fountain" because of its resemblance to a fountain in the wind (Figure 38).

At lower latitudes there is less distortion of the dipole field and the magnetic field lines are closed, forming a torus around the Earth called the plasmasphere. At the outer edge of this plasmasphere, significant perpendicular electrical fields penetrate this region during magnetic substorms and deplete it of plasma. The plasma remaining then redistributes itself to balance the plasma pressure. If the magnetic storm is strong enough, a field line can be almost emptied of plasma. After the magnetic substorm resides, ion outflow from the ionosphere replenishes the plasma in the outer plasmasphere. If one ionospheric source is dominant, which can occur during solstice when the solar radiation is more intense in the summer hemisphere than in the winter, interhemispheric ion flow will occur in the plasmasphere. On occasion, different ions will have their dominant source in opposite hemispheres and ions will flow from the dominant source across the equatorial plane into the opposite

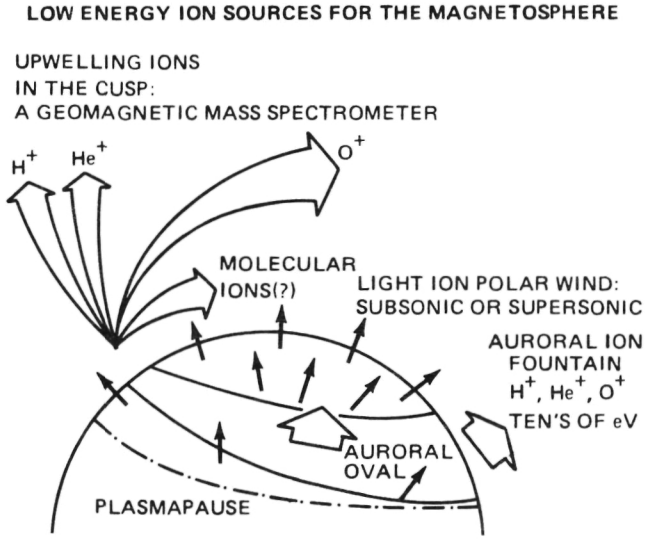

Figure 38. Low-Energy Ion Sources for the Magnetosphere.

hemisphere and counterstreaming of the ions will occur. Observations in the outer plasmasphere following magnetic storms have shown this type of counterstreaming with H^+ ions flowing from the summer hemisphere and He^+ ions flowing from the winter hemisphere. Both plasmaspheric ion flows and high-latitude plasma outflow indicate a continual interaction and interchange of plasma between the

ionosphere and magnetosphere. The Dynamics Explorer 1 and 2 Retarding Ion Mass Spectrometer data have contributed greatly to our understanding of the low-energy plasma motions near Earth and have clearly shown that the ionosphere is the primary source of magnetospheric plasma. During the past year a new source of low energy ion outflow was identified in the dayside auroral zone, and the first measurements of inter-hemisphereic plasma flows were made and modeled theoretically.

Lockwood, M., Waite, J. H., Jr., Moore, T. E., Johnson, J. F. and Chappell, C. R.: A New Source of Suprathermal O+ Ions Near the Dayside Polar Cap Boundary. Journal of Geophysical Research, 90, p. 4099, 1985.

Moore, T. E., Chappell, C. R., Lockwood, M. and Waite, J. H., Jr.: Superthermal Ion Signatures of Auroral Acceleration Processes. Journal of Geophysical Research, 90, p. 1611, 1985.

Waite, J. H., Jr., Nagai, T., Johnson, J. F. E., Chappell, C. R. Burch, J. L., Killeen, T. L. Hays, P. B., Carignan, G. R., Peterson, W. K., and Shelley, E. G.: Escape of Suprathermal O+ Ions in the Polar Cap. Journal of Geophysical Research, 90, p. 1619, 1985.

J. H. Waite, Jr./ES53
(205) 453-3918
Sponsor: OSSA

Spacecraft Charging at High Altitudes Data Analysis

The Spacecraft Charging at High Altitudes (SCATHA) satellite was launched in 1979 to study spacecraft potential effects and spacecraft electrostatic charging with a wide variety of scientific instruments. The orbit was near-geosynchronous (5.3-7.8 RE) so the SCATHA satellite was an ideal platform for studying the regions of the outer plasmasphere and plasma sheet. The passage of the spacecraft through these areas of widely varying plasma parameters also afforded an excellent opportunity to study effects of changes the spacecraft would undergo as a result of the different plasma parameters. Among the SCATHA instruments was the Light Ion Mass Spectrometer (LIMS) developed at MSFC. This instrument is capable of measuring the density, temperature, and flow velocity of hydrogen, helium, and oxygen ions with energies less than 100 eV.

The LIMS data have been used to study plasma temperature and density and to characterize the occurrences of various types of plasma distributions. A cold ($T<1$ eV) plasmasphere population was seen in the dusk sector, and, in addition, a warm plasma component ($T=5-20$ eV) was also seen. This warm plasma displayed a rich structure in pitch angle distributions (i.e., the orientation of the particle velocity vector and the magnetic field direction) and in ion composition. Figure 39 shows the

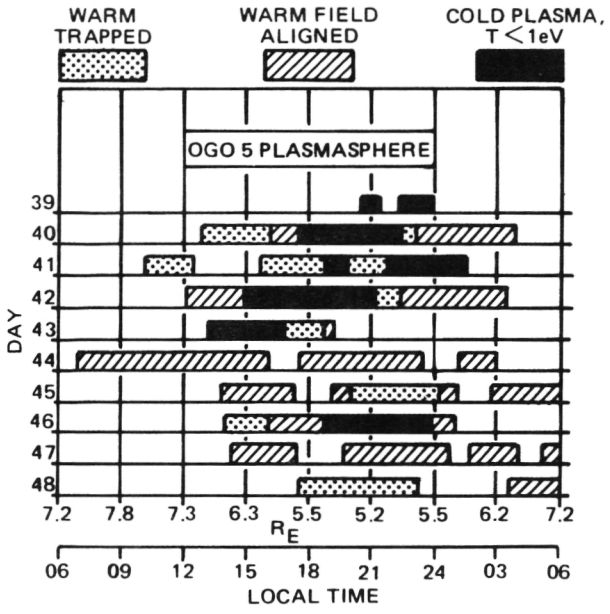

Figure 39. Occurrence in Local Time of Three Types of Thermal Plasma.

variation of the temperature and pitch angle of the plasma throughout the day. The cold plasma component, when seen at geosynchronous altitudes, can be immersed in the warm plasma and can be preceded and followed by plasma with pitch angle distributions that vary from day to day. Such variation indicates that several processes are possible depending on geomagnetic conditions.

The effects of the spacecraft potential upon low-energy plasma measurements have been

studied in detail, and it was found that the satellite potential underwent a modulation of approximately 1 V with spin. By means of an intensive correlative study using several instruments on the spacecraft, this modulation was found to be the result of different photoemissive properties of the various materials used on the satellite surface. Figure 40 shows a comparison of the calculated photocurrent emitted from the spacecraft with low-energy

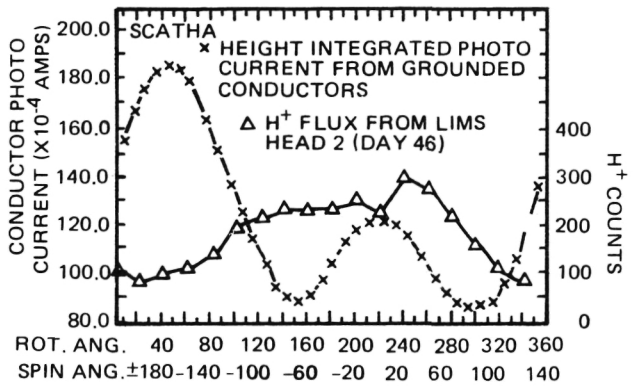

Figure 40. The Total Photocurrent of Illuminated Grounded Conducting Surfaces as a Function of Spin Angle.

H^+ flux measured by a LIMS sensor looking along the spin axis. The flux measured by this sensor should not be spin modulated. The data are plotted as a function of spin angle, i.e., an angle measured in the plane perpendicular to the spin axis of the satellite. The data clearly show that as the photoemission, and hence the positive potential increases, the measured thermal H^+ flux decreases due to the retarding effect. Such a subtle modulation has little effect on measurements of ions with superthermal energies. However, when measuring ions with thermal energies, the effect of a 1 V modulation seriously impedes the detection of these low-energy ions. It is therefore necessary to understand the potential modulation in order to avoid it on future spacecraft. This study, using the SCATHA data, adds valuable information to understanding the causes and effects of potential modulations due to small variations in material properties. In summary, the studies conducted during fiscal year 1985 revealed that the SCATHA spacecraft floating potential suffers appreciable spin modulation due to the nonuniformity of its surface properties.

Craven, P. D. and Reasoner, D. L.: Instrumental Effects on the Temperature an Density Derived from the Light Ion Mass Spectrometer. NASA TM-82536, June 1983.

Horwitz, J. L., Chappell, C. R., Reasoner, D. L., Craven, P. D., Green, J. L. and Baugher, C. R.: Observations of Low-Energy Plasma Composition from the ISEE-1 and SCATHA Satellites. Energetic Ion Composition in the Earth's Magnetosphere, pp. 263-286, Terra Scientific Publishing Co., Tokyo, 1983.

Reasoner, D. L. Craven, P. D. and Chappell, C. R.: Characteristics of Low-Energy Plasma in the Plasmasphere and Plasma Trough. Journal of Geophysical Research, 88(A10), pp. 7913-7925, 1983.

Paul D. Craven/ES53
(205) 453-0029
Sponsor: OSSA

Superthermal Ion Composition Studies

The auroral zones are regions of complex interaction between the solar wind and magnetospheric plasma. This is the site of rapid horizontal flows of ionospheric plasma and strong shears within those flows. They are driven by the solar wind in contact along the magnetic field lines. The electromagnetic transmission of shear forces in the region gives rise to quasi-steady electric fields which accelerate ions and electrons in opposite directions along the magnetic field lines. Several instabilities lead to quasi-steady wave emission in this region. Part of the auroral energy dissipated in the ionosphere causes acceleration or heating of the ionospheric ions which produces non-thermal features in the ion velocity distribution.

New evidence on the altitude distribution of ion heating in the auroral zone has been provided by the Superthermal Ion Composition Spectrometer (STICS) developed with NASA support

and flown on the NASA Topside Probe of the Auroral Zone (TOPAZ), a sounding rocket payload. It has shown that the heating responsible for enhanced ion outflow exists at altitudes as low as 700 km. In one observation a superthermal energetic tail was formed in the otherwise thermal O^+ as shown in Figure 41. The detector was observing upgoing ions at the time of the heating event. Note the clear distinction between the thermal core of the O^+ distribution and the enhanced hot tail, evident from the change of slope. This is believed to be the first documented case of preferential heating of the heavy ions at low altitude.

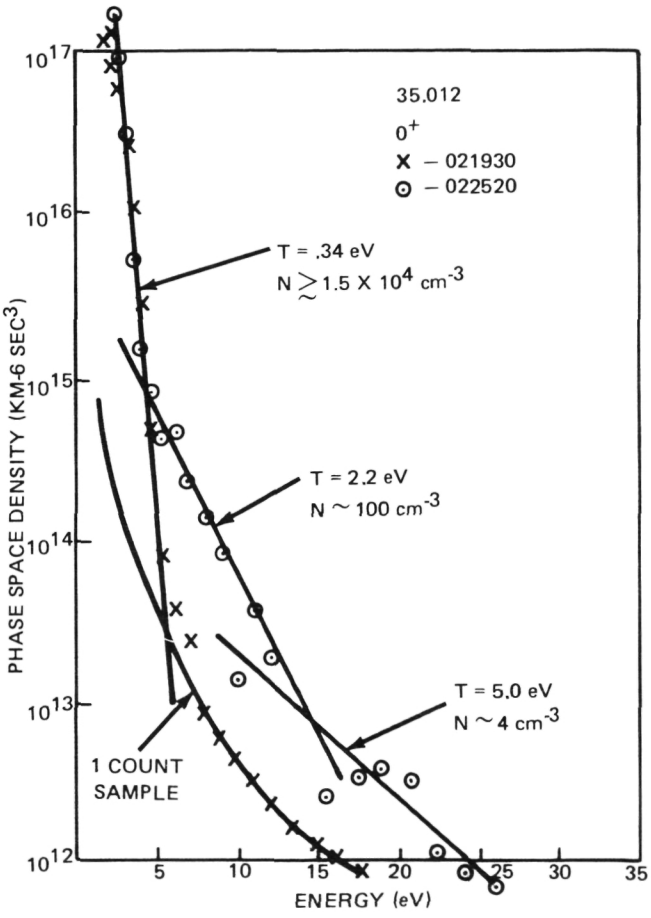

Figure 41. Data from the superthermal ion composition spectrometer on the TOPAZ rocket flight (35.012), showing an upgoing superthermal O^+ component at an altitude of approximately 700 km. Light ion species did not exhibit this feature.

The STICS observations of thermal and superthermal ions suggest that the high temperature ion populations observed at higher altitudes by the Dynamics Explorer – 1 Satellite originate in such superthermal populations created at relatively low altitudes. If the creation of such populations in the topside ionosphere turns out to be an important mechanism for upward transport of heavy ions, significant revisions of current theoretical concepts will be required. Ionospheric transport is generally treated in a hydrodynamic formulation which assumes only minor departures from Maxwell – Boltzmann distributions.

One of the consequences of low – altitude superthermal heating mechanisms lies in the ion – neutral chemistry of the topside ionosphere, which tends to prevent O^+ outflow by conversion to H^+ and O via a charge exchange reaction with H. Those O^+ ions which are energized to significantly superthermal energies are effectively decoupled from this chemistry due to their high velocity, and O^+ escape is significantly enhanced if such acceleration occurs low enough to bypass the ion – neutral chemistry. The state of the neutral atmosphere varies dependent upon the energy input, mainly the solar cycle modulation of the ultraviolet portion of the solar spectrum which is absorbed in the upper atmosphere. These effects have been described in modeling efforts, which predicted a solar cycle increase in the amount of O^+ outflow, assuming relatively constant acceleration and heating processes. This prediction has recently been confirmed, and improved models are now being explored for other predictable effects.

A related study has examined the hypothesis that an observed polar depletion of the Earth's geocorona of neutral hydrogen is caused by enhanced neutral H escape due to the charge exchange of fast, transversely heated H^+ ions on the neutral H or O, forming fast neutral H and slow H^+ or O^+ ions. It was concluded that the neutral heating recently observed in the vicinity of the dayside auroral zone by the Dynamics Explorer 2 satellite is more effective in depleting the neutral hydrogen than super-

thermal effects associated with auroral zone transverse ion heating.

Recent observations, made possible by the development of instruments capable of overcoming the traditional problems of low-energy plasma observations, have revealed a wealth of exciting new phenomena which was largely unanticipated. The predictions of ionospheric plasma transport theory, so long untested by relevant observations, have been resoundingly confirmed. The newly discovered phenomena fit in context as the result of energetic processes occurring in the auroral zone ionosphere, leading to superthermal heating, acceleration, and outflow of the auroral ionospheric plasma. The mechanisms by which ionospheric mass transport is so influenced by the input of solar wind energy remain an issue in space plasma physics. Much work remains to be done, both in the development of more sophisticated models of superthermal ion flows, and in the development of instrumentation capable of studying the phenomena. The evidence amassed during fiscal year 1985 has been found for intense heating and nonthermal conditions in the topside ionosphere. A sounding rocket instrument has returned the first direct evidence that this heating operates preferentially on the heavy ion species.

Moore, T. E. Biddle, A. P., Waite, J. H., Jr. and Killeen, T. L.: Auroral Zone Effects on Hydrogen Geocorona Structure and Variability. Planetary Space Science, 33, pp. 499-506, 1985.

Moore, T. E., Chappell, C. R. Lockwood, M. and Waite, J. H., Jr.: Superthermal Ion Signatures of Auroral Acceleration Processes. Journal of Geophysical Research, 90, p. 1611, 1985.

Thomas E. Moore/ES53
(205) 453-3695
Sponsor: OSSA

Body-Plasma Electrodynamic Interaction Studies

Laboratory testing of the electrodynamic interaction of a body flowing, rarefied plasma continues to be an area of investigation with potential application to solar system plasma physics and to the spacecraft-space plasma electrodynamic interaction. From a technical point of view, the spacecraft-space plasma interaction creates a disturbed region in the ambient medium in which diagnostic instruments must operate to determine plasma characteristics. Laboratory results along with in situ data from Ariel 1 and Explorer 31 satellites and the early Space Shuttle missions have been used in planning experimental objectives and methods for Spacelab 2 investigation.

Studies have been made of the anomalous ionization of neutrals in the vicinity of positively charged surfaces in a background plasma which have revealed significant levels of ionization observed under "collisionless" conditions when surfaces were biased a few tens of volts positive. The investigation may have application to large structures in space and to the electrodynamic missions of the Tethered Satellite System (TSS). This ground-based effort is a predecessor to orbital experiments which will make use of the same experimental techniques and instrumentation for simulation of such solar system body-plasma interactions as those caused by the moon, Io, moving within the Jovian magnetosphere.

The expansion of collisionless plasma across a strong density gradient has been studied experimentally with good agreement between the data and the results of leading theoretical calculations (Figure 42). Plasma expansion is a fundamental process that must occur in the presence of a sufficient pressure gradient. It is very probable, therefore, that it is an important mechanism in numerous space plasma and astrophysical phenomena where strong density or temperature gradients are known to exist.

Laboratory studies have continued the investigation of binary (two ion species) plasma flows in order to accurately simulate the multi-constituent ionospheric plasma. The interaction between combinations of heavy and light ions in the presence of strong density and potential gradients is believed to generate instabilities and oscillations in the wakes of io-

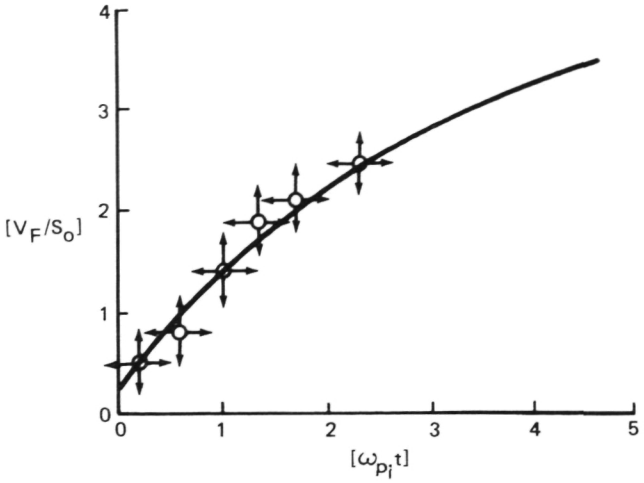

Figure 42. Plasma expansion across a strong density gradient. The data points are from MSFC experimental work, and the line represents a theoretical fit to a numerical model by Crow et al. (1975).

nospheric satellites and in the vicinity of natural density gradients produced in various solar system plasmas and specifically, the plasma dynamics of the Jovian satellite, Io, which involves light protons and heavy SO_2 ions.

A dual ion plasma accelerator for providing a more characteristic environment for flight instrument tests and calibration has been designed, and the construction is nearing completion. This binary plasma source will allow the generation of two completely independent streams of ions which are then superimposed and neutralized to form a single plasma stream. This will permit the selection of different masses, drift energies, and densities for each species of the stream.

During the 1985 reporting period "anomalous" ionization processes in the vicinity of positively charged conductors in plasma were observed as well as plasma expansion into the wake region behind a body in plasma flow. This compares favorably with theory. A useful new plasma generator has been designed and breadboarded for our laboratory plasma wind tunnel.

Wright, K. H., Jr., Stone, N. H. and Samir, U.: A Study of Plasma Expansion Phenomena in Laboratory-Generated Plasma Wakes: Preliminary Results. Journal of Plasma Physics, 33, p. 71, 1985.

Nobie H. Stone/ES53
(205) 453-0029
Sponsor: OSSA

Retarding Potential Analyzer/ Differential Ion Flux Probe

The Retarding Potential Analyzer/Differential Ion Flux Probe (RPA/DIFP) was successfully flown on the Plasma Diagnostics Package on the third Space Shuttle (STS-3) Mission, and reflown on Spacelab 2. The primary scientific objective of the instrument is to study the plasma environment around the Space Shuttle Orbiter with particular emphasis upon perturbations to the plasma environment produced by the Orbiter wake and sheath effects, by electron beam emissions from the Fast Pulse Electron Gun A Experiment, and by neutral gas emissions from the Orbiter. The instrument performed perfectly in all respects, and approximately 64 hours of flight data were received. The data show that the Orbiter produces significant perturbations to the local plasma. Analysis of directional ion flow data has revealed the presence of multiple ion streams near the Orbiter due to its interaction with the ionospheric plasma.

Experience gained from this and other flights of the probe has been used to improve the instrument design and operation. An improved design has been incorporated into flight instruments currently being prepared for two Centaur flights in January 1988. The purpose of the Centaur Sounding Rocket Program is to investigate charged particle acceleration mechanisms in the polar regions of the ionosphere to altitudes of approximately 700 km. Significant ion flows, shears, and reversals were observed on previous missions which passed through the cusp region.

Future instrument development will incorporate a mass analysis capability into the probe to provide a Differential Ion Flux and Mass Analy-

zer (DIF MA) instrument. This will provide the unique capability to separate complex, nonparallel plasma flows and analyze the ion energy and mass consistency of each independent ion stream. The results from STS-3 have shown this capability to be essential in the highly complex, contaminated Orbiter plasma environment. Flight instruments based on the resulting DIF MA design have been proposed for the electrodynamic Tethered Satellite System (TSS) Missions, TSS-1 and TSS-3, and for the Air Force Geophysical Laboratory (AFGL) Interactions Measurement Payload for Shuttle (IMPS) experiment to be flown on an early polar orbit Shuttle mission.

Nobie H. Stone/ES53
(205) 453-0029
Sponsor: OSSA

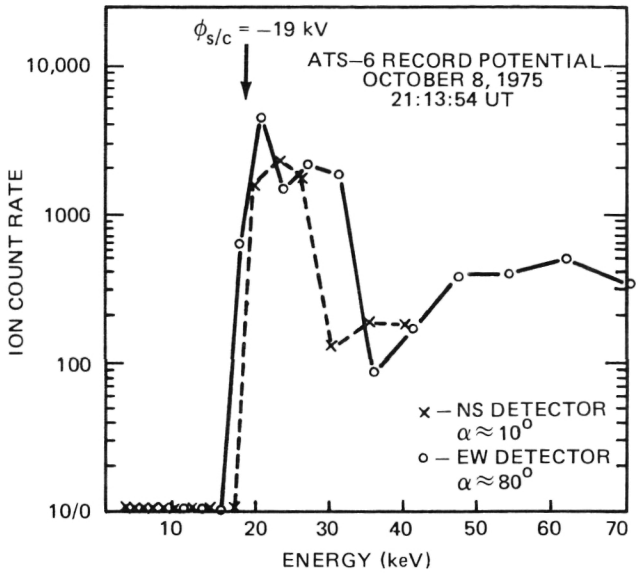

Figure 43. Ion Count Rate as a Function of Energy for the Record Eclipse Charging Event on ATS–6.

Spacecraft Plasma Interactions

Environmental effects on spacecraft include the charging of spacecraft by the ambient plasma. Such charging can affect the plasma measurements on the spacecraft and can even cause the loss of a satellite due to arcing and high-voltage (kilovolt) discharges. The study of such processes is based on the analysis of the interaction between satellite and plasma, using information about the environment inferred from the plasma measurements. These measurements are distorted by the interactions, so the process is an iterative one. The most spectacular case of high voltage charging is the negative 19 kV measurement made on Applied Technology Satellite 6 (ATS) during eclipse in 1975. Figure 43 shows the ion flux as a function of energy, showing how the ions of the magnetosphere are accelerated into the satellite in the electrostatic equivalent of falling into a well.

More subtle effects are found in the analysis of more recent data from the Retarding Ion Mass Spectrometer (RIMS) on the Dynamics Explorer 1 (DE 1) Satellite. RIMS data have been surveyed to determine the satellite potential in eclipse. Within the plasmasphere when the plasma density is over 100 cm^3, potential of a few tenths of a volt negative is observed, as compared to a few tenths of a volt positive in sunlight. Under these conditions the low-energy ions can be measured in sunlight or eclipse. At lower plasma densities (10-20 cm^{-3}), i.e., in the plasmapause region, the satellite potential in sunlight is typically a few volts positive, dropping again to near zero in eclipse. Under these conditions there are elements of the ion population which remain "hidden" in sunlight since they are unable to climb the potential hill to the satellite. These are the ions which become visible in eclipse.

One method of enhancing the ability to measure such ions at any time is to control the detector potential. For RIMS this means biasing the detector assembly and an external aperture plane negative with respect to the satellite. This technique made it possible to observe the supersonic polar wind, and infer a cold plasma background over the polar cap which had not previously been suspected. Analysis of the electrostatic potential distribution around the satellite for such conditions has required the application of large computer codes such as the NASA Charging Analyzer Program (NASCAP). In the future it is anticipated that active plasma sources will be used on individual

satellites to effectively anchor the spacecraft to plasma potential. The spacecraft potential will be monitored by a spacecraft potential monitor which will measure the characteristics of the spacecraft secondary electron energy spectrum from which the relative potential of the spacecraft and the surrounding plasma can be determined. Laboratory studies of the monitoring instrument have been initiated at MSFC.

A. P. Biddle/ES53
(205) 453 – 0818
Sponsor: OSSA

Low – Energy Charged Particle Flight Instrumentation

Information gained by the Retarding Ion Mass Spectrometer on the Dynamics Explorer 1 spacecraft and other instruments has led to a need for a unique, single ion species, low divergence, ion source facility. Such a facility would make possible the testing, development, and calibration of low – energy, mass resolved, low acceptance angle, directional flight instrumentation.

There is no present facility which is capable of combining all of the required parameters necessary to calibrate these instruments, especially with regard to usable fluxes below approximately 10 eV. The system being developed will allow rapid, accurate selection of beam energy, composition, and test article orientation. This unique system makes possible the external adjustment of the magnetic field configuration used to confine and guide the ionizing electrons. This will allow more efficient ionization of the working gas and uniformity of the beam output profile. The chamber diagnostics and manipulators are being upgraded to monitor the beam parameters and characterize the performance of various instruments being tested which will improve the amount of data available during a test. A microcomputer will also be used to integrate the system controls.

The prototype of the new ion source has been designed, fabricated, and tested (Figure 44).

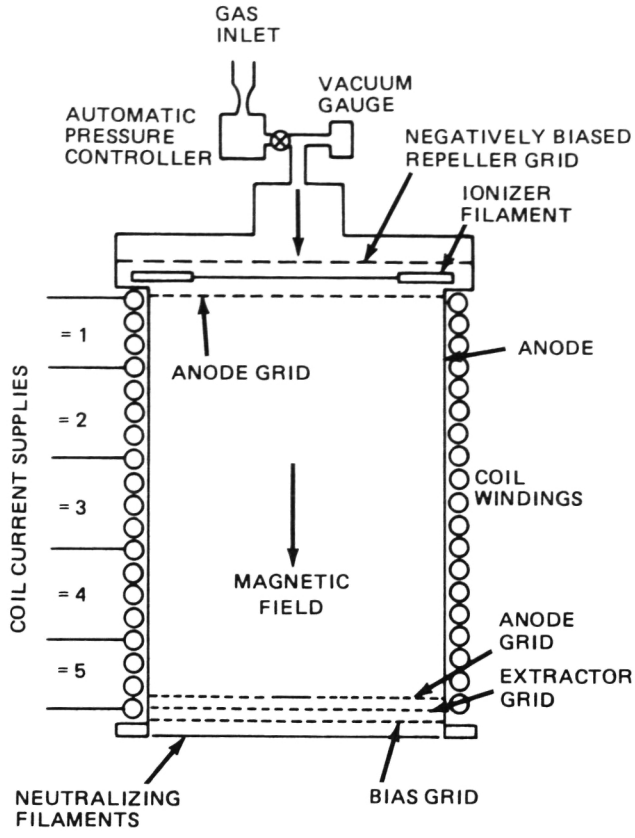

Figure 44. Newly Developed Source with Segmented Magnetic Field Coil and Improved Extractor and Ionizer.

Improvements in reducing beam divergence are evident in Figure 45 which shows current density as a function of beam energy for the baseline system as well as two configurations of the new ion source. The current density is almost independent of beam energy at the 0.24 cm grid spacing. Adding a segmented ionizer coil and an improved ionizer filament geometry has improved productivity and the impurity producing ionization near the ion source walls. This allows the source to run with less total power input, which enhances stability. The beam control system has been completed and an automated data reduction technique to reduce measurement time has been implemented.

The ion source design has been finalized during fiscal year 1985. The instrument chamber has been modified to include electronic focusing of the beam. The instrument facilities and basic chamber operation will be integrated un-

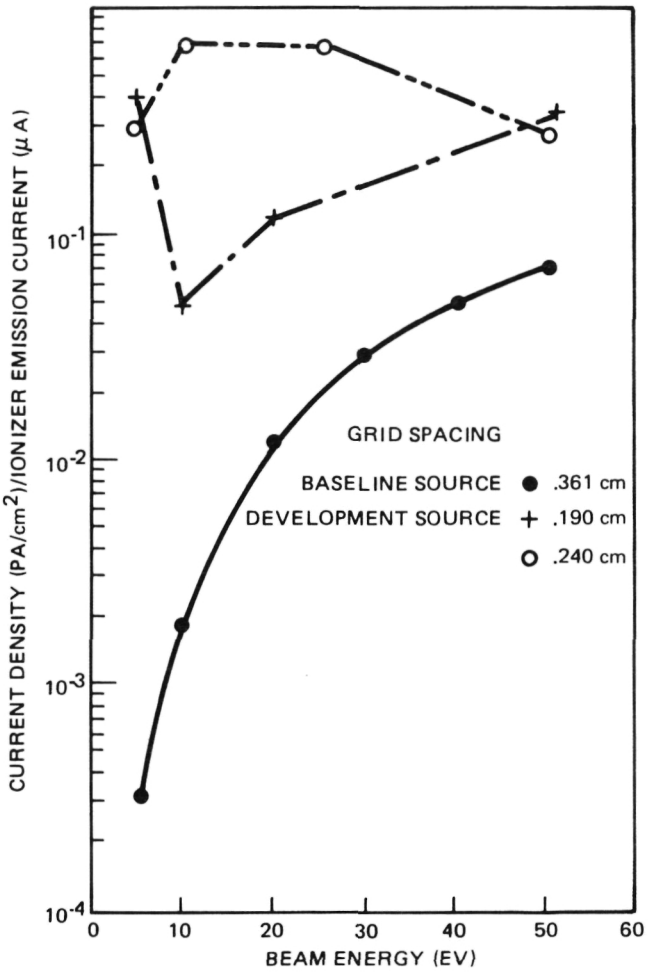

Figure 45. Beam Current Density vs. Beam Energy for Three Source Configurations.

der microprocessor control. The facility has been used during the past year to calibrate the STICS and a University of California at San Diego ion instrument.

A. P. Biddle/ES53
(205) 453-0818
Sponsor: CDDF

Space Physics Analysis Network

NASA scientific researchers are intensifying their data analysis efforts on correlative research by using data from a variety of satellite and ground-based instruments. The space science researchers and their data are located in universities, industry, and government institutions across the United States. Because of this there are fundamental requirements for data and information communication between remote space science investigators NASA scientists and facilities. In order to support these research activities, NASA must develop and demonstrate computer technologies required to facilitate data access, dissemination, retrieval, and space science information exchange.

The Space Physics Analysis Network, or SPAN, is emerging as a viable method for solving the immediate communication problem for the space scientist. SPAN provides low-rate communication capability with co-investigators and colleagues, and access to space science data bases and computational facilities. The SPAN users guide has been distributed to over 450 scientists across the country. The SPAN utilizes up-to-date hardware and software for computer-to-computer communications, allowing binary file transfer and remote log-on capability to over 36 nation-wide space science computer systems. New network nodes include six at MSFC, nine at the Jet Propulsion Laboratory (JPL), two at the University of California-San Diego (UCSD), Applied Physics Laboratory (APL), University of California-Los Angeles (UCLA), Lockheed, National Space Science Data Center (NSSDC), and three at Goddard Space Flight Center (GSFC). SPAN is not discipline or mission limited and scientists in such fields as magnetospheric, ionospheric, planetary, and solar physics participate. The network functions in such a way that the needs of the space science users are addressed while maintaining a stable environment for facilitating correlative space science research and information exchange.

The SPAN system performance is evaluated by the Data Systems Users Working Group (DSUWG). DSUWG consists of scientists and space data system managers from over 40 institutions. DSUWG meets at least once a year for the purpose of SPAN evaluation and acts as the scientific steering committee providing guidelines for data storage, access, and data and software distribution over the network. All

recommendations of DSUWG are carried out including the development and update of the network users guide, development of network facilities land gateways, use of the standard network graphics metafiles, and the use of the Data System Technology Program archive.

The Planetary Pilot Data System (PPDS) recently connected to SPAN will continue to use the network with the addition of three planetary nodes. Astrophysics users at the University of Wisconsin, UCSD, and MSFC have been added as network nodes. The NSSDC node of the SPAN system is providing an on-line data catalog that directs users to the desired data archives. In addition, the NSSDC is starting to serve as a software clearinghouse using the network to enhance software transportability and establish standard practices for documentation. SPAN will be used to transmit data to remote space scientists from the International Comet Encounter spacecraft as it passes by comet Giacobini-Zinner. Post-encounter data comparisons from this mission will also be accomplished through the use of SPAN.

The accomplishments during 1985 have included the establishment of six new nodes on the SPAN network, and the publishing of a SPAN users guide and graphics utilities handbook. A data catalog has also been initiated at the National Space Science Data Center.

It is anticipated that SPAN will grow rapidly over the next few years, not only from the standpoint of more network nodes, but as scientists become more proficient in the use of "telescience" (the use of telecommunications for scientific purposes), more capability will be needed to satisfy the demands.

Gallagher, D. L., Green, J. L. and Newman, R.: SPAN Graphics Display Utilities Handbook (First Edition). NASA TM-86500, May 1985.

Green, J. L., Baker, D. N. and Zwickl, R. D.: SPAN Pilot Project Report. 65, p. 777, 1984.

James L. Green/ES53
(205) 453-0028
Sponsor: OSSA

Space Experiments with Particle Accelerators

Space Experiments with Particle Accelerators (SEPAC) was a multi-component system flown on the Spacelab 1 mission and scheduled for reflight on the Environmental Observation Mission (EOM) 1/2 and Space Plasma Lab. The SEPAC system consists of an electron beam accelerator, a plasma jet generator, a neutral gas plume ejector, and a set of diagnostic instruments.

The system was designed for several scientific objectives, including study of Space Shuttle Orbiter charge neutralization under various conditions, investigating enhancements of charge neutralization by simultaneous plasma or neutral gas ejections, studying the propagation of charged particle and plasma beams in the ionosphere, and creation of "artificial auroras" to study the process of energy transfer from particle beams to the upper atmosphere.

The ejection of charged particle beams from a spacecraft requires a source of return current to the spacecraft to balance the beam current. The potential of the spacecraft will adjust so that the currents are balanced. In the case of the Orbiter, most of the surface is non-conducting except for the main engine nozzles. Figure 46 illustrates the occurrences of Orbiter charging for differing experimental conditions. These are values of Orbiter potential as a function of electron beam current for three different sets of beam firings, or Functional Objectives (FO). In FO-2, the Orbiter position-induced plasma flow from below the right wing and the conducting area of the main engine nozzles was shadowed from the ionospheric plasma. The Orbiter potential quickly exceeded 10 V for small beam currents, and reached several kilovolts for beam currents exceeding 100 mA. By contrast, in FO-5 and FO-7, the Orbiter tail was oriented directly along the velocity vector with the maximum possible conducting area exposed to the plasma flow. In these cases the Orbiter potential stayed below 10 V even for the maximum beam current of 300 mA.

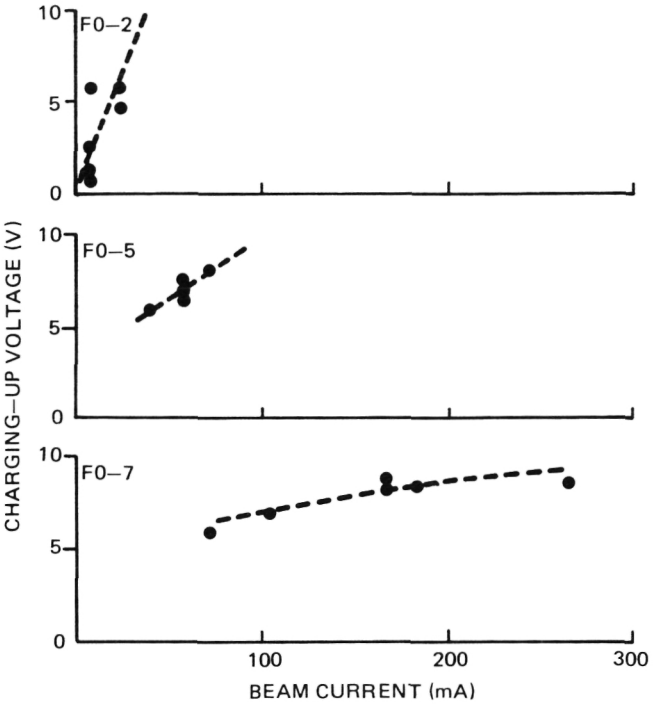

Figure 46. Orbiter Charging for Differing Experimental Conditions.

Orbiter neutralization was enhanced by momentary ejections of plasma or neutral gas. For the brief period that the ejections were activated, about 20 ms, the Orbiter potential returned to a very low value, less than 1 V. Plasma ejection provided a large effective contact area providing an additional path for return current. Ejection of neutral gas provided an enhanced source of secondary electrons produced by ionization of the gas by the primary beam. These electrons provided an additional return current.

Propagation of the electron beam through the ambient ionosphere was studied with diagnostic instruments, including a monochrome television system viewing the region around the exit aperture of the electron gun. For FO-2, a well-collimated beam was observed only for beam currents less than 100 mA. At high currents the primary beam became quickly diffused in both space and the energy spectrum. A diffuse glow surrounded the Orbiter and the measured electrons returning to the Orbiter displayed a wide energy spread with a significant number of electrons having energies up to three times the primary beam energy. This behavior was accompanied by strong electrostatic wave signals, indicating a beam-plasma interaction was occurring, transforming the energy of the primary beam into a wide spectrum of energetic electrons and plasma wave modes. Such behavior was quenched by ejections of plasma or neutral gas. This points to the necessity of insuring adequate charge neutralization when launching an electron beam from an insulated space vehicle without significant modifications of the beam in spatial extent or energy width. It has been established, during fiscal year 1985, that plasma contact with the conducting main engine bells is essential for maintaining neutrality of the Shuttle Orbiter during electron beam operations, unless concurrent with ejections of neutral gas or plasma from the Orbiter. Observations of beam plasma instability indicate that strong wave emission accompanies the disruption of the beam.

SEPAC will be modified for future EOM and Space Plasma Lab flights to include additional conducting area for return current collection and adding a continuous, rather than pulsed, plasma source to effect neutralization for the duration of an electron beam pulse. With these additions, the full capability of the SEPAC system as a space plasma diagnostic instrument will be realized.

David L. Reasoner/ES53
(205) 453-3037
Sponsor: OSSA

Astronomy

The Marshall Space Flight Center's research involvement and commitments in astronomy and astrophysics had its beginnings in early efforts in space science and solar physics associated with the Apollo and Skylab projects. Research and instrument development in gamma ray astronomy and cosmic ray astrophysics was carried out with a successful balloon flight program which led to the present Burst and Transient Source Experiment for the Gamma Ray Observatory and the successful on-going

international Japanese – American Cooperative Emulsion Experiments which observe high energy cosmic rays. The assignment of the HEAO program to MSFC initiated the development of a unique national x – ray telescope calibration facility, and theoretical and experimental research in x – ray astronomy. Recently , MSFC was assigned study responsibility for the Advanced X – Ray Astrophysics Facility. The Center's research activities and expertise in low temperature physics and cryogenics led to a partnership in developing the Spacelab Infrared Telescope. The development of an infrared array camera is the most recent result of a continuing interest in infrared astronomy dating back to Apollo related ground – based lunar observations.

X – Ray Astronomy

The second High Energy Astronomy Observatory (HEAO – 2) provided a wealth of information about x – ray emissions from a wide variety of celestial objects. The Time Interval Processor (TIP) of the Monitor Proportional Counter (MPC) on HEAO – 2 collected high time resolution data which are currently being studied to provide clues to the nature of these x – ray sources. These data are being used for pulse timing and studies of pulse shape variations of x – ray sources containing neutron stars such as LMC X–4, GX 1+4, and the recently discovered 50 millisecond pulsar in the Large Magellanic Cloud. The data are also being used to conduct searches for short periodicities (down to 0.25 ms) for galactic bulge x – ray sources and x – ray burst sources and to characterize the aperiodic time variability of non-pulsing x – ray sources such as black hole candidates Cyg X–1 and LMC X–3.

The study of the time variability of galactic x – ray sources using TIP/MPC data began in 1978 and has provided a useful probe into the physical nature of these exotic astrophysical objects. For example, in 1982 this research program led to the discovery of 69 millisecond x – ray pulses from the 16.7 – day recurring transient x – ray source, A0538 – 66.

Figure 47 is a schematic representation of one model for the A0538 – 66 binary system. Timing of the x – ray pulses led to the conclusion that the neutron star (black dot) moves in an eccentric orbit about its more massive Be star companion (shaded area). Intense x – ray emission occurs only near perihelion where the neutron star accretes material from either the extended and distorted outer atmosphere of the companion, a dense stellar wind escaping from the companion, or other circumstellar material (hatched region). In this way transient x – ray emission is produced every 16.7 days.

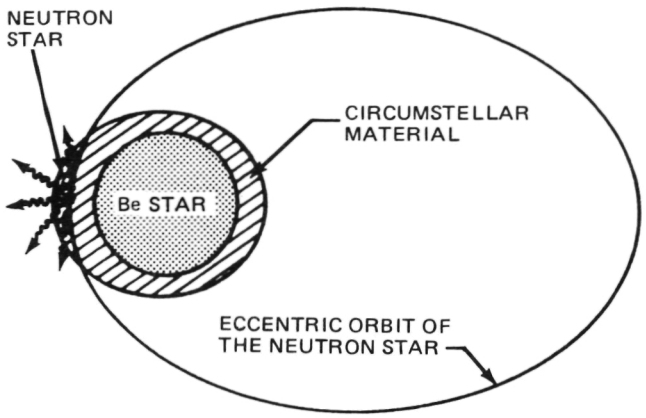

Figure 47. The A0538-66 Binary System.

In 1985 an analysis of the period history of LMC X – 4 has shown little measurable change in its 13.5 sec pulse period with a value for the spin – up time – scale of 4000 years. Assuming disk accretion, this value is consistent with standard accretion and torque models only if LMC X–4 is a fast rotator for which the accretion torques nearly vanish. This result allows an estimate for the neutron star's magnetic field strength of 1.2×10^{13} G. It has been demonstrated that precession of the companion star, a model first proposed in 1974, is unlikely to be responsible for the 1 – 2 month modulations in the x – ray emission from the pulsing x – ray sources LMC X–4, SMC X–1, and Her X–1. Quasi – periodic oscillations in the x – ray emission from GX 5–1 are currently under investigation. Members of the X – Ray Astronomy Branch have also participated during the past year in two Guest Investigator observations of cosmic x – ray sources using the

European Space Agency's X-Ray Satellite EXOSAT.

Associated with the data analysis and interpretation effort is a program of theoretical studies of physical processes that occur in the high temperature ($10^6 - 10^{10}$K), strongly magnetized (field strengths in the range $10^6 - 10^{13}$ G) plasmas expected to exist in the vicinity of accreting neutron stars. This program recently led to calculations of the properties of hydrogen-like atoms in the very strong magnetic fields that are thought to exist at the surface of neutron stars. The variational wave function used in these calculations led to analytic results that provide a useful supplement to more complicated numerical results that appear in the literature. In addition, it has been proposed that a double layer, a thin region separating two thin oppositely charged layers, may form in the accretion column of an accreting neutron star and play an important role in the deceleration of the infalling material. Such double layers in the accretion column of an accreting neutron star may have an impact on future models for the emission of x rays from these objects. This work may provide an important astrophysical application of a phenomenon first observed in terrestrial laboratories when sufficiently strong currents were passed through plasma.

The main experimental effort involves the development of an imaging fluorescent gated x-ray detector. This instrument has greatly improved background rejection over conventional proportional counters and, in addition, has the benefit of improved energy resolution. These improvements arise directly from a discrimination technique which makes use of the detection of the fluorescent K-shell photons emitted in most genuine x-ray interactions above 35,000 eV, the energy region of particular interest for studies of neutron star cyclotron lines. The laboratory prototype has exhibited an enhancement in signal-to-noise of a factor of 20 over that achieved when using ungated instruments.

Recently, funding was received from the Center Director's Discretionary Fund for an investigation into a new two-stage imaging technique that will further enhance the performance of the fluorescent gated detector. In this mode of operation, the usual conflict between high gas gain for good spatial resolution and low gas gain for good energy resolution is avoided by having two separate regions within the detector, one devoted to each parameter.

The fluorescent gated proportional counter seen in Figure 48 is equipped with a two-stage imaging system. The wire mesh visible at the top of the instrument forms a low gain pre-amplification stage from which charge is injected into the main imaging region.

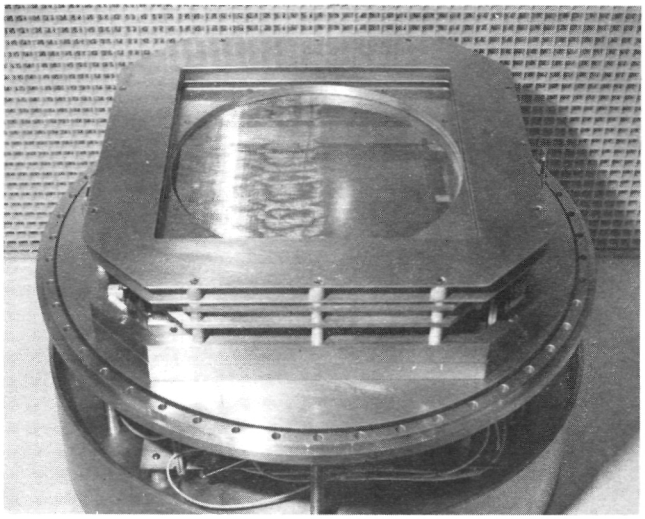

Figure 48. Two–Stage Detector.

The key to operating a detector in this manner is to find a suitable fill gas which will permit charge transfer between the two regions. Characteristics of various gas mixtures are currently under investigation. The addition of this technique to the fluorescent gated detector will provide a versatile astronomical instrument.

M. C. Weisskopf/ES62
(205) 453-3238
Sponsor: OSSA and CDDF

Advanced X-Ray Telescope Designs

The use of x-ray microscopes or relay optics for coupling the high-resolution grazing in-

cidence primary mirrors of x-ray telescopes to detectors or spectrometers promises to be of great value in future NASA x-ray astronomy programs. For many years the spatial resolution, as well as the wavelength coverage and sensitivity of x-ray telescopes, has been limited by the detector rather than by the optics. High-resolution detectors, i.e., photographic film, have poor sensitivity and limited wavelength response. High sensitivity detectors, such as micro-channel plates, Charge Coupled Devices, and position-sensitive proportional counters, can have broad wavelength response but usually restrict the spatial resolution because of large pixel size. X-ray microscope relay optics allow the use of high sensitivity detectors without sacrificing any of the resolving power of the primary mirrors of the x-ray telescope. The MSFC Solar Science Branch is engaged in designing and developing x-ray telescopes based on this concept.

There are two different kinds of x-ray optics that can be used to expand the image from the grazing incidence primary optics. One kind is a grazing incidence microscope that works on the same principles as the primary optics. This type of optic passes the entire spectrum longward of a few angstroms: soft x rays, ultraviolet, and visible. This permits the design of an extended wavelength range x-ray telescope such as in Figure 49. Such a telescope could use the MSFC flight back-up primary optics from the Skylab S-056 X-Ray

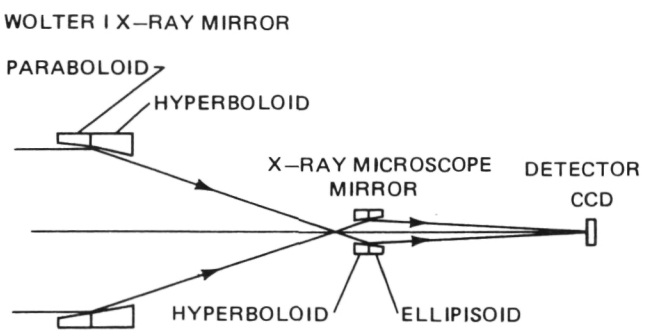

Figure 49. Extended Wavelength Range X-Ray Telescope.

Telescope to produce x-ray images of twice the spatial resolution over fields of view the size of typical solar active regions (a few arc minutes across).

The other type of x-ray magnifying relay optic is the Layered Systematic Microstructure (LSM) Mirror. An LSM mirror is coated with many layers of high Z diffractor material, each of precise thickness and each separated by precise layers of low Z material. The stack of coatings acts as a Bragg crystal to reflect slices of the x-ray spectrum a few tens of angstroms wide determined by the choice of layered material and thickness. LSM mirrors permit the design of dual path x-ray telescopes, such as in Figure 50, which use both the broad spectral

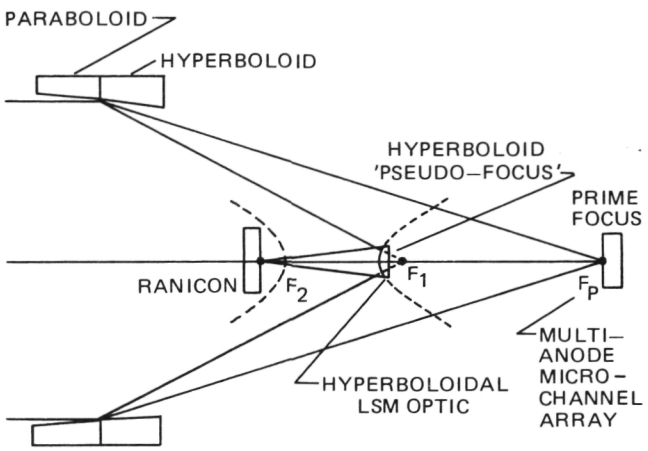

Figure 50. Dual Path LSM X-Ray Telescope.

band pass and wide field of view of the primary mirrors as well as the large collecting area of the secondary (hyperboloid) mirror at selected wavelengths with good spectral resolution.

Theoretical studies, completed in fiscal year 1985, established that the off-axis spatial resolution of an x-ray mirror can be significantly improved by reflecting the primary beam by an appropriately contoured LSM mirror. This allows sub-arc second spatial resolution as a result of general improvement in the system optical aberrations.

High quality LSM mirrors capable of effectively reflecting 44 Å x-rays was also fabricated on contoured spherical substrates during fiscal year 1985. These advanced, high resolution x-ray telescopes are suitable for sounding rocket flights, the Japanese/NASA High Energy Solar Physics Mission, the slit jaw monitor of an XUV spectrometer for the European/NASA

SOHO Mission, and the NASA Max '91 Mission.

R. B. Hoover/ES52
(205) 453 – 0118
Sponsor: CDDF

Gamma Ray Astronomy

Research in gamma ray astronomy has been performed at MSFC for over 10 years, primarily utilizing high – altitude balloons as the research platform. In addition to providing new scientific information, this balloon – borne research has enabled new experimental instruments and techniques to be developed and tested at low cost, before they are proposed as space – borne experiments.

The gamma ray astronomy observational program has used large – area, uncollimated scintillation crystal detectors. MSFC pioneered this technique, which has developed into the Burst and Transient Source Experiment (BATSE) for the Gamma Ray Observatory (GRO). The objective of these balloon flight experiments is to detect and study weak gamma ray bursts below the sensitivity of the first and second generation of satellite – borne gamma ray burst experiments.

The nature of gamma rays remains one of the outstanding puzzles in high energy astrophysics. Their brief duration and random occurrence in time and direction, as well as their lack of identified optical, radio, or x – ray counterparts, make them difficult to study. Most current models of gamma ray bursts are based on isolated old neutron stars. As a result of MSFC balloon – borne observations of weak bursts, it is believed that the burst objects are within our galaxy, although the distance scale is still highly uncertain. Figure 51 shows a weak gamma ray burst found by the four detectors of a 1980 balloon – borne array. The gamma ray balloon flights of 1980 and 1982 were among the longest U.S. scientific balloon flights ever flown, totaling over 70 hours at float altitude for the flights. The longer flights and sensitive detectors combined to provide important data on the frequency of gamma ray bursts at different intensities (Log N – Log S distribution). This distribution is related to the intrinsic luminosity of bursts and their spatial distribution. In 1985, data analysis was completed and published on the frequency of weak bursts using the balloon flight experiment results. Improvements on this measurement are not expected until the BATSE/GRO observations become available.

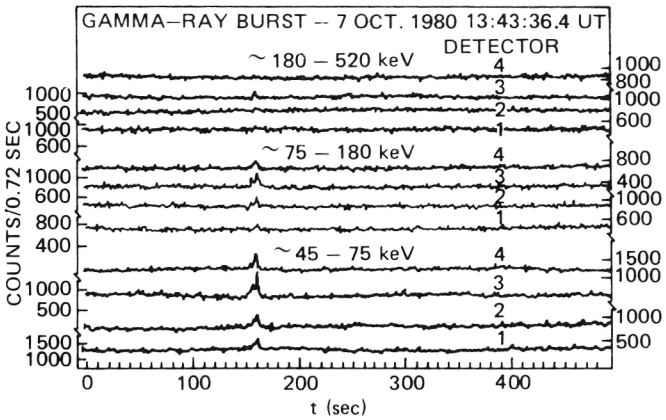

Figure 51. A Gamma Ray Burst Detected by the MSFC Balloon-Borne Detector Array in 1980.

In addition to observations of gamma ray bursts, the large – area detector arrays have proven to be sensitive detectors of other hard x – ray/low – energy gamma ray sources such as the pulsar in the Crab nebula, the x – ray source A0535+26, and solar hard x – ray flares.

At MSFC, measurements of induced radioactivity in spacecraft and detector materials are an important part of the gamma ray astronomy research effort. Measurements of neutron – and – proton – induced radioactivity have been made in metal samples returned from Skylab after 86 days in orbit and from recovered Skylab components after 7 years in orbit. MSFC is continuing these activation measurements, primarily with experiments on the Long Duration Exposure Facility (LDEF) and the Spacelab 2 Nuclear Radiation Monitor (NRM). In addition to activation measurements, calculations and measurements of atmospheric background radiation are expected to contribute to future advances in the reduction of background in gamma ray astronomy observations.

At the present time the supporting research and technology program is concentrating on data analysis and source detection techniques, scintillation detector optimization, and data system improvements. Many of these efforts are closely related to the development of the BATSE/GRO experiment. Preliminary designs for long-duration balloon experiments, and imaging gamma ray astronomy experiments are also being studied.

G. J. Fishman/ES62
(205) 453-5133
Sponsor: OSSA

Cosmic Ray and Particle Physics

In 1978 the Cosmic Ray Group at MSFC joined the Japanese-American Cooperative Emulsion Experiments (JACEE) collaboration, composed of four U.S. and four Japanese groups. The JACEE balloon flight experiments have as objectives the measurement of cosmic ray composition, and interactions spectra above 10^{12} eV. Five JACEE balloon flight experiments have flown three totally passive emulsion chambers and two with supplementary electronic counters.

The JACEE experiments have produced many new results in cosmic ray spectra, composition, and nucleus-nucleus interactions at high energy. The spectra of cosmic ray hydrogen and helium nuclei have been separately measured to 10^{14} eV, showing that both are simple extensions of the lower energy power law spectra. Also, about 50 nuclei heavier than helium at energies above 10^{12} eV have been analyzed, indicating that heavy nuclei above 10^{10} eV are not radically different from those measured by earlier experiments around 10^{10} eV. By microscopic measurements in the emulsion chambers, the number of secondary particles caused by heavy nucleus interactions, their angular distributions, and the fraction of charged and neutral pi mesons may be measured. The angular distribution of charged particles can be used to estimate primary energy. Further analysis produces the transverse momenta of neutral mesons, which is a measure of the "temperature" of the interaction region that produced the mesons.

In the JACEE experiments, the highest energy primary nucleus ever directly observed has been found (a calcium nucleus at 3×10^{15} eV total energy). Also observed was an event with the largest produced particle multiplicity, a 10^{14} eV silicon nucleus which interacted with a silver nucleus and produced 10^{10} charged mesons.

One reason for the strong interest in nucleus-nucleus collisions at high energy is the possibility of observing new states of nuclear matter. Theoretical calculations indicate that at sufficiently high temperature or energy density, protons and neutrons in the nucleus may undergo a phase transition to a plasma of quarks and gluons.

During the past year the fifth in the series of the balloon flight experiments was successfully flown from Palestine, Texas. Data analysis has been completed for experiments JACEE-1 through JACEE-3, yielding new information on cosmic-ray composition and the heavy nucleus interactions.

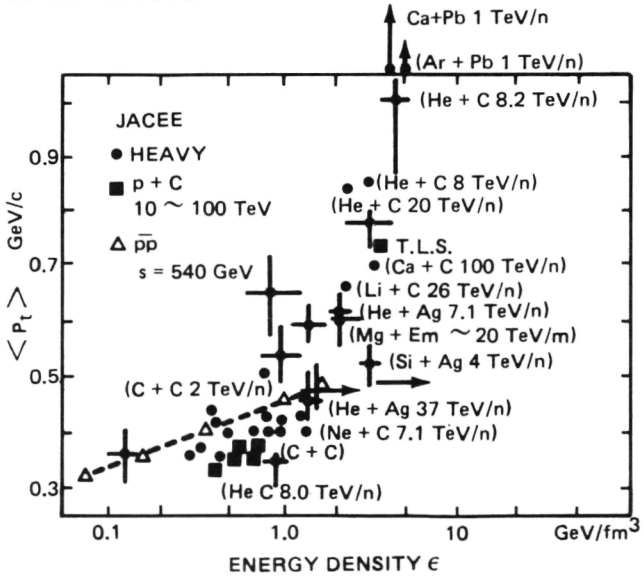

Figure 52. The Average Transverse Momentum of π^0 Mesons and the Energy Density in the Collision Volume is Shown for 30 JACEE Heavy Nucleus Collisions and 6 JACEE Proton-Nucleus Collisions. Data on proton-antiproton interactions at the CERN accelerator are also shown.

A result from this analysis has shown unusual behavior in the distribution of neutral pi meson transverse momentum versus energy density in the collision volume, and has attracted much interest. Figure 56 shows the results of an analysis for all heavy nucleus events that exceed an energy density of ~.5 x 10^9 eV/fm^3. The sharp rise at ~5 x 10^9 eV/fm^3 is near the theoretically predicted energy density for the nuclear matter phase transition. Although this small sample of events does not prove the transition has been observed, such results provide the incentive for future work in the observation of nucleus – nucleus collisions using cosmic rays.

T. A. Parnell/ES62
(205) 453 – 5133
Sponsor: OSSA and CDDF

Mid – Infrared Array Camera

Observation with a sensitive array is often the only practical way to map faint extended astronomical sources. Spatial arrays of detectors make more efficient use of observing time at large telescopes than single detectors. In ground – based, high – thermal – background environments, bolometers are the most sensitive detectors for wavelengths longer than 5 μm. They can be operated broadband ($\Delta^*\lambda/^*\lambda \approx 0.5-1$), are very infrared – sensitive, easy to use, and readily available. MSFC has developed a unique infrared camera detector system containing an array of 20 discrete gallium – doped germanium bolometers capable of imaging relatively large fields of view with very high sensitivity at 5 to 35 μm (Figure 53).

During astronomical observations, the telescope infrared beam enters vertically through the pressure window at the dewar top. The telescope focal plane is then reimaged onto the camera's close – packed array of 20 square field mirrors arranged in four columns and five rows. Each mirror provides a pixel size of 5 arc sec when used at the NASA 3 m Infrared Telescope Facility at Mauna Kea, Hawaii, with a total array size of 20 x 25 arc sec. The radiation incident on each field mirror is focused

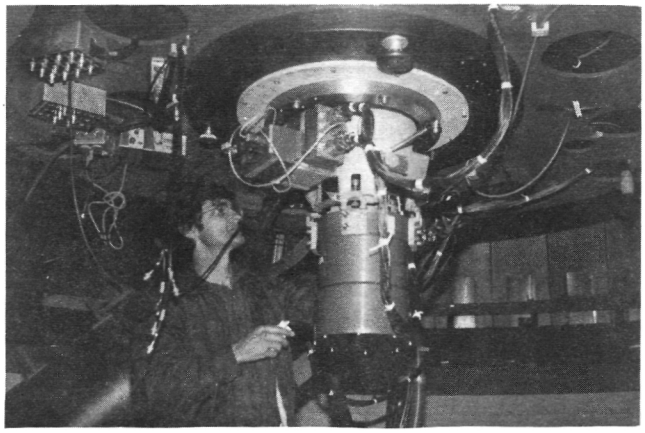

Figure 53. Infrared Array Camera.

onto a 0.3 mm square bolometer detector chip. For sensitivity, bolometers and camera optics are cooled to below 1.6 K using liquid helium.

Additional sensitivity is achieved by the use of an "up – looking" dewar and optics. Since this system is operated at the telescope Cassegrain focus, it views directly along the telescope's optical axis, avoiding additional warm (and, hence, infrared – emitting) beam – diverting optics.

The array has been field tested using the 2.3 m telescope of the Wyoming Infrared Observatory near Laramie. The array has performed well and is undergoing modifications to facilitate maintenance and increase efficiency.

Although this highly sensitive system is applicable to a broad range of programs, its primary purpose is to obtain infrared maps of star – forming regions in the Milky Way and other galaxies and to investigate sources discovered by the Infrared Astronomical Satellite (IRAS). Several university groups, in collaboration with MSFC, will study comets, particularly Halley and Giacobini – Zinner.

Charles M. Telesco/ES63
(205) 453 – 5136
Sponsor: CDDF

Infrared Astronomy

The Infrared Telescope (IRT) experiment for the Spacelab 2 Mission is a joint endeavor of the Smithsonian Astrophysical Observatory, providing the principal investigator, project manage-

ORIGINAL PAGE IS
OF POOR QUALITY

ment, and postflight data analysis; the University of Arizona, responsible for the infrared optics; and Marshall Space Flight Center in collaboration with the University of Alabama in Huntsville, providing the cryogenic system, mechanical equipment, and integration and test functions.

The infrared optics are carried in a helium gas – cooled, articulated cryostat which will scan about a single axis. Coupled with Orbiter motion, this will generate an extensive map of low – surface brightness and diffuse astronomical objects and will produce data on the Orbiter/Spacelab induced environment and its effect on cryogenic infrared astronomy.

Extensive testing has been conducted including mechanical, electrical function, cryogenic performance, acoustic, and thermal vacuum tests. In April 1984, the IRT was installed in the Spacelab 2 payload at Kennedy Space Center and underwent high vacuum and liquid helium servicing testing.

Liquid helium was loaded into the IRT in May 1985 in preparation for the July launch. In June the Spacelab 2 payload was installed into the Space Shuttle. Final liquid helium servicing of IRT will occur two and a half days before launch.

E. W. Urban/ES63
(205) 453 – 5132
Sponsor: OSSA

Atmospheric Sciences

Ground and space – based measurements of atmospheric parameters are used to develop and verify analytical and theoretical models of global and mesoscale atmospheric processes and establish remote sensor requirements. Field experiments provide the data required to verify the operation of air and spaceborne remote sensing instrumentation. Data derived from observations will be used as input to atmospheric model computer codes that can only be accommodated on large computer complexes. Extensive use is also made of interactive data display and access systems to study the time dependent development of atmospheric systems of all scales. The research program consists of theoretical/analytical model development, remote sensor development, flight payload analyses, and the laboratory and field experiments required in these activities.

The Geophysical Fluid Flow Cell

The cloud patterns of planetary atmospheres have long been a mystery to atmospheric scientists. In an effort to better understand the interaction between rotation and convection on a sphere, the Geophysical Fluid Flow Cell (GFFC) experiment was developed.

The GFFC, flown aboard Spacelab 3 (Figure 54), was designed to model the large – scale

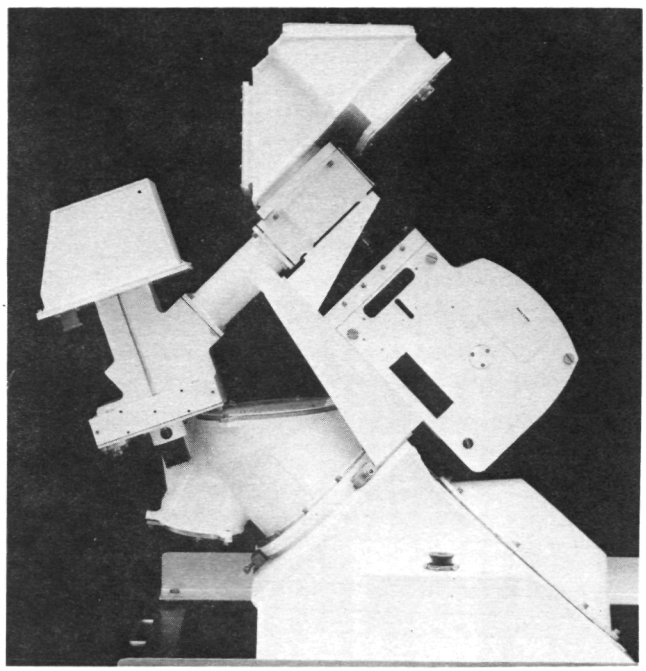

Figure 54. Geophysical Fluid Flow Cell.

fluid dynamics of a rotating, convectively unstable atmosphere similar to Jupiter, the Sun, and even the Earth's own atmosphere and oceans. To accomplish this, a fluid body force normal to the spherical surface was generated in order to properly simulate the relationship between the local gravity vector and the rotation vector of the body. The goal of the experiment was to obtain answers to crucial questions concerning the nonlinear mechanics of global geophysical flows using a spherical model. The results will verify existing theories of

moderately nonlinear fluid systems on spherical surfaces and provide basic data on flows which are more strongly nonlinear than can be currently modeled on a computer. Measurements of the fluid's temperature and velocity fields will determine the critical experiment parameters which lead to the onset of thermal convection.

Six of the experiments modeled the convectively unstable solar atmosphere. The experiments addressed such issues as eddy momentum transport, the equatorial zonal flow acceleration, flow structure of the solar atmosphere and may help to explain the differential rotation of the Sun. The experiments were characterized by an isothermal inner sphere and a cooler, but isothermal, outer sphere. These flows are expected to be both symmetric and asymmetric, as well as convectively unstable.

Six more experiments investigated geophysical atmospheric flows relevant to Jupiter in an attempt to explain its zonal cloud bands. These flows were also convectively unstable, as were the solar experiments; but, in addition, a north – south temperature gradient was superimposed. It is expected that this will produce a meridional torque that will be acted upon by the Coriolis effect to produce a large – scale zonal flow.

Five experiments examined Rayleigh – Taylor instability where the onset and equilibrium states of thermal convection are modified by rotation. Theoretical studies indicate that the onset of thermal convection is suppressed by rotation. Within an experiment the buoyancy is slowly increased by ramping the voltage upward from zero at a prescribed rate. In this manner, the voltage will be continuously known and the critical heating can be determined when convection is first observed.

Three experiments were devoted to the fundamental fluid dynamics of stratified spin – up in which stably stratified fluid which is initially at rest adjusts to the solid – body rotation of its spherical container. The spherical capacitor is initially at rest while the inner sphere temperature is cooler than the outer sphere. Next, the sphere is suddenly set into rotation, generating fluid motion which eventually approaches that of a solid body. Because the reversed temperature distribution is stably stratified, the fluid resists motion in the radial direction and complicates the spin – up process.

The remaining two experiments are relevant to the Earth's oceans in that the fluid will be stably stratified in the radial direction, but driven by baroclinic forces resulting from rotation and latitudinal temperature gradients. The outer sphere also has a similar north – south gradient, but is warmer than the inner sphere. The magnitude of this stable stratification is again controlled by the electric field.

These experiments represent the first ever to study thermal convection on a sphere. The experiment operated in a regime that is unobtainable with analytical methods or even the most powerful supercomputers. The information obtained from this research will give scientists new insights into the atmospheric dynamics of planets, the Sun, and Earth.

Fred Leslie/ED42
(205) 453 – 2047
Sponsor: OSSA

Theoretical and Experimental Studies of Baroclinic Processes

Baroclinicity in a rotating fluid is a state in which the constant pressure and density surfaces do not coincide. This condition is fulfilled when there exist horizontal temperature gradients in the fluid. On all but very small scales, the Earth's atmosphere in midlatitudes is approximately in geostrophic and hydrostatic balance. Because of the Earth's rotation, the horizontal pressure gradient force is balanced by the Coriolis force; furthermore, the pressure at a particular point is the result of the weight of the air above that point. These balances result in the inducement of primarily "zonal" (i.e., east – west) flow with a vertical shear which is proportional to the horizontal temperature gradient. Under strong enough temperature gradients, with resultant strong vertical shear, the basic zonal flow can be unstable to disturbances of various structures and energy

conversion mechanisms. These instabilities organize convection in the atmosphere on scales ranging from about 100 km (60 mi) to 5000 km (3000 mi).

In the laboratory, a working fluid such as water is contained in a cylindrical annulus and the outer cylinder wall is maintained at a colder temperature. The apparatus is rotated about the axis of symmetry. Depending upon the rate of rotation and size of the temperature difference, baroclinic waves may be observed which have a similar dynamic structure to certain of those observed in the atmosphere. The waves may result in steady, vacillating, or chaotic flow depending upon the parameters. Verification of theories of baroclinic flows is done more easily and less ambiguously in the laboratory than by directly observing the atmosphere, since the latter is a much more complicated system with many types of instabilities present. The development of the baroclinic wave into frontal type structures was observed and the results were quite different from the observations in the previous studies. In addition, two new regimes of flow were discovered.

Most of the theoretical research done at MSFC has been of the smaller scale (mesoscale) instabilities. Historically, there has been less work done on these instabilities than on the larger scale phenomena. The primary reason for this is that the smaller scale instabilities are mathematically much more complex than the larger scale phenomena. Numerical (computer) methods have been used to solve the equations of motion and thermodynamics to show how these disturbances create instability in the basic state, what the disturbances look like in the pure situation, and how they feed back to the basic state. The results show that the addition of small viscous and thermal dissipation to the inviscid problem can have quite important effects. The most unstable wave orientation deviates from the "symmetric" orientation that inviscid theory predicts. This allows transition to instability more quickly. The presence of negative potential vorticity is shown not to be required for instability. It has been observed that the basic state can be unstable to a wide spectrum of wavelengths. The energy transfer mechanisms have been studied and have shown that the energy sources for the perturbations can be buoyant, inertial, or a combination, depending upon the parameters. In the fully nonlinear, "symmetric" problem, there is a wave-induced mean circulation such that the net energy flux is zero, and therefore the ultimate energy source is the basic state's potential energy.

This experiment, conducted during fiscal year 1985, is a study in a baroclinic annulus with heating and cooling on the upper and lower horizontal surfaces. The work is completed and four basic regimes were observed. A linear analysis of the three dimensional, non-geostrophic baroclinic instability was also completed, and results have been discussed in an article submitted for publications.

Timothy Miller/ED42
(205) 453-2087
Sponsor: OSSA

Contributions to Monte Carlo Turbulence Simulation

Monte Carlo simulation of turbulence began in the mid 1950's with simple one dimensional simulations, i.e. the turbulence varies only along the flight path. Transverse changes in turbulent gusts were ignored. These variations along the wing of a vehicle are the major contributors to rolling and yawing. Many of the significant advances in Monte Carlo turbulence simulation are concerned with adding three dimensional character to the simulation (Figure 55).

Another concern of turbulence simulators is that the simulation be computationally efficient and the resulting time histories be realistic spectra. In the real atmosphere at the response frequencies of most flight vehicles, turbulence spectra vary as frequency raised to the $-5/3$ power ($f^{-5/3}$). The fact that the spectra do not roll off as integer powers of frequency causes computational problems. Some efforts in the past were directed at fitting these realistic irrational spectra with rational approximations, but either the approximations were

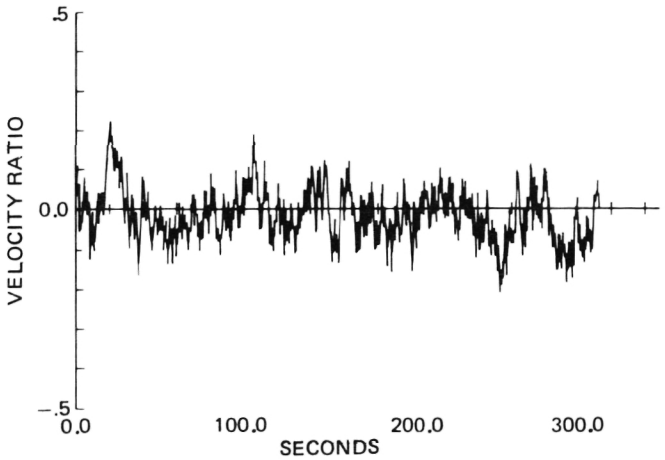

Figure 55. An Example of Simulated Turbulence. The Time History was Generated Using the von Karman Approximate Method and is Usually Indistinguishable from Real Turbulence.

bad or the filters were unstable. In the past year an accurate rational approximation to the irrational spectra was developed with stable filters. The result was an efficient method for generating accurate one-dimensional turbulence.

The method is general enough for application to three-dimensional simulations. One way that three-dimensional realism can be added to flight simulations is to select several points over the body of the vehicle and simulate turbulence at each of these points. The simulated time histories must have accurate signal-to-signal correlations or the correct vehicle response cannot be calculated. Using the rational approximation method, and the multipoint aircraft model, efficient three-dimensional simulations may soon be possible.

C. Warren Campbell/ED42
(205) 453-1886
Sponsor: OAST

Global Wind Measurement by Satellite Doppler Lidar

Present satellite capability makes possible the direct measurement of wind profiles around the Earth. Such measurement is valuable in understanding the dynamics of global atmospheric circulation, climate, and mesoscale processes.

The most advanced wind measuring method for spacecraft usage is Doppler Laser Radar (Lidar) using a CO_2 laser (Figure 56). This

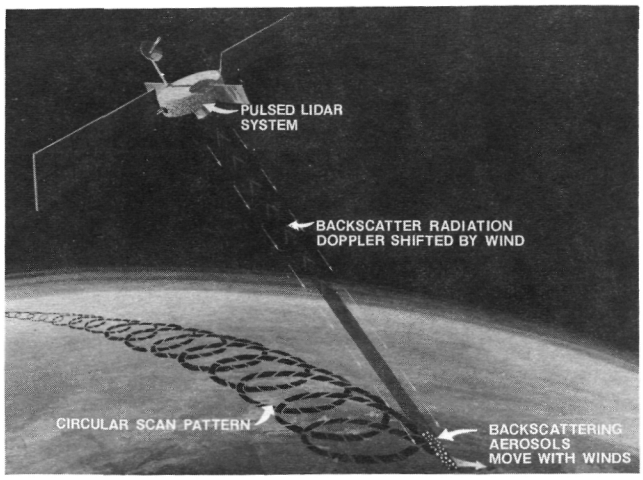

Figure 56. Global Wind Measurement.

instrument determines the velocity of naturally occurring aerosol particles along the laser beam. Adapting CO_2 lidar technology to spaceflight is a straightforward extension of present systems. The largest existing laser usable for Doppler lidar has an energy of 2 J/pulse, while the amount needed for a satellite Doppler lidar is approximately 10 J/pulse. The nature of the velocity measurement requires the development of appropriate scanning techniques. This is crucial to the satellite design since it determines the pulse rate and the power required. Because the effective measurement volume is very small, a scanning and sampling strategy must be developed so that individual velocity measurements can be averaged into a meaningful value.

The amount and distribution of backscattered radiation from atmospheric aerosols must be estimated in order to find the pulse energy required and to make good performance forecasts. These data do not exist in the required wavelength range, so a backscatter assessment program is necessary.

Today, at MSFC, studies are underway to develop a simple design for a Space Shuttle demonstration experiment, to determine optimum scanning strategies and to model a Doppler lidar satellite system response. In fiscal year 1985, a backscatter assessment pro-

gram was organized by MSFC by participating researchers from MSFC and other NASA centers. Ground-based measurements from several laboratories and aircraft flights were included. Benefits of global wind profile measurements are being assessed at Goddard Space Flight Center (GSFC).

Flight opportunities range from the Space Shuttle to a dedicated satellite. A polar orbiting satellite in LEO would be ideal for this instrument, which would allow twice daily coverage of the globe. A satellite in a low inclination orbit could also be used, since little wind data is available for the tropical region.

To summarize the work done during the past year, a Shuttle accommodations study was completed which showed no incompatibilities with using the Shuttle to place a Doppler Lidar in orbit. The laser design was also completed during this reporting period.

Daniel E. Fitzjarrald/ED43
(205) 453-3647
Sponsor: OSSA

Analysis of Airborne and Ground-Based Doppler Lidar Data

The MSFC Doppler Laser-Radar (Lidar) System (DLS) has been used frequently in both ground-based and airborne modes to meet many scientific and engineering objectives. In 1981 and 1984, it was flown aboard the NASA Convair 990 aircraft, while in 1982 it was used in the Joint Airport Weather Studies (JAWS) Project field experiment. The DLS was then returned to MSFC and operated for about a year, again in the ground-based mode, to measure backscattered intensity and winds.

Analysis of lidar data from the JAWS experiment showed for the first time that observations from several lidars can be combined for all three wind components. Findings were consistent with a surface network of anemometers. A collocated comparison with data from a 5 cm Doppler radar, at low elevations in clear air, showed the lidar velocity measurements to be free of bias from ground clutter.

The most significant result of the MSFC studies is measurement of volume backscatter (ß) and absorption (α) coefficients, both integral properties of the aerosol backscatterers. These measurements were made in response to a proposal to measure Earth's troposphere winds using an orbiting carbon dioxide laser. Measurement accuracy of the lidar and design criteria for the lidar itself depends on knowledge of the spatial and temporal distribution of global troposphere backscatter. Vertical profiles of α and ß through the lower troposphere for April 1983 – February 1984 were computed. In a typical vertical profile, the greatest ß occurs in a layer extending from the surface to 1 – 3 km, beyond which ß decreases rapidly. Measurements at different heights show distinct seasonal trends, α and ß being greatest during summer and smallest in winter. Below 1 km, ß follows a monomodal, log-normal probability distribution; above, there is evidence of a bi-modal, log-normal distribution.

Preliminary analysis of fall 1984 flights has commenced with emphasis on two research opportunities: flow around an isolated mountain and flow divergence downstream of a narrow pass. Several racetrack patterns were flown around Mt. Shasta, California, an isolated mountain approximately 3 km above the surrounding terrain. Results show that upwind of the mountain the backscatter was below the limit of detectability of the lidar system. Downwind were broad areas of higher backscatter spreading in a v-shaped pattern behind the peak, indicating that the three-dimensionality of the flow had vertically transported aerosols from a lower level. Wavelike velocity variations were evident.

One research flight was flown downstream of the Carquenez Straits in the Sacramento River Valley. The flight tracks were chosen near the top of the boundary layer normal to the flow to measure flow divergence through the straits from the San Francisco Bay area into the Central Valley. Lidar scan patterns were chosen to measure winds from the aircraft altitude down to the surface. Results show a turning of the wind as it spreads downwind with features and subtleties induced by the topography. These

measurements are unique and are of particular interest to air pollution meteorologists.

Rothermel, J.: Coherent Lidar Measurements of Backscatter and Transmission Loss Profiles. Optical Society of America. Incline Village, NV, 15 – 18 January, 1985.

Jeffry Rothermel/ED43
(205) 453 – 1944
Sponsor: OSSA

Doppler Lidar, Research and Development

MSFC has been actively involved in the research, development, and application of coherent Doppler Lidar systems since the first successful demonstration of wind measurement in 1967. Systems have been developed for various applications, including the measurement of clear air turbulence, wing tip vortices, wind shear, severe storm outflow, wind field mapping, and atmospheric backscatter. These systems have evolved to the point where they are considered valuable tools for research in meteorological applications.

In recent years, system development has been directed toward meteorological research in mesoscale and global scale wind measurement. This year work was concentrated in three primary areas. First, a number of modifications were made to the MSFC pulsed Doppler Lidar to improve its performance in the area of beam pointing and control and to gain a better understanding of system losses for the purpose of accurate system calibration. The system was installed on the Ames Convair (CV) 990 and flown in August and September 1984 to perform wind field mapping around isolated mountain peaks, to examine the inflow into the Central Valley of California, to examine marine boundary layer flows off the coast of California, and to map wind fields in the vicinity of ground – based Doppler wind profilers in Pennsylvania.

In the second area, the 10.6 μm continuous wave backscatter lidar was modified and flown along with the pulsed system in the CV – 990. This instrument was flown to provide data on the atmospheric backscatter, a parameter which heavily influences the potential operation of a space – based Doppler lidar wind measurement system.

The third area of concentration involved the preliminary system definition of a Shuttle Coherent Atmospheric Lidar Experiment (Figure 57). This study is aimed at flying a

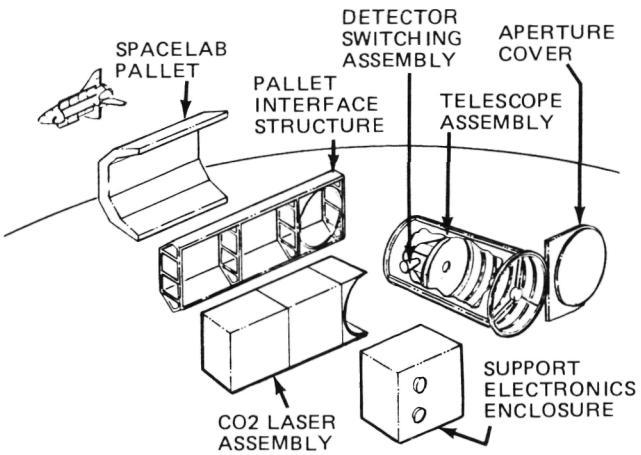

Figure 57. Shuttle Lidar Flight Experiment.

pulsed coherent lidar on the Shuttle to measure atmospheric backscatter, cloud heights, and winds to demonstrate the feasibility of operating such a lidar in space and to demonstrate the capability of performing wind measurements for a free flying space – based system.

Bilbro, James W.: Airborne Doppler Lidar Wind Field Measurement. OSA Topical Meeting on Optical Remote Sensing of the Atmosphere, January 15 – 18, 1985.

James W. Bilbro/EB23
(205) 453 – 1596
Sponsor: OSSA

Low – Altitude Flow Conditions

MSFC is currently studying variable atmospheric conditions which are potentially hazardous to aircraft flying at low altitudes. More information is needed describing phenomena in the lowest 150 m (500 ft) of the Earth's atmosphere, particularly information related to boundary layer conditions hazardous to the ascent and descent of the Space Shuttle and

conventional aircraft. These known hazards include turbulence which produces rapid oscillations such as shaking, pitching and yawing, wind shear which produces changes in air speed, and vertical motion which produces changes in altitude. Wind shear in the zone between relatively calm air in an atmospheric temperature inversion and a strong horizontal wind above the inversion can cause an abrupt turbulence encounter at low altitude. These flow conditions can, and frequently do, occur simultaneously. A classic example of disastrous wind shear and vertical motion occurrence was the crash of Pan American World Airways Flight 759 at New Orleans on July 9, 1982. Between start of takeoff roll and crash (29 sec) the aircraft experienced a decreasing headwind shear of about 19.5 m/sec (38 kts) and a 2.1 m/sec (4.1 kts) downdraft at 30.5 m (100 ft) above the ground.

Research is being conducted to describe and understand these hazards and their effects by using existing data from aircraft and meteorological towers. One available data base is the Atmospheric Sciences Division's high resolution wind and temperature profile measurements from the NASA 150-Meter Ground Winds Tower Facility located at Kennedy Space Center, Florida. The tower is approximately midway between Launch Complex 39B and the Space Shuttle runway. Ongoing empirical investigations are being conducted to determine magnitude, frequency, diurnal, nocturnal, duration, simultaneity of wind shear, turbulence, and vertical motion, along with relevant temperature inversion. Meteorological mechanisms causing strong wind shear are gust fronts formed from mature, severe thunderstorms, fast-moving frontal zones, and in rare occasions low-level inversions formed early in the morning near the surface.

Data on wind speed and direction shear, gustiness and gust factor, updraft and downdraft during strong or gusty winds have been published. Mathematical and graphical descriptions of absolute, positive and negative speed and direction shears both vertically and along a flight path have been determined as functions of intensity categories and significant values. The magnitude and frequency of wind shear would be more valuable for probability estimations, model development and flight simulation if duration were include, therefore, duration of speed and direction shear determinations are also to be published. Other studies planned or in progress include gustiness versus gust factor as measures of turbulence, wind shear and surface inversion at sunrise and sunset, magnitude of maximum downdrafts and heights of maximum occurrence, and shear and turbulence in stable flows found during nighttime conditions.

Alexander, Margaret B. and Camp, Dennis W.: Significant Events in Low-Level Flow Conditions Hazardous to Aircraft. NASA TM 82522, January 1983.

Alexander, Margaret B. and Camp, Dennis W.: Wind Speed and Direction Shears with Associated Vertical Motion During Strong Surface Winds. NASA TM 82566, February 1984.

Alexander, Margaret B. and Camp, Dennis W.: Analysis of Low-Altitude Wind Speed and Direction Shears. Journal of Aircraft, July 1985.

Margaret B. Alexander/ED42
(205) 453-2087
Sponsor: OSSA

Satellite Infrared Remote Sensing of the Formation and Development of Convective Storms

The Man-Computer Interactive Data Access System (MCIDAS) has been used to process infrared and visible critical prestorm imagery obtained from a geosynchronous satellite. This imagery provides information about storm formation, development and dissipation.

The temperature lapse rate above the tropopause affects the potential energy storage of clouds penetrating the tropopause. Potential energy and maximum differences between cloud top and tropopause temperatures have been analyzed for four storms that produced 27 tornadoes. The total potential energy storage for these storm clouds ranged from 10^{12} J to 10^{15} J depending upon the number of tornadoes produced.

Potential energy per unit volume is closely related to the Fujita scale of storm damage. The study showed that an overshooting cloud top with potential energy per unit volume of 32 J/m^3 was responsible for the production of a devastating storm causing damage of F4 on the Fujita scale, with wind speeds of 332 to 416 km/h, while energy levels of 7 – 10 J/m^3 caused storm damage of F3, with wind speeds of 253 to 331 km/h.

Potential energy per unit of volume and the temperature difference between the overshooting cloud top and the tropopause are closely related but not in a linear dependency because the ambient vertical temperature gradient above the tropopause is different for different storms. The potential energy per unit volume calculated from satellite infrared imagery can better characterize the intensity of storms on the Fujita scale of storm damage.

The Tibet Plateau significantly affects development of rain storms in China, as the Rocky Mountains influence weather in the United States. Many rain – bearing synoptic systems in China originate over the Plateau, move east and north, causing heavy rains and severe storms in eastern and northern China. In the First Global Atmospheric Research Program (GARP) Global Experiment (FGGE), the GOES – 1 satellite was moved over the Indian Ocean where its imagery was used to study convective cloud development and the amount of rainfall over the Plateau area in comparison with that over the Rocky Mountains.

The heavy rainfall in the Plateau is usually preceded by high altitude growth of convective clouds followed by a rapid collapse of the cloud tops. The study also shows that the tops of convective clouds associated with heavy rainfall over the Plateau usually lie between the two tropopauses over the Plateau. Collapse of the cloud as observed from the satellite correlates well with the beginning of rainfall observed by the ground stations; and cloud dissipation as seen from the satellite infrared imagery correlates with the ending of rainfall observed by the ground stations. The volumetric dissipation of clouds per unit area over a ground station in comparison with rainfall recorded at that station shows a linear relationship for rainfall amounts exceeding 8 mm. The ratio of observed rainfall at the ground station over the satellite observed cloud volume dissipation per unit area was also computed.

The resulting ratio is almost constant with a value of 9.55 mm/(pixel · km/pixel) for rainfall amounts exceeding 15 mm, and the variation is less than 10 percent for rainfall amounts between 8 and 15 mm (Figure 58). The results of the 1985 analyses show that in the U.S. the

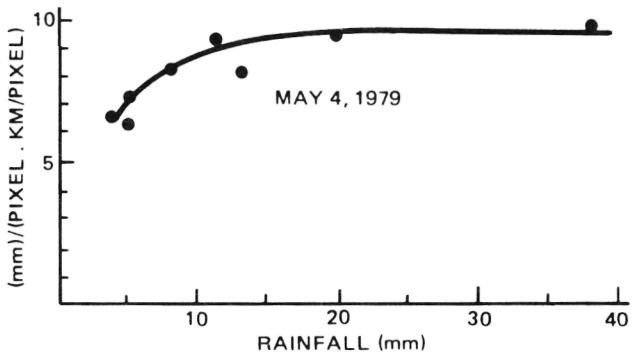

Figure 58. Observed Rainfall – Satellite Observed Cloud Volume Dissipation/Area over Tibet Plateau.

potential energy per unit volume of convective cloud turrets above the tropopause is proportional to the severity of the ensuing tornadoes, as measured by the Fujita storm damage scale. It also showed that over the Tibet Plateau the volumetric dissipation of clouds per unit area is linearly related to rainfall amounts over eight mm on the ground, and the ratio of observed rainfall amounts on the ground to the cloud volume dissipation per unit area is constant for rainfall amounts exceeding 15 mm.

Hung, R. J., and Smith, R. E.: Computer Image Processing of Up – Draft Motion and Severe Storm Formation Observed from Satellite. Flow Visualization, 3, pp. 686 – 693, 1985.

Hung, R. J., Liu, J. M., Tsao, D. Y. and Smith, R. E.: Relationship Between Convective Clouds and Precipitation Over the Qinghai – Xizang Plateau Area from Satellite Remote Sensing and Ground – Based Observation. International Journal of Remote Sensing, 6, pp. 217 – 237, 1985.

Robert E. Smith/ED41
(205) 453 – 3101
Sponsor: OSSA

Technology Programs

The initial assignment of responsibility for design and development of large launch vehicles and their associated rocket propulsion systems to MSFC a quarter of a century ago represented a significant technological challenge. The extraordinary success in carrying out this responsibility from the initial task of modifying the Redstone rocket for manned space flight to today's Space Shuttles is fitting testimony to the many technological achievements necessary to attain this level of excellence. New assignments given to MSFC over the intervening twenty-five years and the transition to a multi-program development center for complex space flight systems have significantly expanded the breadth of the Center's technology programs. In addition to propulsion and launch vehicle design, MSFC's technology initiatives include material science, materials processing, space power, structures and dynamics, heat transfer and fluid mechanics, robotics, and information systems. These diverse technology programs have provided additional opportunities to apply the talents of a highly capable and diverse engineering team.

The development of advanced technology has been the cornerstone of our success. The challenges which have been met, and the results produced, have served to advance the state of the art in many fields of engineering and have prepared MSFC to assume even more challenging assignments in the future.

Liquid Propulsion Systems

Application of Powder Metallurgy Techniques to Produce Improved Bearing Materials for Rocket Engine Turbopumps

The Space Shuttle Main Engine (SSME) High Pressure Oxidizer Turbopump (HPOTP) bearings represent perhaps the most demanding cryogenic application for bearing materials today. These bearings operate at high speeds and with practically no lubrication because conventional lubricants cannot be used at cryogenic temperatures. Some of today's best bearing materials used in gas turbine engines, M-50 for instance, are lubricated with oil. However, these bearing materials cannot be used in cryogenic turbopumps because of corrosion problems. Because of this, corrosion resistant, state-of-the-art 440C bearings are used in the SSME. Unfortunately, these bearings have a relatively short life in the HPOTP. Bearing life is limited by excessive wear and spalling by rolling contact fatigue. To improve bearing life, bearing materials with greater resistance to wear and spalling are being developed. The new materials are prepared by powder metallurgy techniques. The main advantage of the powder metallurgy technique lies in the ability to control the volume percentage and the size of the primary carbides which are the most important microstructural constituents in bearing steel. In conventional wrought materials the carbide sizes and distribution are dependent on alloy composition and solidification rates. Large carbides often result because of slow solidification rates and a large volume percentage of carbides. Banding of carbides often occurs with hot rolling, which is detrimental to bearing life. Powder metallurgy

techniques, on the other hand, produce uniformly distributed fine carbides in spite of high volume percent, and tend to improve bearing life. High volume percentage of carbides increases the hardness and hence the wear resistance of bearing materials.

Several promising bearing materials were procured in gas atomized powder form, compacted into cylindrical shapes and isostatically hot pressed to obtain 100 percent density. The cylinders were then hot rolled into half inch round bars. These bars were tested for rolling contact fatigue life, wear resistance, corrosion resistance, and fracture toughness. A comparison of the B_{10} lives (number of cycles to 10 percent failures) for the candidate bearing materials and the 440C bearing alloy is shown in Figure 59. MRC – 2001, X – 405 and

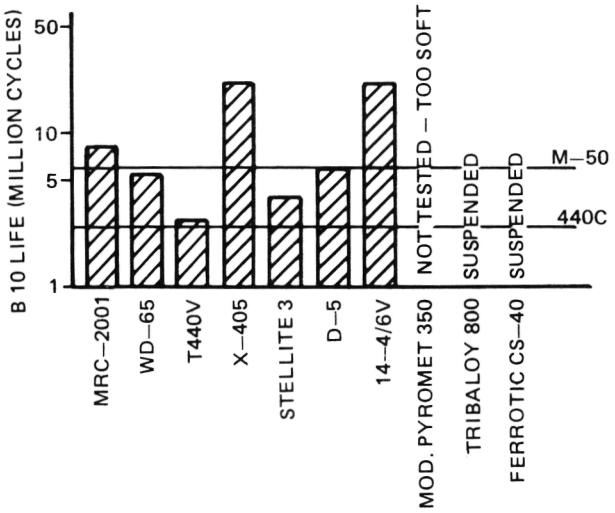

Figure 59. A Comparison of the B_{10} Lives for the Candidate Bearing Materials and the Baseline 440C Bearing Alloy.

14 – 4/6V materials appear to be the most promising. Further testing is under way to verify the preceding findings. The plan is to manufacture full – scale bearings from the candidate materials for testing in the MSFC cryogenic bearing tester.

Biliyar N. Bhat/EH23
(205) 453 – 5509
Sponsor: OAST

Rolling Contact Fatigue Behavior of Ion Plated Bearing Materials

Research is being conducted to improve bearing life by applying coatings, either very hard and wear resistant or very soft to act as a quasi – lubricant. In this program, bearing materials are being coated by ion plating and then tested at two stress levels for rolling contact fatigue resistance. Two different types of coatings are applied. The first is very soft and meant to behave as a lubricant, spreading out the contact stress and preventing asperity – to – asperity contact. Materials to be used are copper, gold, and silver. The second type of coating is extremely hard, wear resistant and has a decreased coefficient of friction. Titanium nitride is the candidate for this "hard coat." The coatings that produce positive results in rolling contact fatigue tests will be applied to full – scale SSME bearings. These bearings will then be tested in the MSFC Bearing and Seal Materials Tester (BSMT). The full – scale tests will duplicate the environment of the actual SSME turbopump bearings experience.

The results of rolling contact fatigue tests on coated bearing materials are very promising. The maximum shear stress which is considered to be the driving force for fatigue failure in this type of test is located about 100 μm below the contact surface. The coatings are applied to thicknesses in the range of 1 μm. Therefore, it was postulated that any cracks which initiated near the areas of maximum shear stress would have little difficulty in passing from the bulk, through the coating, and to the surface. Thus a coating of only 1 μm was thought to be inconsequential in affecting the initiation of or stopping of an internally initiated crack. However, the results have been very positive for rolling contact fatigue resistance of coated bearing materials.

The samples were tested at 4.04 GPa (586 ksi) and 5.42 GPa (786 ksi) maximum Hertz stress. Two materials were used as substrates, 440C and AMS 5749 (Latrobe's BG42). The data are very promising, especially for titanium nitride

coatings of 0.8 μm. Testing of gold and silver coated samples will be done shortly, and the titanium nitride coating of full-scale bearing elements is being developed at this time.

Robert L. Thom/EH14
(205) 453-2010
Sponsor: OAST

Methane Heat Transfer Investigation

Future launch vehicles have a potential need for high pressure rocket engines which use a relatively dense hydrocarbon fuel. System performance studies have indicated that liquefied methane or natural gas composed of approximately 94 percent methane would be one of the leading fuel candidates. This work was initiated to provide information required to further evaluate the feasibility of using either of these propellants as a fuel and coolant in future rocket engine thrust chambers at their anticipated heat flux, temperature, and pressure.

Data were generated using the test fluid to cool a specially constructed, electrically heated, bimetallic tube, while flow rate, tube and fluid temperatures, and power dissipation were recorded. Processing these test data permitted a heat transfer correlation. Monitoring increases in fluid pressure drop across the tube during the testing, coupled with post-test inspection of the internal tube surfaces was used to detect and evaluate the thermal decomposition of the test fluid and the compatibility of the fluid with the copper inner tube wall.

The bimetallic tube consisted of an inner tube of oxygen-free, high-conductivity (OFHC) copper and a stronger outer tube of Monel K500 to provide the required strength at high operating temperatures and pressures. Two bus bar cylinders were brazed to the bimetallic tube and two AN-plug fittings were silver soldered to the tube ends. This in turn was mated with two OFHC bus bars having electrical power cables. The interfacing surfaces of the bus bars and cylindrical plates were silver plated to insure excellent electrical contact. One of the bus bars was fixed to the electrically insulating base, while the other was allowed to slide to accommodate the axial thermal expansion of the tube. This design allowed for quick and easy test specimen changes. The test facility provided a supply of liquefied methane or natural gas to the test assembly. Electrical preheaters allowed for variation in fluid inlet temperature and a turbine flowmeter was used for flow measurement.

The basic test data were analyzed and a recommended heat transfer equation was determined. Although this correlation was established under conditions of axisymmetrical heating in a circular tube, past studies have demonstrated that this is applicable to the asymmetrical heating conditions found in a thrust chamber coolant channel.

This correlation was established over a wide range of test conditions but was limited by the occurrence of a wall roughening phenomenon that was observed at high levels of heat flux and wall temperature. The roughening of the tube wall was shown to correspond to an increase in heat transfer and pressure drop. Detailed examination of the tubes with a scanning electron microscope revealed that the roughening was due to a corrosion type of process that resulted in a significant loss of tube wall (Cu) material.

This project has been successfully completed in fiscal year 1985. Use of the special double wall bimetallic tube allowed testing to heat flux levels never before obtained with these test fluids. No indication of thermal decomposition of the test fluids was detected. Post-test inspection and analysis showed no significant carbon deposits on the inner tube wall.

An important discovery was made that these hydrocarbon test fluids of methane and natural gas have a corrosive or roughening effect on the copper wall surface. The heat transfer data for the smooth tubes were correlated by incorporating a property correction temperature ratio term into the standard Nusselt number formulation.

Morinishi, R., and Cook, R. T.: Methane Heat Transfer Investigation Rocketdyne Division, Rockwell International Corporation, Final Report Contract NAS8 – 34977.1985.

Dale H. Blount/EP26
(205) 453 – 4739
Sponsor: OAST

Rocket Engine Turbopump Bearing & Seal Material Tester

The Space Shuttle main engine high pressure oxidizer turbopump bearings do not meet the 7.5 hr life specification requirement. A program has been initiated to improve the 57 mm bearing life and reliability. In order to understand the bearing environment and loading conditions as well as evaluate various bearing modifications, a bearing tester was conceived, designed, and built.

The first generation bearing tester has been in operation for some time. This tester operates with liquid nitrogen (LN_2) as the coolant, but does not simulate the flow path through the bearings or the loading configuration of the lox turbopump. However, a great deal of data has been obtained which is applicable to the design of a second generation lox bearing tester. A set of instrumentation has been developed and proven with this tester. The resulting data were used to formulate an advanced thermal model of the bearings and flow model of the fluid exiting the bearings. These data have provided an understanding of the bearings' internal dynamics and showed that the instrumentation can detect an imminent failure. The LN_2 tester has also shown the impact of axial loading on bearing life.

This work has aided in the design, during 1985, of a second generation bearing and seal material tester for 57 mm lox turbopump bearings. This tester has been designed to operate with lox as the bearing coolant. It has the capability to test the bearings under various load and lox coolant flow conditions. Load application is via hydrostatic bearings, and the critical speeds are above the operating range. The design provides coolant to the bearings in a manner identical to the lox turbopump. The coolant enters the hollow shaft, then flows through the jet rings to the bearings. The labyrinth seals are also identical to those in the turbopump, thus providing the capability to evaluate the seals as well.

In order to monitor the test bearings' condition, the tester incorporates a great deal of instrumentation as well as borescope ports between and inboard of both bearing pairs. Instrumentation includes temperature and ball pass counter probes on all bearing races and axial and radial displacement probes on the shaft. Coolant temperature and pressure are monitored at all critical internal locations as well as at all inlets and outlets. Six accelerometers (x, y, z at each bearing pair) are mounted internal to the tester on the bearing carrier. Four additional accelerometers are mounted externally on the housing.

Extensive stress, thermal, dynamic, and hazard analyses have been performed to assure the adequacy of the design. With the recent completion of a critical design review, this second generation tester has been approved for fabrication.

Neill Myers/EP33
(205) 453 – 2879
Sponsor: OSF

The Development of Single Crystal Turbine Blades for the Space Shuttle Main Engine

The Space Shuttle Main Engine (SSME) high pressure fuel turbopump contains blades fabricated from a superalloy [MAR – M246 (Hf)]. The turbine blades are directionally investment cast, resulting in a series of long grains each extending the entire length of the blade. When the SSME was designed, this alloy and the directional solidification process were the best combination available. During operation the turbopump blades are subjected to a severe environment that includes high mean

stress, extreme thermal transients and a combination of low and high cycle fatigue. Since the SSME operates in high pressure hydrogen, the blades must also react favorably to this environment. MAR – M246 (Hf) was not specifically developed for the hydrogen environment, which can substantially lower the mechanical properties. Increased blade life will be realized by choosing an alloy with superior mechanical properties and fabricating the blades with an improved casting process.

The most recent development for turbine blades is the single crystal. Single crystals have improved mechanical properties resulting from basic alloy changes and casting processes which eliminate grain boundaries. In this alloy, there is no need for grain boundary strengtheners such as carbides, which frequently act as nucleating sites for cracks; therefore, fatigue life is improved. Reducing the carbide forming elements also raises the operating temperature range, which is highly desirable. Single crystal turbine blades are anisotropic and their orientation can be tailored to optimize the fatigue properties.

A test program has been in progress during fiscal year 1985 for evaluating single crystal alloys in high pressure hydrogen. The tests basically consist of candidate materials being notch tensile tested in high pressure hydrogen and in high pressure helium. The ratio of strength in hydrogen to that in helium is the relative response to the hydrogen. Test results are shown in Table 4 for four alloys, and alloy PWA 1480 appears to be the least embrittled.

Table 4. Notched Tensile Tests at 20°C (68°F) in 34.5 MPa (5 KSI) Hydrogen.

ALLOY	NOTCHED TENSILE STRENGTH MPa (KSI) H_2	He	NOTCHED RATIO H_2/He
CM SX–2	215.9 (31.3)	1498.5 (217.3)	0.14
CM SX–4C	546.8 (79.3)	1536.6 (222.9)	0.36
Rene' N-4	677.6 (98.3	1472.8 (213.6)	0.46
PWA 1480	739.6 (107.3)	1518.0 (220.2)	0.49

Four other alloys scheduled for testing include MAR – M246 (Hf) (D.S.), MAR – M246 (Hf) single crystal, AF56, and CM SX – 2 (ONERA). Those alloys that react favorably in high pressure hydrogen will be further evaluated for use in a low and high cycle fatigue environment encountered in the SSME. Anticipated accomplishments for 1985 are: continuation of the hydrogen environment embrittlement (HEE) screening program; relationship between crystal orientation and HEE for the PWA 1480 alloy; upgrading the screening program to 10 KSI hydrogen/steam at 1600°F; and finally modeling crystallographically and dynamically a SSME turbine blade to optimize mechanical properties and resistance to HEE.

Richard A. Parr/EH22
(205) 453 – 5513
Sponsor: OAST

Improvements in Turbine Airfoil Low Cycle Fatigue Life

Low Cycle Fatigue (LCF) is one of the life limitations of rocket engine turbines. Thermal stresses caused by the rapid start and shutdown of the engines are high enough to cause local yielding and subsequent cracking in the turbine hot section. This problem is especially severe in the Space Shuttle Main Engine (SSME) where the oxygen – hydrogen combustion products and the high operating pressures combine to increase the heat transfer film coefficient to two orders of magnitude greater than experienced in aircraft engines. As a result, LCF cracking may occur after only a few operating cycles and once started, can propagate to a structural failure through steady state and dynamic loading.

To alleviate the LCF problem, airfoils should be designed to minimize start and shutdown thermal gradients. Two techniques proposed to minimize thermal gradients are hollow core airfoils and circulation of turbine drive gas through the hollow core. In fiscal year 1985 these design techniques were evaluated experimentally in a series of tests in the MSFC Turbine Blade Tester. This facility simulates the

SSME turbine start and shutdown transients. Test airfoils were exposed to temperature gradients of 1050K/sec (1900R/sec) and 1725K/sec (3100R/sec) during start and shutdown, respectively, in oxygen/hydrogen combustion products at pressures experienced in the SSME turbines. The tests consisted of running six blades through approximately 75 thermal cycles with frequent inspections for cracking. The blades included solid airfoil, 0.889 mm (0.035 in) and 1.397 mm (0.055 in) hollow wall thickness airfoils, and a 1.397 mm (0.055 in) hollow wall thickness airfoil with a 1.270 mm (0.050 in) hole in the base of the pressure surface. The airfoil profile approximates the SSME fuel turbine hub profile. All of the airfoils were fabricated from PWA 1480 single crystal material. The test results are summarized in Figure 60, and demonstrate that significant improvements can be made in SSME turbine airfoil LCF life through use of the techniques evaluated.

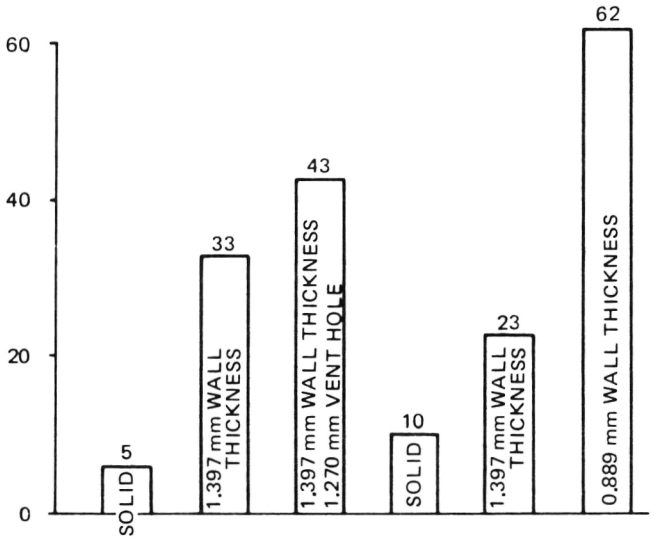

Figure 60. Airfoil Thermal Cycles to First Observed Crack

Loren A. Gross/EP23
(205) 453 – 3812
Sponsor: OAST and OSF

Vacuum Plasma Spray Coating Development

Vacuum plasma coatings of NiCrAlY have been developed that are superior to atmospheric plasma coatings of NiCrAlY currently applied as protective coatings on SSME (Space Shuttle Main Engine) turbine blades. The new coatings are applied in vacuum at Mach 3 velocity with argon/helium as the arc gas, excluding oxides that form during normal atmospheric plasma spraying. The new coatings showed no spalling after 25 Burner Rig tests, cycling between 1700°F and – 423°F, while the current SSME coatings spalled during 25 cycles. Each Burner Rig Test simulates one SSME cycle.

A development program has been initiated with Rocketdyne with initial emphasis on applying durable thermal barrier coatings of ZrO_2 to SSME first stage high – pressure fuel turbopump turbine blades using the vacuum plasma sprayed NiCrAlY as a bond coating. Other SSME applications being investigated include vacuum plasma spraying copper onto the titanium main fuel valve housing and coatings of Incoloy 903 for protection against hydrogen embrittlement.

Richard R. Holmes/EH43
(205) 453 – 0643
Sponsor: OSF

Space Shuttle Main Engine Hot Gas Manifold Analysis

During the development of the Space Shuttle Main Engine (SSME), it was recognized that the hot gas flow through the three transfer tubes on the fuel turbine side was not evenly distributed nor was the tubewise distribution uniform. The three – duct, hot gas manifold system is pictured in Figure 61. Cold flow tests showed that the outer transfer tubes carried 90 percent of the flow. Separated regions in the outer tubes displaced the flow and this in turn led to large gas shear velocities. The resulting impact pressures on the injector posts in the SSME injector cavity caused them to bend under static loads. High turbulence levels of the flow vibrated the posts and caused cracks. It was also observed that these deleterious flow effects were enhanced

as the engine power increased. Due to the asymmetric shape of the flow path, large side forces were developed which had negative effects on the rotor dynamics of the turbine.

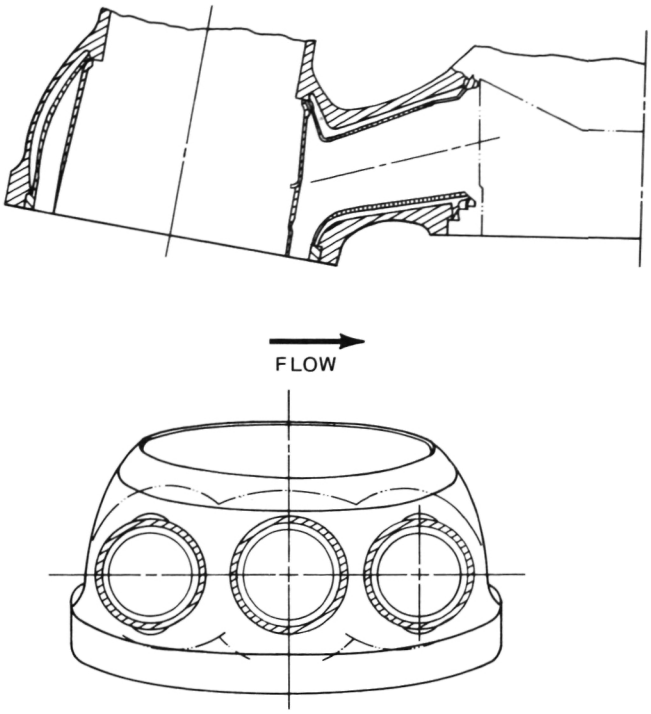

Figure 61. Three-Duct Hot Gas Manifold.

It became obvious that increased power levels could not be attained with the present hot gas manifold configuration. Several new concepts were therefore evaluated, and the one which best satisfied the technical and programmatic criteria was selected (Figure 62). Cold flow tests performed with full-scale hardware established the steady state and dynamic flow parameters in the duct system. During the last year a numerical analysis of the cold flow test results was undertaken. The test data showed clearly that elimination of the center tube and a generous enlargement of the two remaining tubes would solve most of the problems. The two-duct concept reduced the flow velocities by 30 percent and the dynamic pressure was halved. Turbulence levels were also smaller. The total pressure loss was only about 50 percent of the loss with the three-duct system. The turbine side forces were reduced to about 30 percent as compared with those with the three-duct system. Further reductions could be obtained by aerodynamically shaping duct contours. This would also produce a more uniform velocity distribution across the transfer tube.

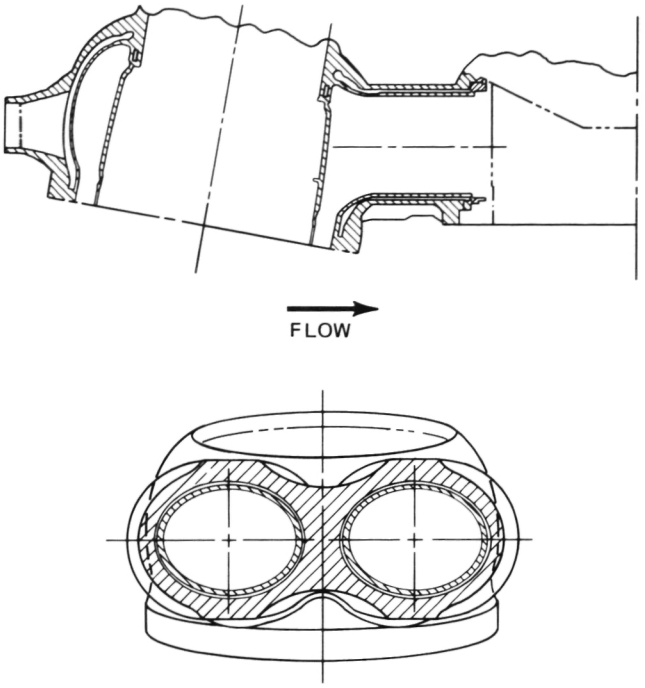

Figure 62. Two-Duct Hot Gas Manifold.

In 1985 a considerable effort was made to obtain numerical solutions to the Navier-Stokes equations which modelled the complex flow in the hot gas manifold. Once a solution is obtained for the basic flow geometry, optimization studies will commence to minimize flow losses and improve the velocity distribution of the hot gas at the entrance to the injector head.

Heinz Struck/ED31
(205) 453-3287
Sponsor: OAST

Turbomachinery Whirl Elimination With Damping Seals

The high pressure turbopumps of the Space Shuttle Main Engine (SSME) operate supercritically and thus are susceptible to subsynchronous rotor whirl. At speeds above a rotor resonance, the rotor can become unstable and orbit in a rotor resonant mode. The High Pres-

sure Oxygen Turbopump (HPOTP) was whirled with 470 Hz at a full power speed near 500 Hz (30,000 RPM). Occasionally the whirl reached a high limitcycle. The 95 percent whirl speed ratio and the limitcycle imply Coulomb friction in rotor joints as the likely cause. The HPOTP has since been modified by adding axial and radial pilots to the preburner pump (PBP) impeller and replacing the labyrinth seals at the inlet and outlet sides of the PBP impeller with damping seals (Figure 63). Damping seals have a stator with deep pockets (Figure 64) which keep leakage low as in labyrinth seals, but add much stiffness and damping. This retrofit suppressed the 470 Hz whirl and reduced PBP bearing loads for larger outer race clearances. Thus, pump speed, thrust, and payload can be increased.

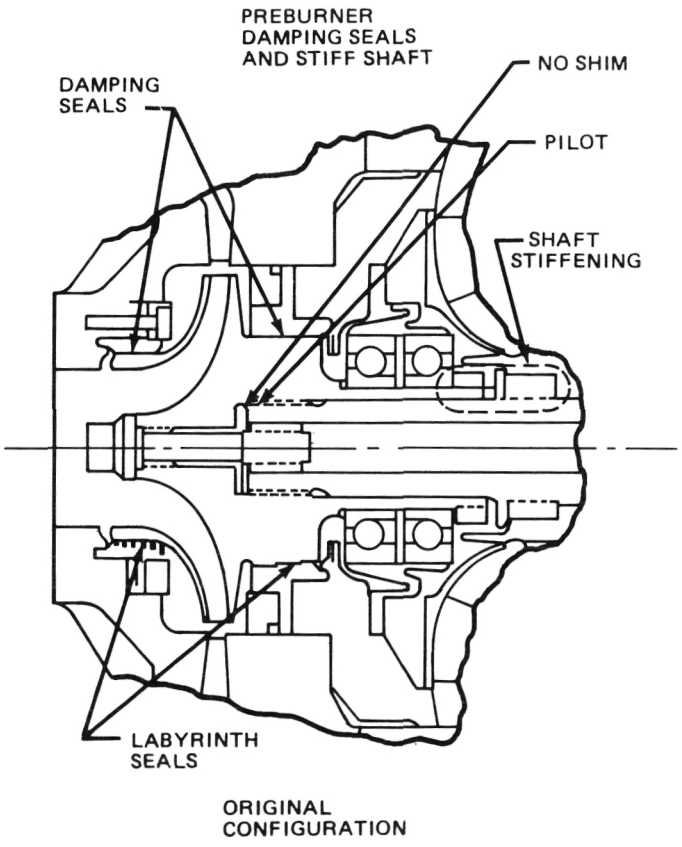

Figure 63. HPOTP Damping Seal Retrofit.

Certification tests of the phase II high-pressure oxygen pump since February 1985 at 109 percent power level showed that the 95 percent subsynchronous whirl has been successfully eliminated. The request for damping seals as retrofits for the floating ring HPOTP turbine seals and the High Pressure Fuel Turbopump (HPFTP) interstage seals has been renewed to 50 percent of the subsynchronous whirl. Low level vibrations near the first critical speeds of 300 Hz are occasionally observed in tests which indicate a low stability margin for the 50 percent whirl. Damping seals are being considered by Aerojet and Pratt & Whitney to damp rotor resonances within the operations range of improved SSME high pressure turbopumps. Wyle Laboratories and the Stein Seal Company are preparing a tester and a test stand to verify the dynamic and sealing properties of damping seals.

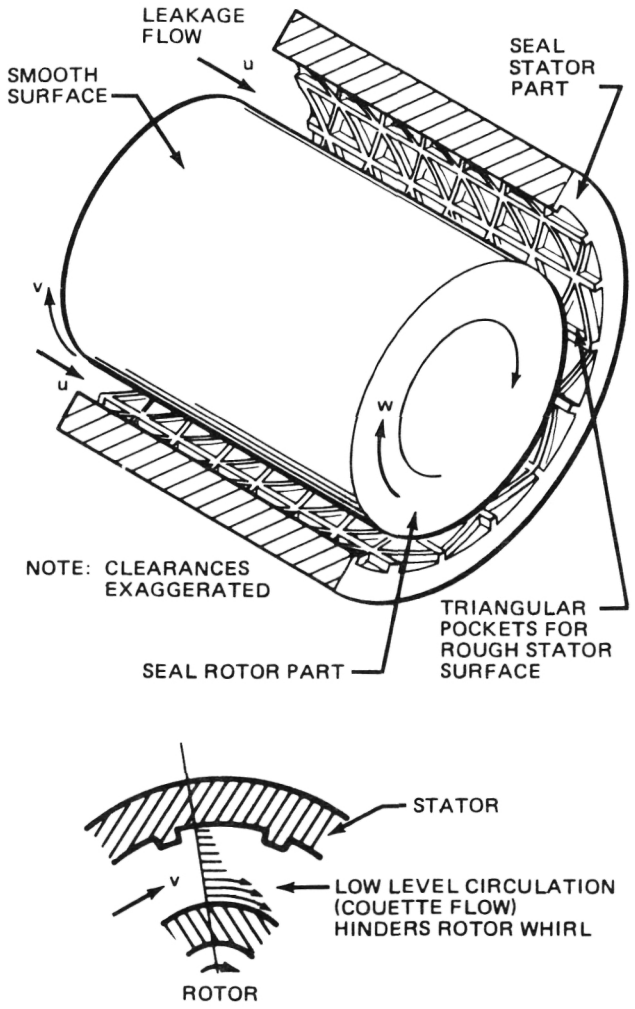

Figure 64. Damping Seal Concept.

Childs, D. W.: SSME Interstage Seal Research Progress Report. Texas A&M University 3123, January 1984.

von Pragenau, G. L.: Damping Seals for Turbomachinery, NASA Technical Paper No. 198. March 1982.

G. L. von Pragenau/ED14
(205) 453 – 4717
Sponsor: OAST

Forces on Turbomachinery Rotors

The objective of this effort was to investigate the latest theoretical definitions of seals, bearings, and other interactive force mechanisms between a high – speed rotor and its housing and to make a comparison with those obtained through test data.

A generic model of the high – speed SSME turbopumps was produced. The model consisted of two linear model subsystems with points of interaction between them. The two subsystems represent the rotor (Figures 65 and 66) and the housing. The housing model is represented by modes which are summed at only the points of interaction. The modes used to represent the housing were chosen from NASA Structural Analysis (NASTRAN) results

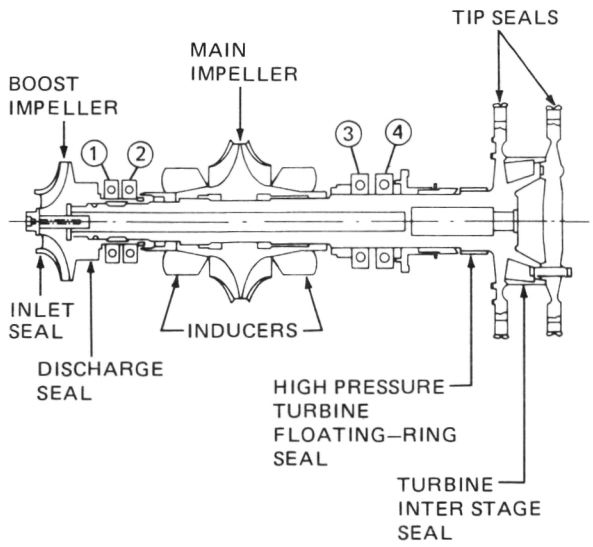

Figure 65. SSME Powerhead Component Arrangement and Local Rotor Coordinate Systems

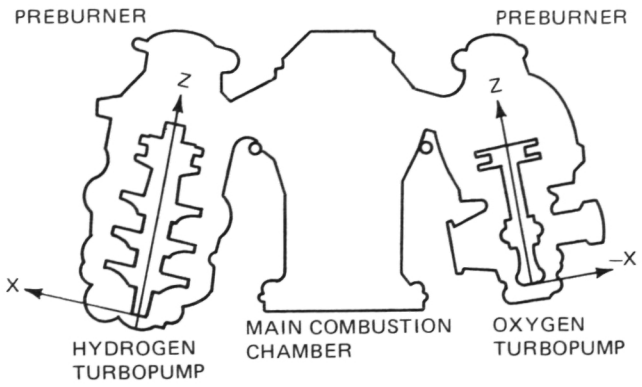

Figure 66. HPOTP Rotating Assembly.

and selected for their high gains at the interaction points and frequency. The rotor was broken into 15 elements and the modes used to represent it were chosen in a similar manner to those of the housing. A rap test verified the frequencies. The interaction points between these two models coincide with the rotor bearing, seal, and impeller interactive points. Forces generated at these points of interaction were calculated from theory modified by test data. The parameters that allowed these models to simulate the high – speed SSME turbopumps were determined from the results of activities of contractors, universities, and MSFC. These were constantly updated due to a better understanding of the fluid forces from test data, design changes, and better theoretical models. The high – speed turbopump model was programmed as a linear analytic model and a time domain nonlinear simulation. The latter was necessary due to the nonlinear interaction of the deadbands in the bearings.

The result of this study was an improvement in the model accuracy due to better definitions of the seals, bearings, and impeller forces. From this model the effectiveness of the different whirl driver suppression techniques can be determined.

Childs, D. W. and Moyer, D. S.: Vibration Characteristics of the High Pressure Oxygen Turbopump (HPOTP) of the Space Shuttle Main Engine (SSME) ASM Report 84 – GT – 31, 1984.

T. H. Fox/ED14
(205) 453 – 4717
Sponsor: OAST

Development of Hydrogen–Resistant Alloys

The most hostile operating environments in the O_2/H_2 Space Shuttle Main Engine are gaseous hydrogen and hydrogen/water vapor. After years of evaluating commercially available alloys, only a few high–strength alloys have been found that perform satisfactorily in these environments.

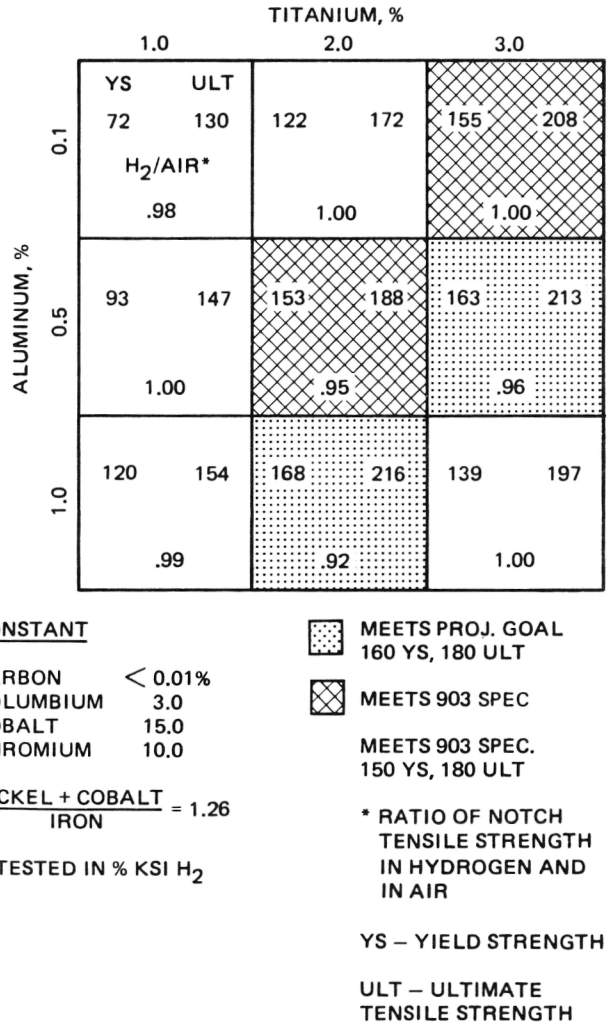

Figure 67. Experimental Matrix with Varying Aluminum and Titanium.

Based on a survey of the literature, the most promising alloy system appeared to be the iron–nickel–cobalt–chromium system. Test matrices were designed to make alloys of the above basic composition with additions of strengtheners, such as aluminum and titanium, and hardeners such as carbon and columbium. The experimental procedure consisted of melting 8 lb heats of the above alloys in a vacuum induction furnace, and then casting and hot rolling them into slabs. The slabs are heat treated with the Inconel 718 treatment.

In early experiments, it was established that the best chromium composition was 10 percent with nickel plus cobalt–to–iron ratio of 1:26. For statistical analyses, a factorial experiment was selected with two variables, each at three levels. One test matrix is illustrated in Figure 67 for aluminum at 0.1, 0.5 and 1.0 percent and titanium at 1.0, 2.0, and 3.0 percent, while the other elements remain constant. The principal screening test is the notch tensile test in 5000 psi hydrogen and reported as the ratio of the notch in hydrogen to the notch strength in air (number at the bottom of each matrix square). In this experiment, only one alloy had over five percent strength reduction in hydrogen; thus none of the alloys should be rejected based on the hydrogen tests. However, the yield and ultimate strength meet the goals in only two cases, with two others close. Based on this experiment, the most promising composition is 37 percent Fe, 32 percent Ni, 15 percent Co, 10 percent Cr, 3 percent Ti and >1.0 percent Al. The next step is to more precisely define the alloy composition and prepare commercial size (200–300 lb) ingots to evaluate welding and corrosion resistance.

William B. McPherson/EH23
(205) 453–5504
Sponsor: OAST

Advanced High Pressure Oxygen–Hydrogen Propulsion Instrumentation

Research efforts to enhance the lifetime, performance, and diagnostics of high pressure oxygen–hydrogen staged combustion rocket engines, particularly the Space Shuttle Main Engine (SSME), have resulted in the identification of critical instrumentation requirements. This instrumentation will provide mathematical

model verification, more accurate and reliable control input data, and component failure prediction. Three areas of instrumentation considered to be of high priority are in the areas of SSME preburner temperature profiling, SSME silicon/microelectronic pressure sensor, and a SSME vortex shedding flowmeter for high velocity cryogenics.

SSME preburner temperature profiling is needed to assess the magnitude of temperature deviations and the effect of engineering improvements. Uniform temperatures are desired across the high-pressure, hydrogen-rich preburners so that thermal stressing of the turbine blades can be alleviated, thereby minimizing turbine blade cracking. Presently, this temperature profiling capability does not exist.

A feasibility study was conducted to determine theoretically if such a measurement could be accomplished. Three laser optical techniques were studied, including Raman scattering, fluorescence, and coherent anti-Stokes Raman spectroscopy. It was concluded that Raman scattering was best suited for this application. Raman scattering can use a single port with the argon laser power transmitted to the engine by fiber optics, allowing the laser, spectrograph, and control electronics to be remotely located from the engine.

A study has been conducted to determine whether laser power can be transmitted through the optical fiber without serious attenuation. In addition, the diagnostic capability of the Raman scattering is being evaluated using a high pressure, high temperature hydrogen cell simulating the SSME preburner.

The second area in which instrumentation is needed is for a SSME pressure sensor. Currently the SSME has conventional strain gage pressure sensors. Reliability problems have been encountered with this design, primarily in the electrical wiring portions of the sensor, i.e., broken wires, bad solder joints, etc. In addition, zero balance and full-scale output of the strain gage bridge are set with resistors located away from the bridge. The bridge is sensitive to temperature and the zero balance point changes with temperature. In an attempt to correct for temperature, compensation resistors are used which correct the bridge output as a function of temperature. The problem with this approach is that the compensation resistors and the strain gages are not at the same loca- equilibrium temperature is reached; therefore, the zero balance is not stable in a transient temperature condition. For diagnostic purposes the data for the transient conditions are of most importance. Current sensor data is lacking for the transient conditions because of poor temperature compensation. As a result of this effect, the current transducers for the cryogenic application are remotely mounted for temperature isolation. This decreases the frequency response.

To improve reliability and temperature compensation, a silicon/microelectronic approach was investigated. The intent is to ion-implant piezoresistive elements into a silicon chip which acts as a pressure sensitive diaphragm. All zero, span, and compensation resistors would also be ion-implanted into this chip. With all the resistors at the same physical location, proper compensation can be achieved. The zero and span can be set precisely by laser trimming the resistors while pressure is applied. The only wire connections are the leads from the chip to the connectors.

A breadboard sensor was designed and built for testing the silicon/microelectronic approach. This sensor showed significant advantages over the strain gage sensors and improved frequency response. The chip design has been finalized, and experimental units have passed thermal and vibrational shock testing. Prototype units are scheduled for delivery in December 1986.

The third area in which instrumentation is needed is the measurement of the flowrate of liquid hydrogen and liquid oxygen in the SSME. The flowmeter originally used for liquid oxygen had to be removed due to structural problems caused by high cycle fatigue. The mathematical flow model of the engine cannot be verified without flow measurements of the oxygen and hydrogen systems.

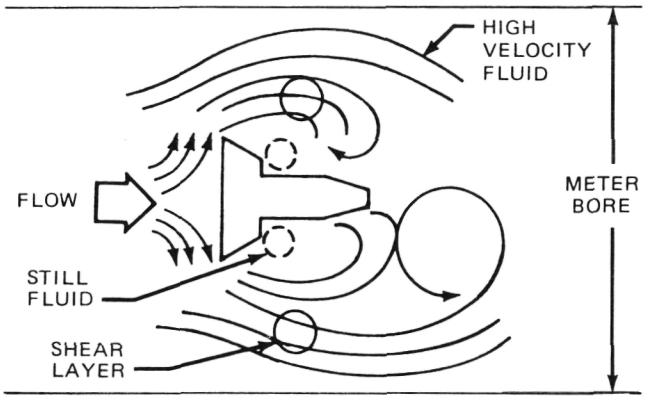

VORTICES ARE SHED ALTERNATELY, CREATING ALTERNATING ΔP ACROSS BLUFF BODY

FREQUENCY = K. $\frac{\text{FLOW VELOCITY}}{\text{WIDTH OF BODY}}$

(a) Vortex Shedding Diagram.

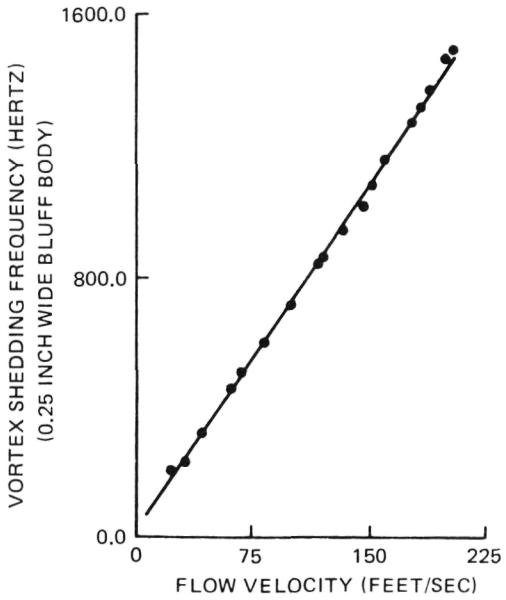

(b) Vortex Shedding Graph.

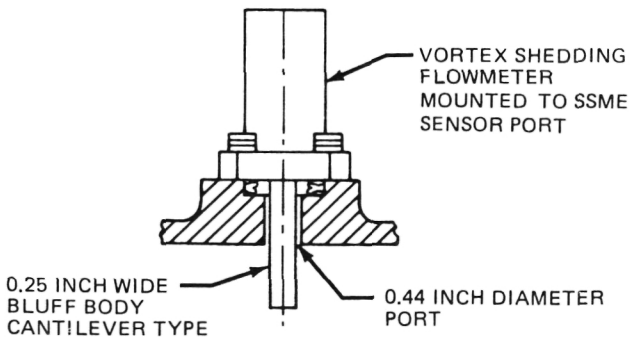

(c) Vortex Shedding Flowmeter.
Figure 68.

The vortex shedding technique along with the engine mounting concept and flow velocity versus shedding frequency are depicted in three illustrations (Figure 68). The shedding frequency is a function of the Strouhal number which is a constant nearly independent of any other fluid property. The alternate shedding of vortices introduce a time varying pressure across the vane. The frequency of this alternating pressure can be measured and is directly proportional to the flow velocity. The magnitiude of the varying pressure does not have to be determined, only the frequency. The vortex shedding flowmeter approach was selected for this research program. To obtain flow velocities similar to that in the SSME main liquid oxygen duct, the penstocks at the Boulder, Colorado, hydroelectric plant were used. The research has shown that the vortex shedding principle is valid at velocities exceeding 55 m/sec, which is close to the flow velocity in the main liquid oxygen duct. The question remaining is the effect of flow swirl on the measurements. This is presently being investigated using SSME liquid oxygen ducts for testing at Boulder to determine whether the measurement can be accomplished without flow straighteners.

Thomas N. Marshall/EB22
(205) 453 – 4626
Sponsor: OAST

Measurement of Very Small Thrust Forces in a Space Environment

The purpose of this investigation was to improve inhouse capability to evaluate microthrusters used on MSFC payloads. To simulate orbital pressure conditions in space required the development of a balance capable of accurate microthruster measurements in a vacuum chamber. The examination of prior research revealed several techniques which could be used to achieve the desired goal. The two most promising techniques were a parallelogram balance and a torsion balance.

A parallelogram balance designed to make drag measurements was modified to measure

thrust. Using this modified parallelogram – type balance, thruster tests were conducted in the MSFC 3.5 ft Low Density Chamber with thrust values from 20 to 250 dynes. These tests revealed that this balance had several serious operational problems, such as limited load – carrying capacity, severe thermal drift, and extreme weakness in response to side loads. For these reasons, development of the parallelogram balance was terminated.

Next, the torsion balance was designed, fabricated, and tested over a range of thrust values from 20 to 500 dynes, with very promising results (Figure 69). It consists of a main frame to which a column is mounted on pivots, allowing the column to rotate freely about the vertical axis. On the column is an arm on which the thruster is mounted to fire tangentially. This causes the column to rotate. The rotation is restricted by an electrically generated counter torque, and the amount of counter torque required to nullify the rotation is the measurement of thrust. Calibration of the completed balance showed very good linearity and repeatability, and very little zero shift.

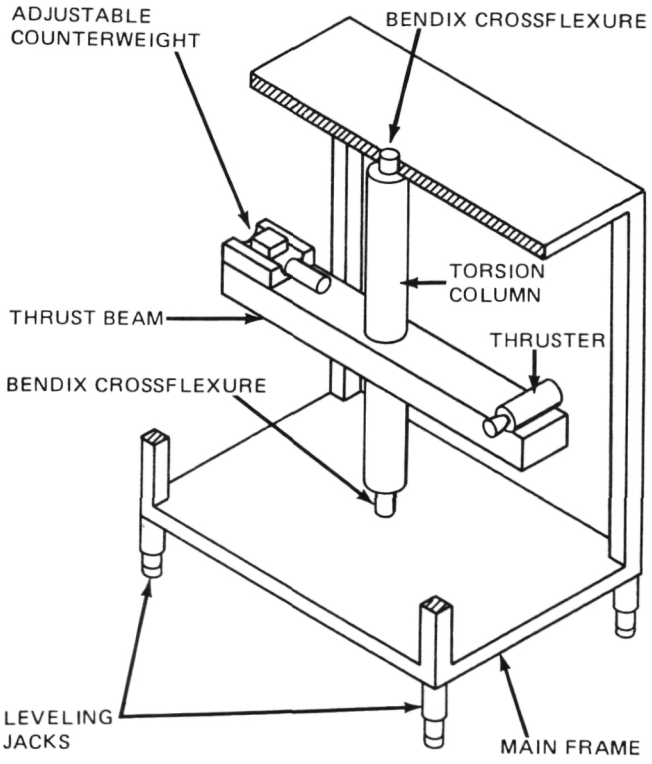

Figure 69. Schematic of Torsion Balance.

Based on the analysis of test and calibration data, the torsion balance provides a significantly better method for making thrust measurements at simulated orbital altitudes. Continuation of this work will improve the capability for accurate microthruster measurements.

A. R. Felix/ED35
(205) 453 – 1848
Sponsor: CDDF

Optically Beamed Energy Transfer Mechanisms

The need to put large mass systems into geosynchronous orbits requires more efficient propulsion schemes. Efficiency in terms of specific impulse for conventional propellant systems has reached its maximum potential, and thus a new approach is necessary. Several concepts exist which are efficient enough to fulfill the projected needs, but nearly all are capable of only low thrust levels. The concept being pursued in this program, beamed energy propulsion, is capable of several hundred pounds of thrust and can provide sufficient thrust to serve as an effective propulsion system for hauling freight to geosynchronous Earth orbit in reasonable trip periods (30 days).

This three – phase research program is now in the third phase. The first stage involved the development of an initiation scheme for the energy transfer medium, a hydrogen plasma. The plasma exchanges energy between an electromagnetic beam, in this case a high energy CO_2 laser, and a working fluid, hydrogen. The goal of the first task was the initiation of the plasma in a stable location within the laser beam. It was achieved by cofocusing a pulsed laser beam from a CO_2 transverse excitation atmospheric laser with the primary beam. Sufficient energy is available within the pulsed beam to initiate a plasma by a series of photon/electron interactions. Experimental development of this technique was accomplished for a range of operating pressures in helium, nitrogen and hydrogen. Figure 70 shows a schematic representation of the developed system.

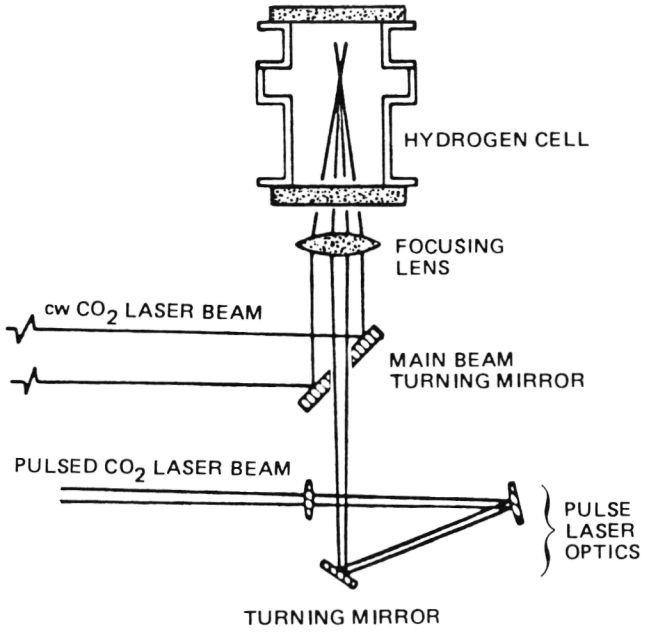

Figure 70. Schematic View of Plasma Test Chamber and Beam Delivery System.

The second phase consists of creating laser-sustained plasma in static gases and determining the effects of fluid entrance velocity on plasma location and absorptivity. The purpose is to evaluate the theoretically-predicted dependence of absorption coefficient on laser flux density. The goal is to produce plasmas with maximum electromagnetic to thermal energy transfer characteristics. These experiments have been concluded in argon and have begun in hydrogen.

The final phase consists of measuring the physical properties of laser-sustained plasma as functions of gas pressure and flow velocity. The primary diagnostics include the measurement of beam energy flux into and through the plasma, heat flux to the chamber wall, and the temperatures within the plasma itself. A special video camera/Abel inversion system has been developed to permit plasma temperature profiles to be measured. The camera system permits individual calibrated pixel data to be recorded. These data are then transferred into an Abel inversion routine which permits absorption coefficient and plasma temperature profiles to be determined. An example of the reduced data for a two-atmosphere argon plasma is shown in Figure 71. Completion of this research will provide the basic physical property data necessary to design a laser thermal thruster with an expected specific impulse capability of 1500 sec.

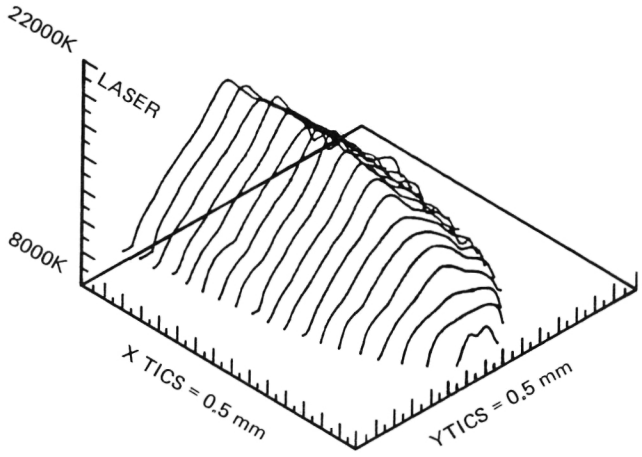

Figure 71. Temperature Profiles Calculated for the Experimental Argon Plasma Radiance Data.

Early in 1985 tests were conducted to produce laser-sustained plasmas in hydrogen. Consistent laser output in excess of 12 kW was reported at this time. The tests were conducted in 3 ATM Hydrogen for durations up to 10 sec. These tests were unsuccessful due to poor beam quality and spherical aberrations in the focusing lens. Subsequent testing was delayed due to supply problems with the NACL test chamber windows and vacuum blower bearing problems with the NASA high energy laser. Currently, negotiations are under way for laser repair and the redesigning of the focusing optical system.

McCay, T. D. and Dexter, C. E.: Chemical Kinetic Performance Losses for a Hydrogen Laser Thermal Thruster, AIAA Paper 85-0907, June 1985.

McCay, T. D. and Thoenes, J.: Numerical Modeling of Laser Thermal Propulsion Flows, and Orbit-Raising and Maneuvering Propulsion: Research Status and Needs, AIAA Progress in Astronautics and Aeronautics, 89, February 1984.

McCay, T. D., Van Zandt, D. M., and Eskridge, R. E.: An Experimental Study of Laser Supported Hydrogen Plasmas, AIAA Paper 84-1572, June 1984.

T. Dwayne McCay/EP26
(205) 453 – 1056
Sponsor: CDDF and OAST

Solid Rocket Propulsion Systems

Ignition Overpressure from Solid Rocket Motor Firings

The importance of predicting pressure waves propagated from rocket nozzles when solid propellant ignition begins led to an investigation of the basic mechanisms influencing ignition overpressure and the control or suppression of the output. This is important because pressure waves become quite critical in inducing loads on aerospace vehicles and launch structures with large surface areas. The control of pressure waves via design of operational limitations is being investigated through experimental means.

Analytical and empirical test methods which can provide guidelines for overpressure suppression techniques developed. Solid propellant rocket motors (scaled at one percent of the Shuttle's Solid Rocket Boosters) were utilized with variable chamber pressure rise rates (80,000 – 140,000 psi/sec) to provide an ignition overpressure (IOP) source. Using a simplified test geometry (cylindrical duct), the pressure field was defined as a function of the chamber pressure rise rate. After providing water injection into the duct, overpressure suppression as a function of water was assessed. In addition, suppression via aerosol mixing and via injection distance down duct was evaluated.

During 1985 the data base has been acquired for a basic duct. IOP was verified to increase approximately linearly with chamber pressure rise rate. Water injection tests were completed using a water flow rate to propellant flow rate (w_w/w_p) of 0.6 and, 0.3, respectively. A time history of the overpressure wave with and without water injection is shown in Figure 72. The water injection rate of $w_w/w_p = 0.6$ provided a suppression of the IOP to eight times depending on the duct location. Tests have also been completed using aerosol foam as a means of suppression. Results indicated that, because of the very low density of the foam, the volume of aerosol required would necessarily have to be very large relative to the source to provide

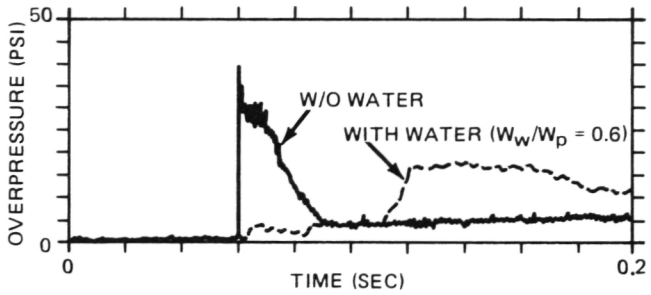

Figure 72. 1% SRM Ignition Overpressure Test Overpressure Measurement K10.

suppression of the overpressure wave. Figure 73 shows a summary of the results. The IOP has been verified as a function of the chamber pressure rise rate. Significant suppression of

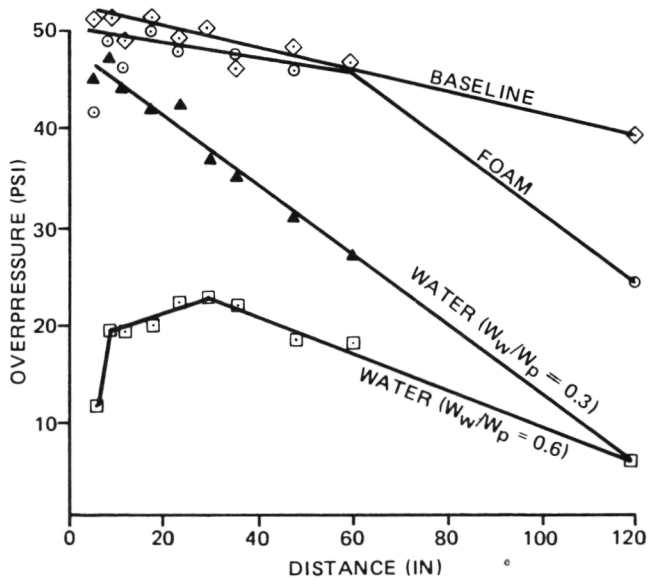

◇ BASELINE – DRY (TEST 5, 6)
⊙ FOAM – (TEST 10, 11)
⊡ WATER – W_w/W_p = 0.6 (TEST 8, 9)
▲ WATER – W_w/W_p = 0.3 (TEST 13)

Figure 73. Duct Overpressure for 2 x 4 Solid Motor Versus Downstream Location.

the output was accomplished with water injection as a function of both flow rate and flow location. A relationship between water injection rate and overpressure suppression was developed. The IOP was also passed through a volume of fixed aerosol foam that provided some IOP suppression; but the number of test cases were limited, and further testing is required to fully assess the foams effectiveness in suppressing IOP.

S. H. Guest/ED24
(205) 453 – 1841
Sponsor: CDDF

Effects of Sodium Hydroxide on Carbon–Phenolic Material

In a continuing effort to provide a basic understanding of constituent materials' properties and interactions, further work with doped carbon phenolic (C – P) systems has been performed. In 1984 it was reported that sodium affected both mechanical and physical properties of solid rocket motor (SRM) C – P systems.

During cure of the phenolic resin, a condensation polymerization takes place where hydroxyl groups lost in the cross – linking process form water. At the resin B – stage state, sodium can attack OH^- groups yielding sodium phenolate (a more active compound consistent with production of para – substituted phenol); it is clear that the effects of hydroxide content will dominate during resin cure. Recent work has confirmed that hydroxide effects during cure subtend sodium precursor variance for post cure physical and mechanical properties.

This phase of the on – going investigation has been divided into three stages delineated by the sodium anion moiety. Sodium chloride, sodium hydroxide, and sodium carbonate were chosen to assess the above effects. Sodium chloride, chosen for the relative inactivity of the dissociated chlorine, was observed to have negligible effect on pertinent resin properties. Therefore it may be concluded that sodium alone in concentrations up to 5000 ppm does not provide measurable kinetic changes in the resin system.

Sodium carbonate, the second contaminant investigated, provided similar results. It is apparent, that while a basic system will direct the cure reaction, a weak system (CO_3^{--}) is insufficient for measurable kinetic perturbations. Finally, effects of sodium hydroxide are being tested in a neat resin system. It is anticipated that these results will parallel those obtained in the earlier study.

Clinton, R. G., Goldberg, B. E., and Semmel, M. L.: Effects of Sodium on Processing and Properties of Carbon/Phenolic Materials. NASA – 8647, p. 101, Huntsville, Al, November 1984.

Clinton, R. G., Jr., Semmel, M. L., and Goldberg, B. E.: Investigation of the Effects of NaOH Dopant Level on the Physical and Mechanical Properties of Carbon/Phenolic Composite Material. NASA CR – 171317, Huntsville, Al, January 1985.

B. E. Goldberg/EH34
(205) 453 – 1227
Sponsor: OSF

Solid Rocket Booster High Temperature Sealants Development

To allow for heat processing and the removal of some thermal protective materials from fastener close – out areas, two high – temperature candidate sealant materials are being evaluated/qualified for use on the Space Shuttle Solid Rocket Boosters (SRBs) to replace the present PR – 1422 sealant. In the initial build – up of the SRB System components (Aft Skirt, Forward Skirt, Frustum and Nose Cap) the fasteners are installed wet with PR – 1422 (polysulfide) sealant. In addition, the heads of all fasteners are covered with the PR – 1422, resulting in encapsulated fasteners. This encapsulation protects the high – strength fasteners from the salt water when the boosters are being recovered after flight. The presently used sealant, PR – 1422, was developed for use over a temperature range of –65°F to 275°F; there-

ORIGINAL PAGE IS
OF POOR QUALITY

fore, an overcoat of thermal protective material is required to protect the sealant from the thermal environment of Space Shuttle launch and flight. The two candidate sealant materials being evaluated this year were developed for use over wider temperature ranges. Both candidate sealants, PR-1750 and PR-812, are two-part, liquid polymer compounds that cure at room temperature to form a resilient sealant material. Either candidate, when mixed, is a thixotropic paste readily applied by extrusion or injection gun which does not flow from vertical or overhead surfaces (Figure 74).

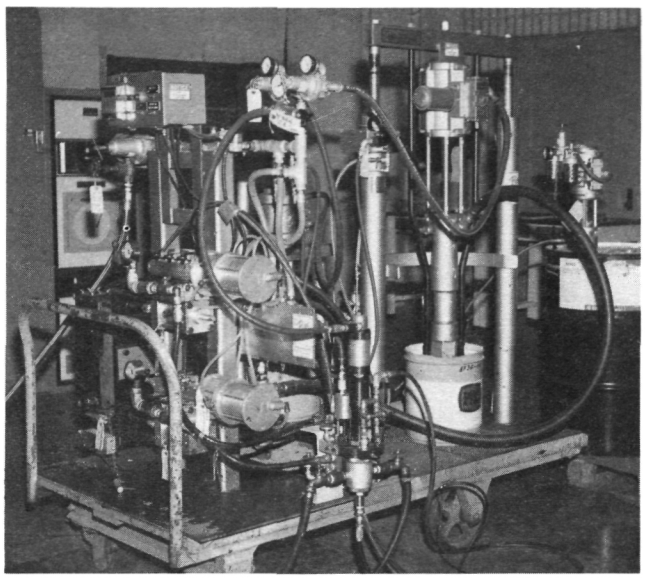

Figure 74. PYLES Meter-Mix-Dispense System for Applying High Temperature Sealants Over Fasteners on the SRB.

It is anticipated that the PR-1750 can be used on the SRB Frustums and Aft Skirts where rows of fasteners are exposed on the exterior hardware surfaces. In addition, it can be used without using K5NA over the sealant for thermal protection and with significant savings in production manpower, serial time, and material costs. Because of its higher temperature performance characteristics, the PR-812 sealant is expected to provide for similar productivity enhancement in protuberance areas where higher temperatures are experienced during launch, flight and recovery.

Charles Jackson/EH43
(205) 453-0643
Sponsor: OSF

Filament Winding Automation and Kinematic Simulation

Process engineers at MSFC and Morton-Thiokol are developing algorithms and techniques for graphic modeling and kinematic simulation of filament winding manufacturing. When fully developed, this system will provide unlimited versatility in the design and implementation of filament winding patterns. Engineers will be able to calculate and generate the data points that describe a given fiber path, and then, in a real-time sequence, simulate the winding of the pattern as it would be wound in the manufacturing sequence. Utilizing this technique, the filament winding sequence can be monitored and evaluated before it is implemented. Once the winding pattern is determined to be satisfactory, the data can be downloaded over a serial link to the machine computer, which converts it to numerical control machine commands. An unsatisfactory winding program can be regenerated and modeled with minimum labor and cost until an acceptable pattern is obtained.

The past year has seen a critical milestone in the development of a system that integrates a computer-controlled filament winding machine (Figure 75), with capability to receive digital commands over a serial link. A VAX 11/780 computer for data manipulation and an Evans and Sutherland PS-300 Real-Time Kinematic Modeling Computer for graphic simulation

Figure 75. Filament Winding.

are used. An extensive software package is being developed to enhance the process control software commercially available through manufacturers of filament winding equipment. This package includes a pattern calculator program that mathematically describes a fiber path over a mandrel configuration, a pattern simulator program to graphically display the calculated fiber path, a machine coordinate generator program, and a motion simulator program used for calculating winding machine positions with its graphical verification. A machine command converter program is also being developed to convert data points and position coordinates to usable numerical control machine commands. The filament winding process simulator program combines the pattern and machine simulator programs to graphically display the laying of fiber in the part. Future plans include the development of simulation techniques to evaluate, in real-time, material behavior and response when subjected to external forces such as thermal loads during cure, debulking (compaction) cycles, and hydroproof testing.

Wendell Colberg/EH43
(205) 453-0643
Sponsor: OSF

Processes

Variable Polarity Plasma Arc Welding on the Space Shuttle External Tank

Over 915 m (36,000 in) of aluminum welds are required for fabrication of an External Tank (ET). These welds were made with the Gas Tungsten Arc (GTA) welding process during assembly of the first 18 units. Historically the GTA welding process has resulted in some defects in the finished welds which has dictated the use of radiographic inspection of them. These defects must be repaired and radiographically checked to meet the design requirements, which is expensive and time consuming.

Since 1979 MSFC has been involved in developing a Variable Polarity Plasma Arc (VPPA) welding system for use on the External Tank. The benefits of the VPPA process include welds free of defects, reduced preweld cleaning, and reduced distortion due to the welding process.

Welding engineers from Martin Marietta Corporation have worked closely with MSFC to convert from the GTA to VPPA welding process in ET production. A master plan, incorporating process development on the large weld tools at the Marshall Space Flight Center, was devised so as not to interfere with ET hardware delivery schedules. Production implementation of the VPPA weld process at the Michoud Assembly Facility began in 1983 on one major weld fixture. Two additional fixtures were added in 1984, and during 1985, five additional fixtures will be added. Conversion of all 16 major ET welding fixtures from the GTA to the VPPA welding process will be completed by 1987.

To date over 1778 m (70,000 in) of VPPA welds have been made on the ET without any radiographic detectable defects. The process, which is completely controlled by a computer, is proving so successful that we have recommended the elimination of radiography of welds which are proof tested.

Nunes, A. C., Jr.; Bayless, E. O., Jr. and Wilson, W. A.: The Variable Polarity Arc Welding Process: Its Application to the Space Shuttle External Tank - Second Interim Report. NASA TM-86482, 1984.

Nunes, A. C., Jr.; Bayless, E. O.; Jr., Jones, C. S.,III; Munafo, P. M.; Biddle, A. P. and Wilson, W. A. The Variable Polarity Plasma Arc Welding Process: Its Application to the Space Shuttle External Tank - First Interim Report. NASA TM-82532, 1983.

Ernest O. Bayless, Jr./EH42
(205) 453-0011
Sponsor: OSF

C-2

Large Weld Tooling Technology Development

Full-scale assembly tooling, simulating the major weld fixtures for the Shuttle External Tank (ET), has been designed, fabricated, and installed during this fiscal reporting period. The tooling consists of two separate horizontal and vertical weld fixtures. The horizontal tooling has been utilized to determine the production impact of tooling and assembly improvements for the ET. In addition, this installation is being used to develop welding parameters and process controls for changing the major weld tooling for the ET at Michoud to Variable Polarity Plasma Arc (VPPA) welding.

The new welding process and tooling improvements developed will significantly reduce manpower and flow time requirements for assembly of the ET. Two innovations in assembly tooling have been developed and are in the process of being implemented at the Michoud Shuttle ET Assembly Facility. These are greatly simplified internal and external clamping tools that offer greater ease in jigging for welding and improvements in peaking and mismatch for the welded joints. In addition, a true track system for separating welded joints has been developed. Work continues on weld parameter development/refinement and on other tooling developments for the ET (Figure 76).

The vertical weld fixture has been installed and checked out. This fixture will be used for developing a reliable method of seam tracking to be used with VPPA welding and to determine if welding can be accomplished from the outside (instead of inside as is the current process). Development of an outside welding process holds promise of tooling simplification and some improvement in diameter tolerance control.

James H. Ehl/EH44
(205) 453-1520
Sponsor: OSF

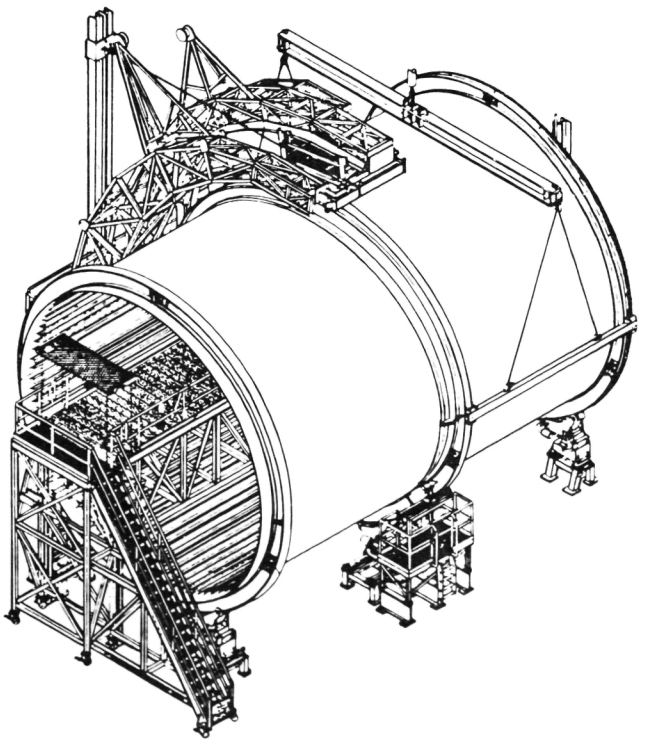

Figure 76. Large Horizontal Weld Development Tool.

Space Shuttle Main Engine Robotic Weld System

Fabrication of the Space Shuttle Main Engine (SSME) requires approximately 584 m (23,000 in) of welding, of which 60 percent is performed by automatic equipment. The remainder of the welds are made manually, at a defect rate more than twice that of the automated welds. Application of conventional automatic welding equipment is not practical for these welds because of the complex geometry of the joints and the need for adaptation during the weld.

An investigation called the Master Weld Program is an interactive computer program to allow welding engineers and operators to quantify all weld process parameters associated with an automatic weld. It was designed to be combined with graphically generated motion path information for a weld joint and converted to commands to a welding workcell robot.

In addition to its use for robotic welding, the Master Weld Program may be used alone to record parameters for any of 16 weld processes. These records may be used for quality control documentation for each weld made by automatic equipment in the form of a library of weld schedules.

Due to the large number of parameters required to specify each weld, mistakes in the programming can cause significant reductions in efficiency. The Master Weld Program incorporates some artificial intelligence (AI) techniques to assist the programmer and cross-check the entered values to eliminate errors. A proficient programmer will not be bogged down by instructions designed for a novice. The result is a structured, standardized approach to automated welding programming.

After the appropriate weld schedule has been entered into the computer database, it may be graphically displayed to verify the time-sequence of program operation. This function, called Graph, allows the operator to quickly scan the entire weld schedule for mistakes before execution on actual hardware. In summary, this system provides data to the welding robot, tabulates welding parameters, generates a cross reference library of welding schedules, documents all the weld schedules, improves programming efficiency and allows a "dry-run" of welds in graphic form before execution.

The SSME robotic welding system being developed by MSFC represents a distinct improvement over conventional welding automation because of the extensive positioning capability of its five-axis torch manipulator as well as the ability to tilt and rotate the part as it is welded. The robot controller also programs the operation of all welding process equipment to a degree of repeatability unatainable by its human counterparts. The system is equipped with a computer interface to a vision-based welding sensor that can compensate for variations in seam alignment and puddle size as the weld is being made (Figure 77).

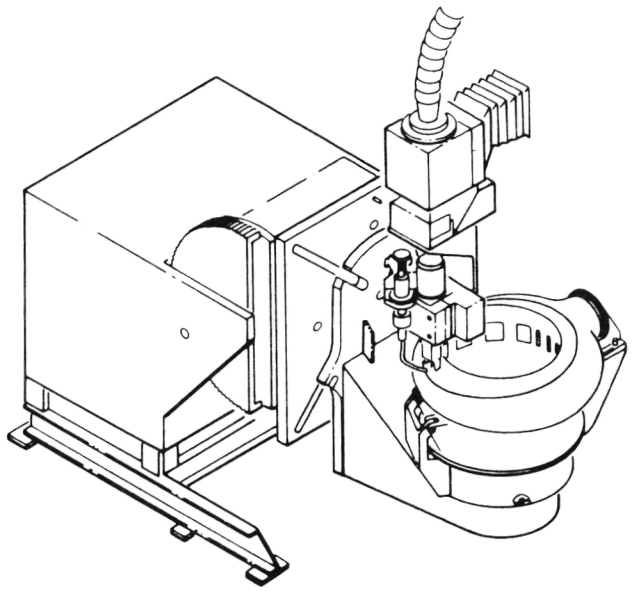

Figure 77. SSME Fuel Preburner Welding Tool.

During fiscal year 1985 engineers from Rocketdyne have been working with NASA engineers to characterize the parameters necessary to develop equipment and processes for welding SSME hardware. The group is jointly working to modify the robot to make it more suitable for the high-quality welds required in SSME manufacture.

The robot is located in the Process Engineering Division's Productivity Enhancement Facility at MSFC, and representative parts are being welded to develop sensors and tooling that will be used in production. Candidate welds for robotics are being demonstrated on fixturing developed at MSFC. Once the welds on a tool are proven on the MSFC system, the tool will be sent to the production facility to be used on the manufacturing robots.

The vision-based welding sensor developed by Ohio State University has demonstrated its ability to track the weld joint and compensate for varying gaps by modifying the filler wire feed rate. During the past year tests have been made to determine the critical sensor control parameters for tracking joints on SSME hardware. Computer programs are being developed to allow an operator to generate the robot programs from a graphic representation

on a computer terminal. This will permit more accurate programs to be written for the robot than can be done by hand.

Clyde S. Jones/EH42
(205) 453 – 0011
Sponsor: OSF

Weld Modeling

At first glance the fusion welding process seems simple enough; a puddle of metal is melted at the surface of a seam by application of intense heat, and as the puddle is moved, its solidified wake remains to join the edges of the seam together. Welders control the puddle by watching it and adjusting machine parameters to get the puddle they believe best for the job. When it is attempted to control the weld puddle without the welder, it becomes apparent that weld puddle physics is not yet well understood.

The application of a moving heat source model to a fusion weld in 1935 by Daniel Rosenthal at the University of Brussels may be considered the classical starting point for modeling welds. Although this model does represent the temperature distribution away from the weld puddle, it fails to determine puddle shape. Although this is in part due to variations in thermal conductivity neglected by the model, the key factor emerging from current research as controlling puddle shape seems to be circulations of molten metal in the weld puddle driven by magnetic pumping and by variations in surface tension on the puddle surface.

Finite element analysis currently underway is complex and will take time to develop; therefore, a simplified compromise has been worked out and now runs on a minicomputer. Instead of using the Rosenthal model as is, the model has been generalized by adding higher order terms from a multipole expansion of the moving heat source. Dipoles can represent latent heat effects by extracting heat where metal is melted and putting it back where the metal resolidifies. Quadrupoles can represent internal circulation of molten metal which remove heat from the puddle center and deliver it to the puddle edges, or bottom, or vice versa. The temperature fields of these high order multipoles decrease more rapidly than the basic Rosenthal monopole heat source term as distance away from the weld puddle increases. At far distances the higher order terms are negligible, but close to the puddle their effects can be pronounced.

It remains to be seen how well higher order multipoles can represent weld puddle phenomena. It would appear that whether surface temperature measurements can give useful information about weld penetration depends upon whether these measurements can be used to determine higher order thermal multipoles. It is anticipated that the extended Rosenthal weld model will prove to be a most useful analytical tool.

The computer model user's manual and documentation are being prepared for delivery to Coherent Optical System of Modular Imaging Collectors (COSMIC) for distribution in November 1985. Current application of the model includes R. Beil at Vanderbilt University who is modifying the model to compute weld metal cooling rates as part of the NASA sponsored study (through Martin Marietta Co.) of factors affecting weld strength in 2219 – T87 aluminum used for the Space Shuttle External Tank; and MSFC which plans to use the model as a general mathematical tool and has recently estimated the laser power required to penetrate 0.125 inch aluminum as part of an experiment planning effort. It is also being used as a model in a study of the feasibility of a front side weld pentrameter based upon infrared thermography.

Arthur C. Nunes, Jr./EH42
(205) 453 – 0011
Sponsor: OSF

External Tank Spray–On Foam Insulation Flowrate Instrumentation System

A method of accurately measuring the mass flow rates of the catalyst and resin used during the application of foam on the External Tank (ET) was needed to improve ET productivity. The ratio of the catalyst flow rate to the resin flow rate affects the quality and properties of the foam produced. Small deviations in the ratio can produce unacceptable foam. Integrating a system consisting of Model C – 50 Micro Motion Flowmeters, a PDP – 11 Computer, and an Industrial Products Subsystem, including software, provides this measurement capability.

Two Model C – 50 Motion Mass Flowmeters provide a real – time measurement of catalyst to resin ratio. Each flowmeter consists of a nonintrusive sensor unit, an electronics unit with analog output, and a remote display unit which displays the flowrate in pounds per second and total flow in pounds. The flowmeters measure resin and catalyst parameters between the formulator and the gun.

The sensor unit consists of a U – shaped tube on a vibration – free mounting. The tube is vibrated and twisted as fluid flows through it. The amount of twist is measured by two magnetic sensors and depends on the mass of fluid passing through the tube. The electronics unit generates signals to drive the remote display unit as well as provide auxiliary output. The remote display unit is located in the operator's console and displays mass totals.

The analog output from the electronics unit is converted to digital values by a Digital Equipment Corporation (DEC) Industrial Products (IP) Subsystem. During 1985 an applications program on the DEC PDP – 11 Computer was implemented which processes the data from the IP Subsystem and monitors flow rate, determines catalyst – to – resin ratio, checks value tolerance, provides real – time data display and stores data for processing. Flowmeter data is sampled every second. This sample rate produces an occasional out – of – tolerance condition due to flowmeter sensitivity. A program is then developed which calculates the ratio based on a 10 sec average. When an out – of – ratio condition occurs the operator is alerted via the terminal, a condition that would have gone unnoticed before.

In addition, a composite, three – mode Proportional – Integral – Derivative (PID) control is being used to monitor and control temperatures in flowing liquids and inside an autoclave even though the two processes have radically different reaction times. Temperatures for both types of processes are sampled every tenth of a second, but the proportional, integral, and derivative gains for each process are determined by the Ziegler and Nichols method, first described in 1942.

Temperature control of flowing liquids is required for catalysts and resins that are sprayed on a test section of the Space Shuttle External Tank in Spray – On Foam Insulation (SOFI) research. The catalyst and resin are kept in separate containers. Lines from these containers are separate all the way to the spray gun where the components are mixed. Each component is heated to the desired temperature in heater blocks after being pumped from the containers. Heaters along the lines also add heat equal to component heat lost due to travel through the hoses. A computerized robot arm points the spray gun to control foam application. A Digital Equipment Corporation PDP 11/23+ Host Computer operates the computerized robot and environmental controllers. It also controls turntable speed and acquires data for analysis.

Accurate temperature control for a 2.74 m by 3.66 m (9 ft x 12 ft) autoclave used to cure parts made from composite materials is required. Twenty – four heaters, controlled by four power controllers, heat the interior of the autoclave to 343°C (650°F). There is a long time delay between changes of power to the heaters and changes in temperature inside the autoclave. Since the part in the autoclave is large, part temperature lags far behind autoclave temperature. The process variable tem-

perature used in the PID control equation is set equal to a percentage of both the desired autoclave and the part temperatures. Autoclave temperature is controlled by a Fluke 2400B computer front end, which in turn is controlled by the Digital Equipment Corporation PDP 11/23+ Host Computer (Figure 78).

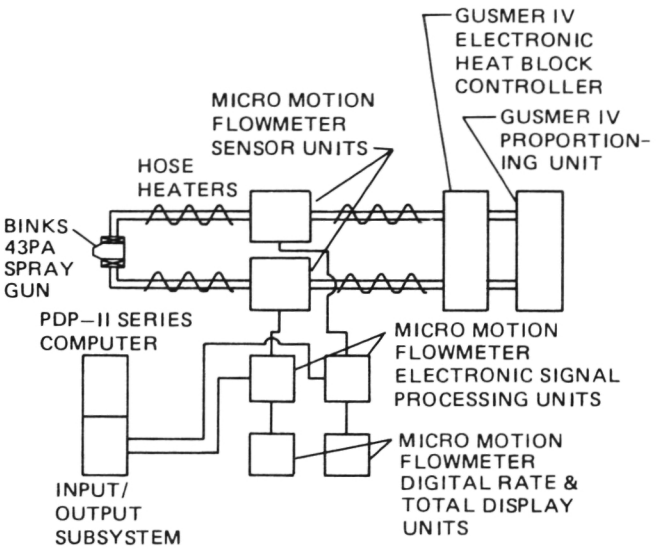

Figure 78. ET–SOFI Flowmeter Block Diagram.

Both processes described could be potentially hazardous in the case of equipment malfunction. Critical processing parameters are monitored to assure that they are maintained safely. If limits are exceeded, audio and visual alarms are initiated and emergency shutdown is performed. The program continues to monitor critical parameters even though the equipment has ceased to function.

Eutiquio Martinez/EH43
(205) 453 – 0643
Sponsor: OSF

Space Shuttle External Tank – Foam Application Development

A new technique of applying insulating foam to the External Tank (ET) Intertank segment is under development that will be more efficient and cost effective than present procedures. The present ET Intertank consists basically of two surface configurations. One part has vertical "hat" shaped stringers and the other part has narrow vertical ribs. At present there are two procedures for the application of foam materials. The vertical "hat" section of the Intertank is sprayed with CPR 488 foam in conventional "barber pole" rotational fashion using three oscillating guns. The Intertank part with the vertical ribs is insulated by spraying between the ribs with BX250 foam, machining the BX250 foam even with the tops of the ribs, and coating the BX250 foam with a tie coat (Isochem) material followed by the application of a top layer of CPR 488 foam.

During fiscal year 1985 development of two opposing spray guns were completed at MSFC as a joint effort with Martin Marietta Corp. (MMC) to define the process control parameters, such as, minimum/maximum gun angles, Intertank rotational speeds and gun(s) raise per revolution. They are set at critical angles, relative to the Intertank, to insure adequate coverage of both sides of the vertical "hat" sections and ribs as the Intertank is rotated and as the guns wave upward. Testing has already proven the feasibility of the concept. The new technique will allow the whole Intertank to be net sprayed with CPR 488 foam with significant savings in manpower and processing and will result in the elimination of two materials (BX250 and Isochem) with potential weight savings.

A second investigation is underway to develop and qualify a sidewall spray foam insulation (SOFI) to be used as a backup/replacement for the CPR – 488 foam presently used on the ET. The CPR – 488 foam presently used as a standard for ET sidewall has a density of 2.3 – 2.6 lb/ft^3; the North Carolina Foam, Inc. (NCFI) 22 – 65 presently used on the ET LH_2 Tank Aft Dome has a density of 2.6 to 3.1 lb/ft^3. The major thrust of the project is to develop a less expensive version/formulation of NCFI foam comparable in physical properties (density, compression/tensile strength, etc.) to the CPR – 488 presently used on the ET sidewalls. The project is a joint development effort by MSFC and MMC utilizing the capabilities of the MSFC Productivity Enhancement Facility and the MMC operated Michoud Assembly Fa-

ORIGINAL PAGE IS
OF POOR QUALITY

cility (MAF) in New Orleans, La., where the ET is manufactured. It will not result in any savings in manpower, serial time or weight; however, material cost savings will be significant since there is a difference of $5.22/lb between the CPR – 488 and the NCFI.

A third investigation is underway to develop a mold to replace hand – poured, foam molding techniques. A Reaction Injection Molding (RIM) process has been developed for use on the Space Shuttle ET. The standard technique for molding of foam protuberance areas on the ET consists of using oversized fiberglass molds that are filled by hand mixing and pouring of small batches of foam until the molds are full. The molds are then removed and the foam is sanded and trimmed to final dimensions by hand (Figure 79). Normally, numerous voids uncovered by the trimming and sanding have to be filled by hand. The voids are a result of air entrapment using the multiple hand – pour, molding technique. During fiscal year 1985, MSFC and Martin Marietta Corp. (MMC) developed a one – shot, net, RIM technique for some protuberance areas on the ET, especially some plumbing bracket ramps on the exterior of the ET. This new machine will provide the MSFC/Contractor Development Team the capability to trouble shoot production problems, off – line, without disruptions to manufacturing flow. The new RIM technique allows the ramps called "Blue Streak Ramps" to be net molded in one effort from the RIM machine with no subsequent work required when the mold is removed.

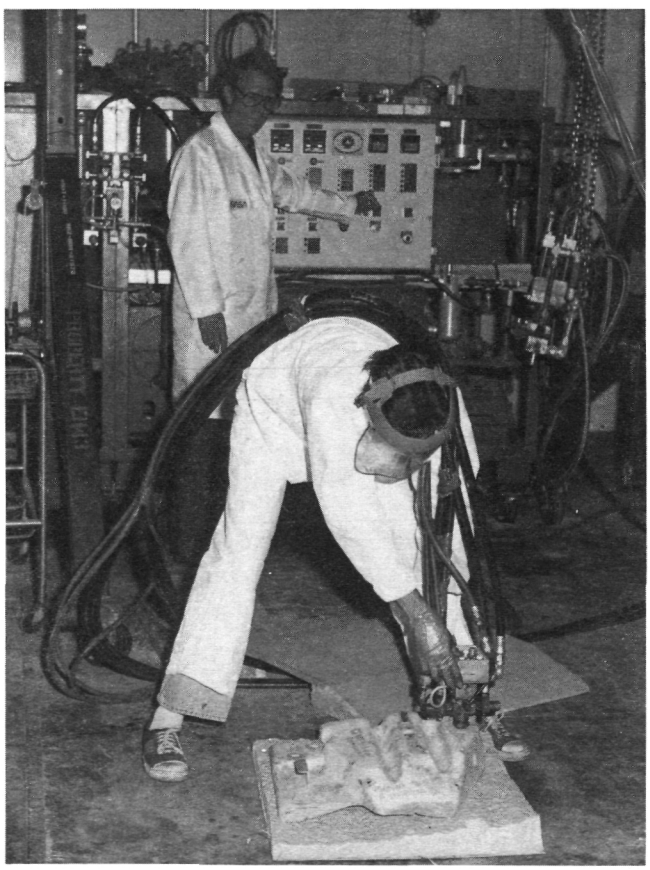

Figure 79. Reaction Injection Molding of Foam.

Technology transfer for the new technique has been made to Michoud Assembly Facility operated by MMC. This technique is scheduled for implementation on the Liquid Oxygen (LO_2) tank "Blue Streak Ramps" in Manufacturing Cells "G" and "H" in August of 1986 and on Lightweight Tank 44. Significant savings will result in the implementation of the RIM techniques because of the reduction in manpower, serial time, and material usage. Other application areas for the RIM technique on the ET are being evaluated by MSFC/MMC engineering personnel.

Charles Jackson/EH43
(205) 453 – 0643
Sponsor: OSF

Process Control Automation

A great deal of progress has been made in the automation of the Process Control Cells in the Productivity Enhancement Area and in establishing a Computer Control Center which links a large host computer to each test cell through a Local Area Network (LAN) known as Ethernet. Three test cells have been fully automated and two others are in the planning stage. A Computer Control Center is being established to support the various activities associated with the test cells. The Control Center will have a large host computer, large peripherals, and a Three – Dimension Color Graphics System for off – line programming.

The Three Process Control Cells that have been fully automated are the External Tank

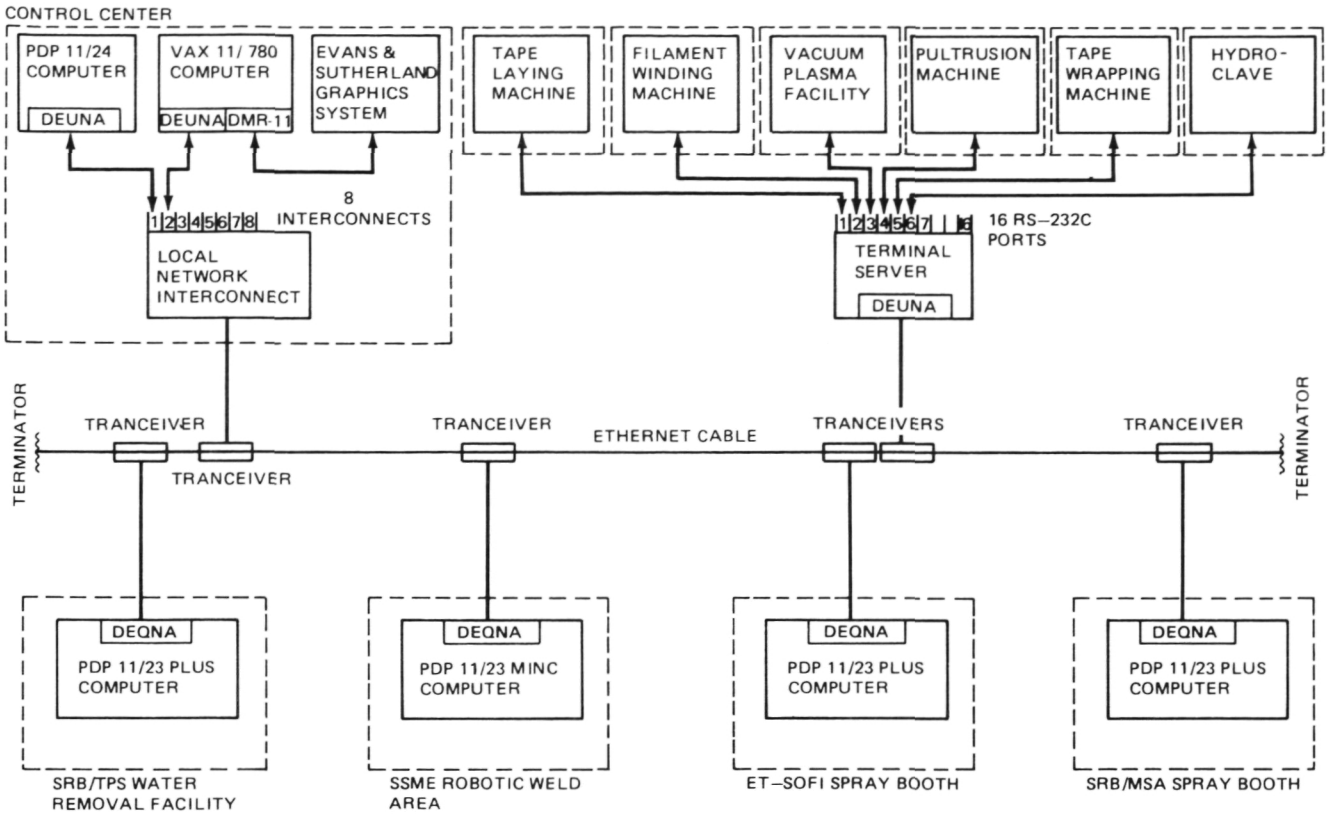

Figure 80. Ethernet Network.

Spray On Foam Insulation (ET – SOFI) Spray Facility, the Marshall Sprayable Ablator (MSA) Spray Facility, and the Thermal Protection System (TPS) Water Removal Facility. The two new areas under development during fiscal year 1985 are the Vacuum Plasma and the Autoclave Facilities. The automation of each test cell includes the installation of a control computer and designing, procuring and installing interface circuits from the computer to the subsystems to be controlled, such as turntables, robots, formulators and data acquisition systems. Finally, to complete the automation process, the application software is developed and tested. This software is especially designed for each application, and it allows the computer to monitor and control the process in a coordinated manner.

The Control Center, which has been implemented during 1985, has a large host computer and a set of large peripherals consisting of magnetic tapes, disk drives, line printers, etc. In addition, a three – dimensional color graphics system is available to model the processes of the test cells in order to optimize the operations and for prediction purposes. Each Process Control Cell is connected via the Ethernet to the others and to the Central Host Computer. This scheme allows the smaller computers in the test cells to share the resources of the host. These resources include data bases and large peripheral devices that, because of space limitations and economics, are not included in each test cell. This link to the central host computer facilitates the task of software development, data acquisition, and process control for each test cell (Figure 80).

Eutiquio Martinez/EH43
(205) 453 – 0643
Sponsor: OSF

Sprayable Ablator Process for Solid Rocket Booster Structures

During fiscal year 1985 a second generation sprayable ablator, designated MSA – 2, and a

highly automated spray application process have been developed at MSFC for use in Solid Rocket Booster (SRB) refurbishment activities at Kennedy Space Center (KSC). MSA – 1, the sprayable ablator currently applied to large areas of the SRB forward structures in coating thicknesses up to 0.64 cm (0.25 in) cannot be used on the aft skirt where up to 1.47 cm (0.50 in) thickness of insulation is required to protect against typical overall thermal loads of 1.367 x 10^3 to 1.249 x 10^3 J/cm^2 (1100 to 1200 Btu/ft^2). Both the MSA – 1 ablator and its successor, MSA – 2, are formulated from epoxy resins filled with phenolic microballoons, glass microspheres, and glass fibers. MSA – 1, however, is subject to cure stresses in applied thicknesses exceeding 0.64 cm (0.25 in). The MSA – 2 formulation incorporates a more flexible epoxy resin binder plus a small amount of ground cork to provide the necessary stress relief and eliminate stress cracking during the 71°C (160°F) cure of MSA – 2 coatings up to 1.47 cm (0.50 in) thick. Automated sprayed – on applications of MSA – 2 will now replace labor – intensive, hand – bonded applications of sheet cork over extensive clean – skin areas of the SRB aft skirt (Figure 81).

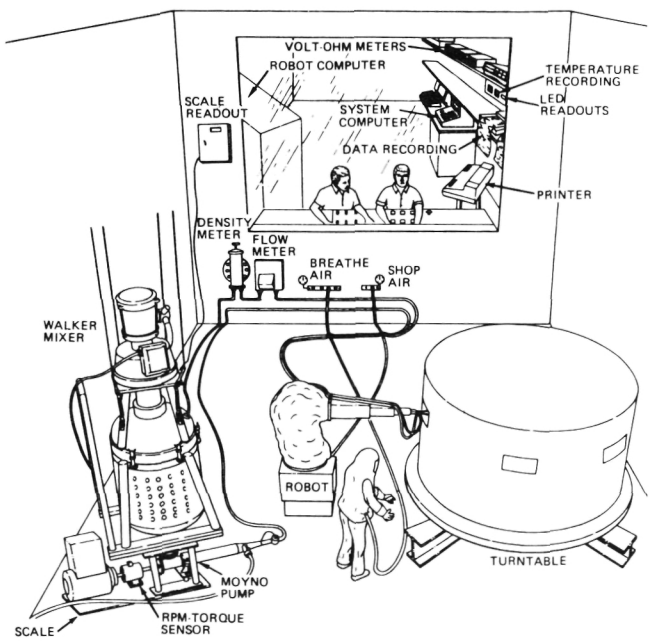

Figure 81. Automatic Robot Spray Processing for Solid Rocket Booster Thermal Protection System.

Development of a successful spray application process for MSA – 1 and its subsequent adaptation and refinement for MSA – 2 was accomplished through identifying the critical processing parameters and developing controls to maintain those parameters within defined limits. For example, for sprayability the ablator formulations are maintained in solution/suspension in halogenated solvents (nonflammable) and are continuously stirred and pumped through a circulation loop that includes mixer, pump, and spray gun by – pass. Acceptable solvent dynamics are maintained through temperature control; too high a temperature of the material or spray booth environment results in rapid solvent evaporation during a spray run, producing an extremely porous, structurally weak coating. Too low readings of the same temperature measurements result in a coating deposition so solvent rich that it is likely to slide off the substrate before it can be cured. In addition, solvent concentration during a spray run is critical. Too little and too much solvent show the same effect as too high and too low temperatures. A continuous reading mass flow densiometer included in the circulation loop responds directly to solvent concentration, confirming conformity of that parameter at the beginning of a spray run and responding to any material abnormalities that may develop during operation. Other monitored and controlled process parameters include pump speed and its corollary, material flow rate through the continuous circulation loop past the spray gun, as well as flow rate through the spray gun onto the substrate.

A Digital Equipment Corporation PDP 11/23 + Host Computer integrates and evaluates incoming parameter measurements and triggers requisite responses to assure programmed process stability. Consistently successful spray application of MSA – 2 ablator onto SRB flight hardware is also expected at KSC, where automated equipment based upon the MSFC system is being installed in the SRB refurbishment area.

William E. Hill/EH43
(205) 453 – 0643
Sponsor: OSF

Materials

An Electrochemical Study of the Corrosion Behavior of Primer Coated 2219–T87 Aluminum

This study, conducted during fiscal year 1985, was directed toward the investigation and development of electrochemical methods for assessing the corrosion of painted aluminum, with special emphasis on the primers used on the External Tank and Solid Rocket Boosters of the Space Shuttle System. Previous work in this area has included many potential – time and potential – current measurements, with varying degrees of success. The scope of this project was expanded to include electrical resistance – time (no previous studies), corrosion potential – time, polarization resistance – time, and corrosion rate – time. The latter measurements were determined using the polarization resistance method, wherein a controlled potential scan is applied to a sample starting at about 20 mV below the corrosion potential and extending to about 20 mV above it. From this information, the corrosion current, and therefore the corrosion rate, may be obtained. Because of the high resistance of the paint film on all samples, it is necessary to correct for the IR – drop caused by the film, and this correction was applied to all polarization resistance measurements. Typical results are illustrated in Figure 82, which shows normalized resistance – time and corrosion rate – time curves for TT – P – 1757 primers with various thicknesses.

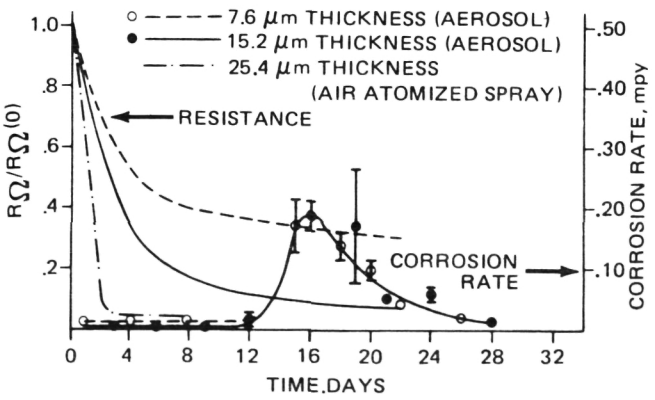

Figure 82. Normalized Resistance-Time and Corrosion Rate-Time Curves for TT-P-1757 Primers.

The electrical resistance – time curves give useful information concerning the porosity of paint films, while corrosion rate – time curves give important information concerning overall corrosion rates and corrosion mechanisms. In general, the corrosion rate – time curves all exhibited at least one peak during the 30 – day test period employed in this work, which is attributed, according to the proposed mechanisms, to the onset of the hydrogen evolution reaction and the beginning of destruction of the protective properties of the paint film. Similar information was obtained for the primers employed for the Solid Rocket Boosters (SRBs) of the Space Shuttle Transportation System. It was determined from this work that the Bostik 463 – 6 – 3 primer employed for the SRB has excellent resistance to water penetration, with extremely low corrosion rates occurring under the paint film. The DeSoto 513 – 346 primer used for the External Tank (ET) shows higher corrosion rates for a nominal coat (15.2 μm thick), with the peak in the corrosion rate – time curve occurring at a relatively early time (11 days). This primer is also relatively porous, with rapid penetration of the paint film by water. A primer coat 35.6 μm thick showed a much lower corrosion rate under the paint film.

Danford, M. D. and Higgins, R. H.:
An Electrochemical Study of the Corrosion Behavior of Primer Coated 2219 – T87 Aluminum. NASA Technical Paper 2459, April 1985.

Merlin D. Danford/EH24
(205) 453 – 4355
Sponsor: OSF

Formulation/Cure Technology for Ultra–High Molecular Weight Silphenylene–Siloxane Polymers

In the aerospace community a continuing need exists for elastomers capable of performing in extreme thermal/oxidative environments. Desir-

able characteristics for these elastomers include long-term thermal, hydrolytic and oxidative stability, coupled with retention of mechanical properties. A group of elastomers which exhibit some promise in this area are silicone polymers with their inherent thermal/oxidative stability. One class of silicone polymers, aryl-modified siloxane, designated as silphenylene-siloxane (SPS), have been the subject of extensive research.

Previous research had shown that the multi-stage polymerization technique could be utilized to produce SPS polymers with molecular weights in excess of 10^6. This technique involved the initial formation of a silanol-terminated prepolymer using 90 to 98 percent of the aminosilane stoichiometric equivalence. In the current research this prepolymer was isolated and purified by precipitation, then chain-extended to molecular weight in excess of 10^6 by incremental addition of aminosilane. Simultaneous incorporation of the vinyl group randomly along the polymer chain provided cure sites for subsequent conversion to a crosslinked elastomer. The high molecular weight gum stock was typically compounded on a micro rubber mill with fumed silica as a reinforcing filler and dicumyl-peroxide as vulcanization initiator.

Four different lots of the experimental methylvinylsilphenylene-siloxane with molecular weight above 9×10^5 were synthesized from prepolymers whose molecular weights ranged from 5.2×10^4 to 3.48×10^5. Both prepolymer and polymer were successfully synthesized in 200 g quantities. The large-scale prepolymer synthesis resulted in higher molecular weights at lower aminosilane concentrations (92.5 mol percent) than were previously reported. This was attributed to more efficient mixing provided by the mechanical stirrer as opposed to the stirring bar which had been used for the smaller scale syntheses.

The incorporation of the vinyl moiety along the polymer chain provided the expected crosslink sites for vulcanization, as indicated by formation of low-tack, thermoset elastomers following peroxide vulcanization. Equivalent or superior mechanical properties were achieved for the experimental elastomer as compared to an appropriate commercial silicone.

A comparison of prepolymer molecular weights with resulting mechanical properties indicates a positive correlation with both Young's modulus and elongation. Decreasing prepolymer molecular weight (M_W), (which increases cure site and crosslink density) drives the cured elastomer to higher modulus and lower elongation. This is the expected mechanical response of a more highly crosslinked rubber. The mechanical properties did not appear to correlate with final molecular weight of the polymer gum stocks.

The relative thermal/oxidative stability of the vulcanized experimental and commercial materials was assessed by thermographic analysis. The superior thermal/oxidative stability of the experimental polymer is illustrated in Figure 83.

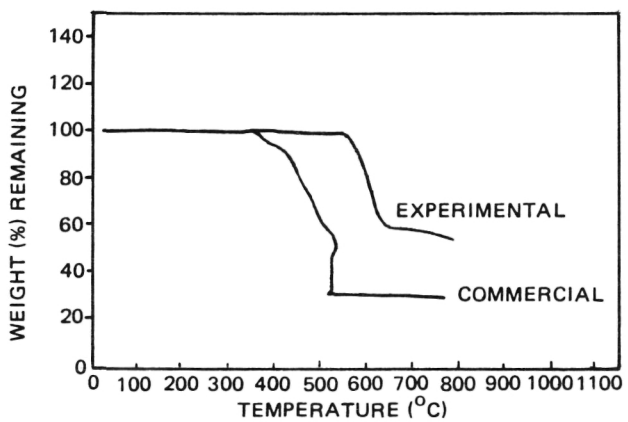

Figure 83. Comparative TGA for Experimental Elastomer Versus Commercial Silicone in Air.

Patterson, W. J., McManus, S. P., and Pittman, C. U.: Macromolecular Syntheses, 6, p.99, 1977.

Patterson, W. J., Hundley, N. H., and Ludwick, L. M.: Ultra-High Molecular Weight Silphenylene-Siloxane Polymers. NASA Technical Paper TP-2295, March 1984.

Hundley, N. H. and Patterson, W. J.:
Formulation/Cure Technology for Ultra – High Molecular Weight Silphenylene – Siloxane Polymers. NASA Technical Paper TP – 2476, May 1985.

N. H. Hundley/EH33
(205) 453 – 1231
Sponsor: CDDF

Cure Monitoring Methodology for Advanced Composite Materials

Composites have become standard engineering materials by replacing equivalent strength metals while yielding significant weight reductions. Much research has been done on composites; however, it is product experience, not scientific knowledge, that governs the materials' processing. Part size, shape, equipment, and material variabilities may produce deviations from an experience – derived optimum. In – process monitoring is warranted to assure reproducibility. Recording of dielectric properties and correlation of these properties to physical cure response provide such an in situ technique.

The two methods of dielectric cure monitoring which have been investigated as having potential application to Shuttle Solid Rocket Motor nozzle and filament wound case processing are parallel plate electrodes (capacitance bridge system) and microchip monoprobe (Micromet). While the capacitance bridge system (CBS) shows potential viability for low conductivity epoxy resin monitoring, it is still of indeterminant value for phenolic composite materials. The CBS is an acceptable method for monitoring cure of neat phenolic resins; however, the introduction of highly conductive fiber/filler reinforcements may lead to conductive transport phenomena capable of supplanting polymer moiety oscillatory responses.

The Micromet System II appears to be a viable means for cure monitoring of both epoxies and phenolic materials. Initial cure monitoring data for phenolic composite materials display reproducible results.

A representative investigation of Micromet – monitored dielectric responses during cure is presented in Figure 84. The onset of flow may be clearly determined at approximately 55°C. The next event occurs during the second temperature hold (95 – 105°C). An inflection is noted on the loss factor and permittivity curves; an endotherm is noted for the temperature display. This event appears tied to the boiling point of trapped volatiles.

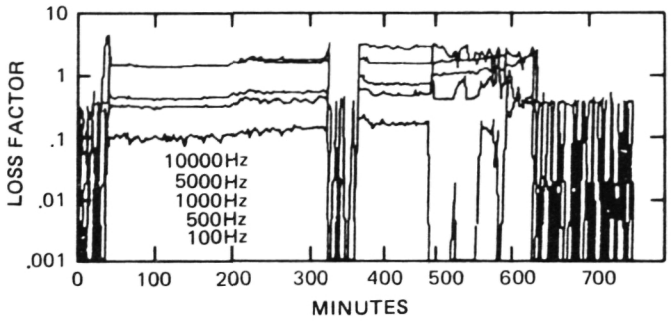

(a) Loss Factor Response for Indirect Lay-Up Procedure for Phenolic Composite Material versus Time.

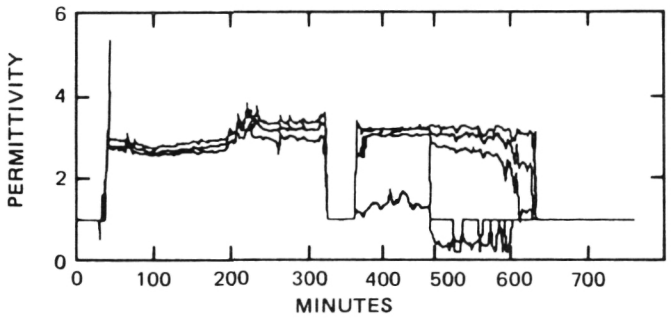

(b) Permittivity Response for Indirect Lay-Up Procedure for Phenolic Composite Material versus Time.

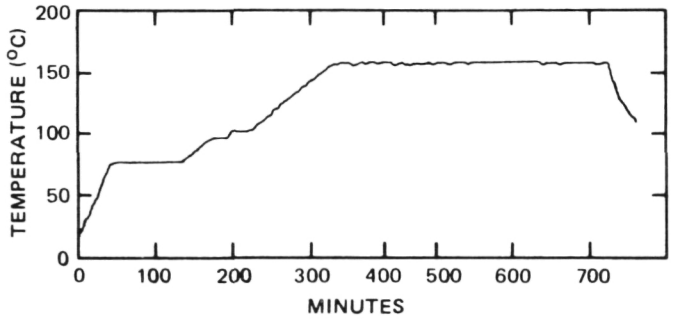

(c) Temperature Response for Indirect Lay-Up Procedure for Phenolic Composite Materials Versus Time.

Figure 84.

At approximately 140°C a deviation in the dielectric responses precedes a loss of signal. This loss of signal is not displayed by the temperature cycle; the problem is not in the sensor. It appears that the dielectric response is masked by thermal activation of the catalytic agents. As the ions are removed during cross-linking, the signal returns. It was noted that a deviation of all signals occurs at approximately 100 min into the final temperature hold, resulting in the subsequent loss of signal. This deviation may indicate water influx during cross-linking on gellation of the system.

While the CBS technique does not appear as sensitive to small deviations in moiety response, it appears to provide a more suitable technique for production-scale monitoring. The temperature ramp rate effects upon cure are clearly represented by this method.

An additional conductivity related term has been indicated for the dielectric permittivity. This term, heretofore unreported, becomes important when boundary layer effects and subsequent electrode shielding are noted. Initial investigations indicate that this term should be diffusion controlled. This work is on-going.

Goldberg, B. E. and Semmel, N. L.: Dielectric Cure Monitoring: Preliminary Studies. NASA TM-86452, May 1984.

Senturia, S. D., Sheppard, N. F., Jr., et al., SAMPE Journal, p. 22, July/August 1983.

B. E. Goldberg/EH34
(205) 453-1227
Sponsor: OSF

Orbital Atomic Oxygen Effects on Thermal Control and Optical Materials

An experiment on the effects of atomic oxygen on thermal control and optical materials was flown on the eighth Space Shuttle Mission (STS-8). The experiment was designed to expose a large number of material specimen disks to assess reactivity and investigate temperature dependence, influence of ultraviolet (UV) irradiation, and material transfer aspects. The experiment provided an atomic oxygen fluence of 3.5×10^{20} atoms/cm^2 incident perpendicular to the experiment material surfaces over a period of 41.17 hours at 120 nmi orbital altitude. Various paints, metals, organic and inorganic optical materials with applications to Space Telescope (ST), Tethered Satellite, and Advanced Solar Array Technology were flown on STS-8 to determine quantitative effects resulting from exposure to the orbital atomic oxygen environment.

Six material application areas on the ST that have been of major concern include the magnesium fluoride-coated mirrors, Chemglaze Z302 painted aperture door, Chemglaze Z306 painted light shields and baffles, Kapton H solar array blanket substrate, silver solar cell interconnects, and the Chemglaze Z853 coated crew aids (Figure 85). Short-term (approximately seven days) data generated to date, on the exposure of magnesium fluoride indicate no atomic oxygen effects either from chemical reactivity or diffusion. Oxygen diffusion at ST orbital altitude (approximately 593 km) cannot be determined at this time because of mission duration but oxygen density necessary to support diffusion is very low; therefore the effect of

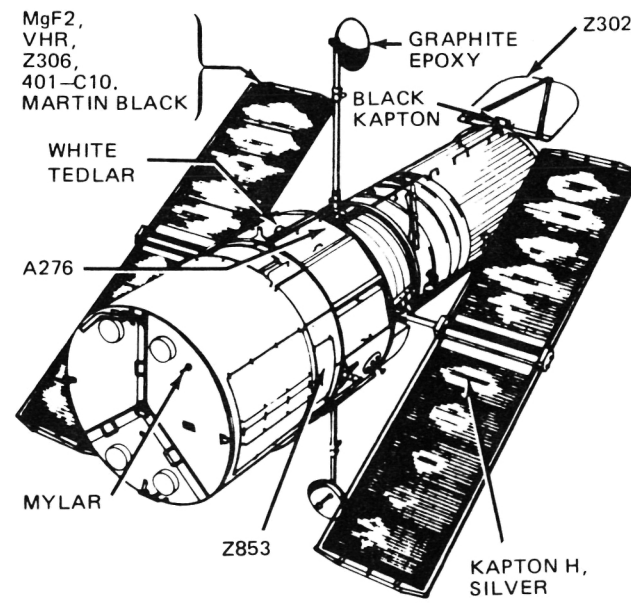

Figure 85. Space Telescope with Non-Metallic Surfaces Identified.

atomic oxygen on the ST mirrors is not expected to be a problem. The erosion of Kapton H has been well documented with reaction efficiencies generated to predict thickness loss based on mission duration, spacecraft altitude and orientation, and solar activity. Recession of Kapton H on the ST solar array blanket has been predicted and the blanket has been redesigned to accommodate the expected loss. Evaluations are currently underway to determine an overcoat for the silver interconnects that will extend ST on-orbit life but not add stress to the interconnect. Atomic oxygen on the Chemglaze Z306 painted baffles and light shields is expected to improve their diffusivity characteristics in the region of direct impact, improving their light suppression characteristics. A silicon coating has also been applied to the Chemglaze Z853 painted ST crew aids to alleviate the concern for transfer of loose surface particles on the exposed Z853 to experiment hardware during astronaut servicing. Finally, overcoats to be applied to the Chemglaze Z302 on the ST aperture door are being evaluated, not only for their low reactivity to atomic oxygen and good adhesion, but also for the ability to maintain the specular qualities of the paint.

Whitaker, Ann F.: LEO Atomic Oxygen Effects on Spacecraft Materials. AIAA Conference on Shuttle Environments and Operations, October 1983.

Whitaker, Ann F., et al: Orbital Atomic Oxygen Effects on Thermal Control and Optical Materials – STS-8 Results. AIAA 23rd Aerospace Sciences Meeting, January 14-17, 1985.

A. F. Whitaker/EH11
(205) 453-4877
Sponsor: OSSA

Liquid Oxygen/Gaseous Oxygen Compatible Elastomers

A substantial effort has been directed toward new elastomeric seal materials that exhibit reliable liquid oxygen/gaseous oxygen (Lox/Gox) compatibility. The major emphasis, particularly in the past few years, has been placed on 6.9 MPa (1000 psi) oxygen impact tests of fluorinated polymers such as those offered under the brand names of Teflon, Viton, Fluorel, and Kel-F, and by the generic name of carboxynitroso rubber. Most tests of Teflon, Viton and Fluorel showed them to be compatible; however, for each polymer, one or more failures were observed. No test data were found for Kel-F elastomer, although Kel-F plastic and oligomers of chlorotrifluoroethylene provided generally successful results. Carbonxynitroso rubber did not burn in oxygen, but was thermally unstable and not readily available.

A relatively new perfluorocarbon elastomer, Kalrez, was evaluated. High pressure impact tests and high pressure oxygen Differential Scanning Calorimetry (DSC) studies were conducted, focusing primarily on Kalrez and Kel-F variants. Variables included polymer type, effect of extraction, effect of carbon black, and post-vulcanization treatment with fluorine.

Kalrez provided the expected compatibility in 6.9 MPa (1000 psi) liquid oxygen impact tests and Kel-F 3700 elastomer, after treatment with fluorine, also passed the test. A reasonable correlation was found between high-pressure oxygen tests and high-pressure oxygen DSC exotherm temperature. Furthermore, DSC results were interpreted to show that the hydrogen content of the base polymer was inversely related to compatibility.

During the past fiscal year subsequent work was directed toward investigating the effect of hydrogen content and extractables and also the effects of molding and fabrication shop contamination on rubber compatibility with oxygen. Based on resistance to thermoxidation, low sensitivity to contamination, and good performance in standard impact tests, the prime candidate selected was 100 parts Kalrez and 20 parts TiO_2 (by weight). After cure and postcure, the material was treated with fluorine by a stepwise procedure and extracted by perfluorohexane. This material provided a dynamic seal at −196°C (−320°F) and was stable in pure oxygen above 200°C (400°F). It passed impact tests in oxygen at 27.6 MPa (4000 psi).

The elastomer is currently offered in limited commercial availability under the name "Katiflex" (Figure 86). Additional Lox compatibility specimens of the Katiflex perfluorelastomer

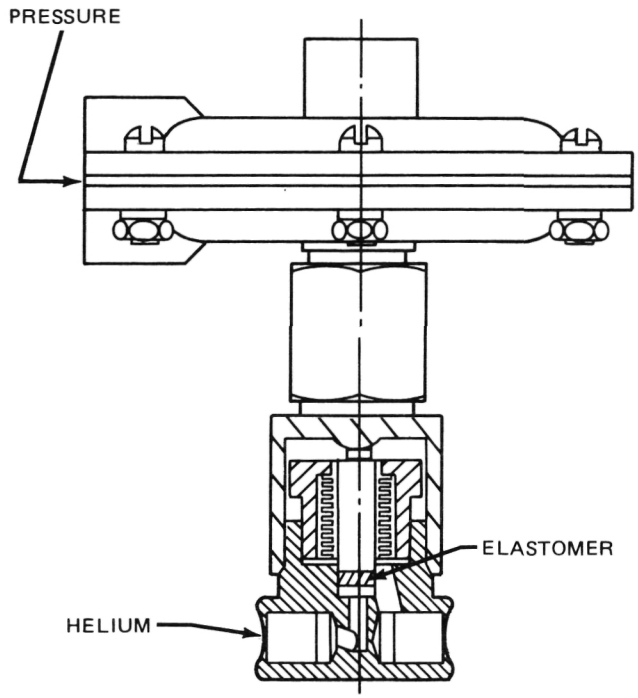

Figure 86. KATIFLEX – A Soft Seal for LOX/GOX Systems.

have been fabricated by TRW and the degree of Lox impact sensitivity has been more carefully studied. TRW is currently under procurement to MSFC for a large number of fabricated mechanical and physical test specimens that will provide for more complete material characterization, including tensile strength, elongation, hardness and compression set as a function of environmental exposure.

Development of Liquid and Gaseous Oxygen Compatible Elastomers for Advanced High Pressure O_2/H_2 Propulsion Systems. Final Report, NAS8 – 34909, TRW, Incorporated, July 3, 1984.

W. J. Patterson/EH33
(205) 453 – 3536
Sponsor: OAST

Space Power

Low–Temperature Semiconductors

The objective of this investigation is to design, fabricate, and test semiconductors which operate at very low temperatures (4K or less). Typically, semiconductors are optimized for operation near room temperature. When cooled, they may operate satisfactorily down to the temperature of liquid nitrogen (approximately 77K). Further cooling causes semiconductor characteristics to degrade. When liquid helium temperature is reached (approximately 4K), the semiconductor active device either behaves like an insulator or its characteristics are degraded, rendering it useless. When returned to room temperature, it is found to operate normally. This low temperature failure is due to a phenomenon known as carrier freeze – out.

The n – type silicon of a typical semiconductor active device, fabricated with normal concentrations of donor dopant, has a bandgap of approximately 0.05 eV between the energy of the donor level electrons and the bottom of the conduction band. At room temperature the thermally induced energy in the donor electrons is sufficient to excite them to the point that they are elevated to positions in the conduction band. This makes the material appear to act like a normal conductor with negative charge carriers. At temperatures near that of liquid helium, however, insufficient thermal energy exists to raise a significant portion of the donor electrons to the conduction band. Because they remain locked to their donor sites with no free current carriers, the material becomes an insulator. A similar energy gap exists between acceptor sites in silicon and the top of the valence band, and the same process affects p – type silicon in the same temperature range.

Although the vast majority of experiments and general processes that require interfacing with

electronic devices can be performed at room temperature, there are many cryogenic applications needing electronics capable of operating close to the point of signal generation. A few examples are the amplification of signals of liquid helium – cooled infrared detectors, the interfacing with superconducting circuits, and ultralow noise measurements in general. Specifically, some of the present bolometer type IR detectors are operated at about 1.5K or less, with the first stage electronics held at a higher temperature such as that of LN_2. Such applications occur in ground – based astronomy looking at radiation of wavelengths to 1000 μm. In a typical application the detector is thermally tied to the helium surface. Its associated first stage preamplifier is mounted to the helium stage on a thermal insulator and cold strapped to the LN_2 jacket so that it operates at about 77K.

An evaluation of the matching requirements between cryogenically operated signal generating devices and first – stage electronics was conducted. This process resulted in a basic course of action for the project. Primarily, silicon – based devices were to be investigated because of the perfected capabilities of silicon suppliers, the body of knowledge of silicon device behavior, MSFC experience with silicon device processing, and availability of an operational MSFC facility designed for silicon processing.

A number of principal design parameters have been identified. The device will be a voltage – controlled semiconductor such as a Metal – Oxide Semiconductor Field Effect Transistor. Layers of highly doped silicon will be used. The device would not be required to operate at room temperature.

Certain results have been achieved. MSFC has the capability of measuring and controlling temperatures from 1.4 K to room temperature; and general device parameters, as well as noise levels in tested devices, can be measured as they are cycled through any part of the temperature range. The low – temperature characteristics of both commercially available and MSFC fabricated devices have been measured. During 1985 the Center developed methods for precisely controlling very thin layers of doped regions in silicon, and designed devices whose physical and electrical layout should enhance their usefulness at low temperatures. The efforts for development and production of low – temperature semiconductor devices are continuing.

Robert F. DeHaye/EB13
(205) 453 – 1505
Sponsor: CDDF

Autonomously Managed Power System

Because of the critical need for substantially reducing orbital power costs, NASA is actively exploring means to increase power system capabilities while lowering the cost per kilowatt hour in order to power a broad range of space systems. A 250 kW, Low Earth Orbit, photovoltaic power system with a technological readiness of 1987 – 1988 has been selected as a focus. The Marshall Space Flight Center has been commissioned by the Office of Aeronautics and Space Technology (OAST) to develop an autonomously managed power system of such magnitude. The objectives of this effort are to generate a reference design, identify and assess the power management and distribution technology deficiencies, develop hardware and software technology, and then demonstrate and evaluate the technology developments in a power management and distribution system breadboard.

A reference design of a 250 kW direct current power system has been completed (Figure 87). This design makes use of cassegrain concentrator solar array power generation and nickel – hydrogen battery energy storage. This system design has seventeen power channels with a per channel capacity of 16 kW.

A breadboard/test facility for subsystem and equipment characterization and verification has been designed and is currently under development. This breadboard/test facility will allow the demonstration of management and control

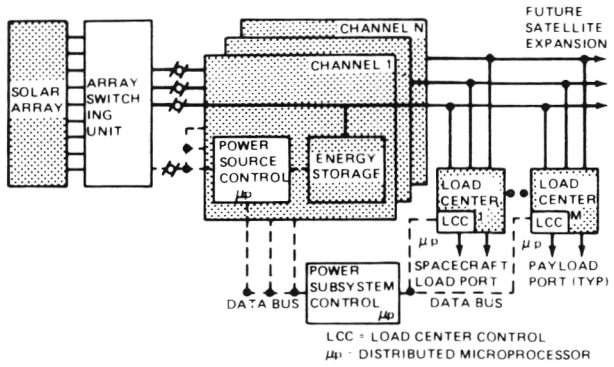

- GENERATION – CASSEGRAIN CONCENTRATOR SOLAR ARRAY
- ENERGY STORAGE – FUEL CELL/ELECTROLYSIS OR BATTERIES
- BATTERY CHARGER – SOLAR ARRAY REGULATION
- REGULATION – ON ARRAY SWITCHING (200–240 VOLTS)
- POWER TRANSMISSION– DIRECT CURRENT AT SOURCE VOLTAGE
- POWER DISTRIBUTION – DIRECT CURRENT AT SOURCE VOLTAGE
- POWER PROCESSING – AS NEEDED WITHIN EACH PAYLOAD OR LOAD CENTER
- CHANNEL QUANTITY – DEFINED BY ENERGY STORAGE CAPACITY (17)
- RELIABILITY – FAIL OPERATIONAL, FAIL SAFE GRACEFUL CAPACITY DEGRADATION WITH FAILURES
- LIFE – INDEFINITE, REPLACE FAILED UNIT AT NEXT SERVICE OPPORTUNITY

Figure 87. Management of Complex Power Systems Using Distributed Microprocessors Linked with Data Bus.

philosophy and autonomous operation of many system functions while providing concise display of system status to the operator/astronaut. Affordable management of a complex system is offered by extending lifetimes of components and subsystems, reducing hardware requirements through software redundancy provisions, and minimizing crew and ground support requirements.

The power system breadboard facility has one power channel and one load center that was completed in 1985. An electrical power subsystem controller, a load center controller, and a power source controller along with many of their algorithms have been completed. A 75 kW solar array simulator for power generation and a 168-cell nickel-cadmium battery for energy storage simulation have been developed. A load center, including loads and switchgear, is under development. Also, under development is the data bus interconnection of the controllers as well as the breadboard facility host computer environment for developing various power system operational scenarios, displaying system status, and simulating various power system interfaces such as the crew and the spacecraft controller.

David J. Weeks/EB12
(205) 453-2514
Sponsor: OAST

Battery Protection and Reconditioning Circuit as Used on the Hubble Space Telescope

The Hubble Space Telescope (HST) uses six nickel-cadmium (Ni-Cd) batteries as the primary means to store electrical energy. The six batteries, each constructed with 23 Ni-Cd cells connected in series, are operated in parallel and connected by diodes to the main power busses. Because of the degradation of the voltage discharge characteristics of the Ni-Cd batteries over time, a battery reconditioning system is required for the lifespan of the HST.

The reconditioning system being built for the HST is a Battery Protection and Reconditioning Circuit (BPRC) developed and tested for several years at Marshall Space Flight Center (Figure 88). The BPRC protects weak cells and low-capacity cells from cell reversal during the discharge cycle, protects low-capacity cells from cell reversal during battery reconditioning, and allows battery discharge to less than 0.5 V/cell for reconditioning. Reconditioning can be accomplished in approximately two days compared with up to 11 days required by previous methods. Each battery on HST houses a BPRC in a module mounted between the 23 Ni-Cd cells and the top cover. The multilayer printed circuit board, output diodes and main transformer are mounted on a metal plate. This modular design allows the BPRC to become an integrated part of the battery, thus minimizing external electrical connections.

The flight design of the BPRC has been finalized with the following results: the BPRC can protect up to two discharged cells without damaging the battery and can provide up to 18

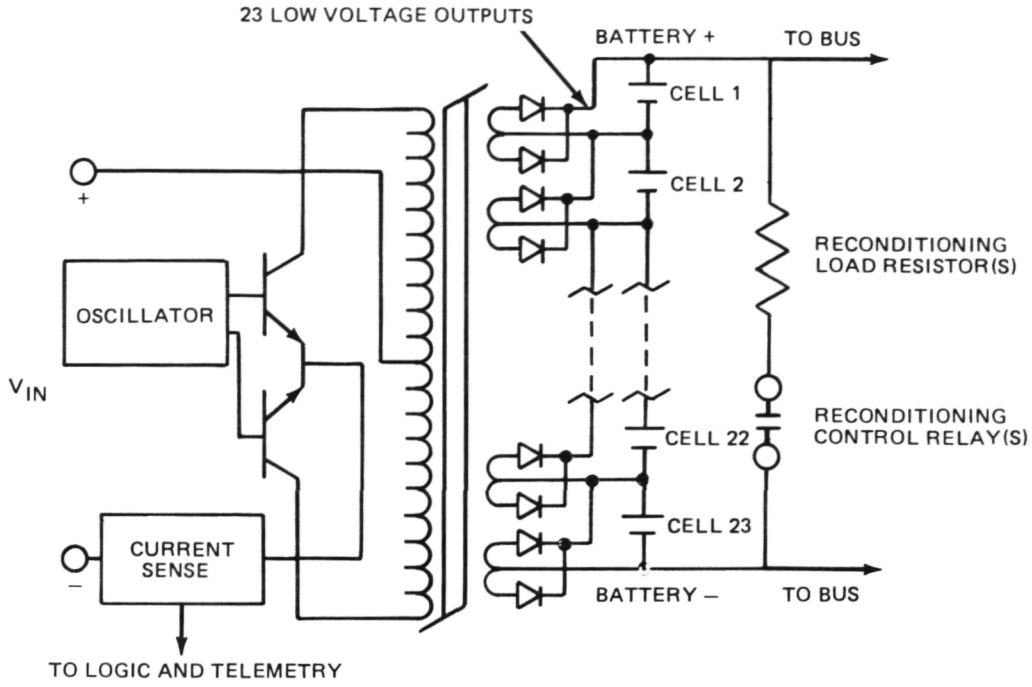

Figure 88. Simplified Flight Reconditioning Circuit.

A of current to a weak cell; the BPRC will provide satisfactory thermal operating characteristics and a good thermal margin of safety for long-term performance; the BPRC has a calculated failure rate of less than 0.8×10^{-6}, a mean time between failure of greater than 1.3×10^{6} hours, and a 2.5 year mission success rate of greater than 98.3 percent. In addition, no failure in the BPRC can cause a battery failure.

Louis F. Lollar/EB12
(205) 453-2510
Sponsor: OAST

Miniature Cassegrainian Concentrator Solar Array

Experimental and analytical evaluation of the miniature Cassegrainian concentrator solar array has indicated that this solar array concept shows significant possibility for reducing both solar array cost and area. Because the element is miniaturized, it operates in Low Earth Orbit at a temperature of about 85°C utilizing only passive, radiative cooling. The efficiency of the element's gallium arsenide (GaAs) cell at this temperature is nearly 20 percent.

Development of the array has been directed at the design, fabrication, and testing of the solar cells and individual elements. Work is being done on a new element design which reduces blockage by the secondary mirror support and is the first design to include consideration of vibrational launch environments. These elements were tested and found to be at predicted levels of performance.

The present emphasis of the program is the development of a structure to which the individual elements are attached to produce a solar array. As a result of analytical studies conducted on the dynamic and thermal response of a large solar array wing, graphite epoxy was chosen as the structural material. The structure consists of a honeycomb grid pattern to which the solar cell elements attach. Four quarter- panels, 63.5 cm by 71.1 cm, were fabricated for testing. Tests of the panels indicate that the required planarity can be achieved and that the panel strength for the model was as expected. The next consideration is an increase of the carbon fiber content

in the design in order to achieve the full strength and weight advantages of graphite epoxy. The study of the element and panel structure design will continue through this fiscal year and into 1986.

M. R. Carruth, Jr./ES53
(205) 453 – 0029
Sponsor: OAST

Robotics and Teleoperations

For several years MSFC has been developing realistic ground – based simulations of teleoperation and robotic systems for the purpose of enhancing future development and application for such programs as the Orbital Maneuvering Vehicle (OMV) and the Space Station. As an integral part of the systems investigations, the characterization and optimization of the performance of the human operator is being investigated. In the MSFC teleoperation and robotics facilities, there exist two elements: the manipulator test bed and the flat – floor, air – bearing facility.

During fiscal year 1985, several improvements were made to the MSFC facilities. A Dynamic Target Simulator Arm, with six degrees of freedom (DOF) was added which provides a capability of attaching large targets. Now more extensive tests can be performed on most control systems concepts, lighting, stereo viewing, various sensors, etc., leading to rendezvous and docking. Earlier, these tests were conducted or planned with targets mounted at fixed locations. In order to allow more comprehensive, higher fidelity testing, other improvements were incorporated. The maneuvering vehicle was modified to allow thrusting through the center of gravity (CG) with a multiplicity of targets (and different weights) attached. A new graphics simulator was installed which allows very rapid, more realistic predictive displays for the manipulator arms. A new six DOF hand controller was also installed.

Several important studies have been completed and others initiated in 1985. A lighting study was completed at the flat – floor facility using floodlights for broad illumination of wide areas, contrasted with visual effects provided by selected spotlights. The results will be used to produce more efficient, and more cost effective, illumination for future teleoperators and robotics, as well as general rendezvous and docking schemes. Another study was completed which investigated systems ramifications of the use of up to four cameras for rendezvous and docking maneuvers.

A new study was initiated with the MSFC Orbital Service System (OSS) to show that modular replacements can be performed on the Multimission Modular Spacecraft (MMS). This effort is relatively comprehensive in that it includes the exchanging of MMS modules on the OSS in three modes of operation which include automation, automation with supervision, and manual augmentation. Another study is leading to establishing a baseline for the Proto-flight Manipulator Arm System. This is designed to allow rigorous comparison of future

Figure 89. Orbital Servicer System with Manipulator Arm.

changes in system performance incurred by any specified subsystem or component change. Parameters in the baseline include such things as lighting combinations, camera locations, human factors, two types of hand controllers, specific end effectors, control modes, etc. The goal is to determine the capabilities and limitations of state-of-the-art, dexterous, manipulator arms involving the total system that would be utilized for satellite servicing (Figure 89).

D. R. Scott/EB24
(205) 453-3369
Sponsors: OSS and OAST

Information Systems

A Laser Optical Disk in a Data Base Management System

The research activity of the Data Base Management System/Mass Memory Assembly (DBMS/MMA) addresses the problems associated with ground processing and handling of large amounts of data generated on board a spacecraft and from independent ground-based systems. New demands are being placed on ground processing facilities by the

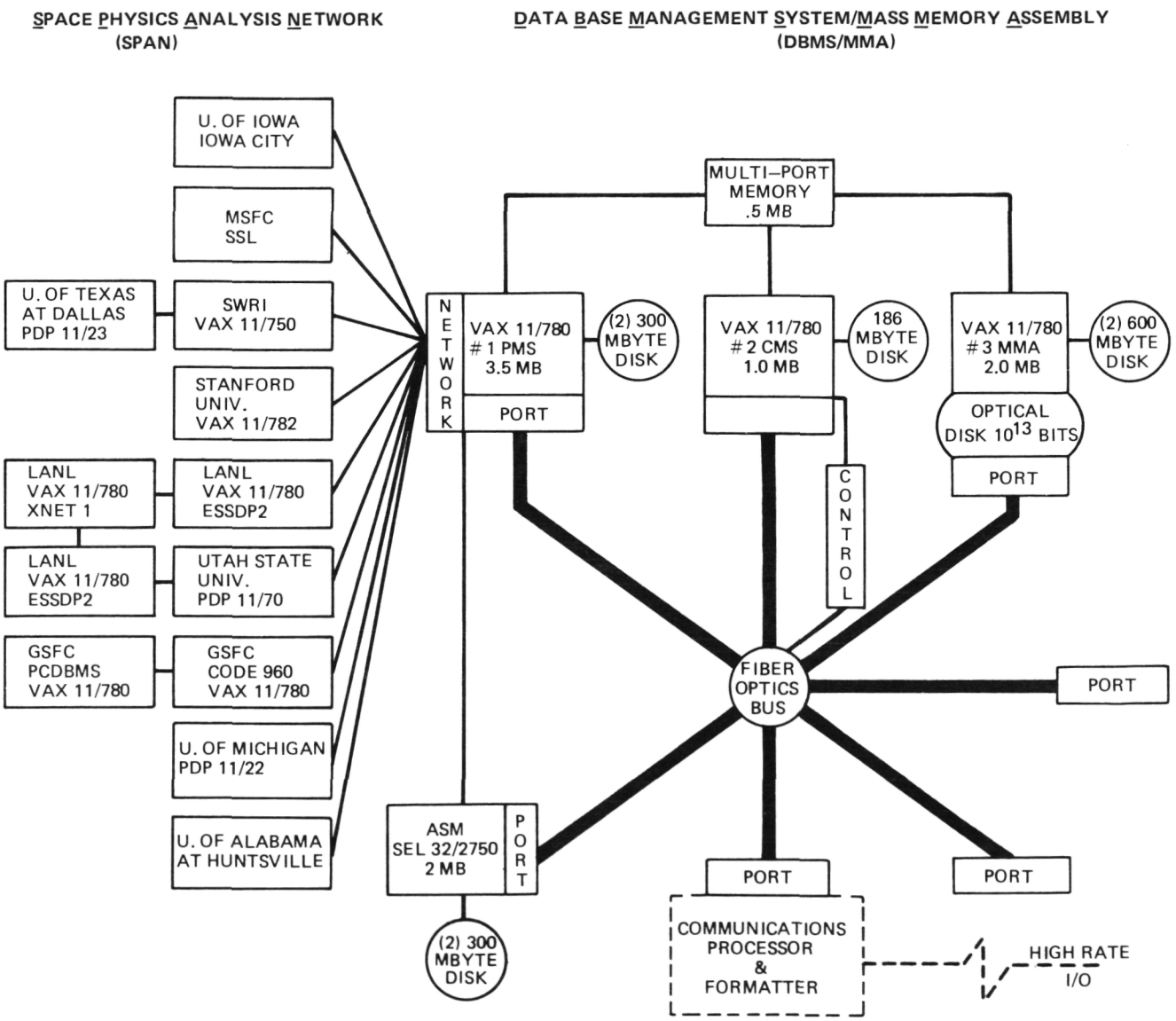

Figure 90. Data Base Management System.

increased bandwidth required to transfer the large volumes of data being generated by sophisticated high rate sensors. There is also a shift from single investigators for a given experiment to experiments by investigative teams whose members are spread across the country.

The DBMS/MMA was installed at MSFC in September 1984. A network of Plasma Physics users was interfaced to the system to help verify its performance, and in the process, has been performed productive analysis on flight data. The design goals for the system, which addresses the new demands, are to accept data from multiple sources at rates up to 50 million bits/sec, record large volumes of the data in an on-line archive, and make the data available to users in near real time. The key components and design elements used to achieve these goals were an autonomous data packet, a distributive processing system, a fiber optic bus, and a laser driven optical disk (Figure 90).

The optical disk recorder, used for the data archive, represents a new concept in data storage. The unit, built by RCA, is the first of its type to be delivered. It utilizes an argon laser to record data onto a 14 in tellurium-coated aluminum disk. Each bit recorded is a .485 μm diameter "pit" made on the disk by the laser. Data is recorded and read at a burst rate of 100 million bits/sec with a sustained rate of up to 50 million bits/sec. One disk has a storage capacity of 8×10^{10} bits or the equivalent of 263 magnetic tapes recorded at 1,600 bits/in. A "juke box," which holds 125 of these disks, provides an on-line capacity of approximately 10^{13} bits of data storage while requiring only 21 ft^2 of floor space. The disk can be written on only once, but read many times. The worst case access time to any data in the system is six seconds. The projected life of a disk is 10 to 15 years without the bit-error-rate exceeding the specified rate of one error per 10^8 bits.

Near-term advances in optical disks, such as implementation of an erasable recording media and replacing the gas laser with newly developed laser diodes, will have an even greater impact on archives and mass storage devices of the future.

Douglas T. Thomas/EB32
(205) 453-0677
Sponsor: OAST

Structures and Dynamics

Space Deployable Structures

During the past several years, interest has increased in the use of deployable structures as building blocks in the construction of large space systems such as the Space Station, the Occulter Facility, large antenna systems, solar arrays, and others. Several concepts were developed and studies were performed to assess their applicability to various programs. The upgrading of existing facilities to extend their capacity was also considered. Two technological programs resulted from these studies; namely, the fabrication of a 0.75 m (30 in) diameter deployable mast with continuous longerons and a 1.3 m (52 in) square deployable/retractable truss.

Coilable-longeron lattice columns varying in diameter from 0.2 to 0.5 m (9-19 in), employing single and double lacing of the mast diagonals, have been used for a variety of spacecraft missions. This program attempted to maximize all performance characteristics, i.e., double lacing and largest possible diameter. The selected design for the work in Phase I was a three-longeron mast with double-laced diagonals and a diameter of 30 in. Phase I consisted of two major activities: four parametric design studies including longeron material investigation and manufacture of a 6.1 m (20 ft) long engineering model. The analytical design study was conducted to establish preliminary sizing of the major mast members incorporating different composite longeron materials. Three materials were considered including S-2 fiberglass, high-elongation graphite, and a hybrid combination of both fibers. Results indicated that S-2 fiberglass is

ORIGINAL PAGE IS
OF POOR QUALITY

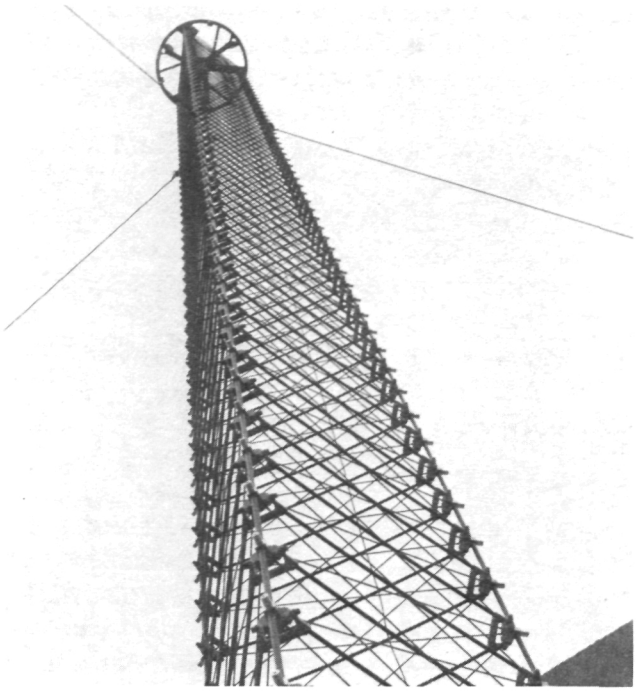

Figure 91. 0.75m Diameter Mast in Deployed Position

the preferred longeron material because of its high strain capability. The fabrication and demonstration of the 6.1 m (20 ft) long demonstration model was also completed during this part of the study. Based on this effort, a 15 m (50 ft) long deployable/retractable mast was built in the second phase of the program. The hardware consists of the actual mast and the support/wench stand which is required for ground testing under one g. Figure 91 shows the deployed structure with predicted mast capabilities as follows: Euler buckling – 8756 N (1,964 lb); bending strength – 4722 N – m (41,748 in – lb); bending stiffness $1.287 \times 10^6 \times N - m^2$ (4.486×10^8 lb – in^2). An extensive test program is planned to verify the capabilities and define dynamic behavior of the structure in fiscal year 1986.

The truss design which was developed in 1985, uses folding longerons and telescoping diagonals in conjunction with a deployment/re-

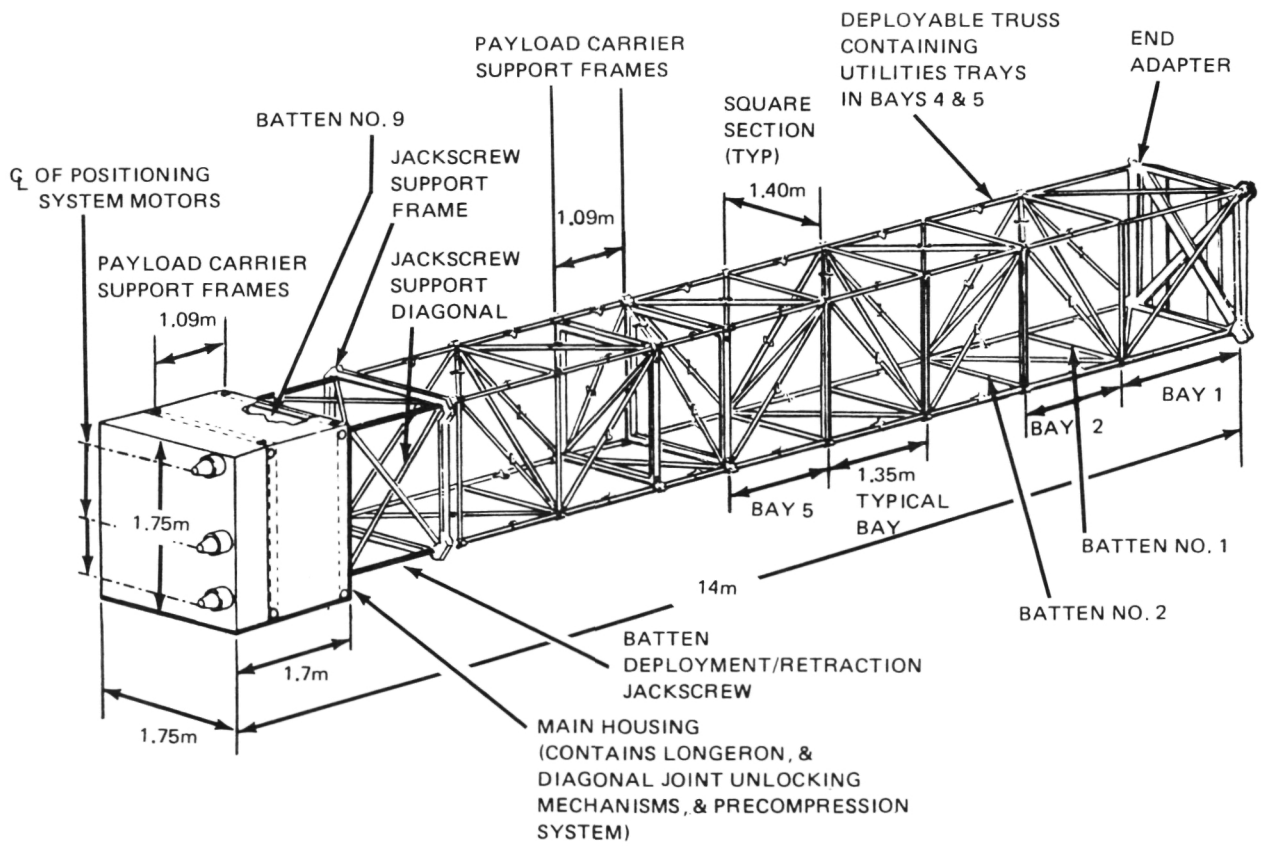

Figure 92. Test Article Design Description.

traction mechanism to provide a stable truss configuration with full structural capability during all phases of deployment and retraction. A bay – by – bay deployment is achieved by using four jackscrews which engage with quarter nuts at the corners of the fixed batten frames. The concept also has a built – in utility tray which unfolds during deployment and provides a 50 cm (20 in) wide surface for installing utility, measurement and data system cables, as well as fluid lines. The design allows for complete ground verification of the operational system before flight. With the exception of steel jackscrews, the present design utilizes aluminum for all structural parts. The application of advanced fiber composites to reduce weight and provide high thermal stability is under investigation. Figure 92 shows the overall truss configuration. This truss and the 30 in mast represent the largest deployable space structure test articles built to date.

E. E. Engler/EP13
(205) 453 – 3958
Sponsor: OAST

Solar Array Flight Experiment/ Dynamic Augmentation Experiment

The SAFE Dynamic Augmentation Experiment (SAFE/DAE) was conceived in 1981 as a Shuttle flight experiment to demonstrate the feasibility of on – orbit measurement and ground processing of the dynamic characteristics of large space structures. These characteristics are frequency, damping, and mode shapes. Test definition or analysis verification provides the dynamic characteristic accuracy required for control systems use. In conventional launch of space vehicles, including the Shuttle, control system/structural interaction could be prevented by placing the control system natural frequency well below the lowest structural natural frequency and still maintain adequate control authority. Large space structures (LSS), however, have such low natural frequencies that the control system natural frequency will have to be "nested" among the structural natural frequencies in order to have adequate control authority. This problem, coupled with the dense rate of LSS structural frequencies, requires a very accurate definition of the structural characteristics. Unfortunately, LSS type structures cannot be tested in the Earth environment, leaving on – orbit tests as the remaining alternative. Fortunately, the Solar Array Flight Experiment (SAFE) was in development at that time and scheduled for a 1984 launch. The SAFE has all the characteristics of an LSS and was a target of opportunity years ahead of the next structure. This opportunity provided the impetus for the SAFE/DAE.

The SAFE/DAE utilizes a retroreflector field tracker (RFT), which is positioned near the base of the solar array. The RFT illuminates 18 – 23 retroreflector targets on the array with 5 laser diodes at the 800 nm spectrum. The sensor portion is an adaptation of a multifield star tracker. The sensor optics focus the retroreflector images on a solid state, charge injection device detector. A remotely located microprocessor controls the data acquisition, interrogates the sensor detector, converts the sensor data to engineering units, and provides a digital output. These units are then multiplexed and stored on a digital tape recorder. Post – flight ground data evaluation processes the ensemble of X and Y motions from all targets to determine the array dynamic characteristics. Evaluation techniques utilize the free decay and time and frequency domain analysis to evaiuate dynamic characteristics.

Six SAFE/DAE tests were run. Data were obtained from all targets during all tests, even though some targets were outside of their anticipated maximum deflections. The reason for this anomaly was that the solar array unexpectedly curved around the mast on the dark or cold portion of the orbit prior to SAFE/DAE data take. This curvature was measured by the SAFE/DAE and is shown in Figures 93 and 94. The small bright dots on the mast top enclosure and blanket are the retroreflector targets. The larger circular targets on the array are the photogrammetric targets.

Evaluation of the measured dynamic characteristics indicates that three modes have been

ORIGINAL PAGE IS
OF POOR QUALITY

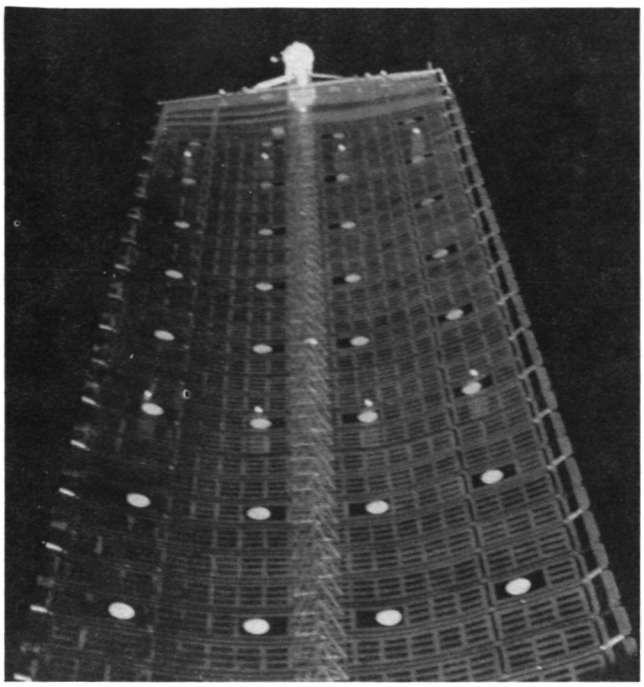

Figure 93. Solar Array Nighttime Curvature.

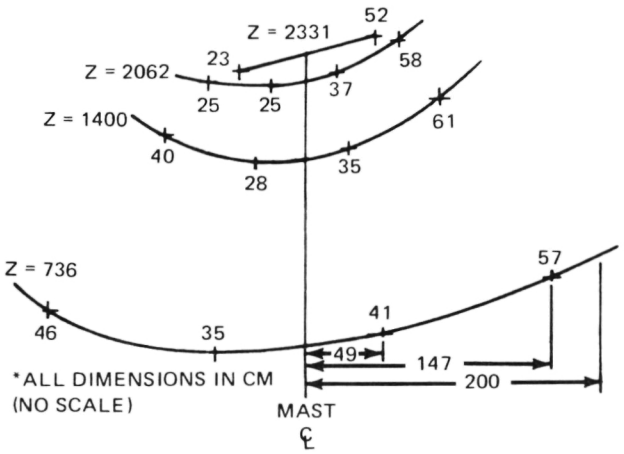

Figure 94. SAFE Nighttime Deflections.

tentatively identified. The modal frequencies tend to vary slightly with different excitation techniques. The first mode damping was very high, 12 to 15 percent, higher mode damping was less, in the three percent range.

Although data analysis and review are not complete, the preliminary evaluation indicates the objectives of the SAFE/DAE have been accomplished. This information indicates that it is technically feasible and viable to perform on-orbit dynamic tests to verify or improve analytical predictions of LSS dynamic characteristics. The data gathering techniques are viable. The data evaluation techniques would certainly need to be extensively expedited or automated but are technologically possible.

Richard W. Schock/ED24
(205) 453-2526
Sponsor: OAST

Composite Structures Development

Recently there has been renewed interest in the use of composite materials in the overall Space Shuttle System to improve performance and reduce weight. A composite structure can be described as the final product formed from the combination of a reinforcing agent and a matrix binder. Such structures offer the distinct advantage of being lightweight, strong and rigid.

Engineers at MSFC, Martin Marietta Corp. (MMC), and the External Tank (ET) prime contractor, have been working to determine which ET parts can be manufactured from composite materials to provide a weight savings of 40 percent when compared to its metal counterpart.

The first prototype part constructed at MSFC has been the forward GH_2 pressure line fairing (Figure 95). The existing fairing, weighing 1.23

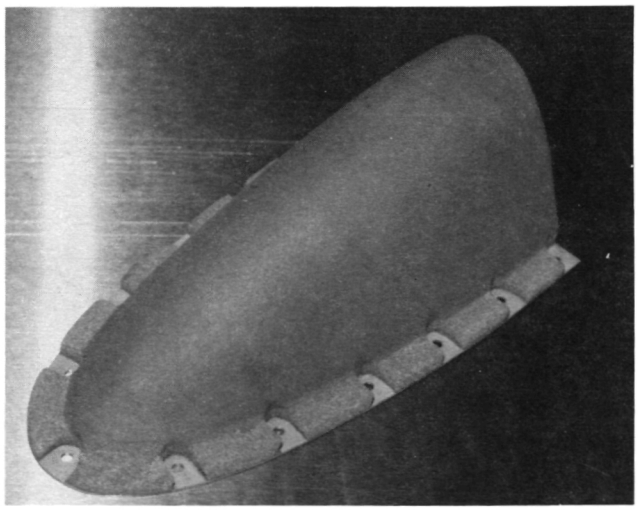

Figure 95. Composite GH_2 Pressure Line Fairing.

kg (2.71 lb), is made of aluminum and coated with a thermal protection system, Super Light Ablator (SLA). The composite fairing, weighing 0.37 kg (.83 lb), is constructed from a graphite/epoxy material system manufactured by Hercules, Inc. (Figure 96). The use of composite materials eliminates the need for the thermal protection system saving additional weight and producing an overall weight savings of 69 percent.

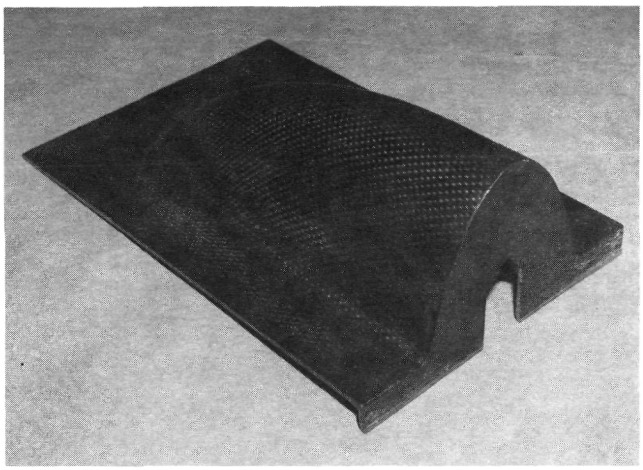

Figure 96. Forward and Aft GH_2 Pressure Line Fairings — Composite Structure.

The fairing is formed in a six-layer sequence. Each of the first five layers is cold debulked after lay-up. Upon completion of the sixth layer, the fairing is hot debulked, cured, and post-cured in an autoclave. The reinforced female tool used during the lay-up was constructed at MSFC using graphite/epoxy composite tooling material manufactured by Fiberite, Inc. The tool was formed using a male mold, cured and reinforced with flat rib sections that provide structural support. Other ET components already identified as candidates for construction from composite materials include cable tray covers, cable tray bracket shields, nose cone fairings and thrust struts.

Gail H. Gordon/EH43
(205) 453-0643
Sponsor: OSF

Development and Test of Advanced Composite Components

Limited technology existed in the design, analysis, and fabrication of advanced composite components typical of those found in large optical structures requiring high thermal stability, such as Space Telescope and Advanced X-Ray Astrophysics Facility (AXAF). Design layups were not generally available, especially for the Pitch 75 graphite fiber system (pyrolized pitch with a 75 x 10^6 psi modulus).

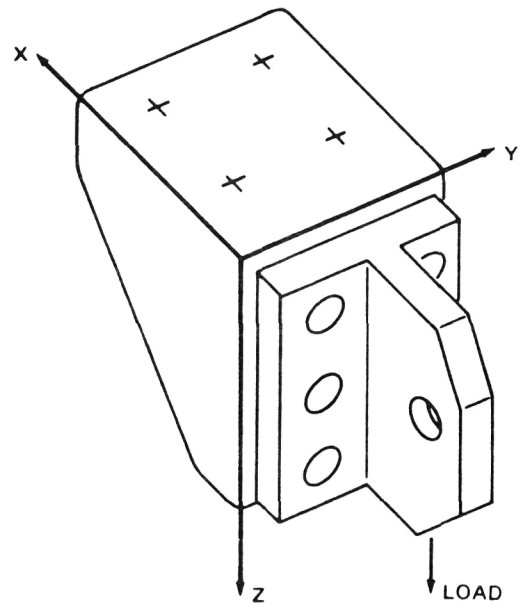

LAYUP DESIGN	SAMPLE NO.	ULTIMATE FAILURE LOAD (LB)
A	1	4,046
	2	3,703
	3	3,492
B	1	4,492
	2	4,083
	3	4,387
C	1	2,229
	2	3,266
	3	3,659
D	1	3,237
	2	3,015

Figure 97. Results of Load Tests on Different Layup Designs.

Four design concepts were selected for development, testing, and characterization. An average of three components of each design and

representative coupon plates were fabricated. Design and structural analysis of the corner fittings, using four different ply orientations, were performed. A total of 11 components and flat panels for material test specimens were obtained through a fabrication contract. The test data were correlated with structural analysis results to establish the validity of the structural model, test method, and component instrumentation (Figure 97).

The results lead to the recommendation that application of advanced composite materials (especially use of the Pitch 75 fiber system) will require structural testing of the specific design selected. Placement of strain gauges should be verified on like components, made from aluminum, to establish stress distribution for complex fittings. Location of strain gages in areas which indicate large changes in the stress field and near edges should be avoided. A progressive failure analysis should be utilized in the analysis process. The test results obtained will give designers and analysts a good understanding of behavior and instrumentation requirements of composite components.

E. E. Engler/EP13
(205) 453 – 3958
Sponsor: CDDF

Heat Transfer/Fluid Mechanics

Fluid Interface and Bubble Experiment

Free surface shapes of rotating liquids play a key role in spacecraft fuel tank design and fluid management systems. In the absence of gravity and temperature gradients along the surface which drive Marangoni convection, the equilibrium shape of the free surface is governed by a balance of capillary and centrifugal forces. Hydrostatic stability is maintained when the additional pressure from the capillary rise is compensated for by the pressure reduction resulting from the curvature of the free surface. In a zero – gravity environment without rotation, the surface is spherical. Whether the sphere encloses the liquid or the vapor depends on the wetability of the container by the liquid. In some spacecraft fuel tank applications, propellant slosh and distribution are controlled by the use of internal baffles which come into contact with the free surface. If the liquid is to be held using capillary forces, the baffle spacing must be small enough to overcome the fluid's inertial forces during small accelerations brought about by thruster firings, crew motion, etc. The problem can be complicated by the rotation of the container. In order to manage the liquid, the distribution of the fluid including its interface shape must be determined.

An experimental apparatus to measure free surface shapes in low gravity was designed and built. It consists of a Plexiglas cylinder 20 cm across and whose depth can be set at 2 cm, 4 cm, or 6.3 cm. The cylinder is partially filled with ethanol. Ethanol was chosen because its surface tension is relatively high and not extremely sensitive to low levels of contamination, its contact line with the container does not stick, and its contact angle is close to zero. The cylinder is fastened to a turntable which rotates about the cylinder's axis. The rotation speed can be varied from 0 to 108 rpm. After the cylinder is filled with ethanol, a prescribed amount is removed to establish the bubble vollume. Overhead and side – mounted video and still cameras record the shape of the fluid interface (Figure 98). A low gravity environment was provided by NASA's KC – 135 aircraft flying a parabolic trajectory. With the apparatus bolted to the floor of the aircraft, 20 to 30 sec of low gravity is produced during the maneuver. Although the gravity fluctuates around zero, typical departures are two percent of terrestrial gravity.

The fluid surface shapes were compared to analytical solutions of Laplace's equation which relates the pressure drop across an in-

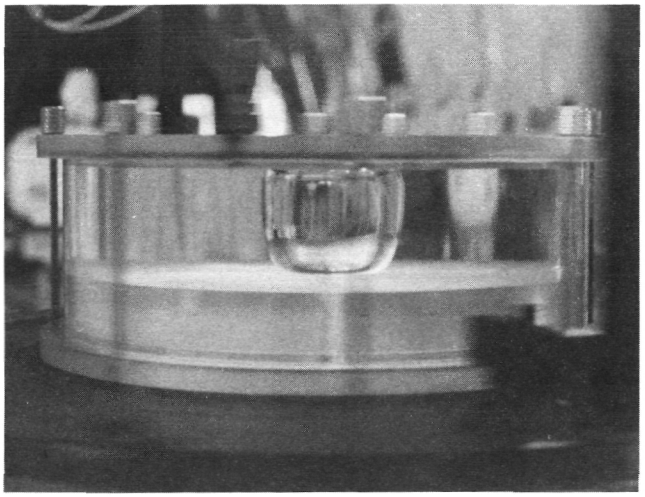

Figure 98. Interface Shape of Rotating Bubble.

terface to the radii of curvature of the surface. Solutions to the equation are dependent upon several parameters, viz F, the ratio of centrifugal to capillary forces, the contact radius of the interface to the boundary, and also the contact angle. For isolated bubbles, F has a maximum value of .5. A further increase in F causes the bubble to break contact with the axis of rotation. For large values of F, the bubble becomes more cylindrical and the capillary rise occurs over a thinner layer. Measurements of the interface shapes performed in the low gravity environment showed good agreement for free surfaces in quasi-equilibrium. Low rotation cases were difficult to evaluate because of the ambient fluctuating gravity environment aboard the aircraft. These cases will have to be examined in Earth orbit where extended periods of microgravity are available.

Fred Leslie/ED42
(205) 453-2047
Sponsor: CDDF

Thermal Energy Storage and Transport Utilizing Microencapsulated Phase Change Materials

An orbiting spacecraft undergoes highly cyclic environmental conditions that have a significant impact upon the vehicle's thermal management system. Radiator systems sized to dissipate heat at maximum design conditions are substantially oversized for average heat loads. Because subsystem elements generally impact system level tradeoff items such as total weight, deployed surface area, and vehicle drag, innovative concepts which minimize radiator areas have been investigated. The concept discussed is the first phase of a project to minimize the required radiator area through storage of peak thermal energy. This energy is later dissipated by the radiator system during more favorable environmental conditions.

Phase I of this study, completed during fiscal year 1984, is a part of NASA Small Business Innovation Research Program. The specific area studied involves microencapsulation of phase change materials (PCM), which have long been utilized as energy storage devices. The unique feature of this effort is the applicability of encapsulated PCM in a stackable, packed-bed energy storage module. A discrete energy storage unit is shown conceptually in Figure 99.

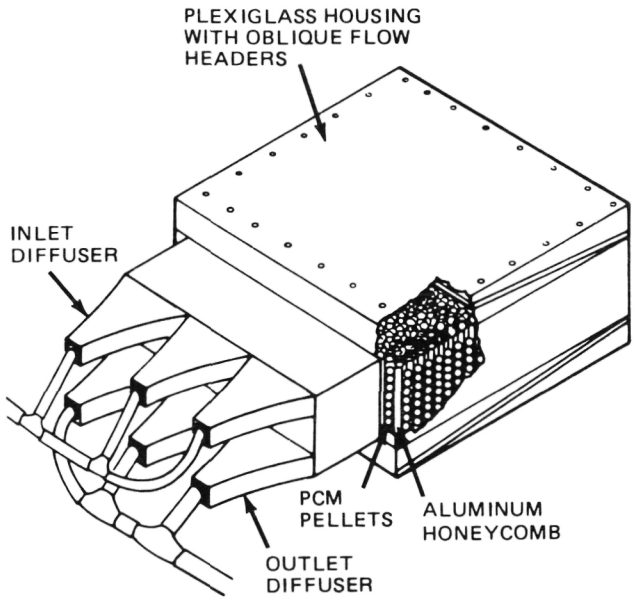

Figure 99. Packed Bed Module with Flow Diffusers.

Microencapsulated PCM in a packed bed arrangement offers the greatest energy storage density and the largest time response of any

of the current storage concepts. Within the packed bed the heat transfer rate is enhanced due to the very large surface area available between the heat transport fluid and the PCM spheres.

In the test unit, an aluminum honeycomb matrix was used to contain the PCM spheres and at the same time prevent the flexible granules from blocking the fluid flow passages. A fine, 150 mesh, stainless steel screen was used to seal the core matrix at each end. The screen was spot welded at six locations around each hexagonal cell and supported by a stronger 18 mesh stainless steel wire cover. The core matrix was then housed in a Plexiglas structure to permit visual observation during experiments; diffusers were used to provide flow distribution across the matrix. The microencapsulated spheres are approximately 3,000 μm in diameter. The PCM used in the study was methyl palmitate (CH_3 $(CH_2)_{14}$ CO_2 CH_3), a non-paraffin wax with a melting point of 30-32°C. The packed bed was loaded with 2159 g (4.8 lb) of PCM spheres to a packed density of 408.5 kg/m^3. The void fraction of the bed was estimated to be approximately 45 percent.

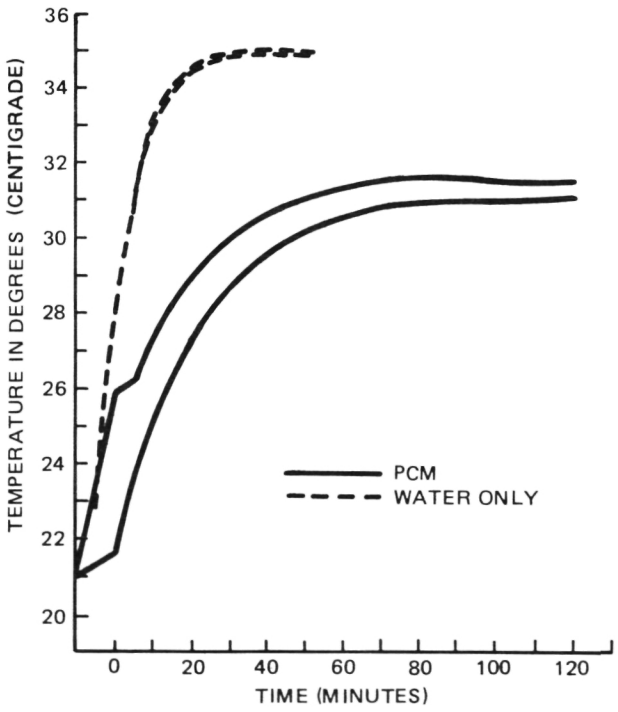

Figure 100. Thermal Response of Packed Bed for PCM and Water.

Typical test results, illustrated in Figure 100, show the temperature response of the PCM packed bed is much better than the water system, which indicates a significant occurrence of phase change, but no discrete melting temperature can be discerned (upper curve is temperature upstream of PCM bed while lower is downstream). During the course of the tests, it was concluded that, not only was the PCM changing phase over a range of temperatures, but supercooling and superheating were occurring, events generally caused by impurities within the PCM. PCM samples of higher purity will be procured and tested in order to more fully understand this phenomenon. The program is now in its second phase of study and the concepts have continued to be developed in fiscal year 1985.

James W. Owen/EP44
(205) 453-5503
Sponsor: SBIR

Heat Transport Across Structural Boundaries

Future NASA spacecraft may evolve in a modular fashion, with initial build-up, as well as growth, accomplished by joining structural elements in orbit. To avoid designing a separate thermal control system for each element, an efficient method of transferring thermal energy across structural interfaces is being investigated. The concept under development involves the transfer of heat alone, without requiring the transport of heat carrying fluids across the boundary. The concept also allows for one degree of freedom (rotation) between the two structural elements.

Because heat pipes offer the potential advantage of efficient heat transport without the need for mechanical pumps, the objective of the current program is to use heat pipe principles in the design of a rotating thermal joint. The operating requirements include a temperature range from 0 to 40°C (32 to 104°F), trans-

fer of up to 10 kW (34,130 BTU/hr.) with an overall temperature drop across the device less than 5°C, (9°F) and a total life of 60,000 revolutions at 2 rpm with a 19.6 kg/m (1700 in/lb) bearing load. The rotating joint is a flat disc 66 cm (26 in) in diameter and approximately 5 cm (2 in) thick, as shown in Figure 101.

A heat pipe is an evacuated, sealed, two-phase heat transfer device which contains a small quantity of a thermodynamic working fluid filling the pores of a capillary structure, or wick. When heat is added, vapor is formed, filling the evacuated space. Conversely, heat removal causes condensation. The resulting condensate is returned to the heat input region, or evaporator, via capillary pumping in the wick. This cyclic process results in efficient transfer of heat with a very small change in temperature from the heat source to the heat sink. The key properties of the fluid are its vapor density, surface tension, and latent heat of vaporization. The vapor density is an exponential function of temperature and determines the minimum operating temperature of the heat pipe. The surface tension, acting in the small pores of the wick, is the predominant factor in determining the capacity of the capillary pump. The latent heat of vaporization determines the mass flow required for a given heat transfer rate, and thus indirectly sets the mass flow requirement in the wick.

The concept, developed during 1984, capitalizes upon these phenomena. The design includes two heat pipe type devices which mate

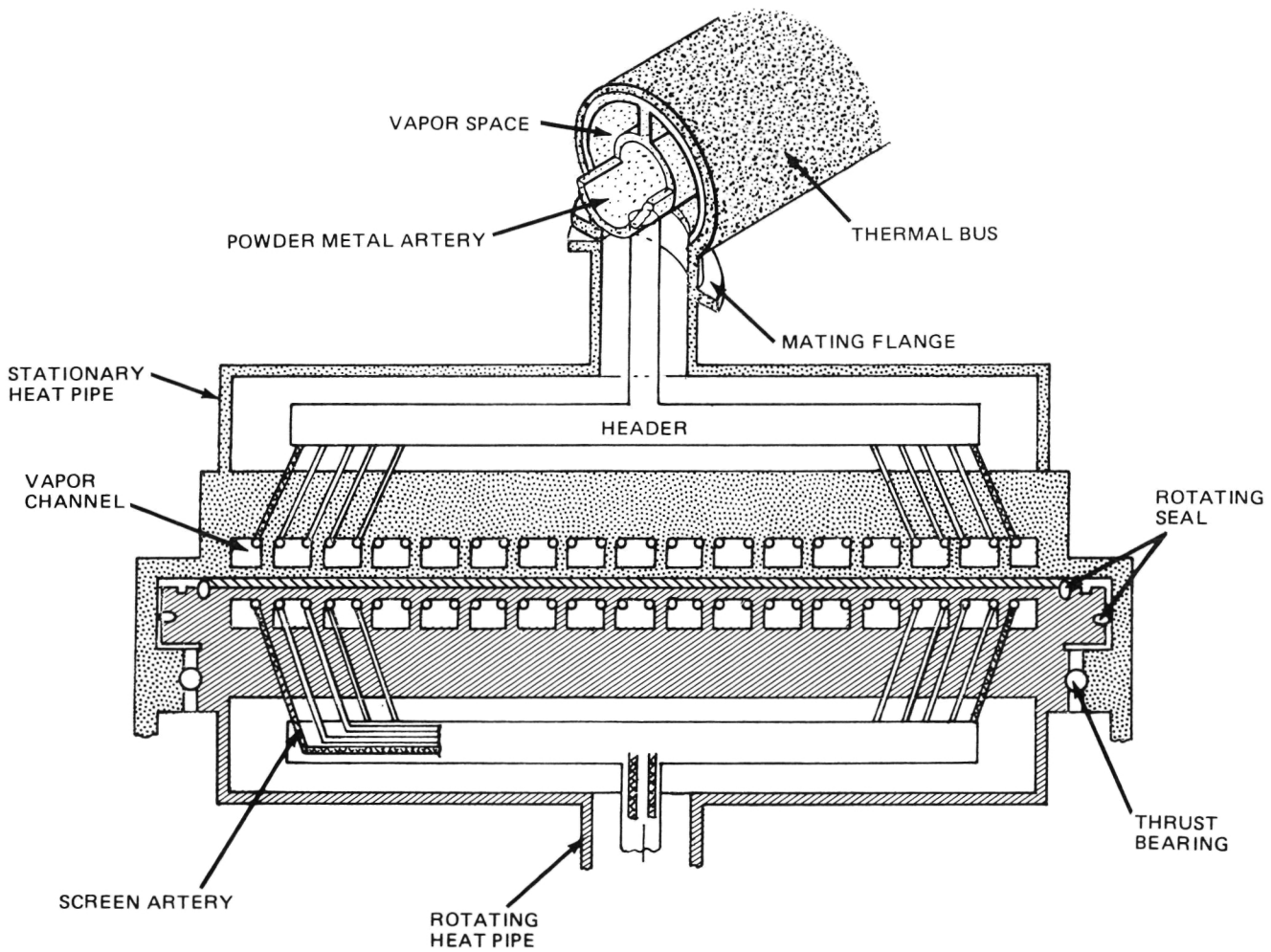

Figure 101. Rotating Heat Pipe Joint.

and form a highly efficient thermal interface unit. Work is continuing with fabrication and testing of a prototype rotating thermal joint.

James W. Owen/EP44
(205) 453-5503
Sponsor: SBIR

Cryogenic Fluid Management Breadboard

The ability to manage fluids in a low gravity environment is a requirement not only for current spacecraft, but especially for future vehicles whose operational scenarios entail orbital propellant storage and refueling. The low gravity environment poses a number of fluid management problems, including the absence of a natural convective heat transfer mechanism and the inability to reliably control the liquid/vapor interface within the vessel. Cryogenic systems pose additional complications for the fluid management system as a result of the extreme thermal control requirements and fluid thermodynamics. Cryogenic fluid management systems must minimize boiloff losses, control tank pressure, and provide pure liquid (or pure vapor) flow on demand without imposing constraints on vehicle maneuvers or attitudes.

A breadboard test article has been developed which contains all the elements of a cryogenic fluid management system (Figure 102). It consists of a 4.96 m^3 (175 ft^3) oblate spheroid liquid hydrogen storage vessel, a purge enclosure, multilayer insulation (MLI), low conductance struts, a thermodynamic vent, and a propellant acquisition device.

During facility and system checkout testing during 1984 the breadboard was loaded with liquid hydrogen and subjected to a 10-hour thermal equilibrium test to determine the thermal control system performance. Though the vacuum facility was unable to maintain the desired 10^{-5} torr (10^{-7} psia) vacuum level, the breadboard steady-state performance was measured at 3×10^{-3} torr (5.8×10^{-5} psia). At this vacuum level, the predicted total heat leak is 88 W (300 Btu/hr), representing a hydrogen boiloff rate of 0.73 kg/hr (1.6 lbm/hr). The measured data for the total heat leak and boiloff rate are 62 W (210 Btu/hr) and 0.50 kg/hr (1.1 lbm/hr), respectively. The data, amassed during fiscal year 1985, are considerably better than predicted and very encouraging since the MLI has been installed on the breadboard for approximately five years with no special environmental protection other than a missile-grade air purge during inactive periods.

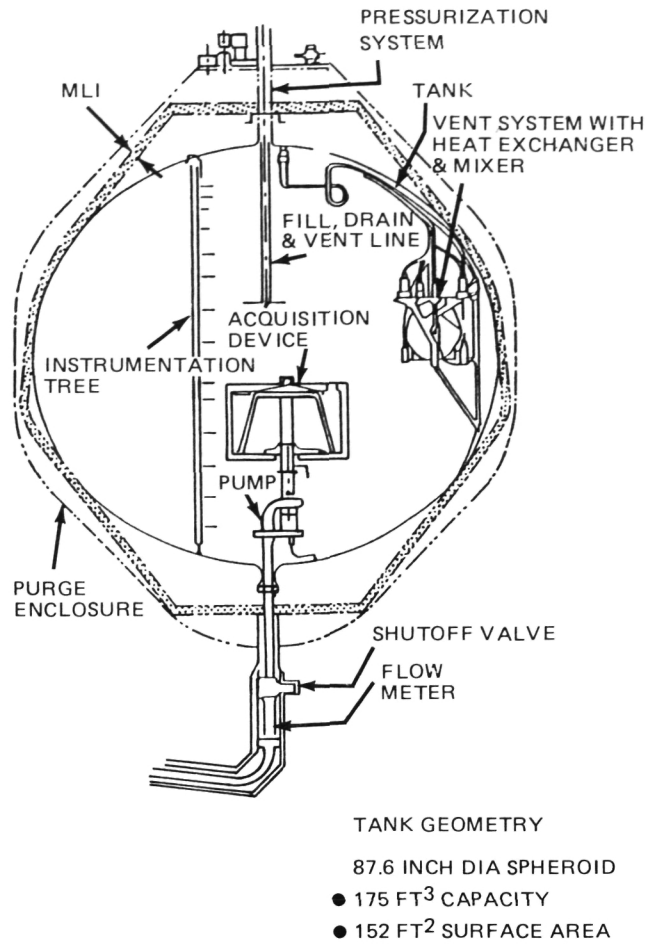

Figure 102. Cryogenic Fluid Management Breadboard.

Both subsystem and integrated system tests are being conducted. The MLI and low conductance strut performance will be determined at simulated space vacuum conditions and compared to the predicted values. To certify the aluminized Kapton MLI as reusable, it will be subjected to 20 mission cycles, including ground hold, ascent, on-orbit, and descent phases, and the performance will be documented to determine any degradation. The ability of the thermodynamic vent and mixer pump to control tank pressure will be verified at representative OTV hydrogen tank heat leak rates, and performance at abnormally high heat loads will be investigated. The capillary acquisition device outflow, refilling, and retention will be characterized as a function of flowrate, pressurant gas type (GH_2 or GHe), and pressurant gas temperature. In addition, integrated system level tests will be conducted to determine the interaction between subsystem and any functional constraints.

Robert A. Brodowski/EP24
(205) 453-0776
Sponsor: OAST

Warm Fog Dispersal Research

Since Space Transportation System (STS) launches and landings are conducted along fog-prone coastal areas, the incidence of fog can cause costly disruption to the Shuttle schedule. Launch delays imposed by visibility restrictions at the return to launch site can result in failure to meet narrow launch window constraints. Low visibility at the landing site can postpone a landing or cause expensive diversion to an alternate site. As the frequency of Shuttle flights increases and as launches are initiated from the West Coast where fog is more prevalent, the potential for fog- induced disruptions will increase.

Various fog dispersal tests have met with only limited success because warm fog, i.e., fog which has a temperature greater than freezing, is both colloidally and thermodynamically stable. Prior to our research, the thermokinetic fog dispersal technique in which fog droplets are evaporated by undersaturating the air, was the best method available. Undersaturation is achieved by either heating the air or mixing it with drier air. It is a very expensive method and produces considerable environmental pollution.

A patent application was filed in the summer of 1984 on a new technique for improving visibility in warm fog. This method uses large volume recycled water sprays, i.e., approximately 6300 l/sec/km (100,000 gal/min/3300 ft) of runway, to create curtains of falling drops through which the fog is processed by the ambient wind and spray induced air flow. Fog droplets are removed by coalescence/rainout.

The curtains of spray are created by propelling water vertically to a height sometimes in excess of 50 m (160 ft) via high capacity nozzles arranged in rows parallel to the runway or other area to be cleared. Unlike the thermokinetic technique, this method cannot completely dissipate a fog, but progressive washout of fog droplets occurs with subsequent visibility improvement in proportion to the quantity of water sprayed. To minimize the amount of spray water required while maximizing the visual range, calculations using available collection efficiencies indicate that the spray drops should ideally be about one tenth of a millimeter in diameter; however, if the spray drops are too small, it is possible that fluctuating ambient winds could carry them into the cleared volume, thus reducing the overall effectiveness of the process. The fact that the air flow induced by the water spray curtain is directed downward near the curtain helps minimize movement of the smaller spray drops into the cleared volume. Therefore, to sustain the beneficial spray induced air circulation and to minimize drift of the spray, it is preferable to work with somewhat larger drops, i.e., 0.3 to 1.0 mm diameter. Still larger drops give lower fog removal efficiencies per volume of water

spray, but otherwise they have no adverse effect if the sprays are recycled.

An initial test program to begin development of the new fog dispersal technique was conducted October 16 – 25, 1984, at MSFC. The results continue to be analyzed during 1985. Although primary emphasis was placed on determining drop size spectra of water sprays produced by individual commercially available firefighting nozzles, a linear nozzle array was also set up to investigate air flow patterns and test the fog dispersal concept should a natural fog occur during the two – week test. A dense fog did occur on one occasion, providing the opportunity to see the concept at work. Despite the fact that the water temperature was initially 4°C warmer than the air temperature, and that the water spray spectra was far from ideal, the visibility in the area downwind of the water spray curtain was measurably improved immediately.

The visual range increased (decreased) by a factor of between two and three each of the four times the water spray was turned on (off). Since only a small fraction of the spray water was contained in drops smaller than 1.0 mm diameter, i.e. the most efficient size range, there exists high potential for increasing the fog clearing efficiency by reducing the mean spray drop size. In fact, doubling the quantity of water in the size range smaller than 1.0 mm diameter through reduction of the mean spray drop size yields an additional factor of two in visibility improvement (Figure 103).

Final evaluation of the operational practicality of this fog clearing system must await further

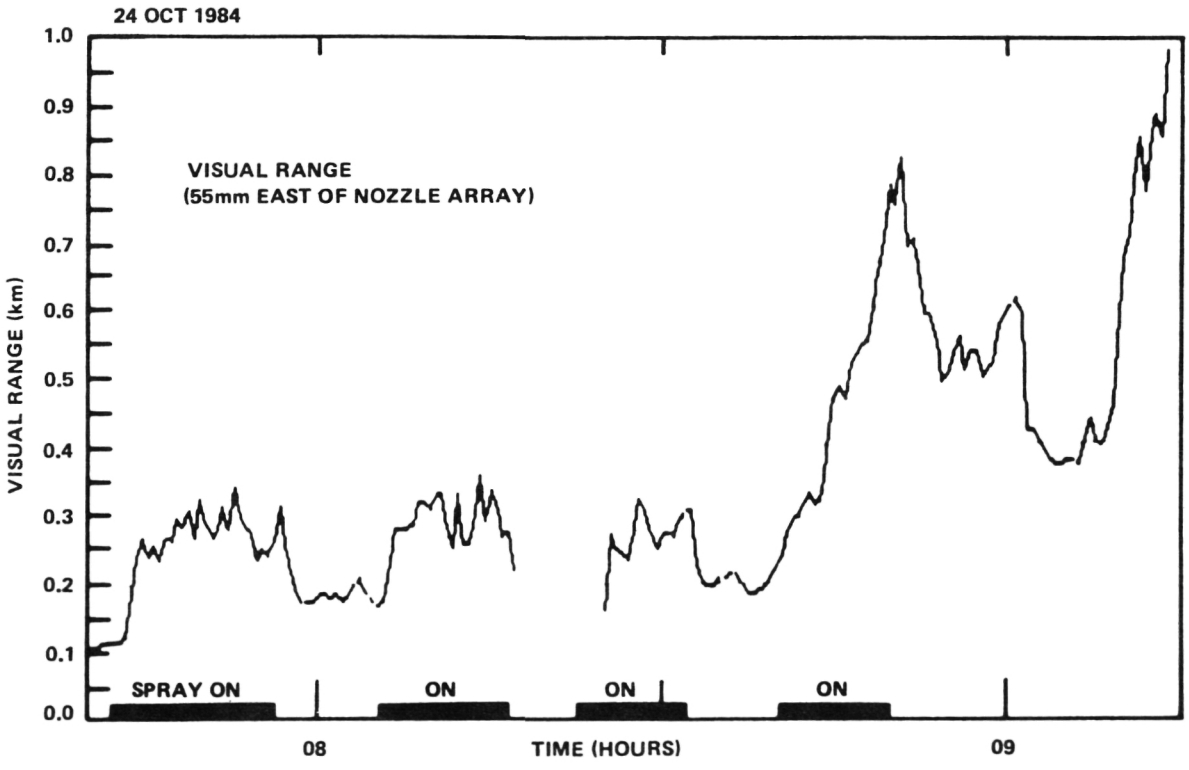

Figure 103. Visual Range Improvement.

analytical development and experimental demonstration, i.e., the operational practicality under a variety of ambient fog, temperature, and wind conditions can only be determined through field testing. Initial results from the completed tests are, however, very encouraging. From a practical standpoint, it should be noted that the energy required to pump 6300 L/s (100,000 gal/min) is an order of magnitude less than that required to operate a thermokinetic fog clearing system. Moreover, when required by changes in wind direction, water can be redistributed to other parts of the runway perimeter by the use of valves, whereas redistribution of heat from the fixed position jet engines used in many thermokinetic fog dispersal schemes is more difficult. An important side benefit of this technique is the considerable emergency fire extinguishing capability it provides.

Keller, V. W.: Warm Fog Dissipation Using Large Volume Water Sprays. NASA Patent Case No. MFS – 25962, 1983.

Keller, V. W.: Status of Warm Fog Dispersal Research. AIAA 23rd Aerospace Sciences Meeting, Reno, Nevada, January 14 – 17, 1985.

Keller, V. W., Anderson, B. J., Burns, R. A., Lala, G. G. and Meyer, M. B.: Large Volume Water Sprays for Dispersing Warm Fog. International Conference on Liquid Atomization and Spray Systems, London, July 8 – 10, 1985.

Vernon W. Keller/ED44
(205) 453 – 0941
Sponsor: CDDF

Technology Utilization

Aerospace technology applications engineering is the dynamic interaction between scientific endeavor and everyday needs. Many of today's new products and processes evolved from technology developed to meet the goals of NASA's aerospace programs. There have been thousands of "spinoffs," each contributing some measure of benefit to the national economy, productivity, or lifestyle.

The most obvious use of technology has been in the areas of information and management. The study of human engineering and propulsion has led to better firefighting methods and equipment; advancements in optics have led to improved visual screening; and the use of small valve technology used in the NASA Viking spacecraft will enable incontinent patients to achieve a measure of dignity and control that had been lost. Man ventured into space because it presented a tremendous challenge and the knowledge and experience gained was an additional benefit of man's exploration outside the Earth's atmosphere.

Advanced Lightweight Firefighting Module

Technology derived from investigation of low vapor pressure liquid flow into rocket engine turbopumps has been applied in the development of a high-flow, high-suction-lift 315 l/sec (5,000 gal/min) pump. It is used in a small, lightweight, helicopter-transportable firefighting module. The module is self-contained and consists of a pump, gas turbine engine, control system, priming system and water discharge system (Figure 104).

Its normal mode of operation is drafting water from any available body of water through three (8 in) 20.3 cm flexible suction hoses and discharging through three (5 in) 12.7 cm firehoses. The physical dimensions are 1.2 m (4 ft) by 2.4 m (8 ft) by 1.8 m (6 ft), and it weighs 1,224 kg (2,700 lb).

Its significant advantages over other available emergency water pumping equipment are its low weight, transportability, high flow, and high lift capabilities. Provided with a network of modules, operators, and a communication system to alert potential users of its availability and capability, this unit can be a real asset in remote areas where units could be flown in by helicopter sling for emergency water pumping and dewatering during natural disasters such as flood, fire, and weather storms. During its development, an earlier version was used to convert a 9.8 m (32 ft) U.S. Coast Guard patrol boat into a fireboat.

The city of Miami, with NASA assistance, adapted a module for use on a surplus military amphibian. The result was a low-cost fireboat which can travel on land as well as water and can be berthed in a firehouse rather than at docksite. It has a free turbine design which allows the compressor and gasifier turbine to rotate up to ignition speed with little rotation of the power turbine and pump during the start sequence. The pump requires 410 kW (550 hp) to produce 315 L/sec (5,000 gal/min) at a 10.5 kg/cm^2 (150 psi) discharge pressure with a

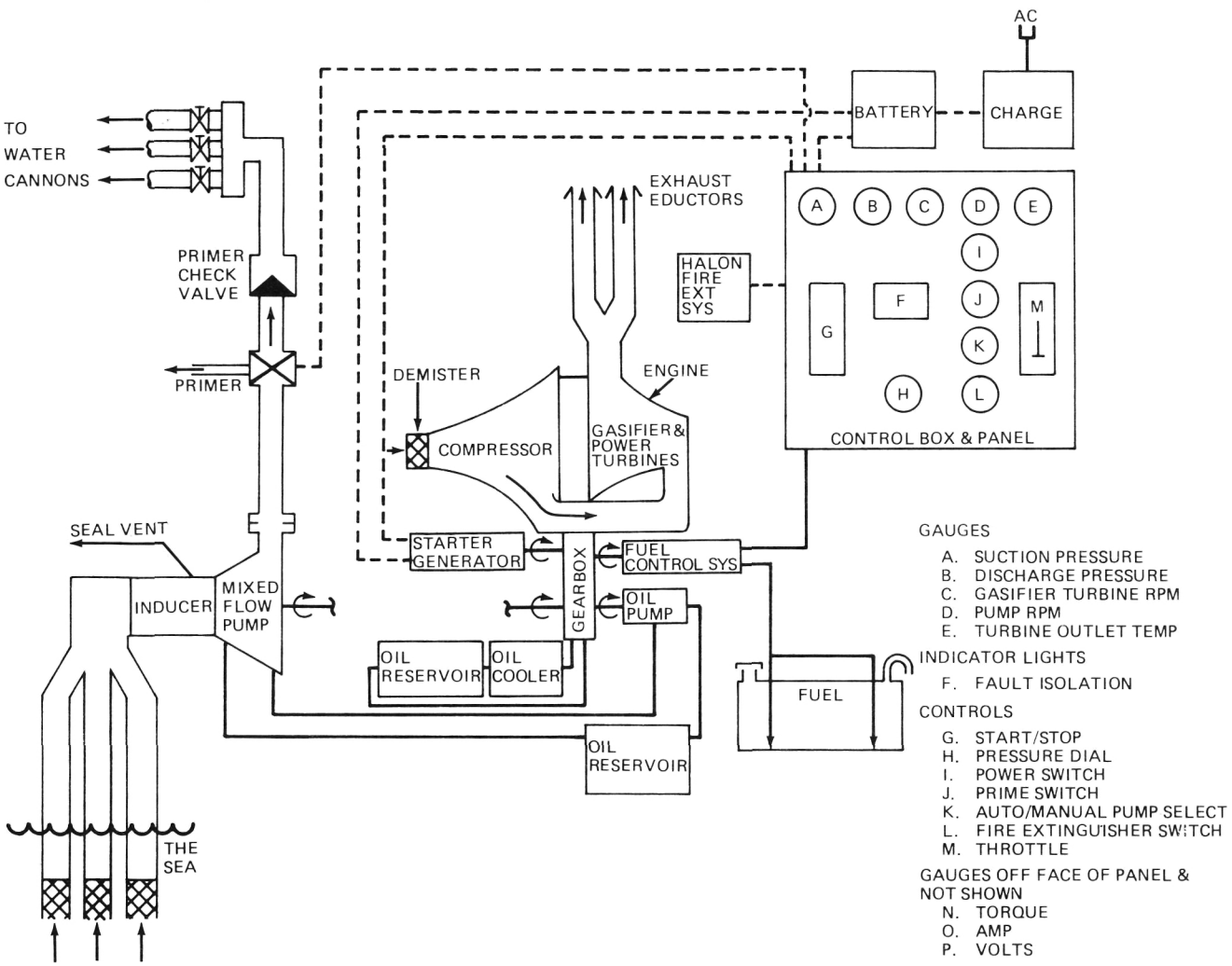

Figure 104. Firefighting Module Block Diagram.

6.1 m (20 ft) suction lift. The module will operate at this condition for three hours without refueling. Operation is simplified by an electronic controller which provides automatic start and automatic shutdown in the event specific preset operating conditions are violated. A two-stage mixed flow pump with inducer was designed specifically for this application. The second-stage impeller shaft is driven directly by the gas turbine engine. A small internally mounted planetary gear train driven by the second-stage shaft drives the first stage impeller and inducer at reduced speed to enhance suction lift performance and to minimize the net positive suction head required. The 315 l/sec (5,000 gal/min) unit was delivered by NASA to the Navy (NAVFAC) in the spring of 1984 and is presently being demonstrated in various situations.

Ralph A. Burns/EP33
(205) 453-2711
Sponsor: USN

Firefighters' Communications Equipment

Using advanced electronics associated with aerospace requirements, MSFC in cooperation with the U.S. Fire Administration and the U.S. Coast Guard initiated a project to improve fireground communications for firefighters and

ORIGINAL PAGE IS
OF POOR QUALITY

other groups including hazardous chemical spill personnel. The project will determine essential operational characteristics of current communications systems, suggest techniques and technology to enhance fireground communications, and demonstrate that moderately priced, reliable communications devices can be produced to meet present and extended needs of the fire service.

Current off-the-shelf transceivers used by firefighters are expensive and not easily adapted to firefighters' conventional equipment or hazardous chemical spill equipment. Hazardous response personnel are normally equipped with bulky equipment, including helmets, air breathing devices, water-based cooling systems, and outer wear to protect them from high temperatures, smoke, and falling debris. For these reasons, their communications equipment requires a design for operational ease, impact resistance, and temperature resistance. It should also be economical and lightweight as well as provide good audio fidelity in noisy environments. The transceiver under development provides firefighters with two-way voice communications with others inside buildings, tunnels, ships, and outside command posts.

The Remic Corp. surveyed communications devices now available and used by fire departments in the United States. During this survey they conducted propagation studies in selected buildings and tunnels, including large steel ships. In addition, a study on the biological effects and possible health hazards of radio transceivers in close proximity to the body was completed. A preliminary design was prepared of a fireground radio communications system (Figure 105). Five pairs of functional and compatible breadboard transceiver systems were constructed and tested.

The U.S. Coast Guard, when responding to spills of hazardous chemicals in or near waters of the United States, has found no single communications system which meets the reqirements of personnel in a fully encapsulated suit. As the work continues this year, the contractor will consult with the Coast Guard Pacific Strike

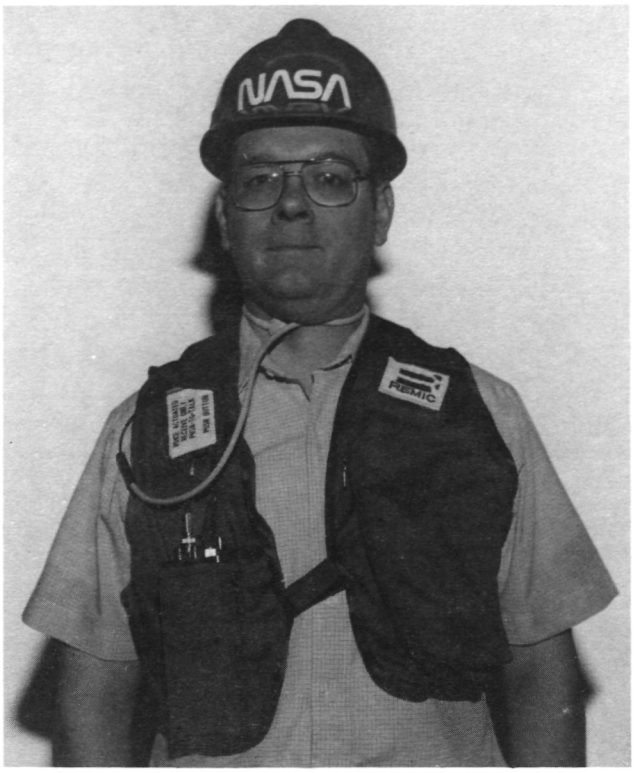

Figure 105. Fire–Ground Radio Communication.

Team in Sacramento to determine specific operational requirements. The contractor will prepare a prototype design that meets configuration requirements of the Coast Guard and will construct eight prototype transceivers and four repeaters for evaluation and testing by NASA and the Coast Guard. Five radios suitable for testing in controlled fireground environments will be fabricated and delivered to the U.S. Fire Administration.

Donald Stone/EB33
(205) 453-1571
Sponsors: USCG and USFA

Emergency Management Computer Aided Trainer

Technology used during Spacelab crew training efforts has been applied to the development of an economical, portable Emergency Management Computer Aided Trainer (EMCAT) for candidates seeking fireground commander positions. When fully developed, the unit

will establish typical and unique firefighting situations with visual response to trainee commands.

Watching the fire's progress on the TV screen, the trainee is presented a sequence of decisions on the computer monitor; his response, tapped out on the keyboard, causes the video fire to change for better or worse. If he makes a series of correct decisions, the fire is extinguished; if he errs, he will see the fire go out of control. At the end of the exercise, he is critiqued by an instructor and informed which decisions were right or where he went wrong.

The unit allows instruction and training in techniques of planning strategy and making real-time decisions in fire and police situations. It will provide realistic simulated environments such as fire scenes or hostage situations with dynamic variables representing typical firefighting or police situations. It includes visual feedback of fire and police scene changes according to decision making input made by the trainee. Video scenes and software data bases are being developed for nine scenarios. Hardware components include a microcomputer using data provided by a floppy disk drive, a computer-to-video disk interface card, a video disk player, a monochrome monitor for text information, operator options, and a color monitor for scenes.

Kenneth A. Smith/EL15
(205) 453-1474
Sponsor: FEMA

Prosthetic Urinary Sphincter System

An implantable artificial sphincter for control of urinary incontinence was ready for human trials during 1985 following a 5-year research and development program. Using miniature valve technology of the type used in experiment packages in two NASA Viking spacecraft that landed on Mars, MSFC joined with Parker-Hannifin Corp., Medical Engineering Corp., and Rochester General Hospital in the development of a simple, reliable implant device to enable urinary incontinent patients to achieve external voluntary control of bladder function. Successful implants have been carried out in 12 dogs at Rochester General Hospital.

Designed for both male and female patients, the system contains a two-chamber inflatable, occlusive cuff around the urethra, a self-sealing storage system, a check valve mechanism and a valve fluid reservoir. All components are either fabricated from or covered with medical grade silicon rubber (Figure 106).

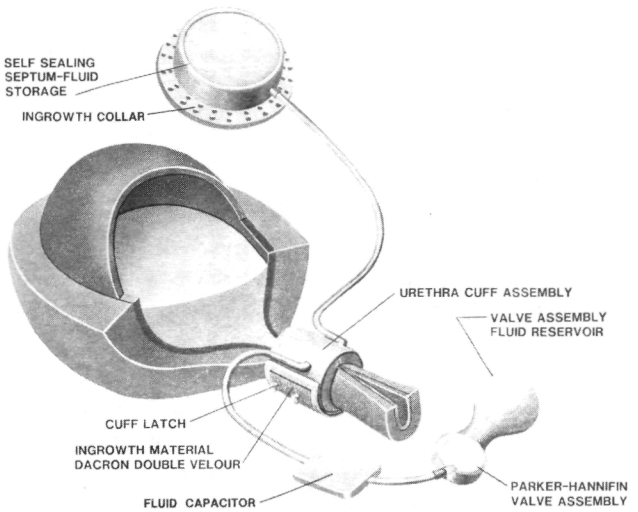

Figure 106. Prosthetic Urinary Sphincter System.

Dr. William G. Montgomery, a researcher treating paraplegics at Bowman Gray School of Medicine at Wake Forest University, asked NASA for assistance in developing a simple, reliable valve that could be surgically implanted and easily controlled by the patient. Aerospace technology, particularly miniaturized fluid control technology, was applied to the problem statement.

Medical Engineering of Racine, Wisconsin, plans to market the device following government approval and clinical trials. Parker-Hannifin's Biomedical Products Division manufactures the valve assemblies evolving from aerospace applications. The system is being further developed for control of fecal matter in persons who have undergone colostomy surgery.

ORIGINAL PAGE IS
OF POOR QUALITY

John Richardson/AT01
(205) 453 – 2223
Sponsor: Medical Engineering Corp.

Photorefractor Ocular Screening System

An economical, highly reliable photorefractor ocular screening system has been developed to detect eye problems in children through a photometric analysis of retinal reflexes. The Generated Retinal Reflex Image System photorefractor is basically a 35mm camera body, a 500 mm tele – macro lens, and an electronic flash (Figure 107). By making a color photograph, the system is capable of testing the human eye for refractive error and obstruction in

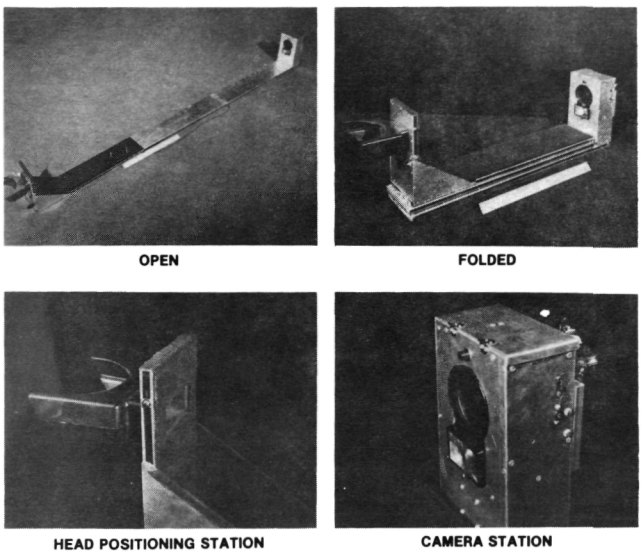

Figure 107. 2.4 Meter Photorefrator Ocular Screening System.

the cornea or lens. Ocular alignment problems are detected by photographing both eyes simultaneously. The color images of each eye are analyzed for alignment defects and differences.

Use of color film is important to detect minimal refractive errors, to determine the difference in refractive error between the two eyes, to detect lens obstructions, and to determine eye alignment defects (Figures 108 and 109).

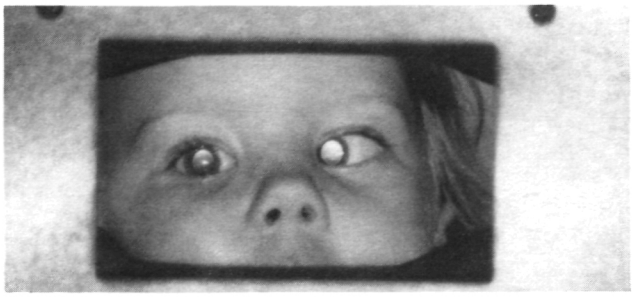

Figure 108. Refractive Error Indication Anomalies.

Figure 109. Refractive Error Indication Anomalies.

Independent tests conducted by the Smith – Kettlewell Eye Research Foundation in San Francisco rated the accuracy of a prototype 4.2 m system at 88 percent. The Generated Retinal Reflex Image System was initially used in a mass screening of students at the Alabama School for the Deaf. It was then used by the Huntsville Lions Club in screening 1,835 kindergarten and first grade students, of whom 507 were found to have abnormal retinal reflexes. University of Alabama researchers are also testing a select group of 441 learning disabled students to determine possible relationships between eye abnormalities and learning disabilities. Of these students, 255 were found to have abnormal retinal reflexes. Researchers also photographed and analyzed ocular images of over 700 normal students, grades 2 through 6, for comparison data.

The new 2.4 m system has a NASA patent pending, and its use has been authorized by the Food and Drug Administration. The portable unit will become commercially available this year.

John Richardson/AT01
(205) 453 – 2223
Sponsor: Medical Sciences Corp.

ACRONYMS AND SPONSORING AGENCIES

OAST	Office of Aeronautics and Space Technology, NASA
ACP	Office of Commercial Programs, NASA
OSF	Office of Space Flight, NASA
OSS	Office of Space Station, NASA
OSSA	Office of Space Science and Applications, NASA
CDDF	Center Director's Discretionary Fund, MSFC
USAF	United States Air Force
USN	United States NAvy
USCG	United States Coast Guard
USFA	United States Fire Administration
SBIR	Small Business Innovative Research Programs
FEMA	Federal Emergency Management Agency

☆U. S. GOVERNMENT PRINTING OFFICE: 1985-551-847/F-09963